University of Southampton Research Repository

UNIVERSITY OF Southampton

Faculty of Medicine

Institute of Developmental Sciences

Human Development and Health

Endothelial Microvesicles Involvement in the Dynamics of Thrombus Formation

Giedo Elamin

Thesis for the degree of Doctor of Philosophy

July 2021

Abstract

Background: In the event of vascular injury, careful organisation of blood platelets and coagulation factor activation functions to stop blood loss. Endothelial-derived microvesicles (EMVs) are involved in coagulation, inflammation and endothelial dysfunction, all important processes in the development of cardiovascular disease (CVD). Contradicting reports suggest that EMVs have both a beneficial and a harmful role to play in these processes.

Aim: Therefore the aim of this research is to understand the role of EMVs in coagulation by examining (I) the impact of EMVs on thrombus formation, (II) the lipid composition of EMVs and (III) the miRNA content of endothelial cells after EMV incubation.

Methods: The effect of EMVs on thrombus formation and anticoagulant activity was determined using the Chandler Loop, immunohistochemistry, flow cytometry and an anticoagulant activated protein C activity assay. Lipidomic interrogated the behaviour of lipid headgroups and chain species, and miRNAs in EMVs were assessed using next generation sequencing in stimulated and unstimulated conditions.

Results: Thrombi formed in the presence of exogenous EMVs were smaller and less solidified and possibly had enhanced anticoagulant activity. EMVs were incorporated into the thrombus. The phospholipid composition of EMVs was found to differ from the secreting cells with a possible enrichment of phosphorylated phosphatidyl inositol. miRNAs in EMVs appeared to target biological pathways involved in cell signalling and thrombus formation, and their content differed in EMVs from stimulated cells.

Conclusion: EMVs are incorporated into the thrombi and may potentially reduce the extent of thrombus formation, protecting against thrombus formation. Some of the effects of EMVs may be mediated by phospholipids and miRNAs.

Table of Contents

List of Figures

List of Tables

Declaration of authorship

I, Giedo Elamin, declare that this thesis and the work presented in it are my own and has been generated by me as the result of my own original research.

I confirm that:

This work was done wholly or mainly while in candidature for a research degree at this University.

Where any part of this thesis has previously been submitted for a degree or any other qualification at this University or any other institution, this has been clearly stated.

Where I have consulted the published work of others, this is always clearly attributed.

Where I have quoted from the work of others, the source is always given. With the exception of such quotations, this thesis is entirely my own work.

I have acknowledged all main sources of help.

Where the thesis is based on work done by myself jointly with others, I have made clear exactly what was done by others and what I have contributed myself.

None of this work has been published before submission

Signed: Giedo Elamin

Date: July 2021

Acknowledgement

One paragraph is not enough to extend my sincere gratitude to my supervisors. Thank you all for accepting and hosting me as one of your PhD students at the University of Southampton.

I consider myself really fortunate to have had the opportunity to complete this work in such great company, under the best supervision I could have possibly had. I consider myself fortunate to be supervised by the four of you. Having great four supervisors, one gets to learn immensely from. I thank all four for their constant and indefatigable support.

Despite her busy engagements, Dr Nicola Englyst always makes time for me and is never hesitant to discuss any idea I have, however absurd it might seem. Her gentle guidance, friendly and informal nature provide a very good atmosphere for learning. Her regular advice, feedback and encouragement are invaluable to my development in all aspects as a scientist and I consider myself fortunate to be a member of her group. I extend my thanks to Dr Judith Holloway, for her support and patience during ethics application that took many months to solve. Her regular friendly advice and ideas, motivating quotes and endless support throughout my PhD. Both Nicola and Jude are always happy to help or have a quick meeting the three of us. Despite all the frustration we had with the some of the data. Nicola and Jude bring cheer to everyone around with their infectious and cherubic smile.

I am grateful to Dr Phil Williamson for all his invaluable support introducing me to NMR and teaching me the essentials of it. His patience, guidance and friendly advice throughout. I envy his experience, curiosity, naivety towards research by NMR.

I would also like to extend my thanks to Prof John Holloway for all his support and friendly advice. John always encourages me to present whenever there is an opportunity within the university. Despite his very busy schedule, he always stops and asks how are things getting on whenever we bump into each other and never fails to offer his help. My thanks to every person in his lab,

"Dedicated to all the lost souls during the Sudanese revolution"

List of abbreviations

ACS	Acute coronary syndromes
APC	Activated protein C
APL	Aminophospholipid
APTT	Activated partial thromboplastin time
APTT	Activated partial thromboplastin time
AT	Antithrombin
B	Magnetic field vector
B_0	Principal component of the magnetic field vector
BAM	Binary alignment map
^{13}C	Carbon-13
BSA	Bovine serum albumin
Ca	Calcium
CAD	Coronary artery disease
Ca^{2+}	Calcium ion
C domain	Carboxyl domain
cDNA	Complementary deoxyribonucleic acid
Ctrl	Control
CSA	Chemical shielding anisotropy
CV	Coefficient of variation
CVD	Cardiovascular disease
DE	Differentially expressed
D_H	Headgroup thickness
DMPA	Dimyristoylphosphatidic acid
DMPC	Dimyristoylphosphatidylcholine

DMPS	Dimyristoylphosphatidylserine
DNA	Deoxyribonucleic acid
dsRNA	double stranded RNA
e	Electric charge
E	Energy
EC	Endothelial cell
ECM	Extracellular matrix
EDHF	Endothelim-derived hyperpolarisation factor
EFG	Electric field gradients
ELISA	enzyme-linked immunosorbent assay
EMV	Endothelial microvesicle
EPAI	Endothelial plasminogen activator inhibitor
EPCR	Endothelial protein C receptor
ER	Endoplasmic reticulum
ESI	Electrospray ionisation
FDR	False discovery rate
FID	Free induction decay
FT	Fourier transform
FV(a)	(activated) coagulation factor V
FVII(a)	(activated) coagulation factor VII
FVIIai	inhibited form of activated factor VII
FVIII(a)	(activated) coagulation factor VIII
FX(a)	(activated) coagulation factor X
FXI(a)	(activated) coagulation factor XI
FXII(a)	(activated) coagulation factor XII
FXIII(a)	(activated) coagulation factor XIII

KEGG	Kyoto encyclopaedia of genes and genomes
Gla	gamma(γ)-carboxyglutamic acid
GO	gene ontology
$\hat{H}$	Hamiltonian Operator
^1H	Proton
^2H	Deuteron
$\hat{H}_{CS}$	Chemical shielding
$\hat{H}_D$	Dipolar coupling
$\hat{H}_J$	J-coupling
HPLC	High performance liquid chromatography
HPPD	High power proton decoupling
$\hat{H}_Q$	Quadrupolar interaction
$\hat{H}z$	Zeeman interaction
HMWK	High molecular weight kininogen
HUVECs	Human umbilical vein endothelial cells
ICAM	Intercellular adhesion molecule
IL	Interleukin
I	Nuclear spin quantum number
k	Rate constant
k_B	Boltzmann's constant
K_{eq}	Equilibrium constant
LMV	Leukocyte microvesicle
LPS	Lipoplysaccharide
M	Magnetisation vector
MAS	Magic angle spinning
MCP	Monocyte chemoattractant protein

MD	Molecular dynamics
Mg-ATP	Magnesium-adenosine triphosphate
Mg2+	Magnesium ion
MI	Myocardial infarction
miRNA	microRNA
MMP	Matrix metalloprotease
MMVs	Monocytes microvesicles
mRNA	messenger RNA
MS	Mass spectrometry
MV	Microvesicle
NA	Numerical aperture
NGS	Next generation sequencing
NMR	Nuclear magnetic resonance
NO	Nitric oxide
NS	not significant
OFL	Out-of-focus light
^{13}P	Phosphorus-31
PAI-1	Plasminogen activator inhibitor 1
PAR	Proteinase activated receptor
PBS	Phosphate-buffered saline
PC	Phosphocholine
PCR	Polymerase chain reaction
PE	Phosphatidylethanolamine
PFA	Paraformaldehyde
PGI$_2$	Prostacyclin
PH	Pleckstrin homology

PI	Phosophatidylinositol
PI3K-Akt	Phosphoinositide-3kinase protein kinase B
PLL	Poly-L-lysine-coated
PLSER	Phospho-lserine
PMV	Platelet microvesicle
PPM	Part per million
Pre-miRNA	Precursor miRNA
Pri-miRNA	Primary miRNA
PS	Phosphatidylserine
PSF	Point Spread Function
PSGL-1	P-selectin glycoprotein ligand-1
qRT-PCR	Quantitative reverse transcription polymerase chain reaction
RBC	Red blood cell
RIN	RNA integrity number
RF	Radiofrequency
RNA	Ribonucleic acid
RPM	Revolution per minute
RT	Room temperature
SAM	Sequence alignment map
SD	Standard deviation
SEM	Scanning electron microscopy
SM	Sphingomyelin
SNR	Signal-to-noise ratio
SS-NMR	Solid state-nuclear magnetic resonance
T_1	Longitudinal relaxation time
TDE	2,2'-thiodiethanol

TGFβ	Transforming growth factor beta
TM	Thrombomodulin
TMM	Trimmed mean of M
T_m	Melting temperature
TMS	Trimethylsilane
TNF-α	Tumour necrosis factor alpha
TF	Tissue factor
TFPI	Tissue factor pathway inhibitor
tPA	Tissue plasminogen activator
t-PA	Tissue-type plasminogen activator
Tris	Hydroxymethyl-aminomethane
u-PA	Urokinase plasminogen activator
VCAM	Vascular cell adhesion molecule
vWf	Von Willebrand factor
WBC	White blood cell
WGS	Whole genome sequencing

Common abbreviations not spelled out in the text

°C	Celsius degrees
cm	Centimetre
γ	Gyromagnetic ratio
g	Gram
l	Litre
μ	Micro
m	Milli
M	Molar
mol	Mole
n	Nano
p	Probability value
sn	Stereospecific number
v/v	Volume/volume
ω_0	Larmor frequency
w/v	Weight/volume
%	Percentage
λ	General anisotropic spin interaction
χ_{CSA}	Chemical shift anisotropy interaction constant
χ_D	Magnetic dipolar interaction constant
χ_Q	Electric quadrupolar interaction constant
$\Delta\omega$	Resonance offset
Ψ	Wavefunction
3'UTR	3' untranslated region
5'UTR	5' untranslated region

Chapter 1: General Introduction

1.1. The Haemostatic System and Thrombus Formation

The circulatory system, also called the cardiovascular system or the vascular system, is an organ system by which cells transport the basic components required for life throughout the body (Ruggeri, 1997; Monahan-Early, Dvorak and Aird 2013). This circulatory system in which the heart pumps blood through a system of arteries, arterioles, capillaries, venules and veins facilitates the efficient delivery of oxygen and nutrients (i.e., amino acids and electrolytes) and removes metabolic waste from all parts of the body (Wohner, 2008). Lining this entire network is a layer of endothelial cells (ECs) that preserve vessel patency by supplying an inert surface which prevents blood cell adhesion (Zimmerman *et al.*, 1990; Monahan-Early, Dvorak and Aird 2013). ECs also secrete soluble mediators (e.g. endothelium-derived hyperpolarisation factor, EDHF, nitric oxide, NO and prostacyclin, PGI_2) (Wu and Thiagarajan, 1996) to actively inhibit thrombus formation, to keep platelets, the primary blood cell accountable for thrombus formation, quiescent (Wohner, 2008).

Upon vascular injury, the blood vessel integrity and the blood flow is disturbed and must be restored within limited time to prevent exsanguination (Mann, Brummel and Butenas, 2003). The system responsible for the arrest of bleeding upon injury, to keep the blood in a fluid state and to remove blood clots after the restoration of vascular integrity is known as the haemostatic system (Figure 1.1), (Kratzer and Born, 2009). This system can be categorised into three phases. Firstly, the vascular phase is triggered by an injury in the blood vessel wall (Figure 1.1a) leading to smooth muscle vasoconstriction which reduces the diameter of the vessel at the site of injury. Next, the platelet phase (Figure 1.1b) begins when platelets attach to the site of injury and become activated due to the release of chemical factors and local hormones by ECs. The third phase is the coagulation phase (Figure 1.1c) which begins 30 seconds or more following damage to the vessel wall. Coagulation leads to a thrombus formation (blood clot); (Figure 1.1d) reinforced with a fibrin mesh which seals off the damaged vessel wall (Kratzer and Born, 2009; Ruggeri, 1997).
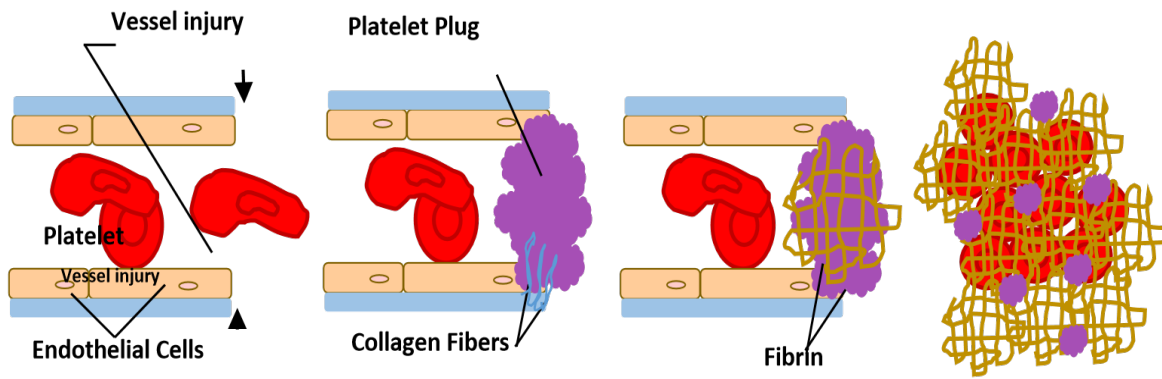
(a) Vascular damage **(b) Platelet plug formation** **(c) Blood clotting** **(d) Thrombus formation**

Figure 1.1: Phases of the haemostatic system. A simplified haemostatic system demonstrating the main phases of injured-vessel healing. Upon onset of injury ECs and other blood vessel wall cells are removed exposing an extracellular matrix that promotes platelet adhesion and activation. Adhered and activated platelets aggregate with newly arriving platelets transported to the injury by blood flow to form a platelet plug. Simultaneously, a series of biochemical reactions (coagulation) are initiated. Both platelets and coagulation are regulated by many biochemical and biophysical mechanisms to ultimately form fibrin which then lead to thrombus formation. Once the thrombus is formed the haemostatic plug must stem the loss of fluid from the vessel. To accomplish this, the plug must be sufficiently impermeable to fluid flow and must possess the mechanical strength to withstand the forces imparted upon it by the flowing blood.

The haemostatic system requires a delicate balance between procoagulant and anticoagulant activity (Palta and Saroa, 2014). Any significant disruption to this system may lead to severe complications such as excessive bleeding or thrombosis as elicited in Figure 1.2. If any injury to the vascular tissue occurs, the procoagulant system is activated in order to prevent blood loss and eventually heal the injury. Several models have attempted to depict and explain the process of coagulation. These models have gradually evolved over time to become more detailed and complex as our understanding of the coagulation system has progressed (Palta and Saroa, 2014); (Kratzer and Born, 2009).

3
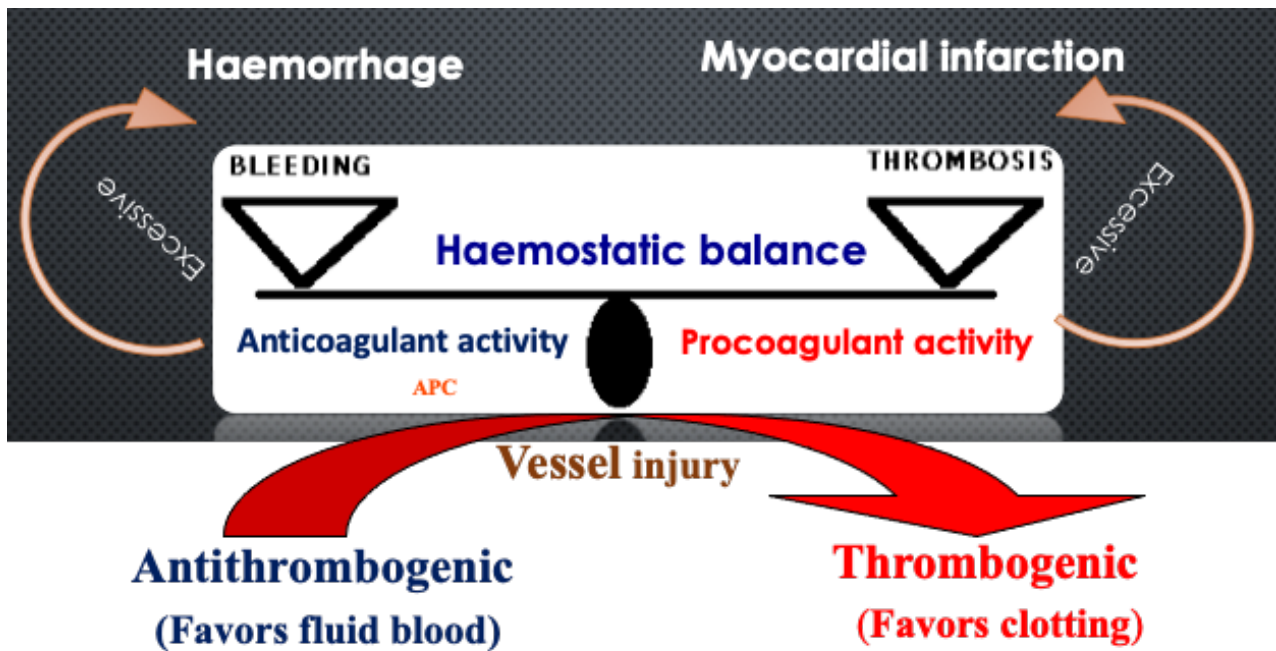
Figure 1.2: Delicate haemostatic balance. *An imbalance in haemostatic system can result in either excessive bleeding (haemorrhage), or excessive clotting (thrombosis) which may lead to myocardial infarction (MI) for instance, which can ultimately result in the obstruction of blood flow through vessels. Haemorrhage can be caused by trauma, deficiencies of coagulation factors, deficiencies in platelet adhesion or aggregation and anticoagulant (e.g. activated protein C, APC). Thrombosis can be caused by perturbations in blood composition that lead to a prothrombotic state (e.g. downregulation of anticoagulation factors), stasis in blood flow, or rupture of atherosclerotic plaques.*

The composition of a thrombus is determined by the nature and extent of injury, the local blood flow velocity and the vascular bed of the injury (Furie and Furie, 2008). For example, in the large arteries where blood flow is rapid, clots tend to be platelet rich, because platelets can adhere and aggregate at high shear stress and coagulation products are characteristically diluted. These known 'white clots' are characteristic of myocardial infarctions (MIs) which form at the site of an atherosclerotic plague rapture (Furie and Furie, 2008; Yong, Koh and Shim, 2013) Whereas, in the veins of the extremities in which blood flow is slower and in regions of recirculating flows i.e., in venous valve pockets, clots tend to be rich in fibrin and red blood cell (RBC, erythrocytes) since coagulation reactions and fibrin polymerisation have a greater residence time (Furie *et al.*, 2005). In these regions, the fibrin entraps RBCs providing what are called 'red clots'. Nevertheless, this so-called white clot/red clot terminology overgeneralises the clot structure because both types of clots enclose both platelets and

4

fibrin. Furthermore, the processes of thrombus formation can be summarised in three categories: hypercoagulability, endothelial injury, stasis, collectively known as Virchow's triad (Wolberg *et al.*, 2012). Hypercoagulability is an increased concentration of platelets, microvesicles (MVs) (Welsh, Holloway and Englyst, 2014) and procoagulant and anticoagulant proteins that affect the bloods ability to form a thrombus. Endothelial injury causes blood to be exposed to procoagulant surfaces triggering platelet plug and fibrin formation (Epstein, Rosenberg and Aird, 1999; Ardion, Shanahan and Pisetsky, 2007). Stasis of blood flow is abnormally slow or stopped blood flow and contributes to coagulation by the accumulation of clotting factors at a single location and through endothelial activation in the immobile blood (Abid Hussein *et al.*, 2007). These categories highlight the significant activities carried by the coagulation cascade as well as MVs thrombus formation (Ardoin, Shanahan and Pisetsky, 2007).

1.2. Coagulation and Thrombin Generation

Originally, the coagulation cascade was appeared to be the classical representation of the coagulation approach (Tanaka, Key and Levy, 2009). It was this cascade approach that majority laboratory tests were based on to explore haemostatic disorders (Wolberg *et al.*, 2012). This earlier theory of haemostasis originally indicated that coagulation factors controlled haemostasis in a system where cells, particularly platelets, merely provided phosphatidylserine (PS)-containing surfaces on which these procoagulant proteins assembled (Wohner, 2008). This theory, however, did not explain haemostatic mechanisms *in vivo*, for example, why certain groups of patients had a bleeding tendency (Johansson and Stensballe, 2009). It did not predict which patients were at risk of bleeding. An example of this is in patients that are deficient in factor XII, high molecular weight kininogen (HMWK) or prekallikrein (Merlo *et al.*, 2002). These patients do not present with a bleeding tendency although they show a prolonged activated partial thromboplastin time (APTT) on analysis (Capoor *et al.*, 2015). In haemophilic C (factor FXI, FXI) deficiency patients, there is an increased risk of haemorrhage but the APTT is not indicative of the extent to which the patient may bleed even though the bleeding is markedly lower than that seen in haemophilia A or B (Capoor *et al.*, 2015). The new cellular model of haemostasis incorporates the cellular components of haemostasis and the role they play in achieving haemostasis (Hoffman and Pawlinski, 2014).

Specific cellular membranes with suitable protein binding surfaces are required in the coagulation process for the purpose of binding enzymes, cofactors and eventually forming haemostasis. All these processes occur sequentially in three distinct coagulation phases: 1) an initiation phase, in which low quantities of active coagulant factors are produced; 2) an amplification phase, where the level of active coagulation factors is enhanced; and 3) a propagation phase, where coagulation factors bind to extremely procoagulant membranes of activated platelets, leading to fibrin clot formation (De Caterina *et al.*, 2013; Tanaka, Key and Levy, 2009).

1.2.1. Initiation

Initiation of coagulation as elicited in Figure 1.3 occurs when sub-endothelial tissue is exposed to the circulation at a site of injury. The tissue factor (TF) expressed in ECs is released and binds to endogenously activated FVII to form a TF/FVIIa complex (Edgington and Mackman, 1991). Therefore, a cellular source of TF is essential. There has been evidence (An *et al.*, 1994); (Meng *et al.*, 2003) showing that initiation of coagulation can occur in the vasculature. This is because certain factors (FVII, FX and FII) infiltrate tissue spaces, depending on their molecular size and are activated by TF (Adam and Bird, 2009). These factors have been detected in lymph and have been assayed along with their activated and inactive peptide forms (GoretzkP *et al.*, 1992). This may imply that activated factors are present at basal states and that thrombin production can take place outside the vasculature as demonstrated in healthy subjects (GoretzkP *et al.*, 1992); (Krishnaswamys *et al.*, 1992) even when the vascular wall is intact. This indicates that the initiation phase is constantly activated contrary to findings of other studies (Silini *et al.*, 2002). To generate a clot, approximately 2nM of thrombin is required. At high concentration of TF, the generation of FXa is predominated by the TF/FVIIa complex rather than the FVIIIa/FIXa complex, as has been shown *in vitro* (Olsen *et al.*, 2006).
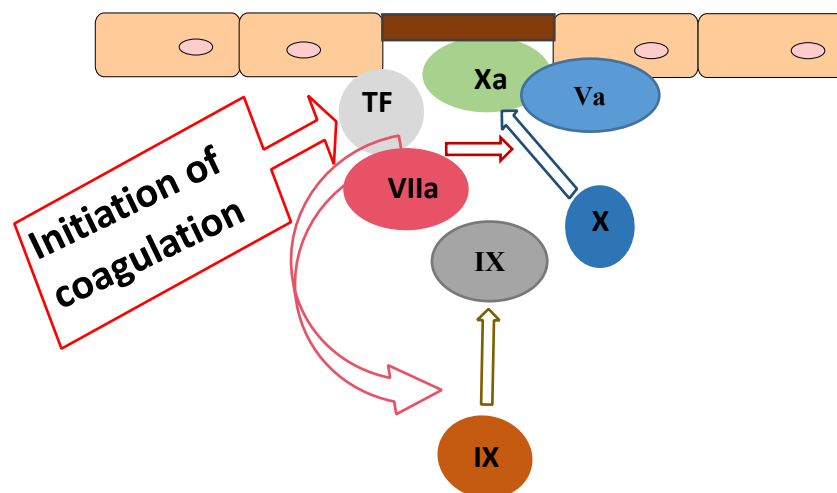
Figure 1.3: Initiation phase of coagulation. *The TF/VIIa complex activates factor X, either directly or indirectly via factor IX, which converts prothrombin into thrombin in small amounts that are insufficient to complete the process of fibrin formation.*

7

Initiation of coagulation produces minute concentrations of thrombin, mainly due to FXa. Thrombin levels produced during initiation were found to be in the ranges of 0.5 – 2nM which are sufficient for the rapid activation of platelets, FV, FXIII and fibrin formation, all of which occur before propagation. It was found that after clotting was started platelet activation followed by FXIII and FV activation was observed at a clot time of 4 minutes and all this activation precedes release of fibrinopeptides (Johansson and Stensballe 2009; Monroe et al. 2002). After the 4-minute clot time, 25-50% of procoagulant substrates were cleaved and 60% of the platelets were activated. All of this occurred with less than 1% of the total thrombin produced (Mann, Brummel and Butenas, 2003).

In conclusion, by the time a clot is visually seen, 25% - 60% of reactions involved in the formation of that clot will already have occurred but 96% of the thrombin has yet to be generated (Mann, Brummel and Butenas, 2003).

1.2.2. Amplification

Under normal circumstances, haemostatic components in the vascular wall cannot escape the endothelial layer because of their size. However, in the presence of vessel wall injury, platelets, FVIII and von Willebrand factor (vWf) leave the vasculature and come into close proximity with the small amount of thrombin generated during initiation. Platelets adhere to the injury site and form a plug on the damaged vessel wall (Wanger & Bonfanti 1991). A minute level of thrombin generated (Figure 1.4) activates these platelets by initiating a conformational change through the "flip-flop" mechanism, allowing them to expose their PS-rich surface (Contreras *et al.*, 2010). This thrombin further activates factor V released from the activated platelets and cleaves FVIII from vWf (Carrim *et al.*, 2015).
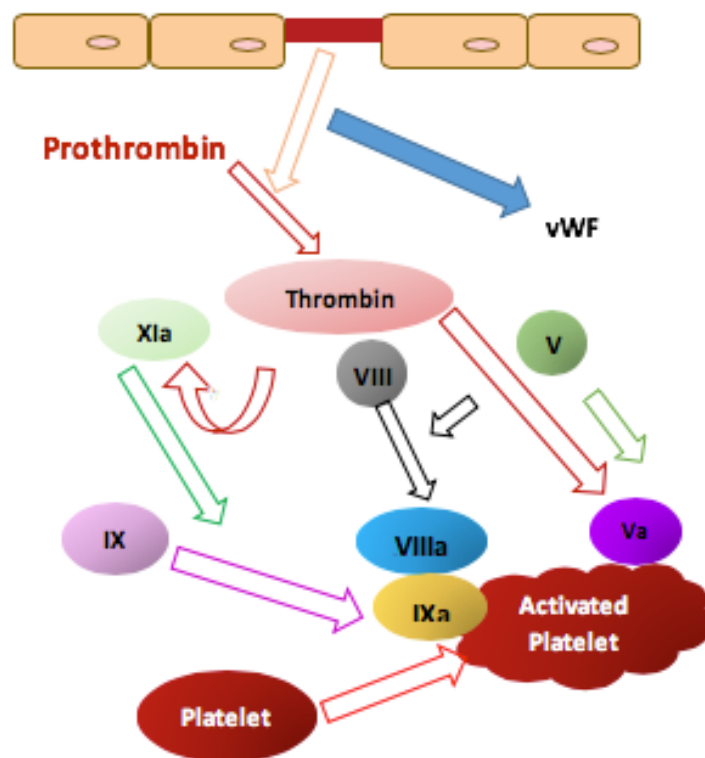
Figure 1.4: Amplification phase of coagulation. *The small amounts of thrombin that have been formed trigger formation of blood thrombus, by actively providing positive feedback for the activation of XI, XI, VIII and V to accelerate platelet activation. Figure adapted from Travers, Smith and Morrissey, 2015; Gaertner and Massberg, 2016).*

During the initiation and amplification phases, there is a priming step which provides an explanation for the recruitment of platelets and the role they play within the thrombus formation (Monroe, Hoffman and Roberts, 2002). During the priming stage, the TF-generated thrombin produced from the initiation stage binds to the platelets that have adhered to the extravascular matrix tissue, mediated in part by vWf binding to collagen. Binding to matrix proteins like collagen activates the platelets and localises them at the TF site. Thrombin then enhances platelet activation via proteinase activated receptor (PAR) mechanisms (Coughlin, 2000). Thrombin is one of the well-known PAR agonists which is a multifunctional serine protein produced during blood coagulation. Proteolysis of the extracellular NH2-terminal of PARs is used by thrombin to interact with cells which leads to exposure of a new tied ligand, binding intramolecularly to the receptor and commencing signal transduction (Behrendts *et al.*, 1990). PAR1 and PAR4 are two of the four PARs that have been reported in human platelets and are accountable for thrombin-induced platelet activation (Kahn *et al.*, 1999; Crawley and Lane, 2008). The dual stimulation via collagen and thrombin results in platelet activation greater than that seen with other agonist stimulation. Collagen stimulation of the platelet receptors results in platelet expressing high levels of FV (Monroe, Hoffman and Roberts, 2002). Thrombin cleaves the partially activated FV to a fully active form. The same cleavage process applies during the activation of FVIII resulting in its release from its cofactor binding molecule (vWf); (Tanaka, Key and Levy, 2009).

The flip-flop mechanism in platelet activation exposes PS which is required for binding to the γ-carboxyglutamic acid (Gla) residues of the clotting factors in a calcium-dependent manner (Aktimur *et al.*, 2002). TF-generated thrombin binds to specific receptors on platelets to prevent being neutralised by antithrombin (AT) (Fritsch et al. 2006). Inactive platelets have at least 3 binding receptors for thrombin that include the GPIb-IX-V complex that binds thrombin at the heparin-binding site, PAR1 that binds thrombin through the substrate-binding site and anion-binding exocite-1 (Travers, Smith and Morrissey, 2015). After the PAR1 is cleaved by thrombin, a new amino terminus with a tethered ligand then binds to other nearby PAR1 receptors, triggering a signalling

cascade. PAR4 has shown some signalling capabilities but is mainly linked to platelet aggregation rather than platelet procoagulant activity, which means that its role in haemostasis occurs much earlier during primary haemostasis (Hoffman and Monroe, 2007). The FVIII-vWf complex allows FVIII to bind to platelets through the vWf binding site on the GPIb-IX-V complex. This brings FVIII in close proximity to thrombin and allows for FVIII activation. FXI binds reversibly to platelets and this binding is enhanced by the presence of prothrombin (Hoffman and Monroe, 2007). Platelet-binding proteins play a major role in propagation. FVa binds tightly to lipids and acts as a binding protein for FXa on the platelet surface. FIXa binds to platelets in the absence of FVIIIa but this depends on the PS content of the lipids. The result of priming is a platelet that readily binds activated FXI, cofactors FVa and FVIIIa (Frey and Gaipl, 2010).

1.2.3. Propagation

At this stage of coagulation, the TF-produced thrombin will have generated several activated proteins that cause a higher concentration of thrombin (approximately 1nM) to be generated during the propagation stage (Mann, Brummel and Butenas, 2003) as shown in Figure 1.5. On the surface of activated platelets, FIXa combines with its co-factor FVIII and this occurs the moment FIXa reaches the platelet surface (Roth, 1992). The initial FIXa is formed by the TF/FVIIa complex and can move to the platelet surface because FIXa is not rapidly inhibited by tissue factor pathway inhibitor (TFPI); (Fritsch et al., 2006) and AT only inhibits it at a very slow rate (Crawley and Lane, 2008). FIXa can also be produced on platelet surfaces by FXIa. Tenase complex activates FX to FXa which immediately combines with FV, forming a more protective complex away from TFPI and AT. This prothrombinase complex converts large amount of prothrombin to thrombin, which cleaves fibrinogen to fibrin monomers that polymerise and fuse the platelet plug into a stable clot (Yamamoto and Loskutoff, 1996).
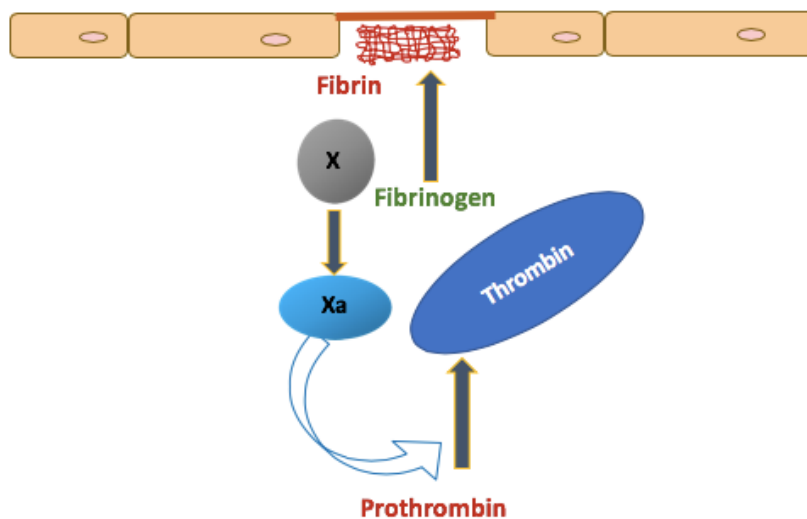
Figure 1.5: Propagation phase of coagulation. *The process through feedback mechanisms involving activation of thrombin, forms the prothrombinase complex to convert prothrombin into thrombin ,and through the action of thrombin, fibrinogen conversion to fibrin.*

In conclusion, initiation is highlighted by the production of low quantity of procoagulant factors. Amplification is highlighted by the enhacement of levels of active procoagulant factors. Propagation is highlighted by coagulation factors bind to extremly procoagulant membranes of activated platelets, leading to fibrin formation.

Coagulation pathways (Figure 1.6) play vital roles in the formation of fibrin clots. For example, the extrinsic pathway produces a low concentration of thrombin on TF- bearing cell surfaces that can trigger the onset of fibrin clot formation (Wolberg *et al.*, 2005). Initially, it was believed that this early fibrin mesh was more porous and that later when more thrombin was produced, a more tightly packed mesh was layered on top of the initial mesh, creating a more condensed and therefore secure clot (Silveira *et al.*, 1994; Mavrommatis *et al.*, 2001). More recently, it has been suggested that after the initial low-thrombin based fibrin clot is formed, the clot itself evolves with the addition of new fibrin strands to the already formed fibrin mesh. These subsequent strands elongate and cross-branch other local strands, creating a dense fibrin clot. This indicates that the final fibrin clot formed is composed of several different sized fibrin fibres (Monroe, Hoffman and Roberts, 2002; Undas and Ariëns, 2011).
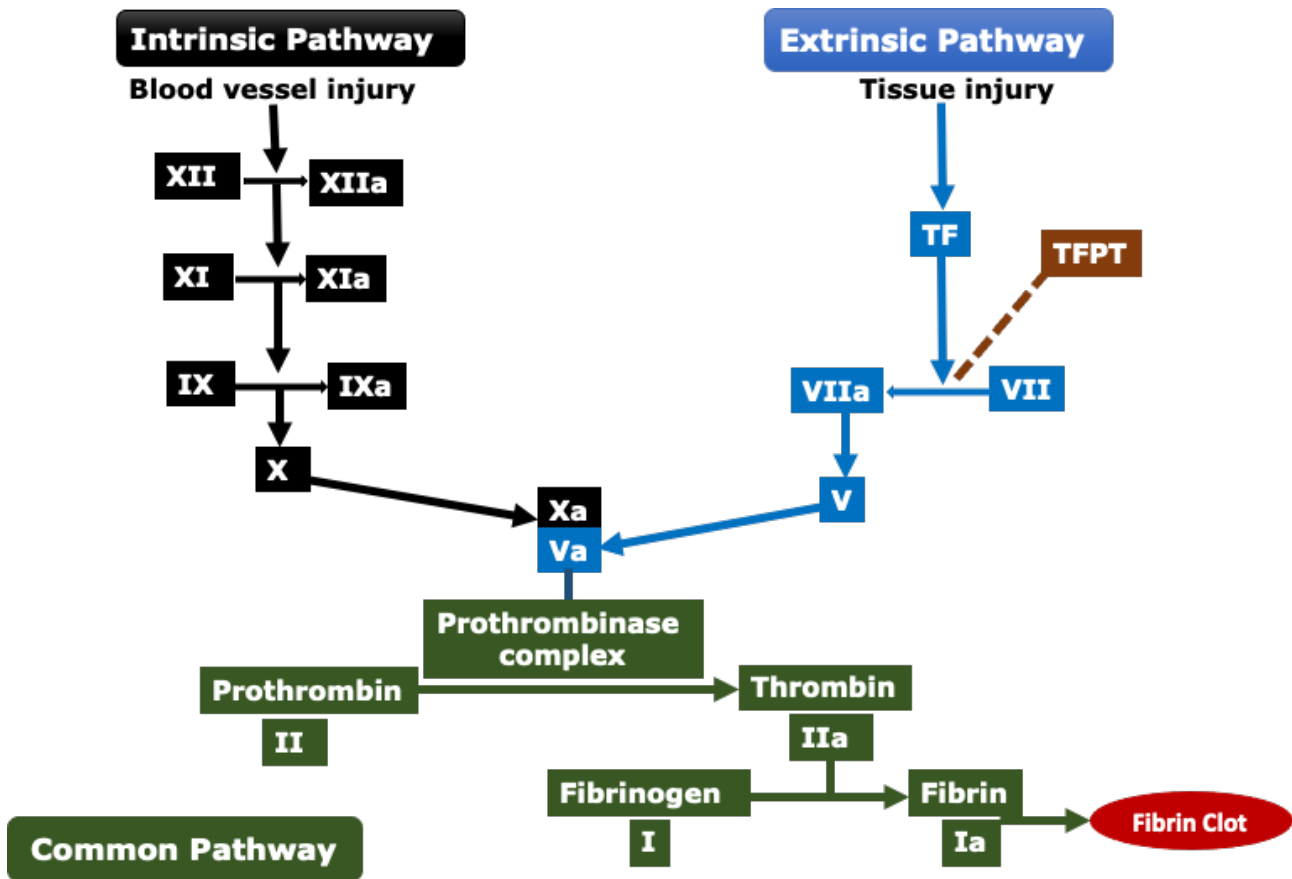
Figure 1.6: The coagulation cascade. *A simplified representation of the blood coagulation which occurs through two separate, however interactable pathways known as the intrinsic and extrinsic pathways. The intrinsic pathway is initiated by internal vascular injury, whereas, the extrinsic pathway is initiated by external injury which causes blood to escape from the vascular system. Coagulation pathways interact through a series of enzymatic reactions where coagulation factors are activated and subsequently activate other factors. These two pathways contribute to the common pathway responsible for fibrin formation.*

In conclusion, a cell-based model of coagulation allows a more general understanding of the coagulation system working order and offers a larger degree of consistency with clinical observations when it comes to coagulation disorders and explains that the presence of procoagulant factors, cellular counterparts as well as thrombin generated during clot formation, all determine the structure and subsequently the stability of the clot.

1.2.4. Inhibition of The Coagulation Cascade by Anticoagulant Pathways

Thrombotic events can occur with excessive thrombin formation and fibrin deposition compromising vascular integrity. Thus, the coagulation cascade is firmly regulated by three different anticoagulant pathways cooperating TFPI, AT and the protein C pathway, each anticoagulant pathway targeting various factors of the coagulation cascade (Figure 1.7). These can maintain and localise the activity and formation of thrombin, regulating haemostasis both temporarily and spatially (Esmon, 2009; Mann, Brummel and Butenas, 2003). Therefore, natural anticoagulant mechanisms are critical in preventing widespread clot formation. This is evident by the fact that mice lacking one of these three major anticoagulant pathways, are not compatible with life (Esmon, 2009; Cowan, Robson and d'Apice, 2011).

The coagulation cascade is triggered by TF exposure and binding to FVIIa in the extrinsic coagulation pathway as stated earlier. TFPI inhibits the extrinsic pathway by blocking TF-FVIIa and FXa on the sub-endothelial and on the developing platelet plug. Since TFPI targets the initiation phase of the coagulation cascade, it can only control generation of the trace quantities of thrombin (mediated by the activity of TF/FVIIa and initial FXa). As soon as more thrombin is formed in the propagation stage, TFPI is unable to efficiently affect the coagulation process (Edgington and Mackman, 1991; Todoroki *et al.*, 2000). Following the positive feedback activation, thrombin formation becomes TF-independent. Following this moment, the protein C pathway operates as the key mechanism controlling thrombin formation (Esmon and Fukudome, 1995; Charles T. Esmon, 2001).
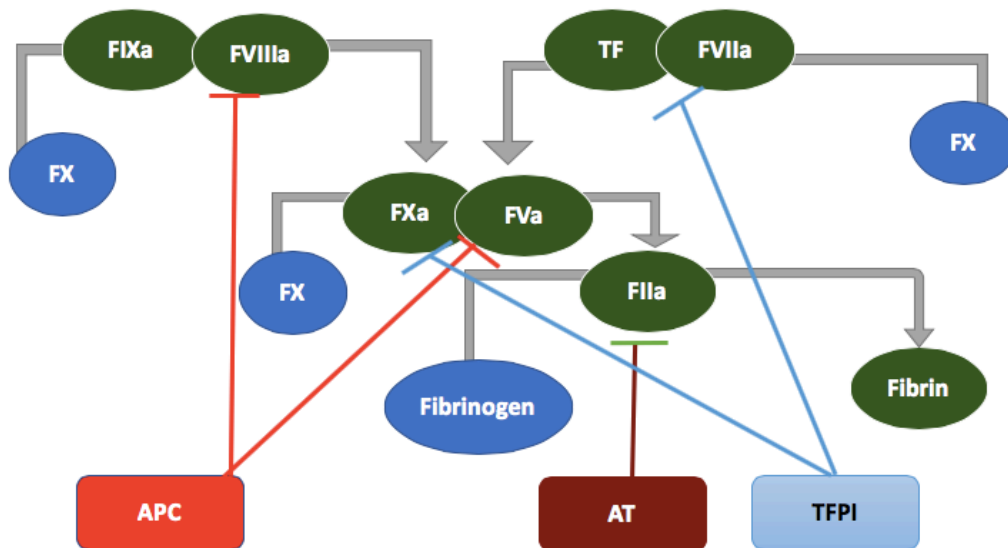
Figure 1.7: Inhibition of the coagulation cascade by the three distinct anticoagulant pathways. *The coagulation cascade is precisely regulated by the three recognised anticoagulant pathways including activated protein C (APC), tissue factor pathway inhibitor (TFPI) and antithrombin (AT), APC inactivates FVa and FVIIIa. TFPI inhibits TF/FVIIa and FXa and AT inhibition of FIIa (Crawley and Lane, 2008; Esmon, 2009).*

The protein C anticoagulant pathway is initiated by the generation of a complex of thrombin and the transmembrane glycoprotein thrombomodulin (TM) forming activated protein C (APC) (Figure 1.8) (Dahlbäck and Villoutreix, 2005). Hence thrombin also has anticoagulant besides procoagulant properties, because upon thrombin-TM binding, the specificity of thrombin is changed, it is no longer able to clot fibrinogen or activate platelets (Bernard *et al.*, 2001; Dahlbäck and Villoutreix, 2005). APC is also profibrinolytic as it can bind to the plasminogen activator inhibitor (PAI) and enables the conversion of plasminogen to plasmin, which then leads to fibrin degradation and anticoagulation (Esmon and Fukudome, 1995). TM receptor of vascular EC surface accelerating the ability of thrombin to activate protein C by >1000-fold (Crawley et al., 2007). The endothelial protein C receptor (EPCR) brings protein C in close range to TM to which thrombin is bound. When protein C is bound to EPCR this process is stimulated another 20-fold and therefore, blocking EPCR significantly reduces the production of APC (Dahlbäck and Villoutreix, 2005). In a response mediated by EPCR, APC acts directly on cells to carry multiple cytoprotective effects including; anti-

16

inflammatory activities (Liaw *et al.*, 2001), alteration of gene expression profiles (Esmon, 2001; Liaw *et al.*, 2001), anti-apoptotic activity and protection of endothelial barrier function (Liaw *et al.*, 2001). Therefore, APC must remain bound to EPCR at the cell surface in order to exert its role in cytoprotection (Bernard *et al.*, 2001; Dahlbäck and Villoutreix, 2005). Once APC is released from EPCR, it is able to carry out its anticoagulation functions by inhibiting the coagulation cascade through proteolytic generation of the two key coagulation factors, activated FVa and FVIIIa (Figure 1.8) (Dahlbäck and Villoutreix, 2005; Navarro *et al.*, 2011), thus inactivating the prothrombinase complex and preventing the formation of additional procoagulant enzymes at sites where a healthy, intact endothelial lining is present (Navarro *et al.*, 2011). This proteolytic reaction is greatly enhanced by the negatively-charged phospholipids present on activated platelets and vascular endothelium and by protein S the non-enzymatic cofactor to APC (Gleeson, O'Donnell and Preston, 2012). Therefore, as previously mentioned, to maintain normal haemostasis, a balance between levels of procoagulant and anticoagulant factors and their activities is required. Any disruption of this balance can lead to increased risk of haemorrhage or thrombosis.
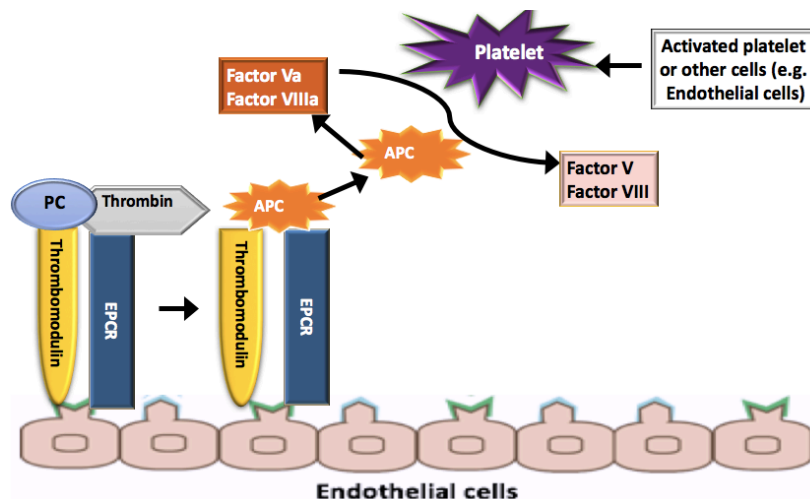
Figure 1.8: Inhibition of FVa and FVIIIa by activated protein C (APC). *Protein C (PC) and thrombin forms a complex with endothelial cell surface receptors, thrombomodulin (TM) and endothelial protein C receptor (EPCR) leading to the formation of APC. APC is secreted into the blood and directly inhibits FVa and FVIIIa (Navarro et al., 2011). Figure adapted from E. Gill, unpublished.*

17

1.2.5. Fibrinolysis

In order to maintain blood flow, the fibrinolytic pathway degrades fibrin clots once they are no longer required to seal a site of injury (Mosnier and Bouma, 2006). Therefore, fibrin formation triggers the activation of the fibrinolytic system, which is also based on conversion of zymogen to enzyme (Khan and James, 1998; Mosnier and Bouma, 2006).

Thrombin act on ECs activating them and finally leading to increased production of tissue plasminogen activator (tPA) and urokinase like plasminogen activator (uPA) (Singh *et al.*, 2003). Both these activators play an important role in the production of plasmin in its active enzymatic configuration from plasminogen (Singh *et al.*, 2003). Out of the two activators, tPA has higher activity and its interaction with fibrin further increases its activity (Vervloet, Thijs and Hack, 1998; Wohner, 2008). The fibrin polymer is broken down by plasmin, thus dissolving the clot (Hoffman and Monroe, 2007).

Fibrinolysis occurs following the steps of the external coagulation pathway and both of these processes are governed by various checks and balances (Hoffman and Monroe, 2007). uPA and tPA play an important role in production of plasmin and also interact with fibrin at the same time (Ryn, Stangier and Haertter, 2010). Thrombin and stimuli like exercise or decreased flow of venous blood stimulate the endothelium to produce tPA (Singh *et al.*, 2003). Thus, leading the entire clot formation or breakdown mechanism, this is dependent on the integrity of the ECs. The reaction between thrombin-TM and protein C results in production of APC, which in turn enhances fibrinolysis by decreasing the activity of PAI-1(Griffin, Fernández and Deguchi, 2001). Once the clotting process is initiated the amount of PAI-1 increases thus decreasing the chances of fibrinolysis by increased formation of fibrin (Smiley, King and Hancock, 2001). Once platelets receive appropriate stimuli they produce PAI-1 and in the presence of thrombin increase the rate of PAI-1 production (Binder *et al.*, 2002). Furthermore, FXIIIa is also produced by activated platelets (Thrombin acts on FXIII to form XIIIa. XIIIa then interacts with antiplasmin and fibrin protecting fibrin from the effect of

plasmin, leading XIIIa to facilitate the fibrin molecules combining with each other thus giving more strength to the clot) (Mosnier and Bouma, 2006; Wohner, 2008).

In conclusion, it can be suggested that fibrin and thrombin both act in the initiation and inhibition of fibrinolysis. Studies have been conducted to stimulate the steps involved in clot breakdown and the changes occurring in the fibrin molecules during fibrinolysis (Undas and Ariëns, 2011). These studies show that the entire process is a time consuming one with larger parts of the clot breaking away from the parent molecule (Wolberg *et al.*, 2005; Undas and Ariëns, 2011). Mechanical stimuli such as large shear stress can also lead to clot breakdown (Wolberg *et al.*, 2012). The rate of clot breakdown and the maximum amount of shear stress it can bear is dependent on the composition of the clot. The number of platelets and fibrin in the clot dictate the amount of stress it can bear (Sadler, 1994; Kratzer and Born, 2009). In addition to the key role in the final coagulation stage, the fibrinolytic system influences inflammatory processes (Mavrommatis *et al.*, 2001). While the products of fibrin degradation increase vascular permeability (Volk and Kox, 2000; Esmon, 2001).

1.2.6. The Role of Membrane Surfaces in Coagulation

Regulation of the coagulation cascade as well as most cell-cell interactions require suitable protein binding-membrane surfaces, typically including membranes of activated platelets and ECs (Yau, Teoh and Verma, 2015).

Cell membranes are composed of a double layer of phospholipids. They can form lipid bilayers because of their amphiphilic characteristics, in which two hydrophobic fatty acid "tails facing intracellular cytoplasmic and a hydrophilic "head" facing the aqueous phase (Yoshida et al., 2005; Dahlbäck and Villoutreix, 2005). The major constituent of a cell membrane is a lipid bilayer mainly comprising phosphatidylcholine (PC), sphingomyelin (SM), phosphatidylethanolamine (PE) cholesterol and PS; (Zwaal and Schroit, 1997; Lemmon, 2008), unevenly distributed between the inner and outer surfaces of the cell. (Frey and Gaipl, 2010). Inside a resting cell, the inner leaflet is enriched mainly with PS and PE as well as phosphatidic acid, whereas the outer leaflet contains large quantities of PC and SM, (Zwaal and Schroit, 1997; Lemmon, 2008). Cellular membrane phospholipid asymmetry is studied to outline functional mechanisms of the membrane (Janmey and Kinnunen, 2006). In a response to stimuli that activates the cell, e.g., in platelet activation, calcium ion ($Ca^{2+)}$ influx enhances negatively-charged PS exposure to the outer surface of the cellular membrane (Van Meer, Voelker and Feigenson, 2008). This modification in phospholipid layer symmetry caused by PS exposure is considered to comprise an optimum surface for blood coagulation in addition to anticoagulant reactions (Kol, De Kroon, Killian, and De Kruijff, 2004). In a standard phase in the blood clotting cascade, a soluble plasma serine protease accumulates with its protein cofactor activating its substrates (Williamson and Schlegel, 2002). These series of actions are significantly supported by the presence of negatively-charged membranes consisting of accessible PS moieties (Contreras et al., 2010; Kagan *et al.*, 2004). The main PS-binding motifs in the blood coagulation cascade, gamma-carboxyglutamic acid (Gla) domains, can coordinate divalent metal ions for example, Ca^{2+} or magnesium ($Mg^{2+)}$ (Villoutreix, Teleman and Dahlbäck, 1997; Morrissey *et al.*, 2009). These metals ions are capable of forming a compound with the PS-phosphate group (Leventis

and Grinstein, 2010). Furthermore, the Gla domain of prothrombin, FVII, FIX and FX in addition to the carboxyl (C) domains of FV and FVIII induce coagulation (Aktimur *et al.*, 2002). Development of such compounds with the cellular membrane causes enhanced formation of the proteases FXa and thrombin, eventually increasing thrombus formation (Aktimur *et al.*, 2002). In contrast, the capability of TFPI and APC anticoagulant activity is also dependent on the phospholipid binding mechanisms of protein S Gla domain (Krishnaswamys *et al.*, 1992; Abid Hussein *et al.*, 2008; Crawley and Lane, 2008). PS in the outer membrane is the key regulator of the TF procoagulant activity on cell surfaces (Wohner, 2008b). Nevertheless, the presence of PE significantly decreases PS requirement for the activation of FX by the TF/FVIIa complex (Garcia, Pavalko, and Patterson, 1995; Abid Hussein *et al.*, 2008). It appears that interactions provided by PE collaborate greatly with small quantities of PS present in the cell membrane to induce efficient FX activation (Heemskerk et al. 2002; Lhermusier et al., 2011).

In conclusion, thrombus formation is a complex process, arising from a balance between procoagulant and anticoagulant processes and fibrinolysis. This governs the rate of thrombus formation, size and persistence. These parameters have significant effects on clinical outcome, for example how long a brain is deprived of oxygen during a stroke and how effective thrombolytic "clot-busting" drugs are on the dissolution of thrombi.

1.3. Extracellular Vesicles

Multicellular organisms develop complex communication systems to regulate biological activities, thus maintaining physiological homeostasis. Disruption of cell-to-cell communication leads to pathological complications and disease progression. Intercellular communication between cells occurs via immobilised molecules and secreted factors. Traditionally, secreted factors include small soluble molecules such as hormones, chemokines, neurotransmitters and cytokines, which can act over short distance and affect the neighbouring cells in a paracrine approach or travel a long distance in an endocrine approach (Morhayim et al., 2014). The past decades have witnessed the discovery of a novel model of mediators of intercellular communication called extracellular vesicles (EVs) (Figure 1.9), which have potential use as biomarkers for disease as well as interesting and relevant functions potentially promoting both health and disease (Sahoo et al., 2021). The term EVs describes a small heterogenous group of membrane-vesicles secreted into the extracellular space by a wide spectrum of cell types in response to cell activation, injury, angiogenesis and apoptosis (Ratajczak and Ratajczak, 2017; Thery et al., 2018). The term encompasses exosomes, microvesicles (MVs) and apoptotic bodies. According to the last update of the International Society for Extracellular Vesicles (ISEV), EVs are defined as a group of different vesicles ranging from 30 – 5000 nanometres (nm) in diameter, secreted by different cell types through a number of mechanisms including endosomal or plasma membranes, blebbing and budding (Sahoo et al., 2021).
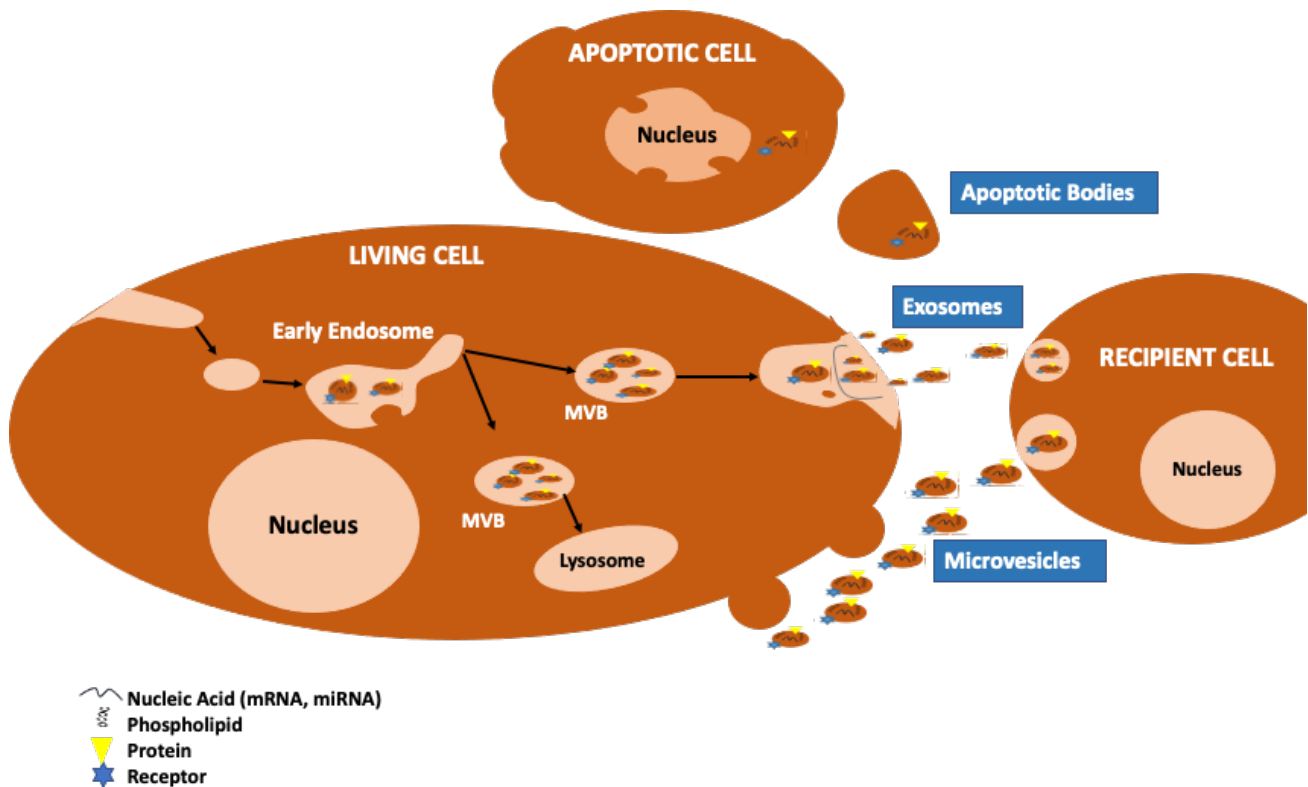
Figure 1.9: Release mechanisms of heterogenous populations of extracellular vesicles (EV) and their contents. *Schematic representation of EVs release from donor cells and interaction with recipient cells. Exosomes are formed as the intraluminal vesicles originating from the endosomal pathway which involves formation of multivesicular bodies (MVBs) that are trafficked to the plasma membrane, where lysosomal degradation or fusion of the MVBs with the plasma membrane releases the exosomes into the extracellular space. Apoptotic bodies are released by membrane blebbing of apoptotic cells as part of cellular apoptosis. Microvesicles (MVs) are formed via direct budding from the cell-membrane surface into the extracellular space, thereby carrying membrane markers of the parent cell. MV formation is calcium-dependent and associated with loss of membrane asymmetry and disruption of cellular cytoskeleton. EVs contain a diverse array of cargo, including transmembrane and globular proteins, lipids and nucleic acids.*

Exosomes are secreted internally from cells in the endosomal compartments (multivesicular bodies, MVBs), and have a diameter of 30–150 nm (Thery et al., 2018). MVs are formed by direct budding from the cell surface and fission of the plasma membrane of the recipient cell, and have a diameter of 100–1000 nm (Hugel *et al.*, 2005; Welsh, Holloway and Englyst, 2014). Apoptotic bodies are organelle-containing EVs generated by membrane blebbing of apoptotic cells. Such vesicles are phagocytosed and ranging in size between 500 and 5000nm (Doyle and Wang, 2019). Details of the

differences between the three populations remain under investigation (Sahoo et al., 2021. Nevertheless, EVs have been classified into a range of characteristics including cellular origin, lipid, surface marker and size (Figure 1.10). Amongst the various EVs population, an intersection of biophysical characteristics, including protein expression and size range, have been reported (Sahoo et al., 2021).

Extracellular vesicles

	Exosomes	Microvesicles	Apoptotic bodies
Size range nm	30 – 150	100 – 1000	500 – 5000
Density g/mL	1.13 – 1.19	1.15 – 1.21	1.16 – 1.28
Origin	Multivesicular body Endosomers	Plasma membrane	Plasma membrane of apoptotic cells
Markers	Tetraspanins: CD9, CD63, CD81 Other: Alix, TSG101, GM1, Rab, chaperones	PS binding: Annexin V, lactadherin Cell surface proteins i.e., Integrins, Glycoproteins, Selectins, VCAMs, ICAMs	PS binding: Annexin V Nuclear material: Propidium iodide

Figure 1.10: Characterisation of extracellular vesicles (EVs). Schematic representation of key features commonly used for EVs classification. The term "EV" is used as a generic term to encompass all cell-derived secretory vesicles, including exosomes, microvesicles (MVs) and apoptotic bodies.

EVs have been proposed as vectors of biological signal transmitters between cells via all major classes of biomolecules to regulate a diverse range of biological processes including transport of bioactive molecules, including lipids, proteins and nucleic acids that can regulate various cellular processes (Figure 1.11) (Thery et al., 2018; Antonova et al., 2019).
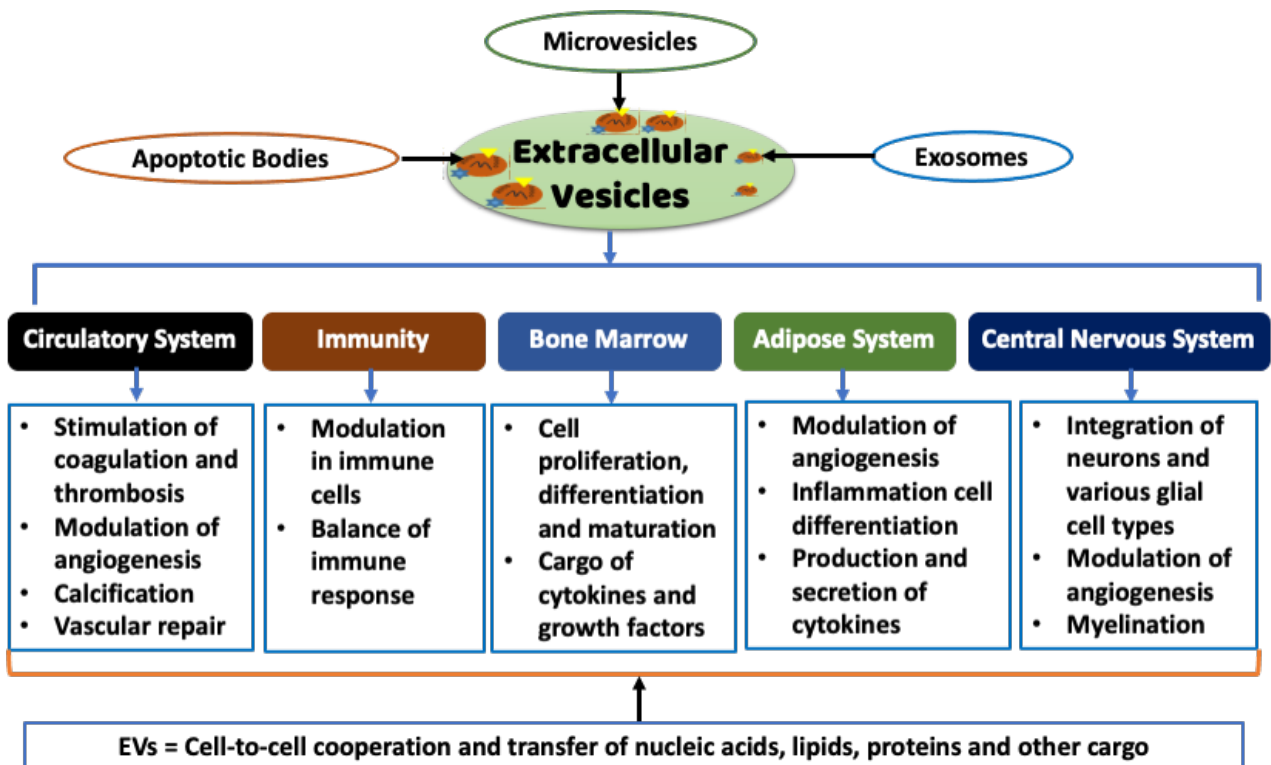
Figure 1.11: Physiological functions of extracellular vesicles (EVs). *A summary of documented physiological roles of EVs in vivo. EVs have a range of biological functions including the key biological functions such as cell-to-cell cooperation and transfer of a range of cargos. For instance, their communication between platelets and endothelial cells (ECs) in coagulation by transfer of cargos such as phospholipids and miRNAs.*

In conclusion, EVs have been broadly studied in the last few decades and have been demonstrated to modulate biological processes important in physiological and pathological processes. Increasing evidence supports a role for MVs as well as other types of EVs, in intercellular communication. Therefore, these vesicles hold exciting possibilities for their use in diagnostic and therapeutic applications. However, there is requirement for general consensus on standardised, multiparameter and high-throughput analysis methods. Further research on biogenesis and biological content of EVs as well as the distinction between EV populations and their isolation is required. This will significantly enable more differentiation between EV populations and functional characterisation of the different subtypes of EVs.

1.4. Blood Microvesicles

Blood MVs are generated from the outward budding of the plasma membrane and released into the extracellular environment. The subsequent sections focus on MVs, particularly endothelial-derived MVs.

1.4.1. Discovery of Microvesicles

The presence of cell-derived MVs in blood was first observed by Chargaff et al., in 1946 (Hargett and Bauer, 2013). They showed that 'plasma, unrestricted from intact platelets, forms thrombin on recalcification and that the rate of this thrombin formation can be decreased by prior high-speed centrifugation of the plasma'. In 1967, Wolf et al. showed that high-speed centrifugation of platelet-free plasma resulted in a pellet, which triggered thrombin formation after recalcification of the plasma (Wolf et al., 1967; Gaamangwe, Peterson and Gorbet, 2014) Originally, Wolf called this coagulant material "platelet dust" and the name was changed into microparticles (MPs) by Crawford et al., in 1971 before more recently being called MVs (Crawford, 1971; Hargett and Bauer, 2013). During the early 1970s, platelet membrane vesiculation following incubation with thrombin was imaged by scanning electron microscopy (SEM) (Webber and Johnson, 1970), delivering some of the initial images of MVs (Hargett and Bauer, 2013). Furthermore, over the following years MVs were measured in several biological fluids by a variety of techniques including; nanoparticle tracking analysis, flow cytometry and enzyme-linked immunosorbent assay (ELISA) (Hargett and Bauer, 2013), with the modern advance of flow cytometer imaging assisting researchers not only measure/quantify the number of MV, but also visualise each MV separately (Shet, 2008; Hargett and Bauer, 2013). Besides, currently, it is known that possibly all eukaryotic cell types, including blood cells such as platelets, monocytes, granulocytes and ECs, release MVs(Tripisciano et al., 2017). Moreover, since extracellular platelet-derived vesicles were the first MVs identified and comprise the largest portion of MVs in blood circulation as shown in Figure 1.12, initial analyses observing their

fundamental mechanisms of generation were established on platelet microvesicles (PMVs) (Vajen, Mause and Koenen, 2015). Nevertheless, advanced research has focused on the agonists accountable for the formation of endothelial microvesicle (EMVs). Additionally, the occurrence of MVs and other EVs is not limited to blood, but they are also present in other human body fluids, such as cerebrospinal fluid, synovial fluid, urine and breast milk (Hugel *et al.*, 2005).
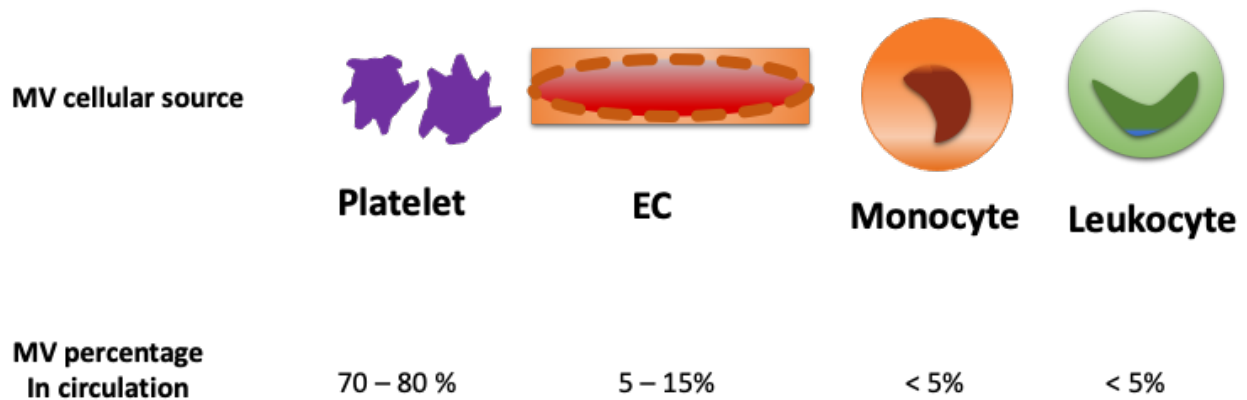
Figure 1.12: The main cellular source of microvesicles (MVs) and proportion in circulation system. MVs are derived from different cell types, however platelets are the main cellular source of MVs, followed by endothelial cells (ECs) and other blood cells such as monocytes an leukocytes.

1.4.2. Formation of Microvesicles

MVs (Figure 1.13) are formed from outward budding/blebbing of the plasma membrane (Muralidharan-Chari *et al.*, 2010). Therefore, MV formation is induced by a flip or budding in the cell membrane. The budding process consists of three key steps: sorting of protein cargo, budding of a portion of the plasma membrane and a loss of standard membrane asymmetry resulting in the exteriorisation of PS to the outer leaflet (Muralidharan-Chari *et al.*, 2009). Nevertheless, the precise mechanism of MV formation remains debatable (Hargett and Bauer, 2013; Batool, 2013). However, investigating membrane remodelling has led to vital breakthroughs in MV formation (Hugel *et al.*, 2005; Simak and Gelderman, 2006; Loyer *et al.*, 2014). Prior to membrane restructuring, the intracellular layer of the membrane of cells typically comprises PE and PS and the extracellular layer of the membrane consists of mainly PC amongst other sub-phospholipids such as SM (Abid Hussein *et al.*, 2008; Shet, 2008; Frey and Gaipl, 2010). The process of MV formation is elicited in Figure 1.14. There are well-established three lipids-transport proteins which carry out a vital role in phospholipids transportation across the bilayer of the cell membrane. These are known as the calcium-dependent scramblase which play a vital role in inward and outward transportation, the PS specific magnesium-adenosine triphosphate (Mg–ATP) dependent flippase/aminophospholipid (APL) translocase playing a role in inward transportation and the Mg-ATP dependent floppase carrying out a role in outward transportation (Janmey and Kinnunen, 2006; van Meer, Voelker and Feigenson, 2008; Contreras *et al.*, 2010). In the literature, these proteins are referred to as scramblase, flippase, and floppase (van Meer, Voelker and Feigenson, 2008; Leventis and Grinstein, 2010).
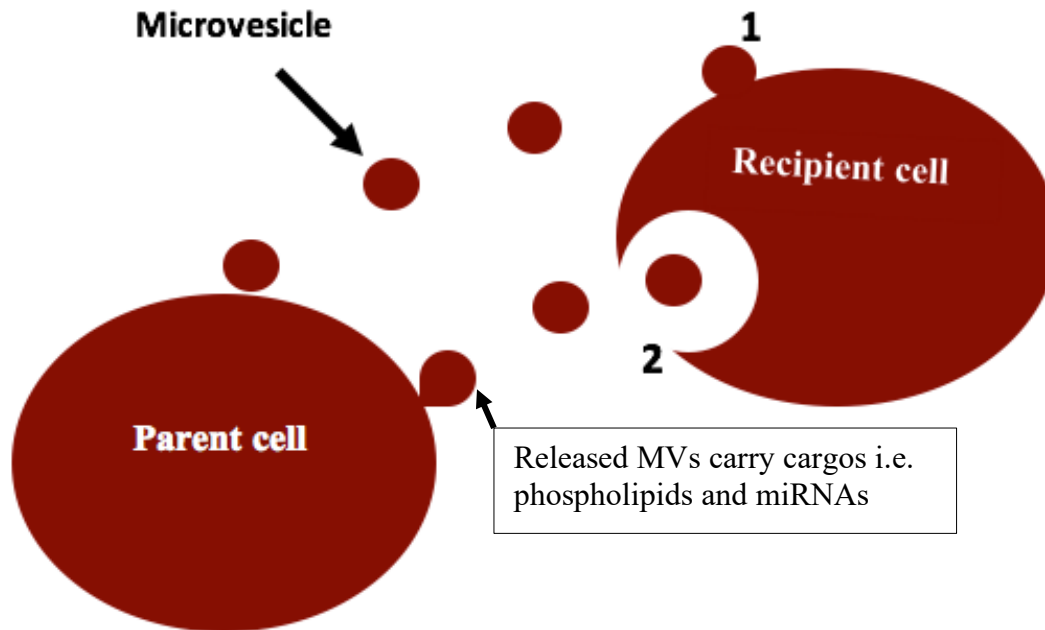
Figure 1.13. The formation and release of microvesicles (MVs). The MVs are released by budding directly from the secreting cell surface into extracellular space and can directly bind on the recipient cell surface via 1) fusion with the recipient cell plasma membrane or 2) via receptor mediated endocytosis and or exocytosis.

Activation signals on cells results in increased calcium ($Ca^{2+)}$) release from the endoplasmic reticulum (ER) (Morrissey *et al.*, 2009). Such increase results in structural variations in the cell membrane (Spector and Yorek, 1985; Hugel *et al.*, 2005; Lemmon, 2008). The rise in intracellular Ca^{2+} activates two enzymes (scramblase and floppase) and downregulates the third enzyme (flippase) activity (Hugel *et al.*, 2005). This results again in a loss in membrane asymmetry (Ardoin, Shanahan and Pisetsky, 2007; Leventis and Grinstein, 2010). High intracellular Ca^{2+} levels, Ca^{2+} influx and Ca^{2+} secreted from within the cell additionally causes the secretion of cysteine proteases (Piccini *et al.*, 2004; Pinton *et al.*, 2008). The cysteine protease for example, calpain, activates integrins which results in reformation and modification of actin filaments and membrane blebbing that ultimately results in MV formation (Abid Hussein *et al.*, 2007; Muralidharan-Chari *et al.*, 2009; Wolberg *et al.*, 2012). Following the processes of remodelling and blebbing of the cell membrane, the once negatively-charged inner layer that comprise amino phospholipid such as PE and PS is then accessible to the extracellular environment because of the activity of phospholipid transport enzymes

(flippase, scramblase and floppase); (Spector and Yorek, 1985; Simak and Gelderman, 2006; Frey and Gaipl, 2010). The negatively-charged membrane layer and the composition of the formed MVs propose some vital functions thereof (Chang *et al.*, 1993; Mareš *et al.*, 2012). This mechanism of MVs formation is proposed for erythrocytes and platelets MVs formation (Heemskerk et al., 2002; Simak and Gelderman, 2006). Nevertheless, it is essential to emphasise that MV release is not a random process such as the degradation of the plasma membrane of dying necrotic cells, but a highly-controlled process associated with different types of cell stimulation.
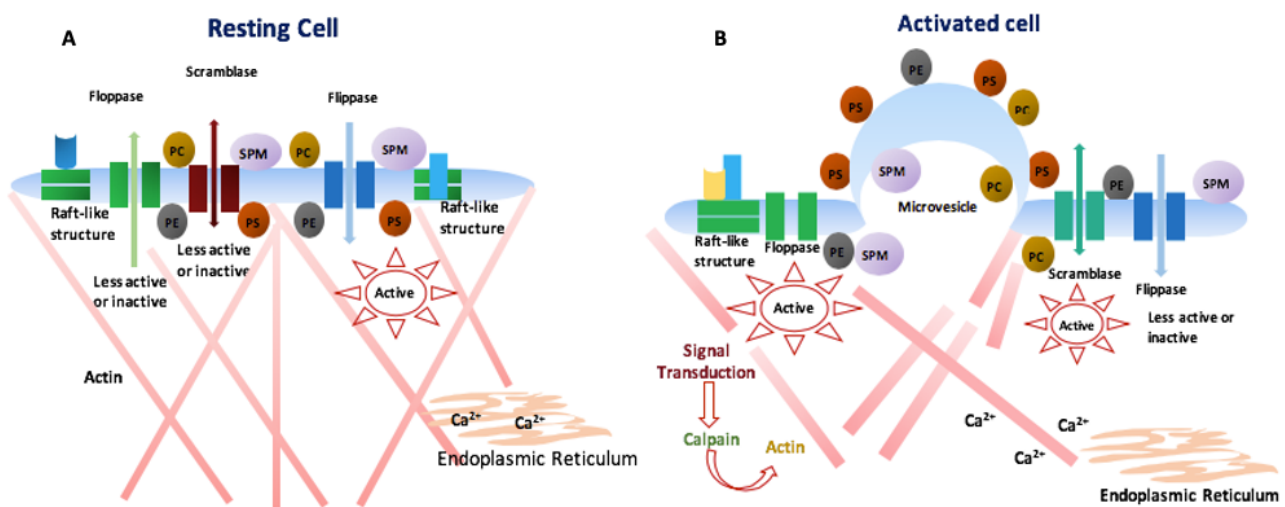
Figure 1.14: The process of microvesicle (MV) formation. *A) A resting cell encountering membrane remodelling leading to MV formation. Phosphatidylcholine (PC) and sphingomyelin (SPM) in a resting cell are typically located mainly on the outer layer of membrane, while phosphatidylethanolamine (PE) and phosphatidylserine (PS) are more generally located on the intracellular membrane layer. Flippase, floppase and scramblase maintain the asymmetric distribution of phospholipids (Lemmon, 2008; Wohner, 2008). There is low cytoplasmic calcium (Ca^{2+}) concentration and only flippase internalising negatively-charged phospholipids is active. B) An activated cell encountering cellular membrane remodelling and MV formation. Following membrane remodelling, flippase is inhibited while floppase and scramblase are activated. Floppase externalises PS and scramblase translocate specifically through the membrane, resulting in membrane asymmetry loss. Increased intracellular Ca^{2+} levels and Ca^{2+} influx from the ER are induced, which then activates calpain. Calpain then mediates cleavage and variation of the actin filaments and cytoskeleton reorganisation, which results in membrane blebbing leading to MV formation and release. Figure adapted from (Mares et al., 2012).*

30

MVs being enriched in exposed PS, enables them to fully organise the assembly of the coagulation cascade components (Abid Hussein *et al.*, 2008; Leventis and Grinstein, 2010). As well as TF, MVs expose P-selectin glycoprotein ligand-1 (PSGL-1) that mediate interactions with P-selectin located on activated platelets surface, leading to the recruitment and binding of more platelets. Once the platelet plug starts to cover the damaged tissue and sub-endothelial cells (Muralidharan-Chari *et al.*, 2010; Dignat-George and Boulanger, 2011), TF is subsequently adhere to activated platelet surfaces to function in the growth of a thrombus (Biró *et al.*, 2003). Thereby MVs-associated TF induces haemostasis, resulting in prompt accumulation of the haemostatic plug (Heemskerk, Bevers and Lindhout, 2002). Elevated levels of MVs has been shown to induce platelet deposition and thrombus formation (Heemskerk, Bevers and Lindhout, 2002; Simak and Gelderman, 2006). Nevertheless, no clear role of MVs in maintaining normal haemostasis has been presented to date.

1.4.3. Functions of Microvesicles

Given the nature of their formation, membrane MVs can act as intercellular communication messengers between cells (Figure 1.15). Therefore; MVs, can transfer an assortment of different types of cargo when released from parental cells, such as membrane associated proteins and lipids, cytokines, transcription factors, cytoplasmic contents, integrins, peptide hormones, messenger RNA (mRNA), micro-RNA (miRNA) and possibly cellular waste products such as cytotoxic agents, cell metabolic waste and misfolded proteins (Ruggeri, 1997; Simak and Gelderman, 2006; Creemers, Tijsen and Pinto, 2012). Moreover, MVs can also alter the activity of recipient cells through the transfer of their cargo (Hugel *et al.*, 2005). Valadi et al., reported that mRNA in MVs from murine mast cells could be transferred to and expressed by, human mast cells (Hugel *et al.*, 2005; Gaertner and Massberg, 2016). Also, murine embryonic stem cells support self-renewal and expansion of adult stem cells by vesicle-mediated transfer of RNA while MVs from endothelial progenitor cells have been shown to activate an angiogenic program in ECs by the transfer of mRNA (Shet, 2008). This capacity has been implicated in long-range cell signalling (Creemers, Tijsen and Pinto, 2012).

31

Therefore, MVs may play a vital role in cellular signalling if such cargo is transferred to recipient cells. Further functions of MVs include procoagulant and anticoagulant roles in thrombus formation are described in Section 1.4.6.
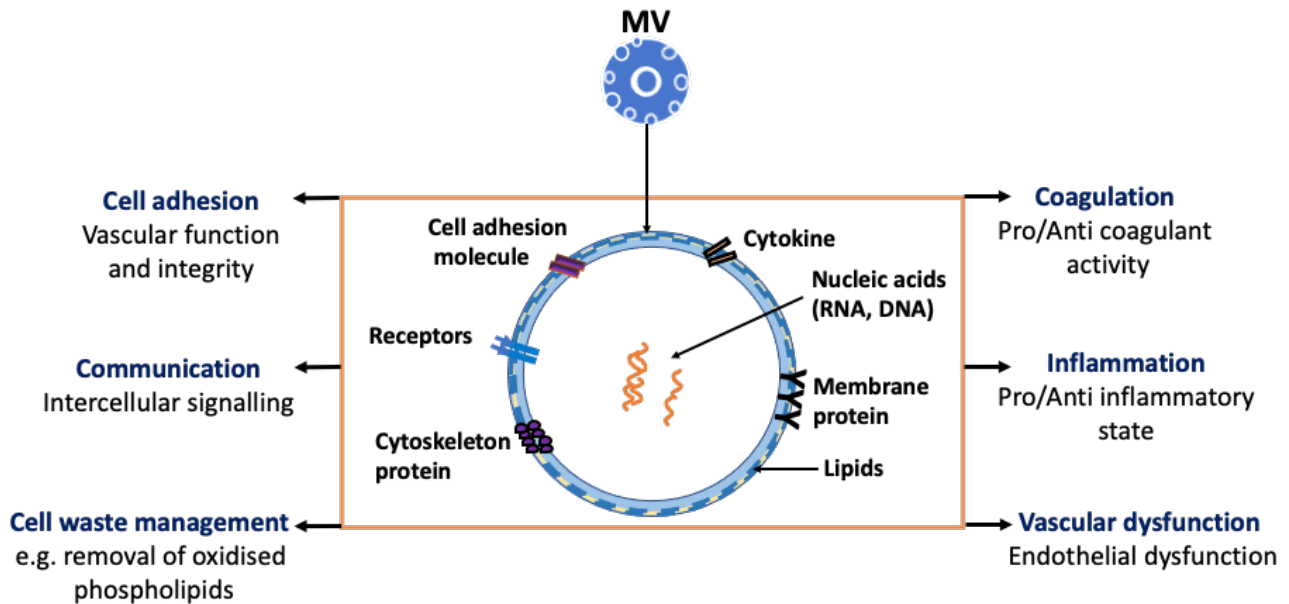
Figure: 1.15: Functions of circulating microvesicles (MVs). Once the budded phospholipid-bilayer-enclosed-MVs released into the blood circulation, they carry a number of functions including cell-to-cell cooperation and transfer of different biomaterials such as phospholipids, proteins and miRNA from secreting cells to recipient cell. MVs bud from the plasma membrane of cells, meaning that their contents closely match that of the parent cell.

1.4.4. Clearance of Microvesicles

The presence of MVs in plasma reflects a balance between MV production by activated and apoptotic cells and their clearance from the circulation (Loyer *et al.*, 2014). It was suggested that, due to their smaller size and greater ability to diffuse and escape phagocytosis, MVs may be able to survive in the circulation longer than the cells they originate from (Vajen, Mause and Koenen, 2015). However, limited information exist on the mechanisms of clearance. MVs are suggested to be cleared from the circulation by phagocytes in the liver or spleen. Phagocytes can recognise PS expressing MVs by receptors that bind PS directly or by receptors for the proteins that opsonise MVs (Dasgupta *et al.*, 2009). It has been shown that procoagulant PMVs are rapidly removed from the circulation following injection into rabbits (Dasgupta *et al.*, 2009), and within 30 minutes following infusion in mice

(Flaumenhaft, 2006). It was demonstrated that the half-life of annexin V positive MVs in humans is 5.8 hours following transfusion of platelet concentrates and that the removal of PMVs was quicker than the removal of platelets (Loyer *et al.*, 2014). However, defects in the clearance of MVs can lead to problems, including increased risk of thrombosis (Yong, Koh and Shim, 2013; Loyer *et al.*, 2014).

1.4.5. Significance of Microvesicles

Currently, it is documented increased MVs concentrations are associated with pathophysiological conditions, with elevated levels reported in inflammation associated conditions, diabetes, sepsis, dyslipidaemia, cancer and coronary artery disease (CAD) (Ardoin, Shanahan and Pisetsky, 2007; Creemers, Tijsen and Pinto, 2012; Yong, Koh and Shim, 2013). Furthermore, several MV populations correlate positively with deprived vascular consequences; for instance, endothelial dysfunction (Vallet and Wiel, 2001; Yong, Koh and Shim, 2013), suggesting MVs function in the pathophysiology of cardiovascular diseases (CVDs). Also, abnormally low MV concentrations have been suggested to be harmful (Engelmann and Massberg, 2013). For instance, decreased blood MV concentrations accompanied by reduced PS expression and deficiency in floppase activity characterise mechanisms associated with Scott syndrome (Yong et al., 2013); whilst, ageing an independent risk factor for CVD, has been associated with a decreased basal MVs level (Barteneva *et al.*, 2013). The above described literature suggests that MVs levels have a biological functional range which assists haemostasis maintenance, outside which they may trigger a pathological phenotype (Loyer *et al.*, 2014). This perception, nevertheless, may be oversimplified to describe the complex role these MVs play, as they have also been shown to enhance a dose dependent protective phenotype in cultured ECs (Gaertner and Massberg, 2016), and have been suggested to present in high levels in certain conditions such as CAD (Dimassi et al., 2016). Therefore, MVs coexist with cells in physiological and pathological conditions (Barteneva *et al.*, 2013).

1.4.6. Microvesicles in Coagulation

MVs provide a phospholipid surface for the assembly of blood coagulation factors, such as prothrombinase complexes, permitting thrombin generation (De Caterina *et al.*, 2013). Removing PMVs from plasma by high-speed centrifugation, prevents clotting of the plasma (Hargett and Bauer, 2013). The role of PMVs in coagulation is further demonstrated by Scott's Syndrome, in which patients have bleeding complications due to impaired release of PMVs (Satta et al., 2010). In autoimmune thrombocytopenia, elevated PMVs play a role in preventing bleeding complications (Morel *et al.*, 2011). It has been suggested that the membranes of PMVs have 50-100-fold higher procoagulant activity than that of activated platelets (Vajen, Mause and Koenen, 2015). The role of MVs in coagulation is however, complex and unclear. MVs can express PS and TF, central components of coagulation. Conversely, PMVs can inactivate coagulation factors Va and VIIIa, suggesting that they also possess anticoagulation properties. In healthy individuals, the level of annexin V positive MVs is inversely correlated to the plasma concentration of thrombin-AT complex, suggesting that in this case MVs have an anticoagulant function (Palta et al., 2014). Whereas under pathological conditions, the number of MVs exposing TF can be elevated, leading to increased coagulation (Biró *et al.*, 2003). The procoagulant potential of MVs is not restricted to PMVs. EMVs express vWF, resulting in platelet aggregate formation and leukocytes-derived MVs (LMVs) can transfer TF between platelets and trigger thrombosis (Wohner, 2008; Barteneva *et al.*, 2013). In fact, at the onset of coagulation, monocyte-derived MVs (MMVs) are the main contributor of TF activity, and are crucial for thrombus formation, whereas PMVs may be more of an indicator of platelet activation (Heemskerk, Bevers and Lindhout, 2002; Simak and Gelderman, 2006). MVs have also been suggested to be involved in anticoagulant pathways (Figure 1.16) through the expression of TM, TFPI, EPCR on the MV surface (Pérez-Casal *et al.*, 2009). TM binds to TF creating a complex that has no procoagulant effects (Weiler *et al.*, 2001). TFPI down regulates activation of TF – FVIIa complex (Crawley and Lane, 2008), while EPCR binds protein C, which once activated inactivates FVa and FVIIIa (Pérez-Casal *et al.*, 2009). Furthermore, it has been suggested that the negatively-

charged PS exposed on MVs may enhance assembly of PC anticoagulant protein complex (Abid Hussein *et al.*, 2008).
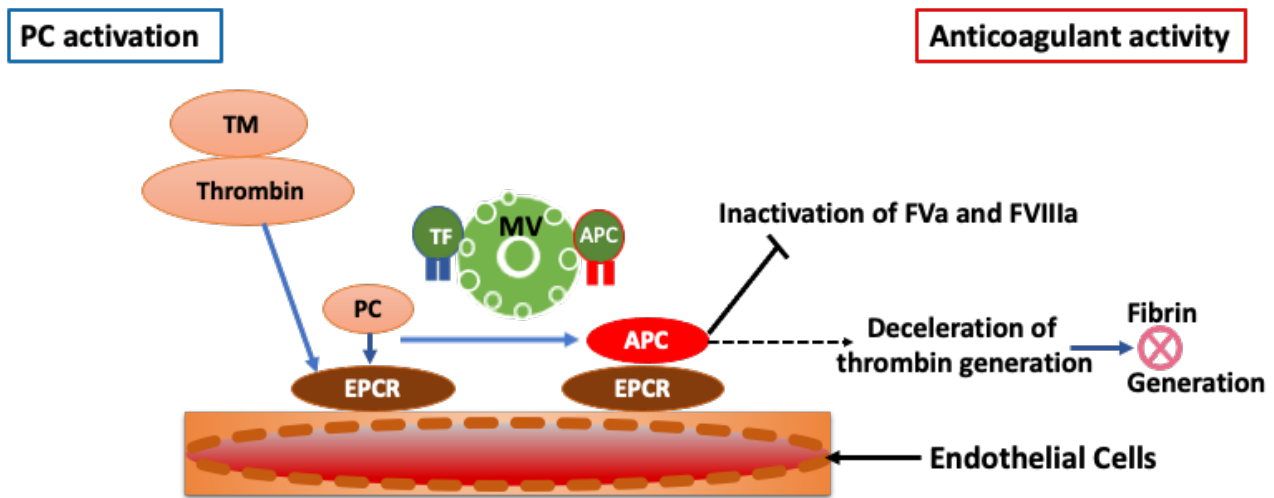
Figure 1.16: Microvesicle (MV) proposed involvement in anticoagulation. *Coagulation tissue factor (TF) expressed on MVs promotes coagulation whereas activated protein C (APC) inhibits coagulation. Activation of protein C (PC) is mediated by thrombin-thrombomodulin (TM) complex and endothelial protein C receptor (EPCR), inactivating factors Va and VIIIa, causing anticoagulant effects. Also, thrombin attaches to TM forming a thrombin-TM complex which inhibits fibrin generation.*

1.4.7. Microvesicles in Inflammation

Inflammation is defined as a reaction to injury or infection and is produced as a net result of interaction between different cells either on a one to one basis or via cytokines and other mechanisms (Ardoin, Shanahan and Pisetsky, 2007). It has recently been discovered that shedding MVs produced by different cell types also play a role in inflammation (Batool, 2013). MVs have both proinflammatory and anti-inflammatory effects on EC as well as the vascular wall (Vallet and Wiel, 2001; Dahlbäck and Villoutreix, 2005). Results from *in vitro* research have reported that MV promote the release of proinflammatory endothelial cytokines for example (Vajen, Mause and Koenen, 2015), monocyte chemoattractant protein-1 (MCP-1) and interleukin-6 (IL-6) which suggested to be induced by MVs and induced expression of endothelial cytoadhesins such as vascular

cell adhesion molecule (VCAM) (Angelillo-Scherrer, 2012; Vajen, Mause and Koenen, 2015) intercellular adhesion molecule (ICAM) and E-selectin (Esmon, 2001; Mohan Rao, Esmon and Pendurthi, 2014). Besides having a proinflammatory role, MVs play an anti-inflammatory role as reported by *in vitro* studies (Eichacker *et al.*, 2002; Simak and Gelderman, 2006; Vajen, Mause and Koenen, 2015). In these studies, MVs promoted the release of anti-inflammatory factors such as IL-10 and transforming growth factor beta-1 (TGFβ-1) from macrophages resulting in a reduction in circulating IL-8 and tumour necrosis factor-alpha (TNF-α) (Ardoin, Shanahan and Pisetsky, 2007; Batool, 2013; Hargett and Bauer, 2013). Since MVs are found at high concentrations in regions with inflammation, it is suggested that they play a vital role in inflammation and inflammation-related disorders.

1.4.8. Endothelial Microvesicles

EMVs are endothelial-derived heterogeneous vesicles (0.1–1μm diameter), resulting from membrane remodelling (Dignat-George and Boulanger, 2011). They express PS and antigens characteristic of EC (Faure et al., 2006). EMVs were initially reported in lupus individuals with lupus anticoagulant displaying thrombotic complications (Dignat-George and Boulanger, 2011). Although the exact mechanism resulting in EMV formation by EC remains unknown (França *et al.*, 2015), most available knowledge of the molecular mechanisms leading to EMVs release has its origin in *in vitro* studies, in which a variety of stimuli (including TNF-α) can induce the release of EMVs by ECs. Furthermore, EC can shed these vesicles upon activation, shear stress or apoptosis (Jimenez *et al.*, 2003). EMVs express VE-Cadherin (CD144), MCAM (CD146), Endoglin (CD105) and PECAM (CD31) are considered to reflect EC apoptosis (Jimenez *et al.*, 2003; Wang *et al.*, 2014). In contrast, E-selectin (CD62E), ICAM (CD54), and VCAM-1 (CD106) are considered to reflect EC activation (Simak and Gelderman, 2006; Abid Hussein *et al.*, 2007). Furthermore, EMVs released upon EC activation express elevated concentrations of inducible antigens while apoptotic EC shed EMVs with procoagulant activity (Dignat-George and Boulanger, 2011). With the exception of CD62E and

CD144, most of these markers are not specific for EMVs and are expressed on other cell types (Simak and Gelderman, 2006; Barteneva *et al.*, 2013). CD105 has been found on bone marrow cell subsets and activated macrophages/monocytes, CD31 has been found on activated platelets, PMVs and leukocyte subsets, CD146 has been found on pericytes, tumour cells and activated T-cells, CD54 has been suggested on leukocytes, and CD51 has been found on activated platelets and monocytes/macrophages (Hugel *et al.*, 2005; Simak and Gelderman, 2006; Dignat-George and Boulanger, 2011; Barteneva *et al.*, 2013).

1.4.8.1. Significance of Endothelial Microvesicles

EMVs may represent a small subtype of circulating MVs, however, their variations in plasma levels may predict pathological significance (Yong, Koh and Shim, 2013). For instance, several studies showed that EMVs provide protective effects to recipient cells (Ardoin, Shanahan and Pisetsky, 2007; Curtis *et al.*, 2010). Furthermore, EMVs carry markers of their parent cells, the analysis of which can provide useful information on endothelial status, for instance, CD54+, CD62E+ and CD106+ EMVs predominantly reflect inflammatory endothelial activation, while TF+ EMVs reflect prothrombotic changes of endothelial and annexin V positive EMVs characterise endothelial apoptosis (Jimenez et al., 2003).

Endothelial-derived MVs and platelet-derived MVs share several surface markers (i.e., CD31, CD105) as shown in Table 1.1, which leads to unclear differentiation, particularly in samples where PMVs and EMVs outnumber those from other cellular sources (Hromada., et al., 2017; Mortbeg et al., 2019). Careful selection of markers for EMVs and PMVs can lead to their correct identification, but poor choice of markers or weak antibody-binding or weak fluorochromes may result in misinterpretation of the MV type (Ahmadzada et al., 2020).

Table 1.1: Surface markers of endothelial microvesicles (EMVs) and platelet microvesicles (PMVs). *A summary of the various identified surface markers of PMVs and EMVs, and endothelial dysfunction-associated diseases.*

Microvesicle Origin	Disease	Surface Marker											Citations
		CD 31	CD 41	CD 42	CD 54	CD 62	CD 63	CD 105	CD 106	CD 141	CD 144	CD 146	
Endothelial													
	Acute coronary syndrome	+	x	x	+	x	x	+	-	x	x	+	(Ridger et al., 2017; Ratajczak M.Z., and Ratajczak J., 2020; Thery et al, 2018)
	Subclinical atherosclerosis	x	x	x	+	-	x	+	+	+	+	x	(Doyle L.M., and Wang M.Z., 2019; Yanez et al., 2015)
	Lupus anticoagulant	=	-	=	+	+	x	-	=	-	+	x	(Sahoo et al., 2021; Ratajczak M.Z., and Ratajczak J., 2020; Sustar et al., 2011)
	Pulmonary arterial hypertension	-	+	+	+	+	x	+	x	-	+	x	(Doyle L.M., and Wang M.Z., 2019; Sahoo et al., 2021; Ratajczak M.Z., and Ratajczak J., 2020)
	Ischemic stroke	+	x	x	-	+	+	+	+	+	+	-	(Lacroix et al., 2013; Sahoo et al., 2021)
	Vascular disease	-	x	x	+	+	x	+	+	x	x	x	(Doyle L.M., and Wang M.Z., 2019; Ratajczak M.Z., and Ratajczak J., 2020)
	Endothelial dysfunction	+	+	-	+	+	x	+	x	+	=	x	Thery et al., 2018; Sahoo et al., 2021; Ratajczak M.Z., and Ratajczak J., 2020)
Platelet													
	Acute coronary syndrome	+	+	+	+	-	+	+	x	=	x	=	(Antonova et al., 2019; Doyle L.M., and Wang M.Z., 2019; Ratajczak M.Z., and Ratajczak J., 2020)
	Subclinical atherosclerosis	x	+	+	+	+	x	=	-	+	x	-	(Sahoo et al., 2021; Ratajczak M.Z., and Ratajczak J., 2020; Sustar et al., 2011)
	Lupus anticoagulant	+	-	+	+	+	x	x	x	+	x	+	(Doyle L.M., and Wang M.Z., 2019; Ratajczak M.Z., and Ratajczak J., 2020; Thery et al 2018)
	Pulmonary arterial hypertension	+	x	=	+	+	-	x	x	-	=	+	(Doyle L.M., and Wang M.Z., 2019, Ratajczak M.Z., and Ratajczak J., 2020; Sahoo et al., 2021)
	Ischemic stroke	+	+	+	=	+	+	-	x	=	-	=	(Doyle L.M., and Wang M.Z., 2019; Ridger et al., 2017; Ratajczak M.Z., and Ratajczak J., 2020)
	Vascular disease	+	+	+	+	=	x	x	-	=	-	+	(Doyle L.M., and Wang M.Z., 2019; Ridger et al., 2017; Sahoo et al., 2021)
	Endothelial dysfunction	+	+	+	+	-	-	+	=	x	x	-	(Doyle L.M., and Wang M.Z., 2019; Sahoo et al., 2021; Ratajczak M.Z., and Ratajczak J., 2020)

(Key: (+) increase, (-) decrease, (=) no change, (x) not measured).

PMVs carry several surface markers which can promote recruitment of inflammatory cells, particularly leukocytes and monocytes, induce adhesion to ECs and influence haemostasis. Also, a number of surface markers are found on the surface of the ECs which can be carried by their derived MVs, particularly during cell activation (Soler-Botija et al., 2019). However, several of the surface markers found on PMVs and EMVs can lead to incorrect identification of MV, as they may overlap. Nevertheless, PMVs and EMVs carry pivotal surface markers which have been demonstrated to be useful biomarkers of atherosclerosis and CVD (Dini et al., 2020).

Controversial evidence is found in the literature about whether the difference in EMVs formed under pathological and non-pathological conditions is related to their functional activities (Figure 1.17). For example, in the investigations by Boulanger et al., and Vanwijk et al., naturally released EMVs situated in the blood of healthy participants did not impair endothelial function (Ardoin et al., 2007). Similarly, EMVs produced spontaneously by unstimulated cells were not associated with the development of a proinflammatory phenotype among recipient ECs (Curtis et al., 2009). In contrast, high levels of EMVs have been suggested to be contributing agents in vascular disorders, mainly initiated by endothelial dysfunction, facilitating potential use in diagnosis and prognosis (Yong, Koh and Shim, 2013). A range of clinical pathologies affecting the vessel wall are phenotypically altered and often have increased numbers of EMVs, these include hypercholesterolemia, acute coronary syndromes (ACS), atherosclerosis, metabolic syndrome, cerebrovascular accident, diabetes, peripheral artery disease, obesity, hypertension and heart failure (Loyer *et al.*, 2014). Most of these conditions, if not all, are associated with endothelial dysfunction and increased risk of thrombosis which may have involvement of EMVs in their pathology (Ardoin, Shanahan and Pisetsky, 2007; Wang *et al.*, 2009; Yong, Koh and Shim, 2013; Welsh, Holloway and Englyst, 2014). One of the key cellular events is an activated, damaged and compromised endothelium, resulting in vesicular release (Yong, Koh and Shim, 2013). This supports the theory that EMV functions vary not only depending on their cellular source, but also on their formation stimulus, with physiological modifications possibly resulting in the release of qualitatively diverse EMVs in comparison to those produced under pathological stresses (Loyer et al., 2014). Therefore, it is important to distinguish the difference in the levels of EMVs in pathological and non-pathological conditions. In this area, Mezentey et al. have performed *in vitro* assay to highlight the various parameters of angiogenesis (cell division rate, capillary formation and apoptosis of ECs), quantifying physiological concentrations of EMVs present in healthy donors ($10^3 - 10^4$ EMVs/ml) and pathological levels (measured in CVD patients, 10^5 EMVs/ml) (Barteneva *et al.*, 2013). Higher levels of EMVs are believed to affect almost all mechanisms linked to angiogenesis. The same researchers had

previously reported that 10^5 EMVs/ml impaired endothelium–dependent relaxation, which was not observed with 10^4 EMVs/ml (Abid Hussein *et al.*, 2008; Loyer *et al.*, 2014; Gaertner and Massberg, 2016). Another study by Bernal-Mizarchi et al., found that depending on the activation or apoptosis of the cell stimulus, various proteins are expressed (Bernal-Mizrachi *et al.*, 2003; Nouman, 2019) Bernal-Mizrachi has also analysed two subtypes of EMVs (CD51+ and CD31+/CD42-) in patients with CAD and have stated that CD31+/CD42- EMVs were expressed most often in unstable angina and acute events of MI and CD51+ EMVs were reported in comparable quantity together in acute and chronic events of stable angina (Bernal-Mizrachi *et al.*, 2003; Barteneva *et al.*, 2013). Furthermore, another study showed the presence of CD144+ EMVs in circulation, with increased levels being observed in patients with diabetes mellitus and coronary disease including atherosclerosis (Barteneva *et al.*, 2013). Therefore, CD144+ EMVs can be an indicator for analysing atherosclerosis via EC dysfunction (Koga *et al.*, 2005). This may explain why EMVs may be suitable as an early marker of vascular dysfunction (França *et al.*, 2015).
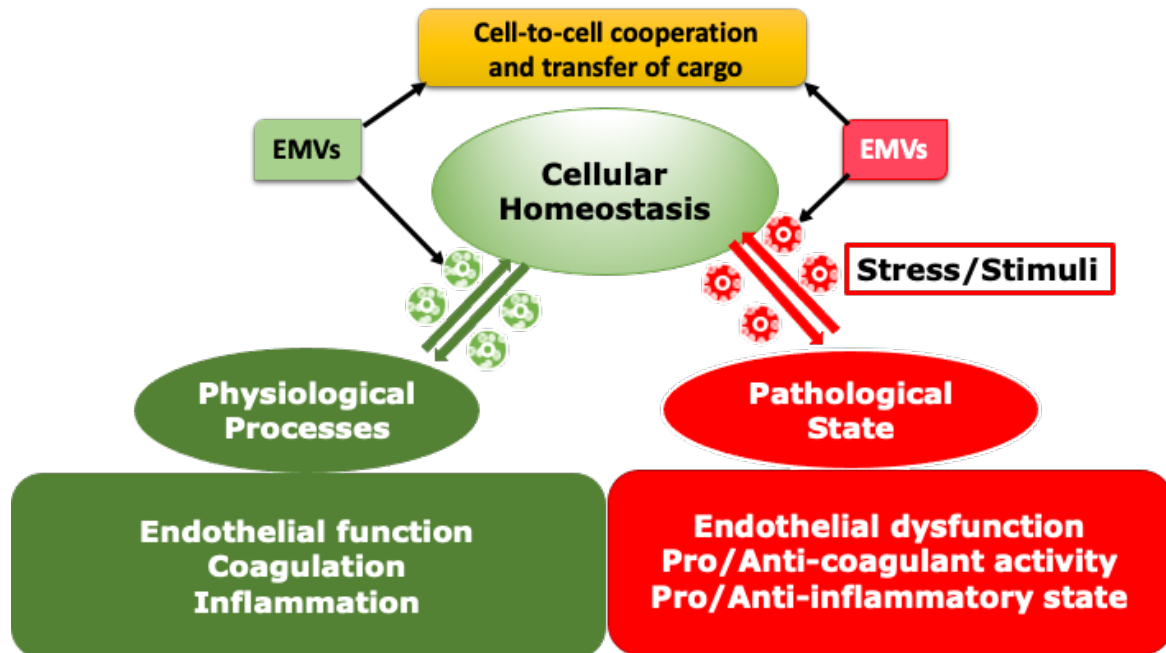
Figure 1.17: Proposed representation of endothelial microvesicles (EMVs) role in cardiovascular health and disease. *ECs secreted EMVs contribute to the regulation of physiological processes and under abnormal conditions, these cells secrete EMVs that differ in number, composition and function resulting in endothelial dysfunction contributing to cardiovascular diseases (CVDs).*

1.4.9. Microvesicles and Membrane Lipids

Characterisation of MV-surfaces has been commonly achieved by analysing membrane-surface-proteins, which lead to signaling function of MVs. In contrast, lipid signalling mediators are the least investigated of the biochemical components of EVs despite being essential precursors and mediators of several signalling pathways (Chen et al., 2020). The importance of the lipid composition is emphasised by the fact that the smallest EVs are ~30 nm in diameter, and with the average bilayer ~5 nm thick this ensures that 60% of its volume is occupied by the encapsulating bilayer (Kreimer et al., 2015; Chen et al., 2020). In contrast to the extended plasma membrane, the formation of MVs demands the creation of a bilayer with a high degree of curvature (Ratajczak and Ratajczak, 2017; Record et al., 2018). In Figure 1.18 A, the lipid formation of MVs is presented according to the experiments of Baker and colleagues. Their analyses demonstrated that most of the lipids in MVs are SM and PC (Baker *et al.*, 2000). These MVs also display a prominent exposure of PS and PE (Abid Hussein *et al.*, 2008; Muralidharan-Chari *et al.*, 2009). However, if MVs are collected from the synovial fluid of inflamed joints (i.e., MVs from lymphocytes, macrophages and monocytes), the membrane composition has a greater variety of composition, as displayed in Figure 1.18 B. The source of MVs in inflamed joints remains unknown because the majority of inflammatory immune cells, because macrophages, lymphocytes and neutrophils as well as ECs can secrete MVs upon inflammatory activation (Leitinger, 2003). Furthermore, it was revealed that the membrane composition of MVs correlate with the membrane composition of parent cell. The phospholipid of MVs membrane correlates strongly with the cell type and the stimulus leading to the budding and the release of the MV (Simak and Gelderman, 2006). This demonstrates the importance of lipids regulation of cells via MVs. This may be due to the lipid composition being a reflection of the MV or regions of the MV enriched in particular types of phospholipids.
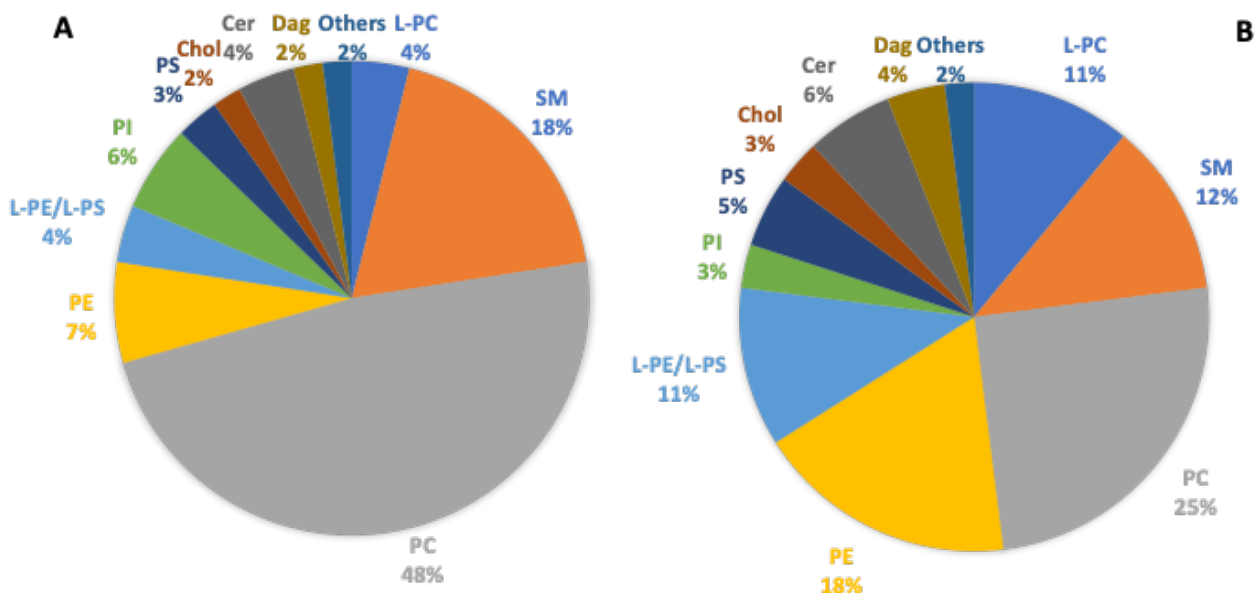
Figure 1.18: Lipid composition of microvesicle (MV) membrane bilayer. *A The composition of the lipids which can be found in the bilayer of MV shed by platelets following activation. B Showing a different composition of MV lipid bilayer found in the synovial fluid of an inflamed joint in comparison to MVs of activated platelets. The data are expressed as weight percent of total phospholipid. Lysphosphatidylcholine (LPC), Sphingomyelin (SM), Phosphatidylcholine (PC), Phosphatidylethanolamine (PE), Lysophosphatidylethanolamine (LPE), Phosphatidylinositol (PI), Phosphatidylserine (PS), Cholesterol (Chol), Ceramide (Cer), Diglyceride (Dag) (Frey and Gaipl, 2010).*

Previously, it has been reported that cell derived MVs collected from venous blood of healthy individuals contained a higher PC and SM, lower PS, PE and PI and small quantities of lysophospholipids LPC, LPE and LPS (Narváez-Rivas and Zhang, 2016; Suárez-García *et al.*, 2017). Those outcomes possibly were influenced by residual plasma present in those preparations. Plasma contains primarily PC and some SM (Simak and Gelderman, 2006; Pérez-Casal *et al.*, 2009). Following subtraction of these phospholipids, the relative contributions of the other phospholipids rises, showing similar levels as data on MVs made *in vitro* (Abid Hussein *et al.*, 2008). Noteworthy that other studies reported were on total plasma MV preparations, with PMVs being the considerable majority, however, not the single component, for example, EMVs were also present. Therefore, the exact lipid composition of released MV is dependent upon the type of parent cell from which it was released and certain pathophysiological and physiological processes that can alter membranes lipid

42

composition (Simak and Gelderman, 2006). Furthermore, stimulated PMVs with collagen contained less PC and more SPM, PS and PE. The lipid composition was different to MVs that were isolated from synovial fluid of inflamed joints (Leitinger, 2003; Simak and Gelderman, 2006). These MVs contained lower PC, higher PE and very high quantities of lysophospholipids in comparison to MVs of healthy subjects (Mori *et al.*, 2003; Simak and Gelderman, 2006). The quantities of lysophospholipids can be explained by the high concentrations of secretory phospholipase A2 (sPLA2) in the synovial compartment, which can hydrolyse the sn-2 ester bond of phospholipids on the MV surface. This would also influence curvature as the chains are then smaller. Noteworthy, These MVs were derived mainly from leukocytes and only to a small extent from platelets and erythrocytes (Heemskerk, Bevers and Lindhout, 2002).

EMVs in healthy participants have shown to correspond with the serum triglyceride concentration, proposing that EMVs may reflect endothelial dysfunction or injury. Moreover, studies revealed that EMV from TNF-α treated ECs expose TF and trigger thrombin generation *in vitro*. More interestingly, however is that such EMV become enriched in both PS and PE and trigger thrombus formation *in vivo* by a TF-initiated pathway (Biró *et al.*, 2003; Abid Hussein *et al.*, 2008). Moreover, another study presented that TF exposed by EMV from activated ECs is responsible for the coagulant activity *in vitro* and *in vivo* (Angelillo-Scherrer, 2012). Therefore, phospholipids have a role in the coagulation cascade, for instance under stimulating conditions, cells and MVs carrying exposed PS provide a catalytic surface to promote various enzyme complex assemblage of the coagulation cascade (Abid Hussein *et al.*, 2008). Furthermore, activated platelet-derived MVs harbour major membrane glycoproteins such as functional adhesive receptors and therefore pose a procoagulant potential which maybe targeted according to the nature of counter ligands (van Meer, Voelker and Feigenson, 2008). Furthermore, MVs can bind to immobilised or soluble fibrinogen and aggregate with platelets, carrying several types of phospholipids facilitating the signalling process between cells. The procoagulant potential of exposed PS cells or MVs is not restricted to platelet MVs

because MVs from ECs and other blood cells also present PS at their surface (Simak and Gelderman, 2006).

In summary, Phospholipids are important components of cell membranes and of MV membranes. Phospholipids of the endothelial membrane play an important role in the regulation of the membrane physicochemical properties related to fluidity as well as in the membrane activity bound enzymes, in signal transduction and membrane transport molecules. A variety of lipids are found in endothelial membrane. These phospholipids form the lipid bilayer of the membrane and their structure is a key factor in the structure and function of cell membranes.

1.4.10. Microvesicles and microRNAs

MicroRNAs (miRNAs, Figure 1.19) are endogenous short RNA molecules, 18-24 nucleotides in length. They are non-coding RNAs that pair up with complementary sequences in target messenger RNAs (mRNAs) directing these protein-coding transcripts to translational repression or degradation (Shaffer, Schlumpberger and Lader, 2012). It is estimated that more than 60% mRNAs are targeted by at least one miRNA and one mRNA can contain binding sites for multiple miRNAs (Muralidharan-Chari *et al.*, 2010; Bugueno el al, 2020). miRNAs are therefore one of the key regulators of cellular processes. It has been suggested that miRNAs play important roles in regulating nearly all aspects of cell physiology, including cell proliferation, differentiation, migration and apoptosis (Shu et al., 2019).
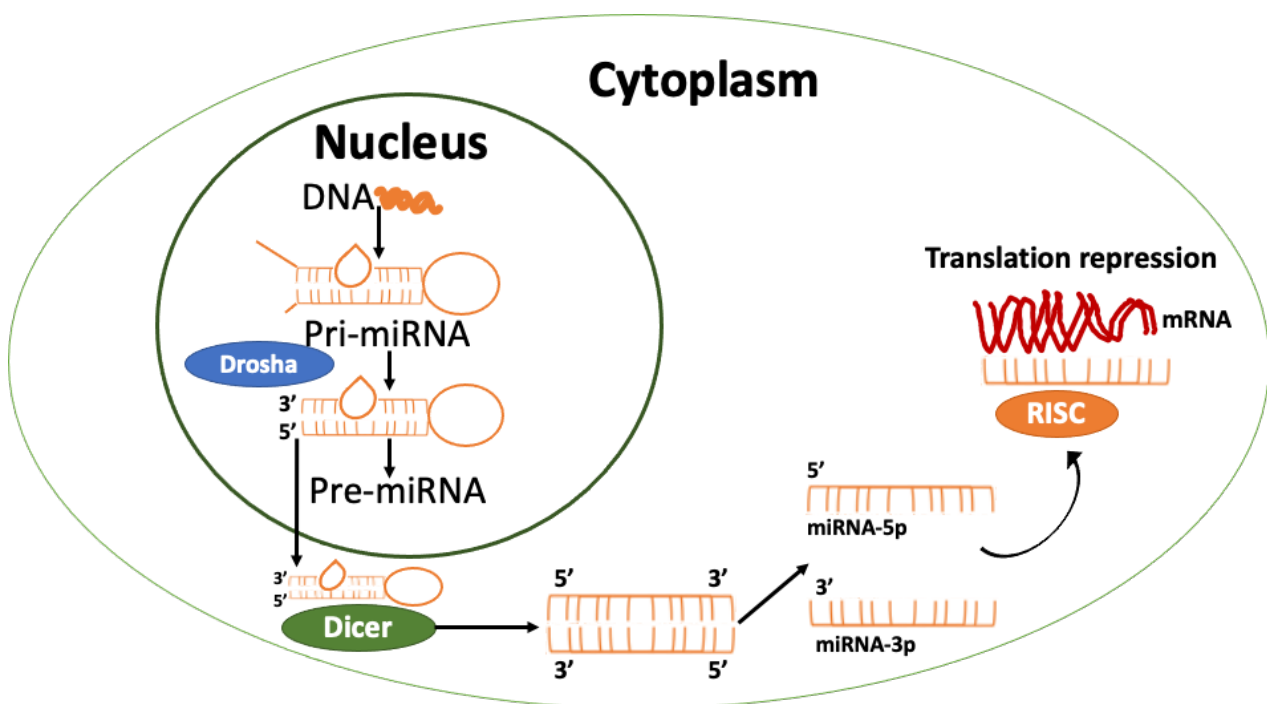
Figure 1.19: miRNA synthesis*. A summary of miRNA formation. A miRNA gene is transcribed to generate pri-miRNA, which is subsequently preprocessed in the nucleus by Dorsha into pre-miRNA. The pre-miRNA is subsequently released in the cytoplasm wherein processed by Dicer to double-stranded miRNA. The mature miRNA molecule, compete for mRNA binding leading to gene silencing. A number of miRNAs are localised intracellularly, however, several are released into the blood circulation packaged into microvesicles (MVs) to deliver information from parent cell to recipient cell.*

In 2008, miRNAs were discovered to be present in blood, detected in platelets and erythrocytes (Mitchell et al., 2008; Xi Chen et al., 2008). Interestingly plasma-based miRNAs are remarkably stable in contrast to synthetic miRNAs added to samples, which degrade rapidly due to the effects of RNase activity in the plasma (Mitchell et al., 2008; Xi Chen et al., 2008). This stability of endogenous miRNAs suggests that plasma miRNAs are protected from RNase activity. One of the ways that plasma-derived miRNAs are protected from degradation is to be packaged into protein or lipid vesicles (Shaffer, Schlumpberger and Lader., 2012; Zeng et al., 2021). Once shed, MVs can travel great distances which enables packaged miRNA to act at distant sites (Muralidharan-Chari et al., 2010; Bugueno el al., 2020). Diehl and colleagues examined miRNA in MVs from human platelets in the setting of CAD. They observed that PMVs contained numerous miRNAs and that these MVs acted as transport vehicles for a large number of miRNAs as well as transfer of molecules from one cell to another via vesicle trafficking (Diehl et al., 2012). These initial studies generated further studies that elucidated the stability of circulating miRNAs, and explained their sources and functions. Since 2008, MVs, exosomes, lipoproteins, and ribonucleoprotein complexes have all been proposed to be carriers of circulating miRNAs (Raimondo et al., 2020).

In summary, MVs have been proposed as a mean for miRNA package and delivery, with intact functionality. Thus, miRNAs carried by MVs may represent one of the possible biological mechanisms by which MVs may alter the functionality of recipient cells. As such MV-miRNAs may provide novel diagnostic biomarkers and therapeutic interventions for a number of CVDs.

1.4.11. Summary of Microvesicles

MVs carry multiple types of cargo, presenting a potent information delivery system between cells. They can influence local cells or can be directed to distant sites. However, the role of MVs in coagulation, inflammation and endothelial dysfunction is still not fully understood. Contradicting reports suggest that MVs have both a beneficial and a harmful role to play in these processes. It may be that a careful balance of MVs of different subtypes is required for haemostasis and when this balance is disturbed by disease, MVs switch to having a pathological role. Furthermore, research on EMVs and thrombus formation is scarce; therefore, the role of EMVs remains unknown. This thesis focuses mainly on the involvement of EMVs in thrombus formation.

1.5. HUVECs and EA.hy926 Models of ECs

1.5.1. HUVECs as a Model of ECs

Primary human umbilical vein endothelial cells (HUVECs) can be defined as cells that are derived from the endothelium of veins from the umbilical cord. They are used as a laboratory model system to study the physiological and pathophysiological mechanisms involved in the development of endothelial dysfunction (Bok et al., 2018). A key part of our knowledge we have today in understanding the EC with blood cells and various mediators comes from *in vitro* experiments with HUVECs (Bok et al., 2018). Therefore, research using HUVEC have been proposed as a suitable model for human studies on human endothelium by containing different cellular markers on HUVEC, i.e., VCAM-1 (CD106), a molecule which is involved in EC adhesion (Onat et al., 2011) (Figure 1.20). While HUVEC model does not characterise all EC types exist in an organism, HUVEC is a well-established *in vitro* model to study vascular endothelium properties and key biological pathways involved in endothelium function (Onat et al., 2011). Also, they are a good arterial cell model as they behave similar to that of arterial cells than venous due to the flow between mother and foetus (Medina-Leyte et al., 2020). In addition, they have been used to investigate the expression of different proteins (Figure 1.20) including anticoagulant surfaces proteins (Medina-Leyte et al., 2020).
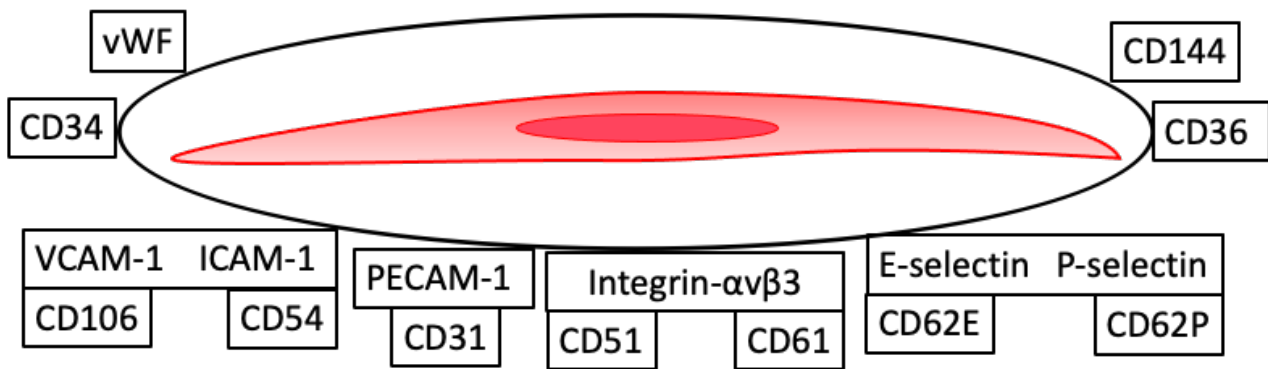
Figure 1.20: Protein markers in human umbilical vein endothelial cells (HUVECs. *Schematic representation of different protein markers which can be identified in HUVECs. These different molecules are involved in cellular activation, proliferation, differentiation, migration, adhesion and apoptosis.*

1.5.2. Properties of HUVECs and EA.hy926

EA.hy926 cell line was produced in 1983 by the hybridisation of epithelial cells A549/8 with HUVECs and since then immortalised EA.hy926 have been widely used (Bouïs et al., 2001; Medina-Leyte et al., 2020). This due to their faster proliferation, extended life span (up to 20 passages) and more stability (Ahn et al., 1995; Bouïs et al., 2001). EA.hy926 have been demonstrated to preserve the general enzymatic characteristics of HUVECs. For instance, the characteristics of endothelin converting enzyme from HUVECs (Bouïs et al., 2001; Medina-Leyte et al., 2020). Moreover, a study investigated leukocyte-EC adhesion interactions using HUVECs and EA.hy926, by comparing the effect of TNF and interleukin-4 (IL-4) on their adhesiveness and expression of VCAM-1, ICAM-1 and E-selectin, demonstrated that HUVECs exhibited increased adhesiveness and adhesion molecule with TNF or IL-4, whilst EA.hy926 cells exhibited these responses with TNF only. Nevertheless, TNF stimulation induced E-selectin expression on HUVECs and EA.hy926 cells (Thornhill et al., 1993). EA.hy926 cells investigated in this study, therefore, demonstrated responses similar to that of HUVECs when stimulated with TNF, however not when stimulated with IL-4 (Ahn et al., 1995; Bok et al., 2018). A study investigated the expression of integrins and adhesive properties of EA.hy926 in comparison to primary HUVECs showed that EA.hy926 retained several endothelial characteristics and can be converted into a proangiogenic phenotype. Nevertheless, they demonstrated a

significantly different proteomic pattern compared to HUVECs and a distinct profile of integrin expression (Baranska et al., 2005). Moreover, a further study comparing gene expression between HUVECs and EA.hy926 cells, demonstrated that most genes which were expressed by untreated HUVCs, were also expressed by untreated EA.hy926 cells, and concluded that EA.hy926 cells retained most of the characteristics of ECs in baseline conditions and following treatment with atorvastatin (Boerma et al., 2006).

1.5.3. Foetal and Adult-derived ECs

HUVECs are suggested to respond differently compared to adult ECs as they are more responsive to inflammatory cytokines compared to HUVECs. For instance, foetal HUVECs are found to express high concentrations of TF following cytokine-stimulation (Brodowski et al., 2017). However, adult ECs are suggested to regulate TF expression more tightly (Andrews et al., 2017). Moreover, studies demonstrated that HUVECs are more receptive to inflammatory cytokines compared to adult saphenous vein ECs, with HUVECs expressing higher concentrations of adhesion molecules in response to TNF-α and IL-1β (Gumina and Su, 2017; Collier, Akinmolayan and Goodall, 2017). Studies assessing the suitability of using EC lines for endothelial/ immune interactions found differences in the ability to respond to cytokines between HUVECs and other immortalised human EC lines i.e., EA.hy926. One of the greatest differences between foetal and adult cells was related to the induction of VCAM-1 and E-selectin in response to TNF-α using primary HUVECs, this induction was indetectable on EA.hy296 (Gumina and Su, 2017). The lack of expression of VCAM-1 in EA.hy926 may reflect the deficiency in migration of lymphocytes and monocytes. However, this disagrees with other studies which suggested that one of the most frequently used and best characterised permanent EC lines is EA.hy926 which present most of the desired primary biological and molecular characteristics of HUVECs, presenting endothelial properties (Thornhill et al., 1993; Andrews et al., 2017).

1.5.4. EC Model-derived EVs

EVs from ECs *in vitro* studies have demonstrated functional activity. For instance, EVs isolated from HUVECs *in vitro* are involved in angiogenesis in physiological and pathophysiological conditions (Mathiesen et al., 2021). EVs play a protective role enhancing repair of the endothelial layer and a number of studies have used HUVEC-derived EVs to explore EC activation, proliferation, migration and adhesion (Tripisciano et al., 2017). These mechanisms play fundamental roles in vascular remodelling during ischemic events (Mathiesen et al., 2021). Moreover, HUVECs have been studied in different stimulated conditions to assess the effect of EVs production, composition and content, as well as EVs communication with other ECs and cell types (Tripisciano et al., 2017). Studies have shown that EVs production increased as well as induced changes in their composition and functionality when HUVECs were exposed to high glucose levels, contributing to the development and progression of endothelial dysfunction (Mathiesen et al., 2021). Also, HUVECs stimulated with TNF-α resulted in changes in EVs protein and miRNA expression. These changes induced functional modifications in the recipient cells, proposing that EVs have an essential mediator role in CV haemostasis (Mathiesen et al., 2021). Moreover, high EV concentrations have been suggested as biomarkers of endothelial dysfunction (Ratajczak and Ratajczak, 2017).

1.5.5. EVs from Quiescent and Proliferating Cells

Quiescence has been characterised by monitoring EVs, a method that offers insight into the distinctive properties of quiescent ECs and may eventually provide a better understanding of EV secretion of quiescent cells (Abdelhamed et al., 2019). Furthermore, it has been proposed that quiescent ECs are distinct from proliferating cells, quiescent ECs downregulating gene expression that involved in cell proliferation as well as acquiring new properties such as differentiation and apoptosis (Abdelhamed et al., 2019; Mathiesen et al., 2021). Levels of EVs as well as VCAM-1 expression were decreased on quiescent ECs compared to proliferating ECs or when cells were

introduced to inflammatory stimuli. This could be due to quiescent ECs being resting and therefore secreting less EVs or expressing VCAM-1. Another hypothesis could be that EVs being protected and remain within quiescent ECs (Mathiesen et al., 2021).

In summary, the forementioned studies highlight the importance of using HUVEC-based models in *in vitro* research. The collection and characterisation of HUVEC-based models have made crucial contributions to vascular biology research and HUVECs have significantly advanced and facilitated the field of CV research. While studies using HUVEC-based models do not replace *in vivo* models, they provide advantages and benefits in in basic research and the proposal of novel therapies and the development of novel diagnostic methods. However, it is important to select the appropriate type of EC, depending on the question being addressed.

1.6. Thrombi Production *in Vitro*

In order to assess changes in thrombus formation, it is important to understand the structure of *in vivo* thrombi and the different methods available for formation *in vitro*. The morphologic and biochemical structure of the thrombus is clearly influenced by different flow conditions inside the blood vessel. This can be demonstrated by the differences between an arterial thrombus formed in high flow and pressure conditions, present in the arteries, compared to a venous thrombus formed in an area of lower pressure (Chandler, 1958; Kawakami et al., 1993). Arterial thrombi display apparent laminations, which are produced by the contrast between dark layers containing red cells and pale areas formed mainly by platelets and fibrin (Dadsetan et al., 2001). They are usually occlusive, greyish, friable and firmly attached to the blood vessel's wall (Chandler, 1958; Beythien et al., 1994). In addition, these thrombi are commonly superimposed on an atherosclerotic lesion and are more difficult to lyse (Sinn et al., 2011). In contrast, venous thrombi, formed in areas of low flow rate, could be mistaken as simple clots, since, like clots, they contain more erythrocytes and fewer platelets than the arterial thrombi, exhibiting reddish colour and not adhering to the blood vessel wall (Amoroso et al., 2001). Thrombi vary in size and shape and usually have an occluding head followed by a tail (Kawakami et al., 1993). In the arterial circulation, the tail builds up in the opposite direction of blood flow, however, in the venous, circulation it develops in the same direction as the flow (Cotran, Kumar and Robbins, 1994). The specific characteristics of arterial and venous thrombi outlined above plus other characteristics influence sensitivity of a thrombus to lysis (Sinn et al., 2011). It is difficult to evaluate accurately the shape and the macroscopic structure of thrombi, since they have irregular external surface, rubbery consistence, and cannot be appropriately visualised inside (Bergen, 2004). The structural integrity of a thrombus formed *in vitro* is affected by the method used to produce the thrombus. Studies that investigate the stability of thrombi to lysis frequently use thrombi obtained *in vitro* by different methods. Thrombi can be produced from whole blood or plasma, using static or dynamic methods, with or without the addition of anticoagulant. The method employed can alter the morphologic structure of the thrombi and consequently its

53

susceptibility to lysis (Robbie et al., 1997). The use of different techniques in different studies limits comparisons between these experiments. In addition, some methods frequently used represent a poor model for human thrombi formed *in vitro,* for instance, static blood clots method which includes drawing approximately 2 ml of venous blood and transferring directly into a glass tube, leaving it upright, undisturbed for 20 -30 min at RT followed by inversion. Following solid clot formation, the intended investigation can be carried out. This method is believed to be a poor model that may not provide useful histological and biochemical information and their results often do not correlate with findings from *in vivo* studies (Oeveren et al, 2012). Therefore, it is important to know the technique used in order to compare the results of different studies and to recognise if it is a method capable of simulating *in vivo* thrombi characteristics.

In addition to the use of clots formed in static systems (Robbie et al., 1997; Amoroso et al., 2001) three types of *in vitro* dynamic models have been used extensively: the Chandler Loop; (Chandler 1958; Robbie et al., 1997), roller pump closed-loop system (Monnik et al., 1999) and a more recent ball valve model (Hemobile) (Romero *et al.*, 2013). The Chandler Loop is an *in vitro* thrombogenicity testing system consisting of a mechanical device which involves a closed tubing partially filled with air and partially with blood. The air remains on top of the vertical rotating circular loop. On rotation, the tubing repetitively circulates through the air-liquid interface, providing geometric and fluid mechanical characteristics similar to *in vivo* circulation (Chandler, 1958). The roller pump closed-loop system contains a length of tubing located inside a curved raceway. This raceway is placed at the travel perimeter of the rollers mounted on the ends of rotating arms. The roller pump causes blood to flow by compressing tubing between the roller and the curved (U-shaped) backing the plate as the roller turns in the raceway (Monnik et al., 1999). The Hemobile consists of a closed tubing filled with liquid (often whole blood) which is forced in a semi-rotating movement. On rotation, devices in the tubing repetitively circulate through the liquid-liquid interface containing no air (van Oeveren, Tielliu and de Hart, 2012) Each model has its advantages and

disadvantages as highlighted in Table 124. Following considerable evaluation of static and dynamic models, the focus will be on the Chandler Loop, because it is considered to be one of the closest models producing thrombi that mimic *in vivo* thrombi.

Table 1.2: Features of different flow models. *The table highlights the main features as well as advantages and disadvantages of each flow model used for thrombus formation and lysis.*

Technique	Advantages	Disadvantages	Citations
Chandler Loop	Efficient, reliable and cost-effective. Could be adjusted to high flow. No mechanical device compressing the tubing. Low platelet adhesion to the tubing. Can be easily loaded with a number of loops at a time.	The continuous blood-air contact may induce leukocyte and platelet aggregation.	(Amoroso, et al, 200; Munch, et al, 2000; Sinn, et al, 2011).
Roller pump closed-loop system	Could be adjusted to high flow. Effective for short circulation times. Cost-effective.	High flow induces haemolysis. Mechanical device compressing the tubing which causes blood damage which reduces sensitivity and does not permit prolonged exposure. High platelet adhesion to the tubing. May cause decreased platelet function.	(Dadsetan, et al, 2001; Oeveren, et al, 2012; Sinn, et al, 2011)
Hemobile ball valve model	Could be adjusted to high flow. No mechanical device compressing the tubing. Can be easily loaded with a number of loops at a time.	High platelet adhesion to the tubing. May cause decreased platelet function.	(Oeveren, et al, 2012; Sinn, et al, 2011).

In 1958, Chandler developed the Chandler Loop thrombogenicity testing device (Figure 3.1) along with defining the definitive features that distinguish a thrombus formed *in vivo* from a clot formed under static conditions (Chandler, 1958). He was the first to propose a technique to produce an *in vitro* thrombus in blood circulation by rotating tubing loops, producing thrombi that mimic those formed under arterial flow with striking morphological and biochemical similarity (Chandler, 1958; van Oeveren, Tielliu and de Hart, 2012). In 1994, Stringer et al, analysed the morphology of Chandler thrombi by light and electron microscopy and found a similar polarised distribution of platelets and erythrocytes to an in arterial thrombi formed *in vivo* (Stringer *et al.*, 1994). In 1997, Robbie et al., performed a detailed microscopic and immunohistochemistry comparison between static blood clots prepared in a test tube, thrombi formed in the Chandler Loop circulation and human venous thrombi formed *in vivo* (Robbie *et al.*, 1997). The Chandler thrombi presented a defined and compact structure, separated in two portions: a dense head of platelets surrounded by erythrocytes, leucocytes and fibrin, and a tail composed of fibrin. They showed very similar morphology to human thrombi formed *in vivo*, in contrast to static clots that lacked defined structure and had a homogeneous distribution of erythrocytes and fibrin. In the immunohistochemistry analysis the authors further demonstrated that thrombi formed in Chandler Loop mimic human arterial thrombi in structure and content and distribution of plasminogen activator inhibitor-1 (PAI-1) which is a serine protein inhibitor found at elevated levels in thrombosis and atherosclerosis (Robbie *et al.*, 1997). The importance of PAI-1 is that it has a profound effect in the resistance of thrombus to lysis. Robbie et al., showed that whole blood clots prepared under static conditions are a poor model for human thrombi formed *in vivo*, as the content of PAI-1 was around 100 times lower in static clots than *in vivo* thrombi, which explains the greater susceptibility to lysis of the static clots (Mutch *et al.*, 2003). However, the PAI-1 content increased significantly in Chandler thrombi, reaching levels comparable with those *in vivo* thrombi (Mutch et al., 2007). The favourable comparison of Chandler thrombi with *in vivo* thrombi has continued with comparison of thrombus lysis (Mutch et al., 2003; Mutch et al., 2007; Mutch et al., 2008). Robbie et al. concluded that Chandler's method provides an appropriate

model for the study of thrombolysis, in contrast to static methods and offered the best model to simulate *in vivo* thrombi both structurally and in terms of PAI-1 content (Robbie et al., 1997; Mutch et al., 2003).

These studies confer a degree of validity to the Chandler Loop method. The design of the Chandler Loop produces thrombi similar to *in vivo* thrombi due to the geometric and fluid mechanical characteristics. The tubing loop alignment offers coiled flow, with a curved axial velocity profile and secondary flow patterns, comparable to that observed in physiological arterial curvatures and bifurcation which have a major impact on the haemodynamics and localisation of thrombi and atherosclerotic lesions *in vivo* (Gardner 1974; Glagov et al., 1988; Sinn et al., 2011). The Chandler method therefore is an appropriate system to study thrombus formation, which enhances its physiological relevance to humans in contrast to static blood clot, reasserting its suitability for flow investigations, which has also been confirmed by other researchers (Gaamangwe, 2014). In addition, Gardner presents a comprehensive study of the fluid mechanics of a Chandler Loop, including details of the menisci behaviour, a prediction of the fluid velocity profile and stress field and an estimate of the height difference between the two free surfaces as a function of the rotation rate (Gardner, 1984). The wall shear stress (WSS) of the Chandler Loop has been converted using the Newtonian relation $\tau = M\Upsilon$, where $\tau = M\Upsilon$, where τ is the fluid shear stress, Υ is the shear rate of the fluid and M is blood dynamic viscosity. Hence it becomes $\tau\omega = 2\pi RO\omega m/15R$. WSS for this model has been previously defined by Gardner (Gardner 1984; Gaamangwe, Peterson and Gorbet, 2014).

The tubing is partially filled with blood to the desired volume ratio, that is, the volume of working blood to the total tubing volume, with the remainder of the tubing filled with air. During operation, a tubing loop on a rotating cradle is rotated about the centre of the torus in a wheel-like motion in a vertical or near vertical plane (Touma *et al.*, 2014). The viscosity and surface tension of the blood causes the meniscus at the air-blood interface on one side of the tube to be elevated with respect to the meniscus on the other side, which establishes a driving toroidal pressure gradient and results in flow of the blood in the direction opposite to the tubing rotation. The moving blood causes a fluid

stress field that, in turn, impacts the suspended cells (Gardner, 1984). By stopping the rotating process at various times, it can be shown that the formation of these artificial thrombi occurs in three stages: (I) small, roughly spherical bodies of the order of 30μm in diameter are formed: (Yau, Teoh and Verma, 2015) each of these consists of a central mass of aggregated platelets surrounded by polymophonuclear leukocytes and monocytes but not lymphocytes or erythrocytes (Wohner, 2008) (II) these bodies coalesce to form a loose coralline structure (the "whitehead"); (III) in the interstices of the "whitehead", around it and extending away from it in the direction in which the tubing travels relative to the blood, a "red tail" forms consisting of fibrin, erythrocytes and lymphocytes (De Caterina *et al.*, 2013). Therefore, the loop configuration provides curved flow, with a skewed axial velocity profile and secondary flow patterns, similar to that observed in physiological arterial curvatures and bifurcations (Gardner 1983; Oeveren, et al, 2012).

The Chandler Loop is an fascinating platform in that it is simple design, construction and utilisation. The tuning loop can be rotated at various speeds for extended periods of time and requires relatively small samples of the blood or other working fluid under investigation. It has been employed in a variety of studies, including work on heparin surface coatings, stents, monocyte activation, heparin surface coatings, monocyte activation, and thrombus formation, lysis and dissolution, to name a few (Chandler, 1958; Mutch *et al.*, 2008; Sinn, et al., 2011). In the present study, the Chandler experimental system will be used to produce *in vitro* thrombi physiologically relevant to human thrombi.

In summary, there are currently a number of *in vitro* models to investigate the complex mechanisms regulating thrombus formation, however, the Chandler Loop have proved to be an attractive device that is simple design, construction and utilisation. The Chandler Loop device will be used in this thesis to produce *in vitro* thrombi physiologically relevant to human thrombi.

1.7. Thesis Hypothesis and Aims

1.7.1. Global Thesis Hypothesis

EMVs will promote thrombus formation.

1.7.2. Global Thesis Aim

The aim of this research is to better understand the role of exogenous EMVs in thrombus formation and inflammation.

1.7.2.1. Specific Thesis Aims:

- To develop a technology that reproducibly produces artificial thrombi that resemble *in vivo* thrombi.

- To determine whether exogenous EMVs alter thrombus formation and to explore the mechanism by which this occurs

- To characterise the lipid composition and understand the impact this may have on the formation of the EMVs and subsequently signalling events underpinning haemostasis.

- To ascertain whether TNF-α stimulation of the cells influences the composition and structure of the parent membrane.

- To establish whether EMVs carry miRNAs that potentially have a role in signalling events underpinning haemostasis.

These aims are summarised in schematically in Figure 1.21.
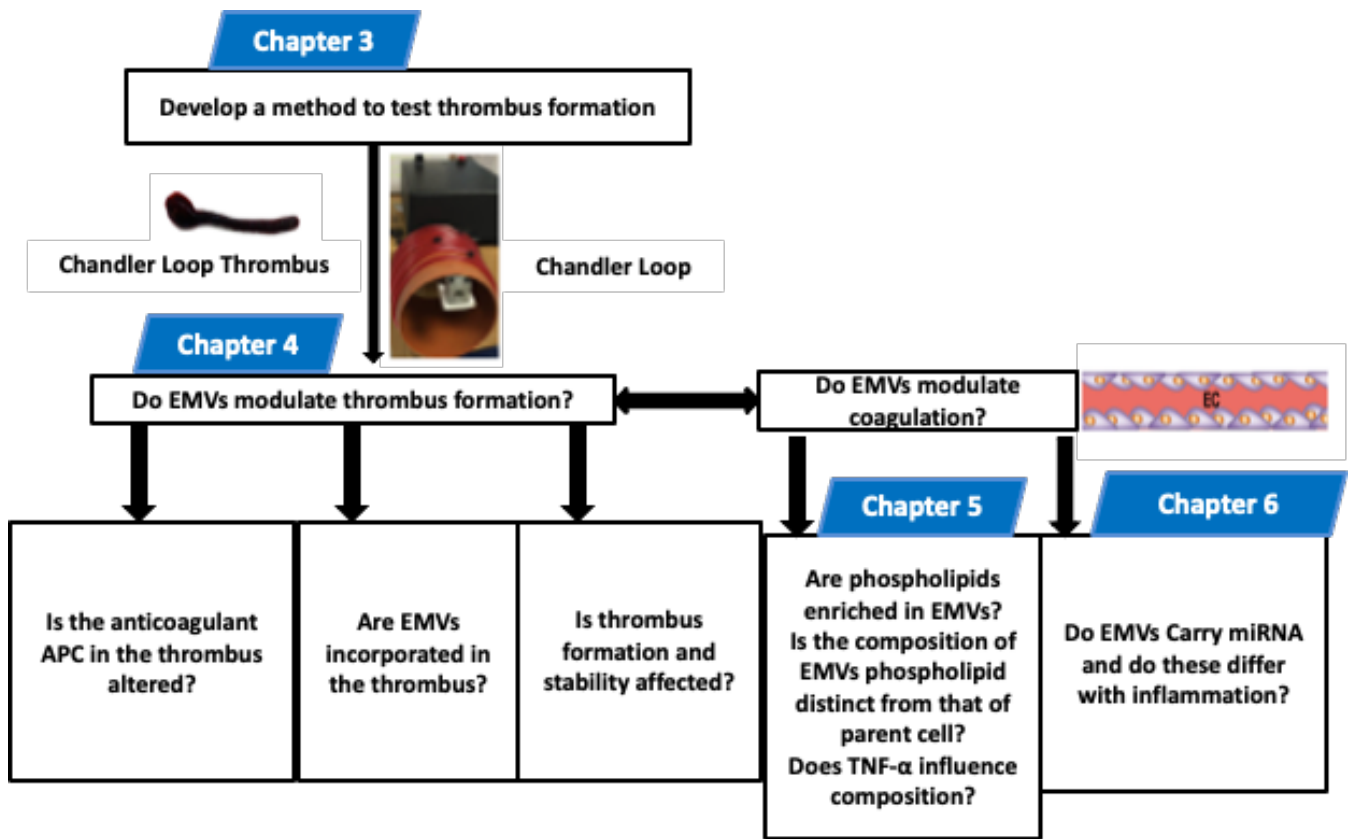
Figure 1.21: Thesis workflow diagram. *Investigations of each chapter are highlighted. Chapter 3 involves development of the Chandler Loop method to test thrombus formation. Chapter 4 investigates the role of EMVs in thrombus formation. Chapter 5 explores the role of EMV-phospholipids in normal and inflamed conditions. Chapter 6 explores the role of EMV-miRNAs in normal and inflamed conditions.*

Chapter 2: General Methods

2.1. Ethical Approval

Ethical approval for this project was obtained from the University of Southampton and local research ethics committees.

2.1.1. Ethics and Funding

This project required the following ethics approvals:

University of Southampton (Faculty of Medicine), ethics and research governance online (ERGO). Ethics study number: 12683.

South West – Cornwall and Plymouth Research Ethics Committee (Appendix 8.1).

This project is funded by The Gerald Kerkut Charitable Trust.

2.1.2. Participant Recruitment and Blood Collection

Males and females were recruited for *in vitro* experiments of this PhD. Participation in all studies was entirely voluntary and participants were given participant information sheet (Appendix 8.2) and informed about risks and procedures of the experiments, as well as were encouraged to ask questions regarding the respective studies. A self-completed health questionnaire (Appendix 8.3) was completed by all participants and verbal and written consent expressing interest in participating in the research was obtained prior to commencing of study (Appendix 8.4). Participants details and baseline parameters were recorded (Table 2.1 and Appendix 8.5). Following consent, an experienced phlebotomist applied tourniquet to the participant's upper arm after thoroughly cleaning the skin with an alcohol wipe. A 21-gauge needle was gently inserted in mainly the median cubital and/or cephalic veins. Blood (~30 ml) was then collected into trisodium citrate 0.106mol/L tubes at a ratio of 9 parts blood and 1 part anticoagulant. Blood samples were then immediately transported to the laboratory in approved biological containers. Experiments were conducted within 10 minutes following blood collection at room temperature (RT).

Table 2.1: Participant details and baseline parameters. For this PhD project, participants were asked to answer general health questions as well as study related health questions, particularly focusing on factors that may affect the results.

Number of participants from whom blood samples were collected	50
Age (years)	Mean: 24 Range: 18 – 35
Ethnicity	95% Caucasian, 5% other
Gender ratio	Male 53% Female 48%
Geographic area	South East/ South West of United Kingdom
Smoking status	100% non-smokers
Educational level	BSc, MSc and PhD
Medication	Excluded if on NSAIDs, anticoagulants, anti-inflammatory or antiplatelet medication.
Presence of infection, cardiovascular, diabetes, haematological disorders, raised cholesterol, allergies	Excluded if they had signs of an infection, or diagnosed CVD, diabetes, haematological disorders, hypercholesterolemia, allergies, pregnancy or breast-feeding

2.2. Thrombus Formation *in vitro*

Citrated whole blood (900µl) was re-calcified with a final concentration of 0.25mM $CaCl_2$ (50µl) to reverse anticoagulation and to permit blood coagulation to occur. The re-calcified blood was placed in low toxic polyvinyl chloride (PVC) tubing (3.0mm internal, 4.2mm external diameter) (VWR, UK product number 228-0106). Tubes were then sealed immediately to form a closed loop and rotated at 30 rpm for 90 minutes, where a chamber of air remained on top of a vertical rotating circular loop and provided for movement of blood during rotation. Tubes were then manually opened, tilted and thrombi were carefully detached (slid out) from the connecting part of the tubing. There was one minute between each loop being filled and placed on the Chandler Loop equipment and one minute between each loop being removed. Thrombi were then placed carefully in 0.9%(w/v) NaCl and the morphology of thrombi observed (head and tail). Each thrombus was then measured individually in terms of weight and length of both head and tail using weighing balance and a ruler. The process of thrombi formation in vitro is summarised in Figure 2.1.
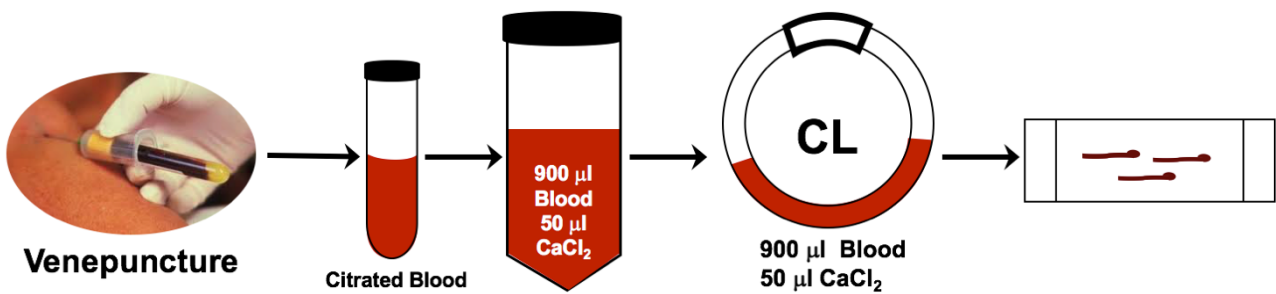
Figure 2.1: The process of thrombi production. *30 ml of blood is drawn from healthy subjects after providing informed written consent into an 8.2 ml vacutainer containing 0.106 ml/L sodium citrate solution. Blood was then transferred into a conical tube and mixed with $CaCl_2$ before was transferred into the tubing and the loops were closed before placed on the Chandler Loop machine. After 90 minutes rotation the loops contained a thrombus consisting of a head and tail.*

2.3. Cell Culture

All cell culture work was carried out in a class II safety cabinet under restrict sterile conditions.

2.3.1. HUVECs

Cell source and basic culture method: A standard method to investigate human endothelial responses *in vitro* is through the cultured of HUVECs. Commercially available primary HUVECs were used in this thesis. 1 vial (10^6 cells) cryopreserved HUVECs [(ThermoFisher, UK, product number: C0035C), passage 5)] were resurrected from liquid nitrogen (-196°C). Cells thawed at 37°C were transferred to growth medium which was made using 100ml M199 [(medium 199), (Sigma Aldrich, UK, product number: M2154), supplemented with 1ml (200μg/ml) EC growth supplement (ECGS) from bovine neural tissue (Sigma Aldrich, UK, product number: E9640), 1 vial glut/pen/strep [(200mM glutamine, 10,000 U/ml penicillin, 10mg/ml streptomycin), (Life Technologies, UK, product number: 10378)], 1ml heparin [(180 USP units/ml), (Sigma Aldrich, UK, product number: H3393)], and 20% heat inactivated foetal bovine serum (FBS), (Sigma Aldrich, UK, product number: F2442). Cells were grown in an incubator at 37°C, 5% CO_2 and fed every 48 hours by replacing old growth medium with fresh growth medium. The removed medium was stored at 4°C for subsequent EMVs isolation as described in Section 2.4.

Passage of primary HUVECs: Cells were checked under phase contrast microscope for confluency and infection every 48 hours. Cells were permitted to grow until they reached approximately 90% confluency and then passaged. Growth medium was removed from the flask and replaced with 10 ml (0.25%) of pre-warmed trypsin-ethylenediaminetetra-acetic (EDTA) solution (Sigma Aldrich, UK, product number: T4299). Flasks were then incubated at 37°C, 5% CO_2 for 5 minutes for cells to detach from the flask's surface. Then 20 ml of growth medium was added to the flask to inhibit the trypsin response and mixed well. Then 15 ml was transferred into a new 0.1% gelatin-coated T75 flask (Sarstedt, UK, product number: 833911), leaving 15 ml in the same flask. Both flasks were then returned to incubator (37°C, 5% CO_2). Each flask then had growth medium replaced every 48 hours.

Cryopreservation of HUVECs for storage: Cells were checked under phase contrast microscope for confluency and infection. After cells reached approximately 90% confluency, they were passaged as describe above, then 20ml of growth medium was added to the flask, mixed well, and transferred into 50ml conical tube and centrifuged at 2,000xg for 10 minutes at RT. The supernatant was discarded, and replaced with 4ml of growth medium, and cold 10% dimethyl sulfoxide (DMSO (Sigma Aldrich, UK, product number: D4540). Cells were distributed equally in new 1ml vials, placed at 4°C then transferred to -20°C for approximately 4 hours respectively then were stored at -80°C until further experiments or analysis.

2.3.2. Immortalised Endothelial EA.hy926

Cell source and basic culture method: 1 vial (10^6 cells) immortalised endothelial EA.hy926 [(ATCC, UK, product number CRL-2922 (passage 3)] were resurrected from liquid nitrogen (-196 °C). Cells thawed at 37°C were transferred to a 0.1% gelatine-coated T75 flask (Sarstedt, UK, product number 833911) along with 20 ml of cells growth medium using sterilised filter (Sigma-Aldrich, UK, product number: SLLG025SS). Growth medium was prepared using 500 ml Dulbecco's Modified Eagle's Medium (DMEM) (Sigma Aldrich, UK, product number: D5546), glutamine/penicillin/streptomycin [(200mM glutamine, 10,000 U/ml penicillin, 10 mg/ml streptomycin), 1 vial of HAT (100 μM hypoxanthine, 0.4μM aminopterin, 16μM thymidine)] (Sigma Aldrich, UK, product number: H0262) and 20% heat inactivated foetal FBS. Cells were grown in an incubator at 37°C, 5% CO_2 and fed every 48 hours by replacing old medium with fresh growth medium. The removed medium was stored at 4°C for subsequent EMV isolation as described in Section 2.4. Cells were checked under phase contrast microscope for confluency and infection every 48 hours (Figure 2.2).

Passage of EA.hy926 cells: Cells were permitted to grow until they reached approximately 90% confluency and then passaged. Growth medium was removed from the flask and replaced with 10 ml (0.25%) of trypsin EDTA solution. Flasks were then incubated at 37°C, 5% CO_2 for 5 minutes for

66

cells to detach from the flask's surface. Then 20 ml of growth medium was added to the flask to reverse the trypsin response and mixed well. Then 15 ml was transferred into a new 0.1% gelatin-coated T75 flask, leaving 15 ml in the same flask. Both flasks were then returned to incubator (37°C, 5% CO_2). Each flask then had growth medium replaced every 48 hours.
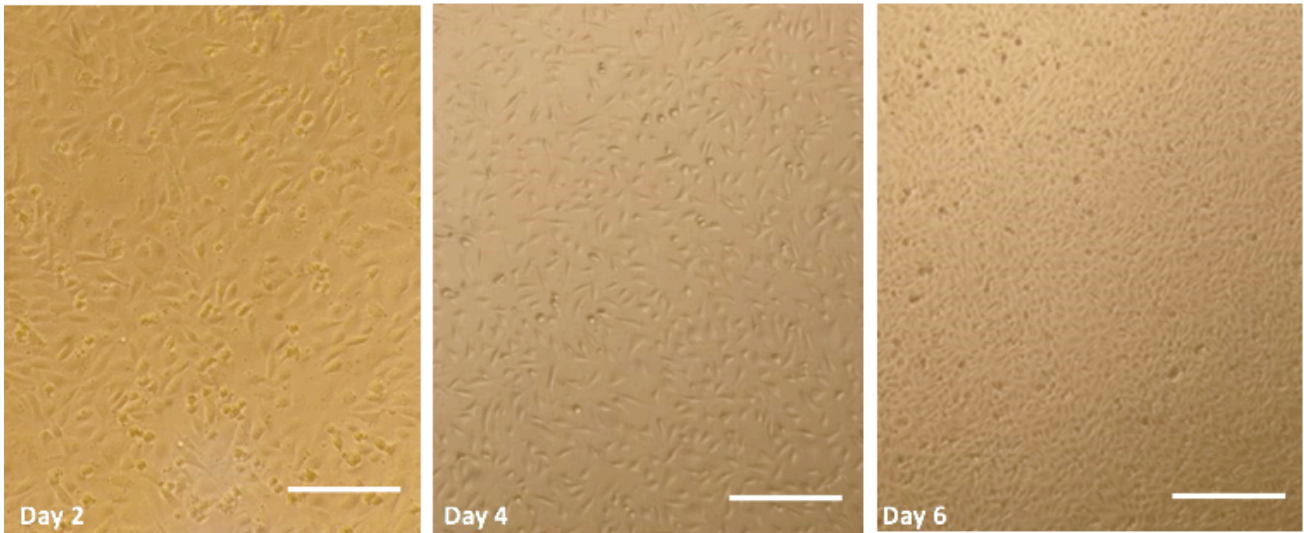
Figure 2.2: Progress of cell culture. *Example images of EA.hy926 cell line taken throughout the cell culture process. Confluency observed under light microscopy in day 2, 4 and 6. Magnification x20. Bar scale 200μm.*

2.4. Harvesting, Storing and Pooling of EMVs

EMVs were produced by cultured ECs, both primary and EA.hy926 cells. EMVs were isolated from growth medium (Figure 2.3). Each time cells were fed (every 48 hours) by replacing old growth medium with fresh growth medium, EMVs were collected. Cell-conditioned medium containing EMVs was collected and centrifuged at 1000xg (4°C) for 5 minutes to remove cells. The supernatant was further centrifuged at 2000 (4°C) for 10 minutes to remove cell debris and large vesicles. The supernatant was transferred into 1.5 ml Eppendorf tubes, leaving pelleted cells and large vesicles at the bottom of the tube. Eppendorf tubes were then centrifuged at 20,000xg for 30 minutes at 4°C to concentrate and pellet EMVs. The top two third of supernatant was discarded and the lower third was retained as it contained concentrated EMVs. EMVs were collected in Eppendorf tubes at 4°C before they were pooled into 50 ml falcon tube. Pooled EMVs were then counted by flow cytometry (10^3/ml). Following counting, EMVs were aliquoted in Eppendorf tubes and stored at -80°C for future experiments.
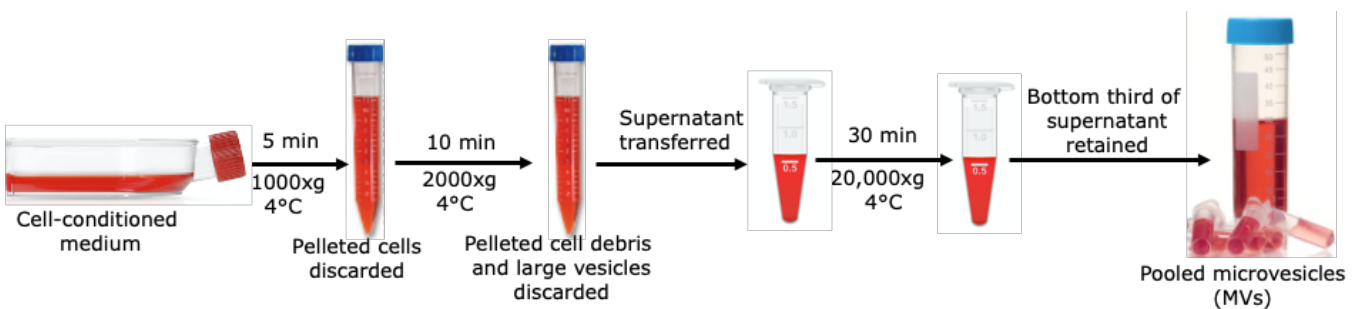
Figure 2.3: Isolation of Endothelial microvesicles (EMVs). *The typical centrifugation steps were used to collect EMVs from conditioned culture media. Number of steps, centrifugal force and times may vary between research groups and biological fluids.*

2.5. TNF-α Cell Stimulation

The confluent cells (90% confluency), subsequently underwent stimulation. TNF-α aliquot (Perotech, UK, product number 300-01A) was defrosted at 37°C water bath and diluted in growth media. The addition of 10ng/ml of TNF-α to stimulate EMV release from HUVECs was used, and the addition of 50ng/ml of TNF-α to stimulate EMV release from EA.hy926. Cells were incubated with TNF-α for 24 hours at 37°C and 5% CO_2.

2.6. Use of Whole-mount Confocal Microscopy of Thrombi to Co-stain MVs with Aleuria Aurantia Lectin (AAL) and CD41

Thrombi were formed as described in Section 2.2. Thrombi were then washed with phosphate buffer saline (PBS) (Sigma Aldrich, UK, product number P4417), (3 times x 5 minutes) fixed in 4% paraformaldehyde solution (PFA) (Qiumigen, UK, 30450002-1) in PBS and left overnight at 4°C. The following day thrombi were taken out of 4°C and washed with PBS (3 times x 5 minutes), then samples were permeabilised and blocked in 1% bovine serum albumin (BSA) (Sigma, UK, product number: P3717) and 1% Triton-X100 (Sigma, UK, product number: 9002-93-1) diluted in PBS to improve the sensitivity by reducing nonspecific binding of antibodies to reaction surfaces and nonspecific binding sites reducing background interference and improving the signal-to-noise ratio. Samples were permeabilised on a rocker for 2 hours at RT. 300 µl/ml FITC-Aleuria Aurantia Lectin (AAL) (Vector Laboratories, UK, product number: B-1395-1) was added to specified tubes and stored overnight at 4°C. On the following day, the solution was removed and the thrombus was rinsed with 1% BSA in PBS each tube for 5 minutes, 3 times. Then PE-conjugated mouse-IgG1 CD41 (BD Biosciences, UK, product number: 561850) was diluted at 1:200 and reconstituted in PBS containing 1% BSA and 1% Triton-X100 to a final concentration of 10 µg/ml was placed in specified tubes and left for 2 hours in the dark at RT on rocker. The thrombus was then washed 3 times with 1% BSA in PBS for 5 minutes. Isotype was used as a negative control using PBS containing 1% Triton-X100 in the absence of anti-CD41 (BD Biosciences, UK, product number: 550617). The tube was rinsed with 1% BSA in PBS 3 times for 5 minutes each time followed by nuclei staining 4′,6-diamidino-2-phenylindole (DAPI 1:500) (ThermoFisher, UK, product number: 62247) for 1 hour at RT. Then the samples were washed 3 times for 20 minutes in 1% BSA in PBS on the rocker. 1%BSA in PBS pipetted out following final washing step and replaced with 300µl/tube 2,2'-thiodiethanol (TDE) (Sigma Aldrich, UK, product number: 166782) clearing solution and samples were cleared using various TDE concentrations (25%, 50%, 75% and - 97%). Following the final clearing step, samples

were left in the final solution (97%) and stored at 4ºC protected from light before being examined by confocal microscopy (Leica Microsystems, Leica TCS-SP5, TCS-SP8 Systems). Following immunostaining, whole-mount TDE – cleared thrombi were placed in glass coverslip bottom chamber slides, covered in 97% TDE and imaged by Leica TCS-SP5 and TCS-SP8 systems confocal laser scanning microscopy running Leica LAS-AF and LAS-X software respectively. Images were captured at 1024 x 1024–pixel resolution with 4-line averaging and appropriate Z-spacing to produce extractable data sets. Images from SP5 were acquired using the following objective lens characteristics; x20 HC PL APO 0.70 NA IMM and x63 HCX PL APO 1.3 NA Glycerol immersion objectives. Furthermore, images from SP8 were acquired using the following objective lens characteristics; x20 HC PL APO CS20.75 NA IMM and x63 HC PL APO CS2 1.3 NA Glycerol immersion objectives. Spectral detection bandwidth windows, laser powers and detector gain sensitivity were adjusted on a sample–by–sample basis to prevent spectral bleed through, with serial imaging applied where required. Detector gains were set to be as sensitive as possible without recording significant signal on these controls and imaging of fully stained samples was observed at those detector gains, or lower gains if the positive staining was bright. Negative controls included: thrombi prepared in the absence of addition EMVs and in the absence of any staining. Fiji Is Just Image J (FIJI), image processing software was used and made qualitative visual-assessments, looked for various MV types as shown by differential antibody and lectin markers binding on fluorescence microscopy (adapted from Professor R. Lewis's laboratory group, University of Southampton).

2.7. Use of Flow Cytometry To Assess Incorporation of EMVs Into The Thrombus

2.7.1. Preparation of Thrombi

Thrombi were prepared in the presence and absence of EMVs as shown in Figure 2.4, and blood/thrombi were collected over a time-course (0 minute, 15 minutes, 30 minutes, 45 minutes, 60 minutes, 75 minutes and 90 minutes). Following collection of blood/blood fragments/thrombi, supernatants were stained using F2N12S dye to identify membranes, following the manufacturer's instructions. F2N12S is dye component of the Violet Ratiometric Membrane Asymmetry Probe/Dead Cell Apoptosis Kit (ThermoFisher, UK, product number: A35137). When excited by a 405nm laser, the F2N12S emits light at 530 and 585 nm.
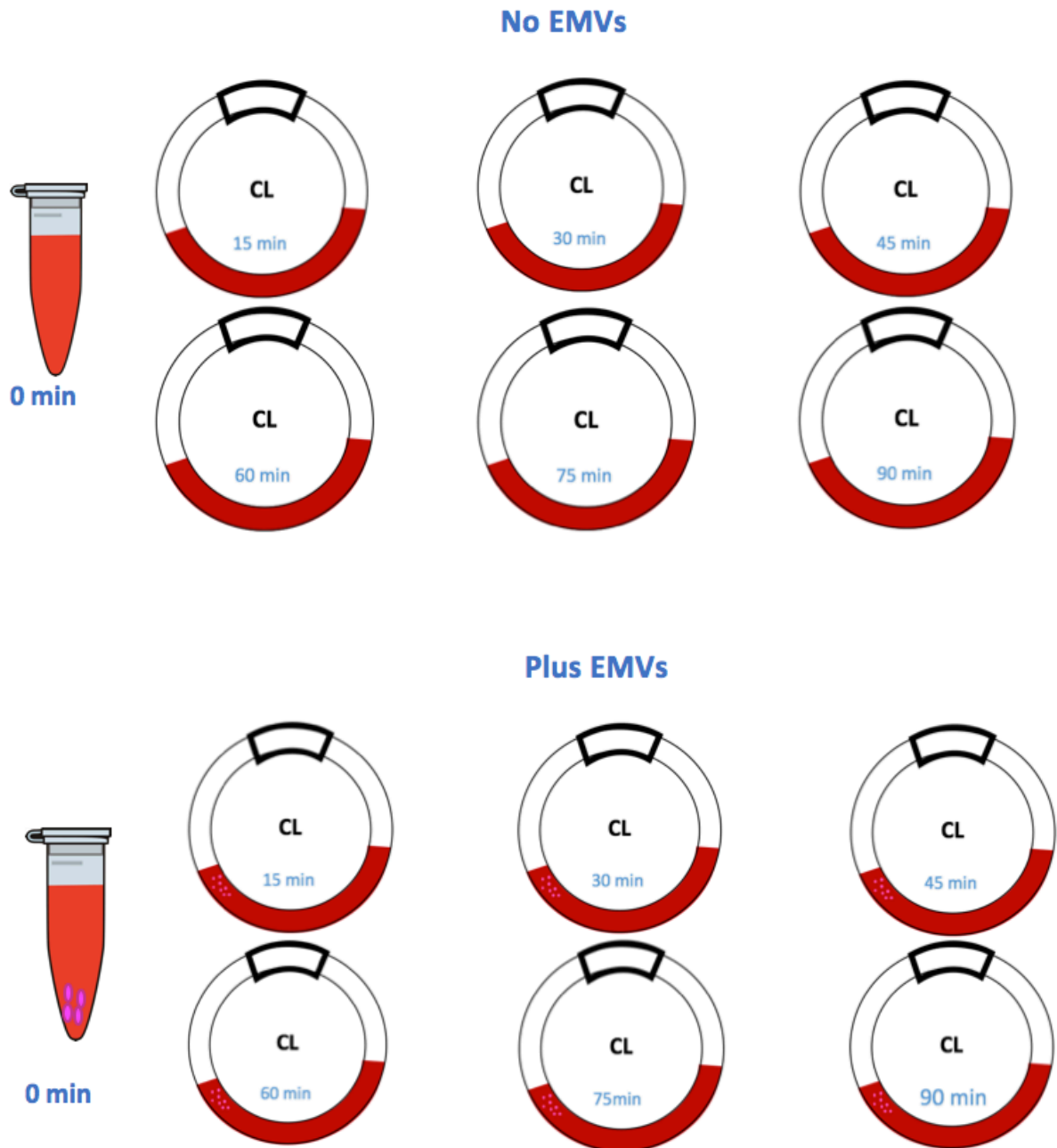
Figure 2.4: Preparation of thrombi in the presence and absence of endothelial microvesicles (EMVs). *Loops used to investigate the effect of adding endothelial microvesicles (EMVs) and allowing thrombi to develop over 0-90 minutes. For each time point, either EMVs (10^3 EMVs/ml) or tissue culture medium (non-EMV control) were added to whole blood before circulating loops on the Chandler Loop apparatus. At the appropriate time point, loops were opened and EMVs in the blood were counted by flow cytometry.*

2.7.2. Identification of EMVs and PMVs by Flow Cytometry

50µl samples were washed in 2ml PBS and concentrated by centrifugation at 20,000xg for 30 minutes. Supernatant was removed and the final volume was 200 µl. Samples were then incubated for 20 minutes on ice in the dark, with panels of antibodies that were used at the manufacturers recommended concentrations. Isotype controls were included (Table 2.2). Panel include IgG1 FITC (BioLegend, UK, product number: 406606), IgG1 PerCP-Cy5.5 (BioLegend, UK, product number: 400929), IgG1 BV711 (BioLegend, UK, product number: 400963), CD31 FITC (BioLegend, UK, product number: 102405), CD105 FITC (BioLegend, UK, product number: 323203), CD106 PerCP-Cy5.5 (BioLegend, UK, product number: 105715), CD41a BV711 (BioLegend, UK, product number: 303729), CD42b BV711 (BioLegend, UK, product number: 303359). F2N12S stock was diluted 1/10 in DMSO was then added to each sample at 1/100 dilution and incubated at RT for 5 minutes, protected from the light.

A single tube contained the violet ratiometric dye (VRD, F2N12S) and CD41/42 and either CD31, CD105 or CD106 (or their isotype controls), allowing identification of the MV membrane and gating to identify either PMVs or EMVs.

Table 2.2: Antibodies and dyes used. *Antibody-fluorochromes or dyes used are highlighted and the reason for including in panel.*

Antibody-fluorochrome or dye	Reason for including in panel
IgG1 FITC, IgG1 PerCP-Cy5.5, IgG1 BV711	Isotype controls
CD41 BV711 CD42 BV711	Identifies platelet microvesicles (PMVs), allowing negative gating to exclude PMVs (important for CD31 especially)
CD31 FITC CD105 FITC CD106 PerCP-Cy5.5	Identifies endothelial microvesicles (EMVs). CD31 is expressed on both PMVs and EMVs and therefore CD31$^+$/CD41a$^+$/42b$^+$ MVs will be PMVs
F2N12S	Detects phospholipid (proxy MV membrane marker) which was included in all panels.

Samples were then analysed on a two-laser dedicated Attune NxT flow cytometer (ThermoFisher, USA), adapted for MV measurement (details restricted due to a confidentiality disclosure agreement). To identify the MVs, samples were gated as shown in Figure 2.5. Bang Beads of known size (0.2μm, 0.5μm, 0.8μm) (Bangs Laboratories Inc, USA, product number: TN303) were analysed and the results used to create Region 1 (R1, quantification gate) from 0.2μm to 0.8μm which allows the identification of particles of MV size. R6 defines the swarm gate, using side scatter to ensure that samples are analysed at a flow rate that is low enough to include only single events are included in the analysis. R16 defines the F2N12S positive events, i.e. all particles with biological membranes. Gates were combined using the Boolean logic AND, specifically R1 AND R6 AND R16.
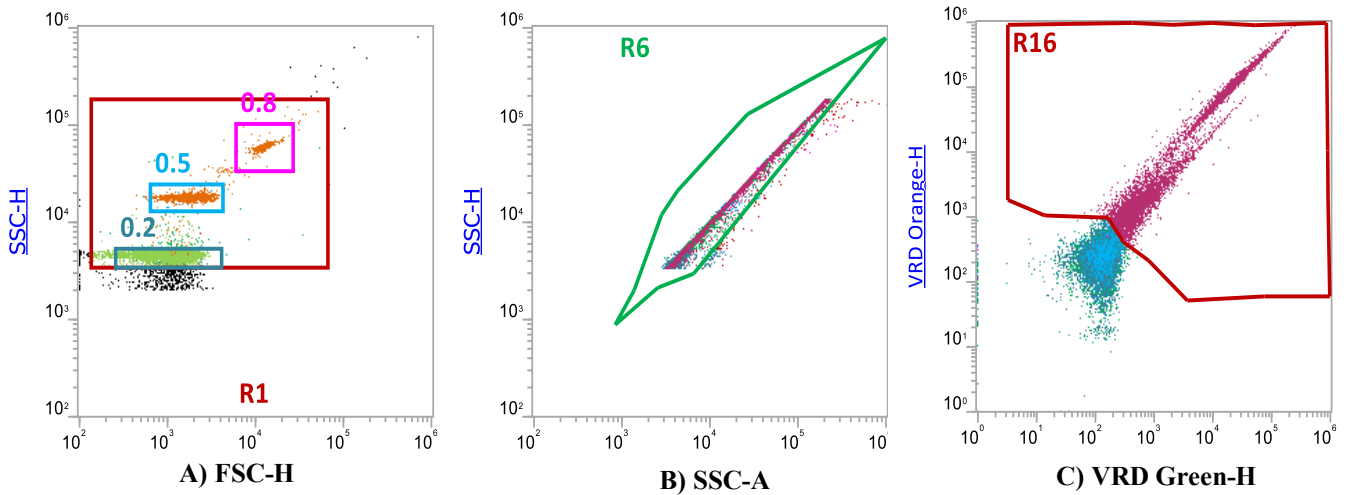
Figure 2.5: Identification of endothelial microvesicles (EMVs). *EMVs identified using (A) Bang Beads (0.2μm, 0.5μm, 0.8μm) to draw size regions for EMV identification. (B) a swarm gate to confirm swarm detection of multiple particles is minimised. (C) Violet ratiometric membrane dye (VRD, F2N12S) to positively discriminate biological signals (R16) from electronic noise.*

The resulting gated particles were analysed using histograms were used to show the percentage of EMVs and PMVs in the population, along with the density of receptor expression, namely the median fluorescence intensity (MFI), using specific fluorochrome-conjugated antibodies. PMV were identified by CD41/42 expression. EMVs were identified as negative for CD41/42 and positive for either CD31/105 or CD106. All staining was compared to isotype specific conjugated controls. Representative examples are shown in Figure 2.6. Concentrations of MVs were calculated using the flow cytometer and adjusted for dilution factor (400μl).
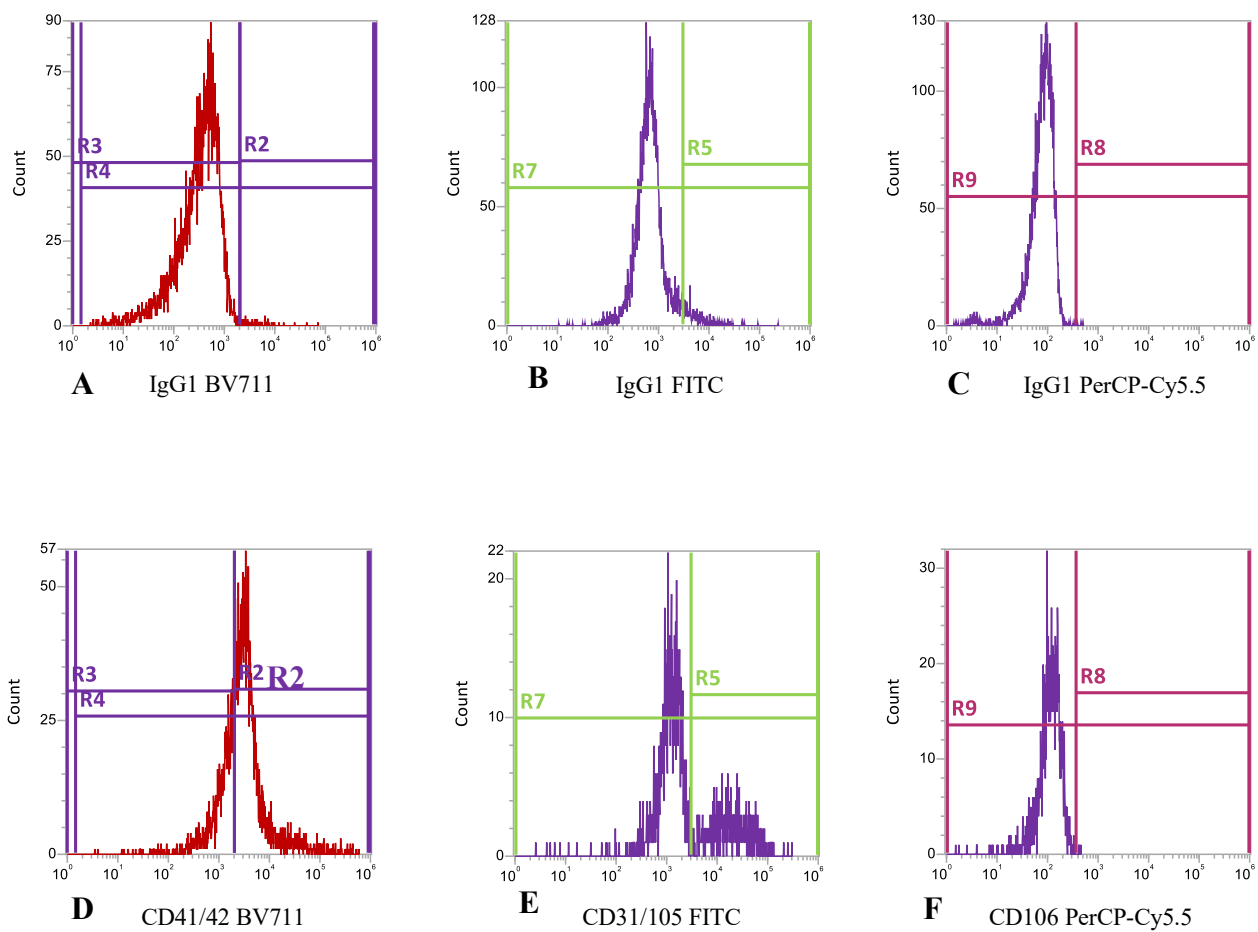
Figure 2.6: Flow cytometry histograms of plasma. *Histograms showing plasma prepared from Chandler Loop at 0 minute. Antibodies used are (a-c) relevant isotype controls, (d) CD41/42-BV711, (e) CD31/105 FITC, (f) CD106 PerCP-Cy5.5.*

2.8. Preparation of Lipids

Membrane lipids of both cells and EMVs were investigated using lipidomic techniques (Chapter 5). However, lipid preparation was required first as described below in Section 2.8.1 and 2.8.2.

2.8.1. Preparation of Cell-Membrane Lipids

HUVECs and E.A.hy926 were cultured (Section 2.3) to extract lipids (20mg) from these cells. First cells were homogenised for 3 minutes and then centrifuged at 1000xg for 5 minutes to breakdown nuclei/unbroken cells, this step was repeated. The resulting suspension was then centrifuged at 10,000xg for 10 minutes to bring down mitochondria. The supernatant was subsequently decanted and further centrifuged at 10,000xg for 10 minutes to bring down remaining membrane fractions. The sample was then resuspended in 25mM hydroxymethyl aminomethane (Tris) solution (pH 7.2) (Sigma-Aldrich, UK, product number: 5567027). Following resuspension in Tris, material was centrifuged at 30,000xg for 10 minutes. Then dispersing 1520mg of dried lipid of pelleted membrane was then packed into a 3.2mm Agilent rotor for ^{31}P-ssNMR analysis.

2.8.2. Preparation of EMV-Lipids

EMVs were collected (Section 2.4) to extract lipids of these vesicles. First EMVs were homogenised for 3 minutes and then centrifuged at 1000xg for 5 minutes to breakdown unbroken EMVs, this step was repeated. The resulting suspension was then centrifuged at 10,000xg for 10 minutes to bring down mitochondria. The supernatant was subsequently decanted and further centrifuged at 10,000xg for 10 minutes to bring down remaining membrane fractions. Sample was then resuspended in 25mM Tris solution (pH 7.2). Following resuspension in Tris, sample was centrifuged at 100,000xg for 10 minutes to collect the pellet (20mg). The pellet was then resuspended in D_2O (Merk, UK, product number: 151882) and pelleted a further time before the dried lipid of pelleted membrane was transferred into a 3.2 Agilent rotor for ^{31}P-ssNMR analysis. Where sample concentration was

required, lyophilisation process was carried out (Section 2.8.3). This was used as a concentration mechanism as well to ensure that protein components remain in the bilayer which could influence lateral segregation.

2.8.3. Lyophilisation of Lipids

Concentration of the EMV samples obtained by centrifugation for NMR analysis. EMV were vacuumed and left to freeze-dry overnight to remove excess water. Following overnight lyophilisation, the dry powder was resuspended in 20μl of D_2O to rehydrate the samples. Samples were then transferred into a 3.2mm rotor. Although, this does not necessarily preserve the phase properties of the sample, the phospholipid composition should remain unchanged.

2.9. Preparation of EMVs miRNAs

All RNA work was completed in a designated RNA workstation. HUVECs were cultured as described in Section 2.3.1. A total of twenty T75 flasks of HUVECs were cultured for the miRNA experiments, 10 of which were treated with TNF-α (Section 2.5) and 10 were cultured untreated. EMVs were collected as described in Section 2.4 and RNA isolation was performed as described in Section 2.9.1.

2.9.1. Total RNA Isolation

Total RNA isolation protocols were conducted according to manufacturers' instructions (Total Exosome RNA and Protein Isolation Kit, Life Technologies, UK, product number: 4478545). Total MV-RNA isolation process is summarised in Figure 2.7. Samples were resuspended and placed in 1 ml (37°C) 2X-denaturing lysis solution in 375 µl 2-mercaptoethanol, mixed thoroughly and incubated on ice for 5 minutes. Two ml of acid:phenol:chloroform was added to each sample to separate the nucleic acids and samples were then mixed well by vortexing for 1 minute. Samples were then centrifuged for 5 minutes at 10,000xg at RT to separate the mixture into aqueous and organic phases. The aqueous phase which contains RNA was carefully removed without disturbing the organic phase which contains proteins and DNA or the interphase which contains DNA and transferred to a fresh tube. The recovered volume was noted. 1.25 volumes 100% ethanol was added to the aqueous phase and mixed thoroughly. For each sample, a spin column was placed into one of the collection tubes. 700µl of the lysate/ethanol mixture was pipetted onto the spin column. As sample volumes were >700µl, the mixture was applied in successive applications to the same spin column. The mixture was then centrifuged at 10,000xg for 15 seconds or until the mixture has passed through the spin column. The supernatant was discarded, and the process was repeated until all the lysate/ ethanol mixture has been passed through the spin column. The collection tubes, containing the RNA, were saved for the washing steps. 700µl RNA wash solution-1 was added to the spin column

and centrifuged at 10,000xg for 15 seconds to remove protein and salt residues through the spin column, discarded the supernatant from the collection tube and replaced the spin column into the same collection tube. This wash step was repeated twice. After discarding the supernatant from the last wash, the spin column was replaced in the same collection tube and centrifuged the assembly at 10,000xg for 1 minute to remove residual proteins from the spin column. The spin column was transferred into a fresh collection tube. 30μl of preheated (95°C) elution solution was applied to the centre of the spin column and centrifuged for 30 seconds to remove residual DNA. The elution process was repeated once more with an addition aliquot of 30μl of elution solution. The elute which contained the isolated RNA (including miRNA) was collected and stored at ≥ -80°C prior to use.
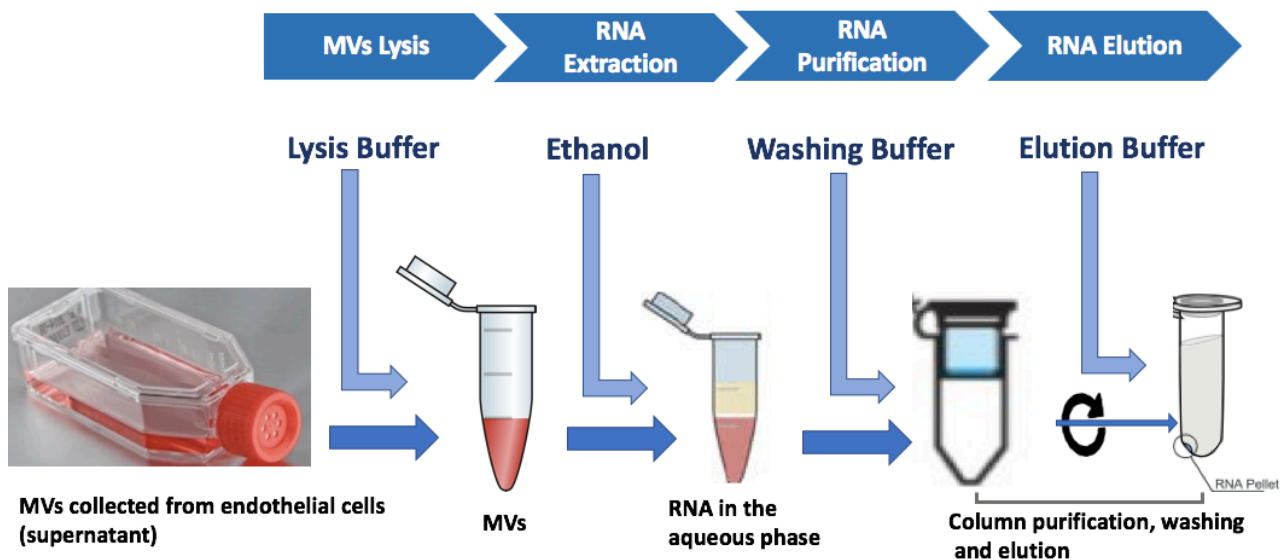
Figure 2.7: MV-RNA Isolation Kit. *The total MV-RNA isolation kit is designed to isolate RNAs from an enriched MV preparation. Resuspended MVs are utilised for organic isolation and purification of total RNA. Maximal yields of ultra-pure RNA are suitable for studies of miRNA processing and function. The isolated RNA is used for next generation sequencing (NGS) to assess miRNA expression.*

2.9.2. Total RNA Quantification

To determine the concentration and purity of total RNA (including miRNA), spectrophotometry (Nanodrop 1000 Spectrophotometer, ThermoFisher, UK, product number: M141300) was performed. Nanodrop software was selected to initialise and nucleic acid mode was selected. The spectrophotometer was initialised by adding 1.5μl of ultrapure water (ThermoFisher, UK, product number: 10977049) the lower optic surface and covering with the upper optic surface. "Initialise" was selected and optical surfaces were wiped clean with RNase decontamination wipes (ThermoFisher, UK, product number: AM9786). 'RNA-40' was selected for measurements. A blank measurement was carried out before the actual sample by loading 1.5μl of RNase free distilled water onto the lower optical surfaces, the upper optical surfaces were lowered and 'blank' was selected, after which the optical surfaces were again wiped clean with RNase decontamination wipes. Then the sample was loaded in the same volume (1.5μl) and the respective cells were activated and labelled. "Measure" was selected that gave the peaks with values representing the quality and quantity of RNA isolated. The Nanodrop calculated the concentration of RNA in the units of ng/μl. The yield of RNA was mostly dependent on the number of EMVs isolated. The purity of RNA was determined by displaying the ratio of optical density (OD) 260/280 and OD 260/230 where 260nm is the peak nucleic acid absorbance and 280nm peak protein absorbance. 230nm is the peak absorbance of peptides, aromatic compounds, phenols, and carbohydrates. OD260/280 values in range of 1.8-2.1 were considered acceptable for RNA integrity number (RIN) analysis indicating low contamination of RNA with protein and for 260/230 values in range of 1.8-2.2 were considered acceptable for RIN indicating low contamination of RNA with compounds that absorb at 230nm (Ibberson et al., 2009; Koufaris 2011). To achieve a more accurate quantification prior to RNA-sequencing, the data from the nanodrop were validated using the qubit fluorometer that uses fluorescent dyes to determine the concentration of the RNA in a sample. All quantification protocols were performed according manufacturers' instructions (Qubit RNA Assay Kits, Life Technologies, UK, product number: Q32852). RNA samples with a volume of ≥ 3μg and concentration of ≥ 50ng/μl were considered

suitable for sequencing (as suggested by Novogene). Samples were prepared in 1.5ml screw-cap DNase-RNase-free microcentrifuge tubes, placed in 50ml tubes, packed in dry ice and placed into a secured biological-sample-box and shipped to Novogene for RNA sequencing (Novogene, China, product number: 17080430).

2.9.3. Small RNA Sequencing

Once samples were received by Novogene, RNA integrity was assessed using an Agilent 2100 Bioanalyzer (Agilent, USA, product number: G2939BA) and measured as RNA Integrity Numbers (RINs). Samples with RIN values $\geq$ 7.0 (as suggested by Novogene and typically used for NGS analysis (Koufaris, 2011) were considered acceptable to small RNA library construction for miRNA sequencing analysis. Of the 20 received samples, 3 had poor RINs (1 control and 2 TNF-α treated) (Appendix 8.8.1).

2.9.4. Library Preparation and Construction

RNA-library preparation was performed using Illumina Small-RNA Library Preparation Kit, according to manufacturers' instructions (Illumina, USA, product number: 63610). Quality control was conducted on each step of the procedure (Figure 2.8) to guarantee the reliability of the data.
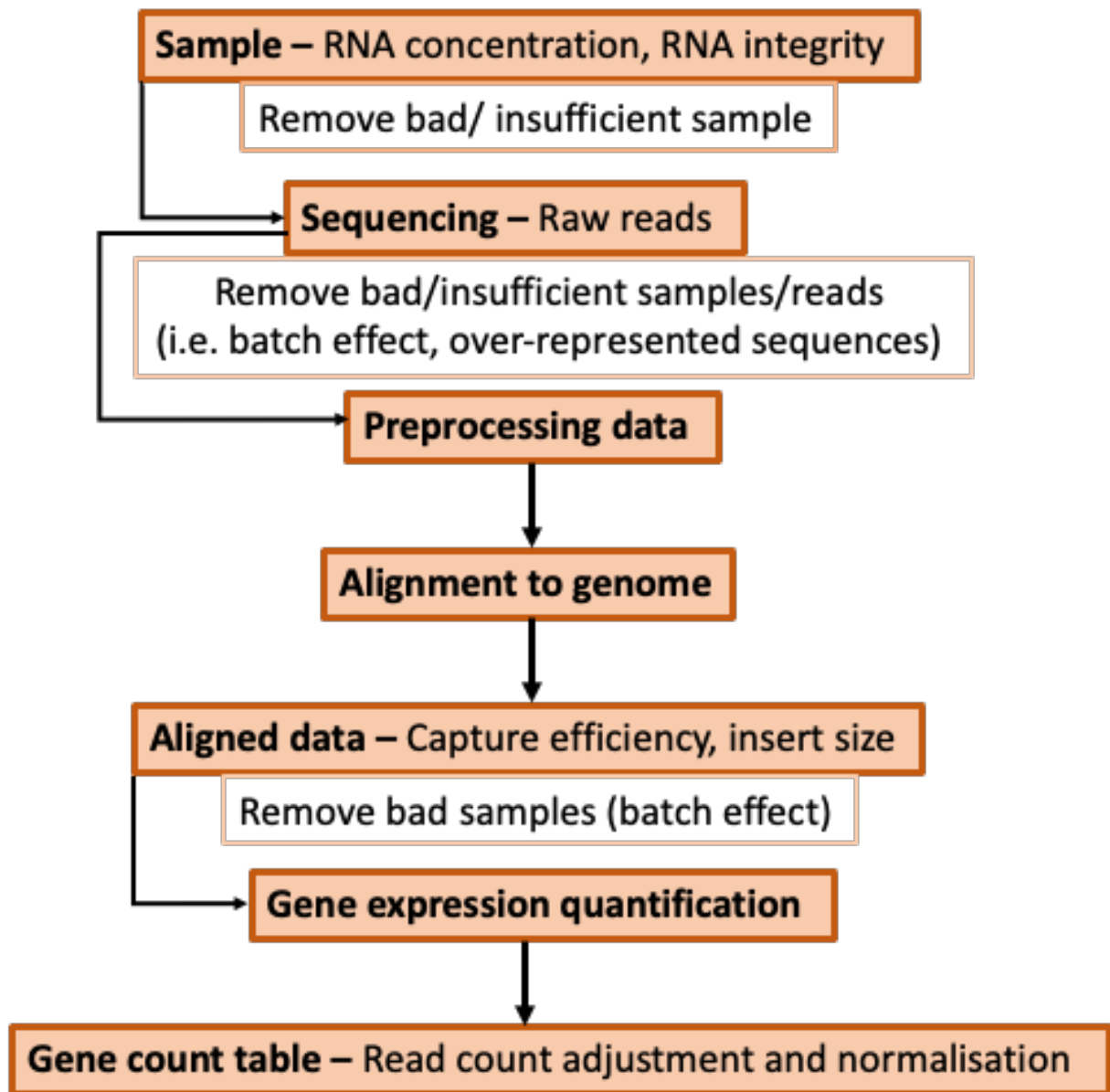
Figure 2.8: RNA-sequencing quality control workflow. *Initially a quality control of the input data (raw reads) is performed. The next step is to preprocess the raw reads to improve their quality. After the alignment of the preprocessed reads, efficiency can be captured, which then gene expression quantification can be applied to read count adjustment and normalisation.*

The prepared library subsequently underwent library construction (Figure 2.8) using Novogene Small RNA Sample Kit (Novogene, China, product number: 17080430). cDNA libraries for sequencing were constructed by Novogene Small RNA Sample Preparation Kit (Novogene, China, product number: 3080670). In brief, the 3' and 5' adapters were sequentially ligated to the ends of small RNA < 200 nucleotides long and reverse transcribed to generate cDNA. The cDNA was amplified by PCR using a common primer complementary to the 3' adapter, and a 5' primer. Samples were size-selected (100bp fragments), purified, quantified, and pooled for sequencing (Figure 2.9).
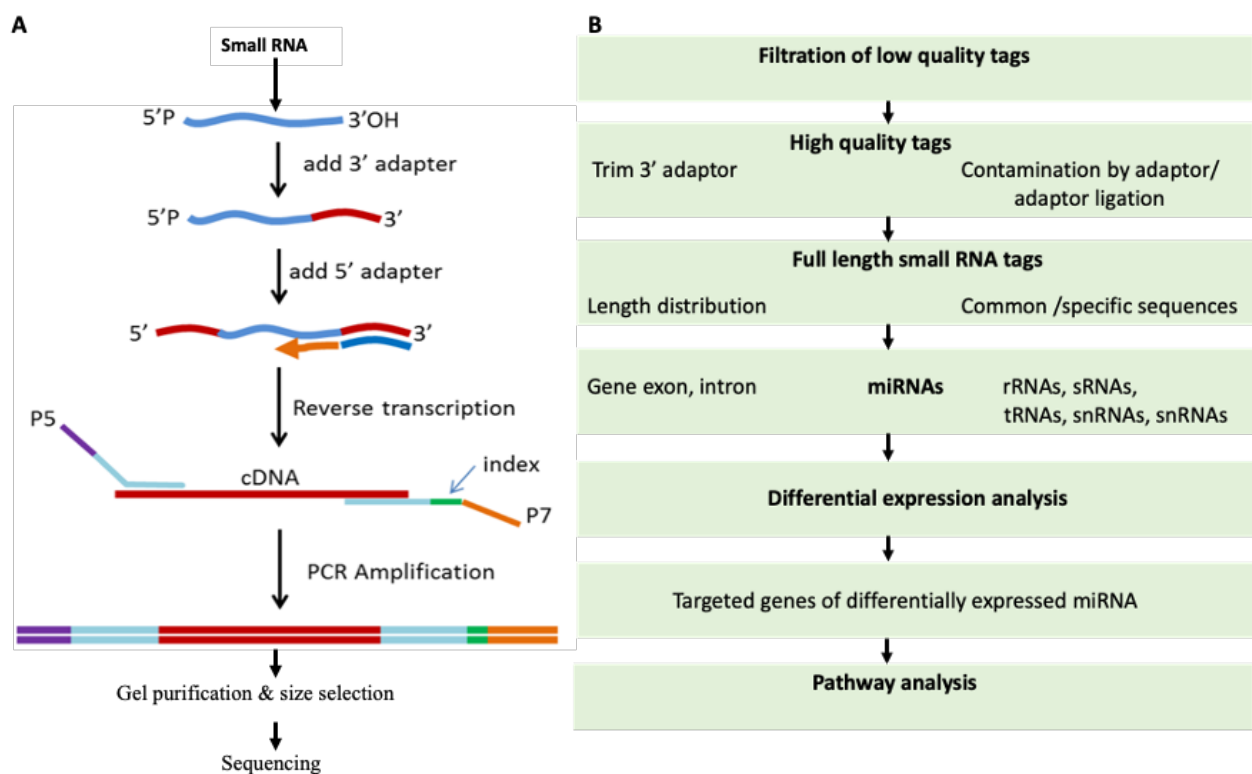
*Figure 2.9: **Workflow of library construction and sequence of miRNA.** A) Flowchart representing miRNA sample preparation and sequencing. Following RNA isolation, small-RNAs (18 -30 nt) are selected, 5' RNA adapter ligation and 3'RNA adapter ligation, the library products are ready for sequencing analysis. B) Flowchart representing bioinformatic processing and analysis. Following sequencing, raw reads are cleaned by the removal of low quality and short reads.*

2.10. Analysis of Data

The statistical analysis was performed with GraphPad Prism version (v7.0) complemented with Microsoft Excel (v16.50). Normality of the data was evaluated by the Kolmogorov-Smirnov and Shapiro-Wilk tests. Data are expressed as mean ± SD or mean ± SEM. Predetermined pair-wise differences were analysed by paired t-test and in case of a non-Gaussian distribution, the Wilcoxon matched paired test was used. For non-pairwise comparison, unpaired t-test (Gaussian distribution) and Mann-Whitney test (non-Gaussian) were used. ANOVA with Bonferroni post-test correction (Gaussian distribution) or Kruskal-Wallis test with Dunn's post-test correction (non-Gaussian distribution) were used for multiple group comparison. P values ≤ 0.05 were considered as statistically significant. Statistical testing was not possible, where sample size was small for statistical testing.

Chapter 3: Development of *in vitro* Method

for Assessment of Thrombus Formation

3.1. Introduction

It is essential to produce thrombi *in vitro* that mimic *in vivo* thrombi as comparably as possible, including a distinctive morphology of head and tail, in order to assess the role of EMVs in conditions that relate to *in vivo* conditions.

3.1.1. The Chandler Loop

The Chandler Loop system is an experimental platform that enables researchers to investigate interactions of blood with artificial materials and surfaces, haemocompatibility and haemorheological effects, and the cellular and molecular interactions that occur when blood samples are perfused over polymeric conduits (Slee et al., 2014). The Chandler Loop consists of several interrelated features such as circular precision cutter which ensures high precision of the circular form, connector tube lock that provides form-fit sealing at the splice, loop cradle that supports the loop while an electric motor drives the apparatus and a rotation unit that enables precise movement of the loop (Figure 3.1).
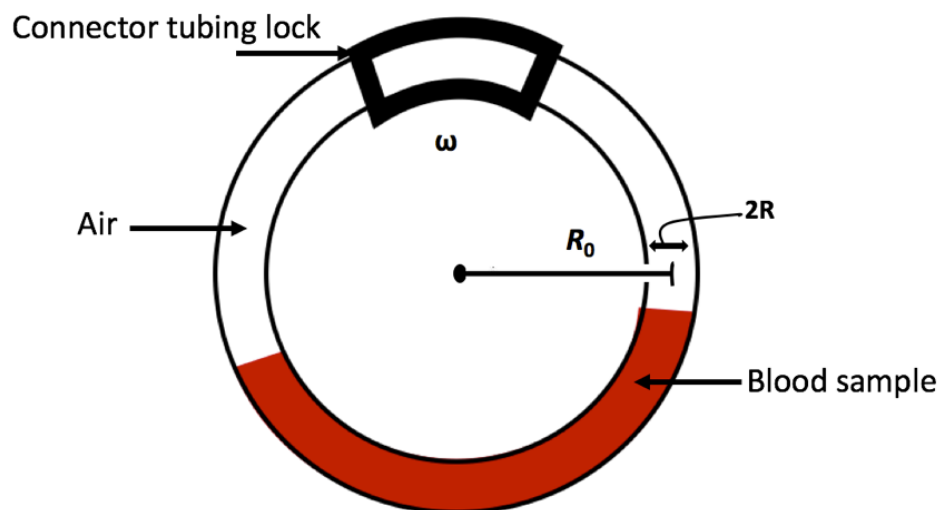
Figure 3.1: The Chandler Loop device. *A sealed Chandler Loop consisting of a hollow tube with its ends connected to form a toroidal loop, where R_0 is the loop curvature radius, 2R is the tube internal radius, and ω is angular velocity in RPM.*

3.1.2. Hypothesis and aims

It is important to produce a thrombus that mimics *in vivo* thrombi as closely as possible, including a distinctive morphology of head and tail, in order for the role of EMVs on thrombus formation to be assessed in conditions that relate to *in vivo* conditions.

3.1.2.1. Hypothesis

It is possible to produce *in vitro* thrombi that mimic *in vivo* thrombi

3.1.2.2. Aims

- To develop and optimise a method to produce thrombi that resemble those *in vivo*
- To test thrombi formation reproducibility
- To test whether thrombi formation over 90-minute time-course is optimal

Figure 3.2 shows the workflow process, with this chapter highlighted in red.
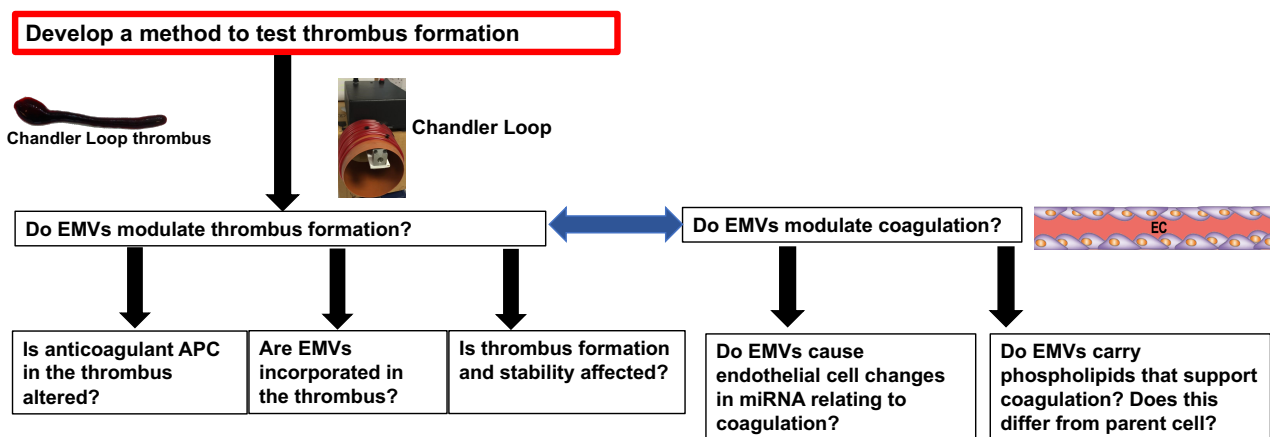
Figure 3.2: Process workflow diagram. *Development of in vitro method (Chandler Loop) for assessment of thrombus formation. This chapter is highlighted in red.*

3.2. Methods

3.2.1. Development and Optimisation of the Chandler Loop

To build the Chandler Loop equipment, key aspects and conditions had to be researched and identified from the literature including variable speed and temperature, diameter of rotating tubing loops and power of flow inducer. This information was then used with the help of Dr David Smith to build the equipment that consists of three main interrelated components as described in Figure 3.3.
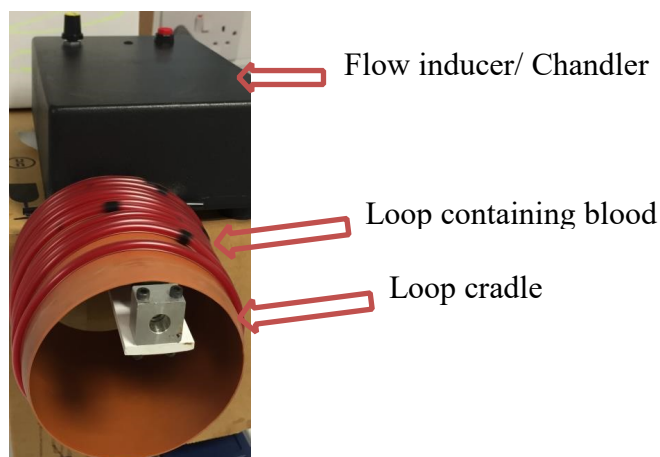
Figure 3.3: Chandler Loop device. Main components of the Chandler Loop, with 15 tubing loops containing blood circulating on the loop cradle (10.7cm in diameter).

Flow inducer: Also known as the Chandler pump or the power source. This is a motor that permits the tubing to rotate supplying electrical power causing a speed of rotation between 10 and 50 revolutions per minute (rpm). The flow conditions used are equivalent to 400-600 s^{-1}.

This is achieved by setting the Chandler pump to 30 rpm. This is to mimic the velocity of an *in vivo* arterial system (Gardner 1974, Vafa Homann et al. 2016).

Tubing loops: Tubing loops are non-sterile transparent, PVC tubing, 3.0 mm internal, 4.2 mm external diameter (VWR, UK, product number: 228-0106). This tubing is cut to a length of 35 cm for each loop. These loops were closed using connectors (tubing of 4.0mm internal, 6.8 external

diameter, cut to a length of 0.5mm) (Romero *et al.*, 2013). Tubes contained whole blood and rotated for 90 minute to form thrombi (Mutch *et al.*, 2008).

Loop cradle: The loop cradle is a circular rotating holder that acts as a frame to support the loops while the flow inducer rotates the apparatus. This frame can hold up to fifteen loops, allowing multiple comparisons to be completed in one experiment.

Variable speed: The Chandler Loop has various speeds depending on the experiments required. For this research, a 30rpm (3.5xg) speed was used to mimic the relative speed of the circulatory system (Gardner 1974, Vafa Homann et al. 2016).

Temperature: According to Dr Mutch, the appropriate temperature to use is 37°C, however, RT has been suggested to work well and has no significant effects on thrombi formation (Dr Mutch, University of Aberdeen, personal communication; Mutch *et al.*, 2008). Therefore, thrombi are formed at RT.

To determine optimal conditions for production of reproducible thrombi in terms of weight and length, the following parameters were altered:

- Blood volume added to loops (0.9 ml – 1.3 ml)

- $CaCl_2$ concentration and/or volume (0.25 mM – 0.50 mM)

- Rotation period (60min – 90min)

Following literature researching, discussion and observation of the Chandler Loop system used by Dr Nicola Mutch and her research group (University of Aberdeen), parameters were adjusted to produce consistent thrombi with length of 1cm and weight of 4mg. Following development of the Chandler Loop, whole blood was collected according to Section 2.1.2 and thrombi were produced (Figure 3.6) using the method described in Section 2.2.

3.2.2. Development and Optimisation of Thrombi Production

Whole blood was collected (Section 2.1.2) and thrombi were produced according to method described in Section 2.2. Initially, produced thrombi were variable in shape and morphology as shown in Figure 3.4. This figure shows the production of initial inconsistent and irreproducible thrombi with different variables in terms of length and weight. Following correct blood volume (0.9 ml) and correct $CaCl_2$ concentration (0.25mM), thrombi were measured in terms of length, width and weight. The method that has been developed has now allowed production of reproducible thrombi (Table 3.1) with a discernible head and tail (Figure 3.6).
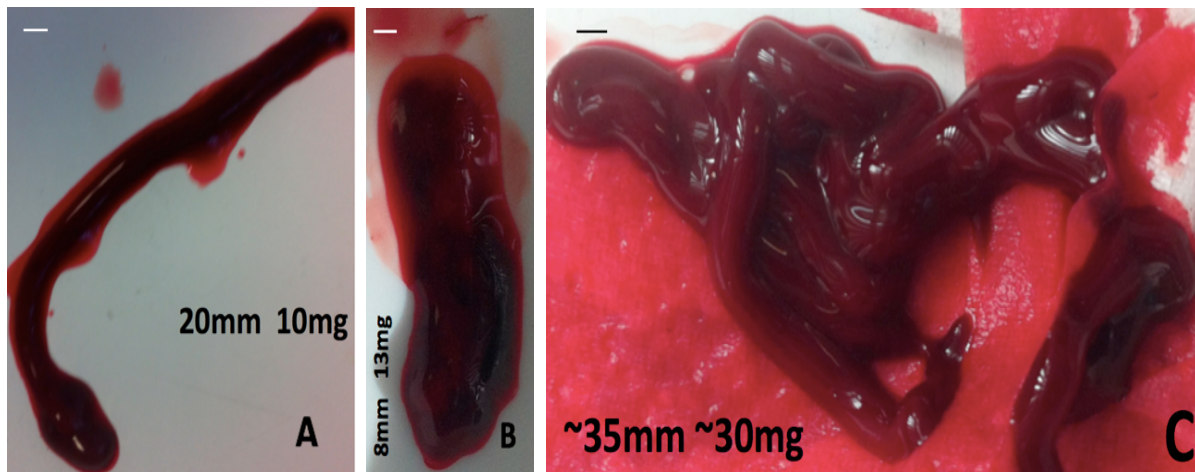
Figure 3.4: Variable thrombi. *Inconsistent and irreproducible thrombi with variable length, weight and morphology under the same initial conditions from same donor. Varied Blood volume (0.9 ml – 1.3 ml), varied CaCl₂ volume (0.25mM – 0.50mM). Scale bar = 1mm. n=10.*

3.2.3. Thrombi Reproducibility

Whole blood was collected (Section 2.1.2) and thrombi were produced according to method described in Section 2.2. In order to express the reproducibility of thrombus formation which was required to show consistency and experimental accuracy in order to determine whether changes are likely to be due to experimental errors rather than biological variations. This was conducted using two measures of the Coefficient of Variability (CoV): The Intra-Assay-CoV (IA-CoV) and the Inter-CoV (IEA-CoV). The IA-CoV was achieved by repeating the same experiment on eleven different blood donors. The IEA-CoV was achieved by working out the mean of fifteen identical loops in the same experiment at the same time, from one individual's whole blood. This experiment was repeated on blood from eleven different donors.

3.2.4. Thrombi Formation Time-course

Whole blood was collected (Section 2.2). Briefly, the method involved preparing 1 Eppendorf for the 0 minute timepoint and 6 identical sets of tubing for the Chandler equipment, and removing them after 15, 30, 45, 60, 75 and 90 minutes rotation (Figure 3.5). The contents of the Eppendorf/loops were collected, photographed and if appropriate thrombi measurements were made. Data from each of the eleven donors were measured and the mean of the data for each donor were calculated. These means were then used to calculate the data (Figure 3.7). Moreover, data from each of the eight donors were measured (Figure 3.8).

Data were tested for normality using Shapiro-Wilk normality test and the data are normally distributed. They are continuous data of more than two groups, therefore a one-way ANOVA is an appropriate test to use. Followed by paired T-test on 60, 75 and 90 mins.
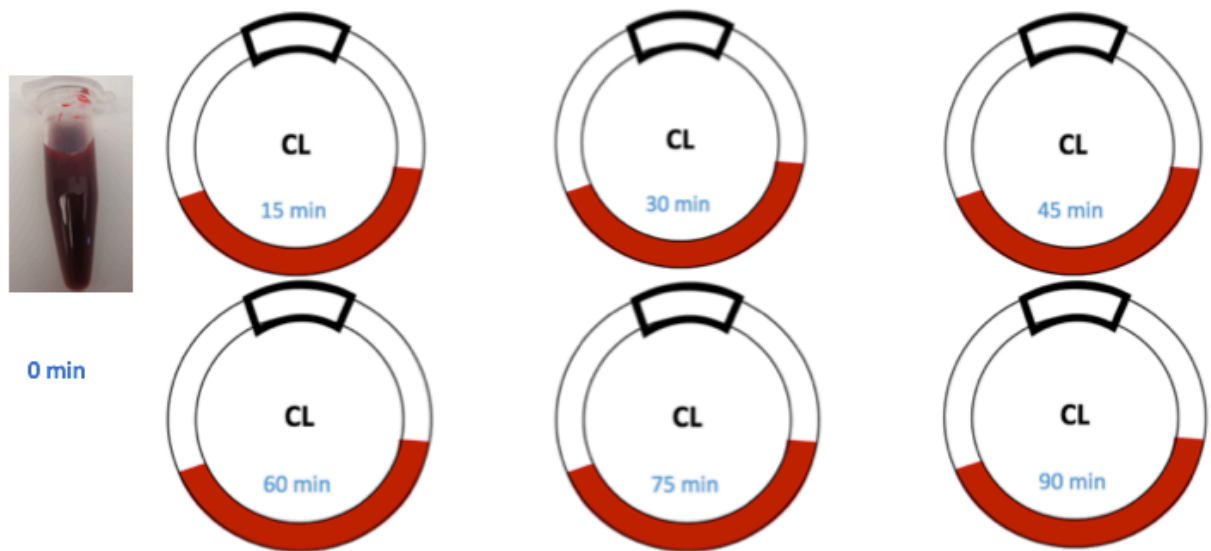
Figure 3.5: Whole blood exposed to different incubation time intervals. *Each loop was rotated for the times shown (15, 30, 45, 60, 75 and 90 minutes) before the appropriate loop was removed from the Chandler device, opened and the thrombus removed and measured.*

3.3. Results

Initially, produced thrombi were variable in shape and morphology as shown in Figure 3.4. Following number of experimental trials performing various troubleshooting approaches, a thrombus was produced as shown in Figure 3.6. This achieved following correct blood volume (0.9 ml) and correct $CaCl_2$ concentration (0.25mM). Consistent and reproducible thrombi were measured in terms of length, width and weight as shown in Table 3.1.
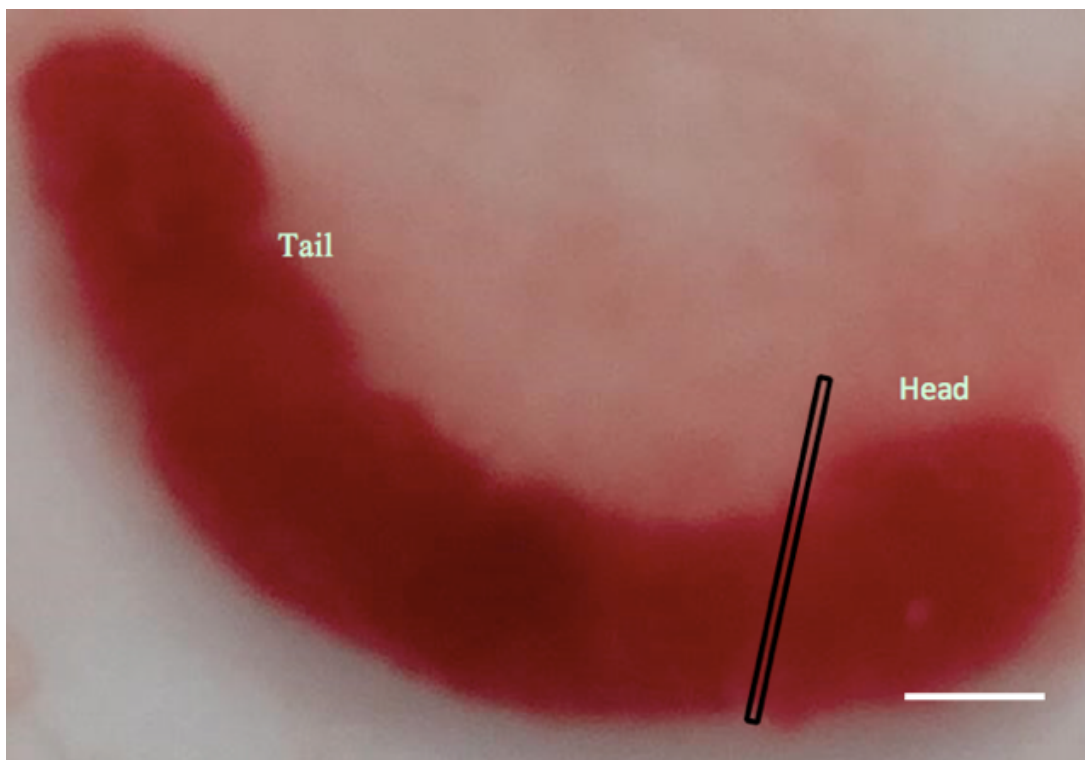
Figure 3.6: Consistent and reproducible thrombi. *A 10mm thrombus consisting of head and tail region. Head length is 3mm and tail length is 7mm. Width for both head and tail is 2mm. The weight of head is 1mg, weight of tail is 3mg. This thrombus was produced using correct blood volume (0.9 ml) and correct $CaCl_2$ concentration (0.25mM). Scale bar = 1mm. n=10.*

Following a number of experimental implementations, i.e. using different $CaCl_2$ concentrations, as well as different blood volume, the developed method has now permitted production of reproducible thrombi as shown in Table 3.1. Head length is approximately 33% and tail length is approximately 66%. Width for whole thrombus, head and tail is 2mm. The weight of head is approximately 25% and weight of tail is approximately 75% of whole thrombus. Data expressed as mean +/- standard deviation (SD).

Table 3.1: Measurements of thrombi for eleven different donors. *Using the new conditions, fifteen different thrombi were made from each of the eleven donors and measured and the mean of the data for each donor were calculated. These means were then used to calculate the data in Table 3.1. n= 11 donors (11x15 loops).*

	Length (mm)	Width (mm)	Weight (mg)
Whole Thrombus	10+/-0.5	2+/-0.5	4+/-0.2
Thrombus Head	3+/-0.5	2+/-0.2	1+/-0.5
Thrombus Tail	7+/-0.5	2+/-0.5	3+/-0.2

3.3.1. Thrombus Reproducibility

The mean and SD of eleven donors were used to calculate the IA-CoV (Table 3.2) by dividing SD by the mean and multiplying it by 100 to achieve CoV percentage. The higher the percentage, the higher the experimental error. The lowest IA-CoV for length is 0.59% whilst the highest IA-CoV is 2.23%. The lowest IA-CoV for width is 0% and the highest is 5.10%. The lowest IA-CoV for weight is 1.29% and the highest is 2.69%. The cut-off for length, width and weight used here is 6%, any percentage above 6% is considered a biological difference (ThermoFisher Scientific).
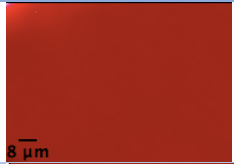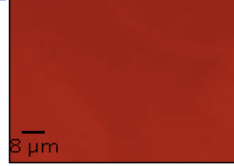
Table 3.2. IA-CoV% from eleven different donors. *Eleven participants' blood samples were used to run fifteen different loops at a time. The mean, SD and IA-CoV were calculated for length, width and weight for each donor. n=11.*

Donor	Length IA-CoV%	Width IA-CoV%	Weight IA-CoV%
1	2.23	2.95	1.89
2	2.02	3.83	2.69
3	2.07	5.10	2.27
4	1.64	2.56	1.30
5	0.59	0.01	1.29
6	0.92	0.00	1.89
7	2.07	3.83	2.27
8	1.10	2.56	1.30
9	0.96	2.98	1.48
10	2.00	2.98	1.48
11	0.59	2.96	1.49

3.3.2. Time-course of Thrombi Formation

The method described in Section 3.2.4 was used to observe macroscopic observations on formation of different stages of thrombi over 90 minute time-course (Table 3.3), as well as to observe blood for thrombus formation in order to determine the approximate time at which thrombi were fully formed (Figure 3.7 and Figure 3.8).

Table 3.3: Observations on blood/thrombi formation with different incubation times. Blood shows no changes in terms of formation at 0 and 15 minutes. However, blood started to produce blood fragments at 30 and 45 minutes (becoming jellified) and formed a smaller (thicker but shorter) thrombus at 60 and 75 minutes. A typical thrombus formed at 90 minutes. *n=8.*

Time (min)	Blood/ Thrombus	Length (mm)	Weight (mg)	Width (mm)	Macroscopic observations
0		NA	NA	NA	No thrombus formation
15		NA	NA	NA	No thrombus formation
30		NA	NA	NA	Blood thickened and fragments can be observed.
45		NA	NA	NA	Blood started to form a jelly-like fragments.
60		7.4	2.3	2.2	A smaller than usual thrombus formed. Scale bar=0.8mm.
75		9.7	3.7	2.1	A shorter, thicker than usual thrombus formed. Scale bar=0.8mm
90		10.0	4.0	2.0	A typical thrombus formed, consisting of head and tail. Scale bar =0.8mm

NA= not applicable

Following macroscopic observations on thrombus formation, investigated the thrombus formation in terms of length, width and weight over the 90 minute time-course (Figure 3.7). No thrombi were apparent up to 30 minutes of incubation (represented as 0 on the graph below) but thrombi dimensions increased incrementally after 45 minutes incubation, however, thrombi begin to increase after 45 minutes and begin to plateau off at 90 minute.
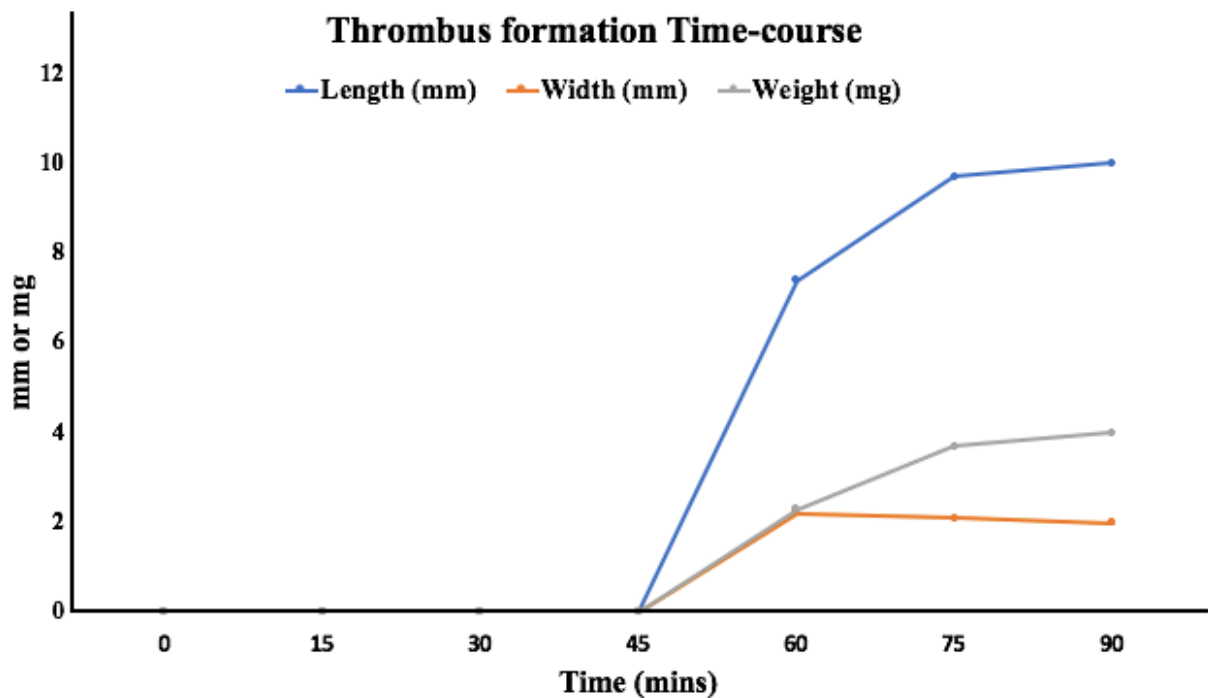
Figure 3.7: Thrombus formation time-course. *Identical loops were made and left to incubate circulating on the Chandler Loop device for 0, 15, 30, 45, 60, 75 and 90 minutes. At each of these time points, each loop was removed and the measurements completed immediately. No thrombus formation is visible until 45 minutes, however, thrombus formation started to become visible at 45 minutes and formation increases until fully forming at 90 minutes before started to plateau off. n=11.*

The next step was to quantify the time-course of thrombus formation using method described in Section 2.2. Then it was decided to use absorbance of the thrombus in the plate reader as a proxy measure for thrombus formation. Other options for investigating overall haemostasis are discussed in Section 4.3.1 and 7.4.1). The absorbance of the blood/thrombi was then measured in Figure 3.8.

Time in Chandler Loop and thrombus formation
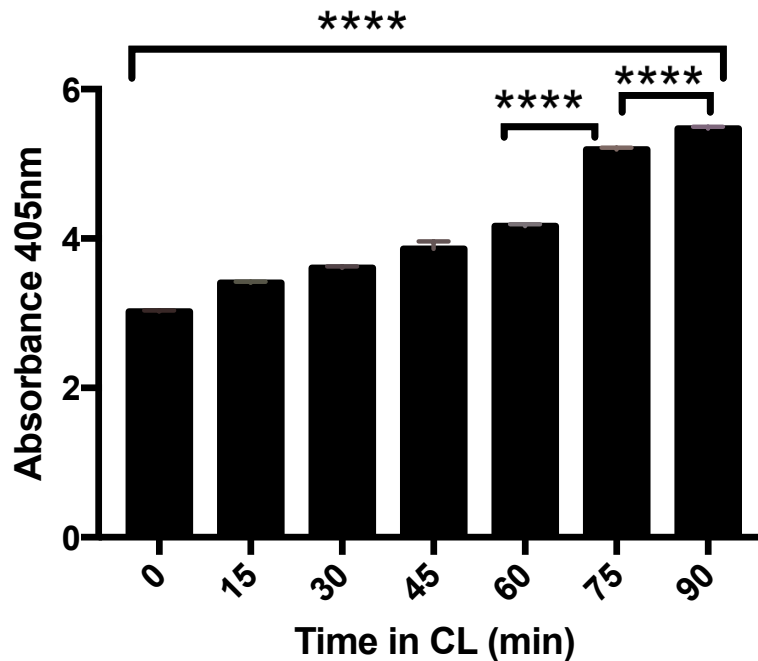
Figure 3.8: The effect of time in Chandler Loop on thrombus formation. *Identical loops were made and left to incubate circulating on the Chandler Loop for 0, 15, 30, 45, 60, 75 and 90 minutes. Samples were removed and absorbance was measured on a plate reader. n=8.*

There is a significant difference across time in the Chandler Loop, where absorbance of blood/thrombi increases with time spent circulating in the Chandler Loop (Figure 3.8, p value =0.0001). A noticeable increase in the absorbance (p value = <0.0001) can be observed at 75 minutes which is when the thrombus shows a recognisable thrombus forming into a distinctive structure before fully forming at 90 minutes. By 90 minutes, the absorbance is highest and the thrombus has fully formed, showing a distinctive structure of head and tail as shown in Section 3.3.1. The likely changes in thrombus formation are illustrated in Figure 3.9.

To summarise, an absorbance-based assay concurs with measurement data and the observed changes in thrombus formation at different time points of circulation in the Chandler Loop. These data suggest that thrombi begin to take a recognisable form between 60 and 75 minutes, however, the final structure is only observed at 90 minutes.
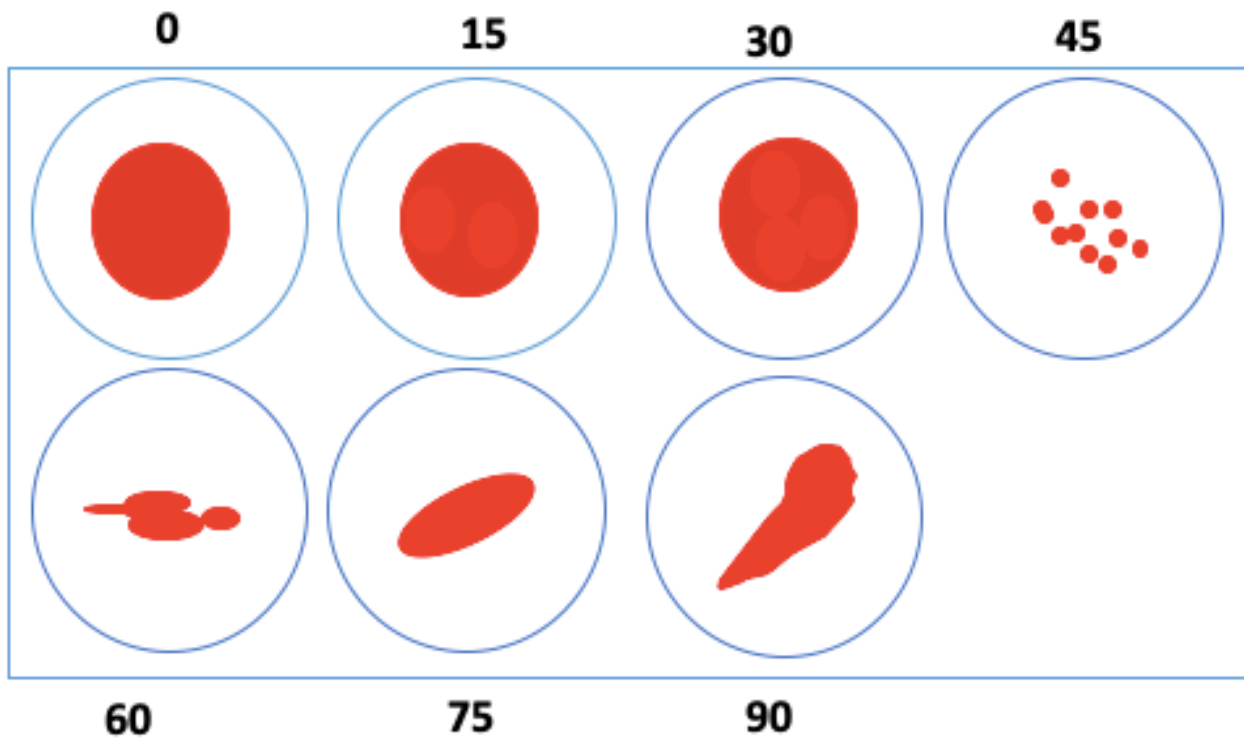
Figure 3.9: Schematic diagram of production stages in thrombus. *The changes in thrombus production at each time point (in minutes), explaining the increase in absorbance over time in minutes.*

3.4. Discussion

The modified Chandler Loop device developed in this study supported fifteen tubing loops that were simultaneously submitted to rotation, optimising the capacity of device, which is capable to form fifteen thrombi at the same time. The device required optimising applicable parameters and experimental conditions. Furthermore, appropriate parameters such as tubing diameters and speed rotation were required. According to Homann et al., the original Chandler Loop experiments used PCV tubing of 3.0mm diameter because saphenous vein (left over cardiopulmonary bypass) possessed the same antithrombotic binding capacity at the same 3.0mm diameter (Homann *et al.*, 2016). This type of material was and is today a good reference to apply (Homann *et al.*, 2016). These measurements are comparable to venous blood vessel diameter which typically measures between 3 – 5mm (Homann *et al.*, 2016). Furthermore, the conventional way of closing the loop is to connect the open ends into the inside opening of a short piece of a bigger sized tubing. The advantage of this system is that the connecting side of the loop mimics natural thrombus formation in humans. This works by attaching the two ends of the tubing loops which act as a vascular injury site mimicking physiological blood formation (Robbie *et al.*, 1997; Mutch *et al.*, 2008).

The handling of blood in this model used sodium citrate for blood collection which functions as an anticoagulant by chelating ionised calcium and preventing activation of calcium dependent clotting factors and the formation of thrombin (Mann et al., 2007; Oslen and Long, 2018). Calcium chloride has the ability to recalcify blood samples to reverse the effects of sodium citrate, to permit coagulation to occur and allow for the precise control of the time of coagulation initiation.

Initially, thrombi formation varied in terms of length, weight and morphology. This may be due to the high levels of $CaCl_2$ initially added (i.e. 50mM) to blood which is reported to not only resulted in complete turnover of fibrinogen but also accelerated formation and prevented spontaneous thrombolysis (Undas and Ariëns, 2011). However, following the use of a lower $CaCl_2$ final concentration (0.25mM) resulted in complete turnover of fibrinogen only (Mutch *et al.*, 2008). This leads to successfully producing consistently sized thrombi (Figure 3.6; Table 3.1). Following

successful thrombi production, it was important to test thrombus formation reproducibility and reproducible thrombi were achieved from eleven different blood donors with a maximum experimental error of 5.10 % (Table 3.2). According to ThermoFisher Scientific and Salimetrics, IA-CoV% of less than 10 – 15% is generally acceptable for whole blood and saliva experiments. However, this acceptable low variability maybe due to inter-donor variability (Reed et al., 2002). These results could be influenced by some factors including the presence of air in the loop, the correct sealing of the loop and the high viscosity of blood can make pipetting especially difficult. It seems that these factors can contribute to raise the IA-CoV *in vitro* studies on thrombus formation. However, these variations approximate them to the conditions found *in vivo*, where thrombi are not identical (Gaamangwe, 2014). According to previous publications (Robbie *et al.*, 1997; Mutch *et al.*, 2008), experiments were performed without a heat source which produced thrombi the same size as those formed with a heat source (Mutch *et al.*, 2008), (personal communication, Dr Mutch, University of Aberdeen). Therefore, this system followed their protocol without a heating source, conducted at RT.

Thrombi formation was then examined at various intervals over 90 minutes in the Chandler Loop (Figures 3.7 and 3.8). Physiologically, thrombus formation initiates seconds-minutes following vascular eruption, however, the full thrombus formation process and lysis can take much longer. By stopping the rotation process at various time intervals (every consecutive 15 minutes), it can be shown that the formation of *in vitro* thrombi occurs in three phases; initially consisting of small, incompletely spherical bodies (30 μm in diameter) which was thought to be macroscopically observed between 30- 45 minutes (Table 3.3, Figure 3.8). However, thrombus becomes evident having distinctive structure of head and tail at 90 minutes of rotation, mimicking those *in vivo*. It was challenging to distinguish between head and tail prior to 90 minutes. As mentioned previously, physiologically, thrombus formation initiates within seconds-minutes following vascular eruption, however, the full thrombus formation process can take much longer. This has been described in Figure 3.8 which was adapted from results in Table 3.3. The figure shows that small spherical bodies

103

are formed at 45 minutes, followed by a more dense, incomplete thrombus at 60-75 minute, which can indicate going from single cells (blood clusters) to thrombus (dense/3D structure thrombus) at 90 minutes (Figure 3.8).

Unlike thrombi produced in a static system, the Chandler Loop is capable of generating thrombi that mimics those formed in humans, with a remarkable morphological and biochemical similarity (Chandler 1958, Robbie et al., 1997). A thrombus formed using a static system has a uniform structure in which all blood cells are randomly distributed and none are aggregated. A thrombus formed using Chandler Loop system, on the contrary displays a complicated structure of aggregated cells, having a white head formed mainly of platelets and followed by a red tail formed mainly of erythrocytes and fibrin strands (Mutch *et al.*, 2008). Thrombi produced in this chapter resemble those produced by flow systems used by other researchers in the field, in terms of morphology. Furthermore, those researchers have examined Chandler thrombi histologically and microscopically and found to resemble those found *in vivo* (Chandler 1958; Robbie *et al.*, 1997; Mutch *et al.*, 2008). The differences between static clots and Chandler thrombi are summarised in Figure 3.10. Therefore, the Chandler thrombus resembles those formed *in vivo* and is suitable for the next objective, to study the role of MVs in thrombus formation, for example to analyse the incorporation of MVs into the thrombus that similar to human thrombus formed *in vivo*.

Static Clots

Clots prepared in test tubes lacked defined structure, with a homogenous distribution of erythrocytes and fibrin.

The process of aggregation that concentrates platelets in the head of the thrombus does not occur during static blood clotting.

There are evidences that thrombi prepared under static conditions consist in a poor model for human thrombi formed in vivo and are not appropriated for the study of thrombolysis

Modified Chandler Loop thrombi

Dense head – composed of platelet-derived material surrounded by erythrocytes, leucocytes and fibrin.

Tail – composed largely of fibrin with fewer erythrocytes and leucocytes than in the head.

The artificial thrombi produced in the Chandler loop circulation provided a much superior model of human thrombi. Their overall structure and staining for fibrin was comparable to in vivo.

In vivo thrombi

In arterial thrombi obtained from the vasculature during surgery or autopsy, platelet-derived masses, erythrocytes, leucocytes and fibrin-containing areas could clearly be identified, all similar to the Chandler thrombi.

The majority of thrombi in patients illustrate a comparable macro and microstructure like the thrombi build in the Chandler Loop.

Figure 3.10: Common features of static vs modified Chandler vs in vivo thrombi. These observations validate Chandler's basic finding, that when blood is made to flow round a closed circular loop of plastic tubing a structure is formed which resembles a naturally occurring thrombus in its microscopical appearance (Chandler, 1958; Robbie et al., 1997; Marder et al,, 2006).

3.5. Conclusion

A fully functioning in-house Chandler Loop system has been developed and optimised, capable of reproducibly producing up to 15 thrombi at a time to allow multiple comparisons of experimental conditions. The typical thrombi obtained present with similar physiological characteristics to those described by Chandler having discernible heads and tails and resemble *in vivo* thrombi. This appropriate *in vitro* system and experimental protocol developed will now be used to investigate the role of EMVs in thrombus formation and thrombolysis. Furthermore, thrombi were fully formed after 90 minutes of tubing rotation, whilst prior to 90 minutes, head and tail were not evident and therefore, thrombi formed at 90 minutes were the most appropriate to study, mimicking those *in vivo*.

Chapter 4: The Effect of EMVs on Thrombus Formation

4.1. Introduction

EMVs can modulate cellular functions and can activate cells in the local microenvironment by travelling through blood circulation (Iba and Ogura, 2018). Several studies have reported that MVs have interactions with coagulation, however, research on EMVs particularly have been limited (Zhang et al., 2014; Tripisciano et al., 2017). A number of studies show high levels of EMVs associated with vascular diseases, however, there is insufficient evidence of their direct pathophysiological link to vascular disease (Shantsila et al., 2010; Iba and Ogura, 2018). The fact that EMVs contain not only procoagulant surface antigens but also anticoagulant antigens such TM and protein C receptor adds to the complexity. Moreover, the procoagulant/anticoagulant balance appears to alter according on the conditions; hence the precise role of EMVs in coagulation remains uncertain (Tripisciano et al., 2017; Iba and Ogura, 2018). Although the literature contains scarce evidence on the exact role of EMVs in haemostasis, the potential links have been suggested between EMVs and APC production in normal physiological circumstances, as proposed in Figure 4.1. However, the precise role of the relationship remains in debate and needs to be determined. Therefore, this chapter will investigate the effect of EMVs on thrombus macro-structure and the means by which the EMVs have these effects, particularly investigating a potential link between EMVs and APC production. Furthermore, this chapter will investigate whether EMVs modulate thrombus formation and whether they are incorporated into the thrombus.
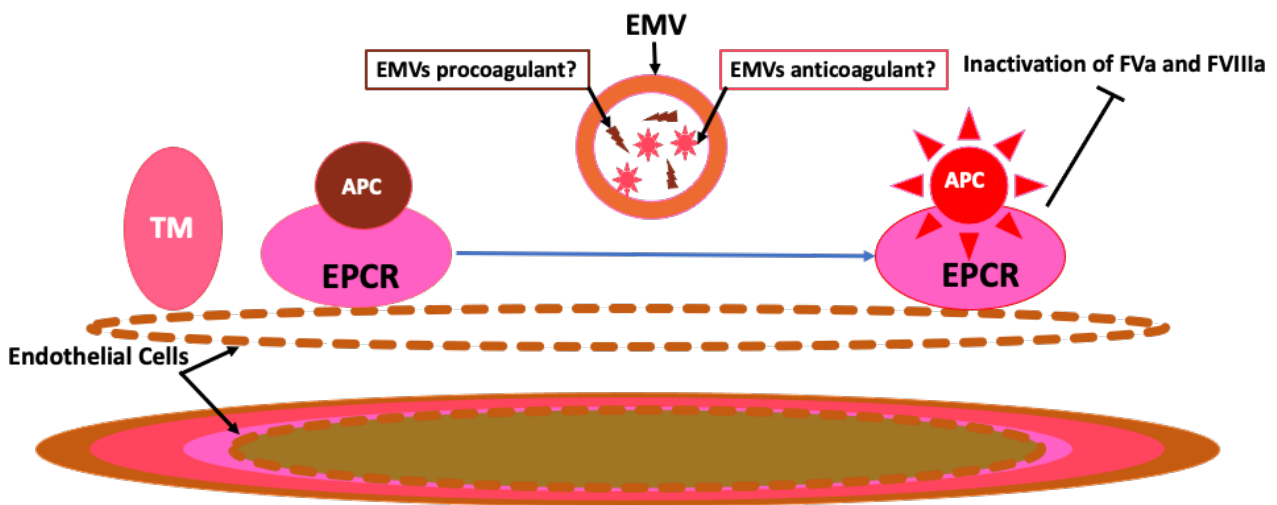
Figure 4.1: Endothelial microvesicle (EMVs) proposed involvement in anticoagulat properties. *EMVs are suggested to be involved in anticoagulant pathways through the expression of membrane associated thrombomodulin (TM) and endothelial protein C receptor (EPCR). Activated protein C (APC) inhibits coagulation, inactivating factors Va and VIIIa effects.*

4.1.1. Hypotheses and Aims

The overall hypothesis of this chapter is that exogenous EMVs affect thrombus formation via modulation of haemostasis. Below are the hypotheses and aims for each subchapter.

4.1.1.1. Do EMVs modulate thrombus formation and structure?

Hypothesis: EMVs increase the extent of thrombus formation

Aims: To investigate whether EMVs contribute to bigger and stronger thrombus production, by measuring the I) length, II) weight and III) macrostructural components.

4.1.1.2. Are EMVs incorporated into the thrombus?

Hypothesis: EMVs are incorporated into thrombi.

Aims: To investigate whether EMVs are:

- Incorporated from blood into developing thrombi

- Reduced in blood as thrombi develop.

4.1.1.3. Do EMVs reduce thrombus size via anticoagulant APC activity?

Hypothesis: EMVs alter thrombus formation via changes in APC production

Aims: To investigate whether the effect of adding exogenous EMVs to a developing thrombus is related to APC. In particular, to determine whether:

- EMVs contribute by carrying/generating APC on their surfaces

- EMVs contribute by altering APC generation in the plasma around the thrombus

- EMVs contribute by altering APC generation on the surface of or inside the thrombus

- EMVs affect the amount of TM found in or around the thrombus.

This chapter is set to explore the influences affecting thrombus formation and the effect of EMVs on thrombus formation and structure, with a more in-depth study of the activated protein C pathway. The contribution of this chapter to the overall thesis is shown in red in Figure 4.2 below.
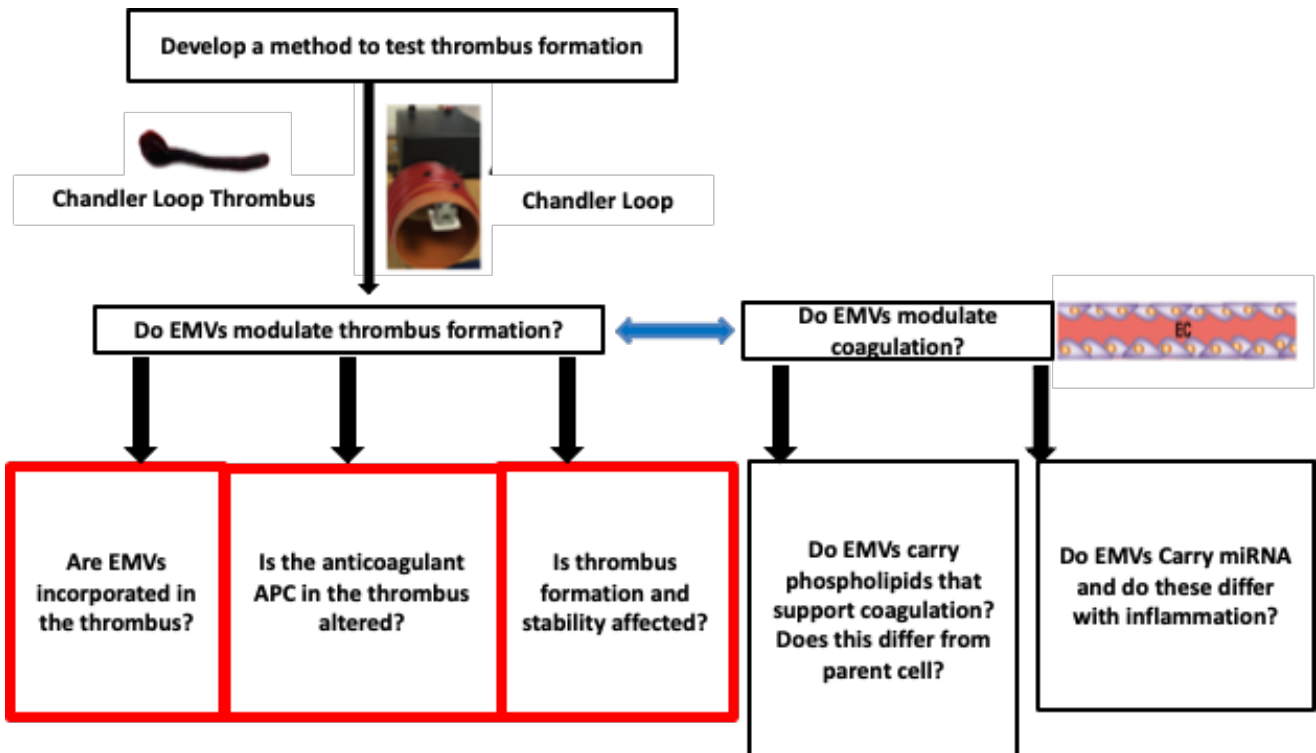
Figure 4.2: Process workflow diagram. In the previous chapter (chapter 3) the Chandler Loop was developed to investigate thrombus formation. In this chapter EMVs will be added to blood to see whether these exogenous EMVs modulate thrombus formation. This chapter is highlighted in red.

4.2. Methods

4.2.1. Preparation and Analysis of Thrombi in The Presence and Absence of EMVs

Thrombi were prepared using the Chandler Loop as described in Section 2.2 from different donors. EMVs (10^3 EMVs/ml) were added to whole blood or an equal volume of tissue culture medium was added as the control. These EMVs had been previously collected from resting HUVEC cells at the following concentrations as described in Section 2.4.

For the dose response experiments in Section 4.3.1, different concentrations of EMVs were added to whole blood (10^4 EMVs/ml, 10^5 EMVs/ml and 10^6 EMVs/ml). After 90 minutes, thrombi were removed from the Chandler Loop and analysed as described in Section 3.2.4.

In the temporal experiments, thrombus formation was stopped at a variety of times as described in Section 3.2.4. Length and weight were measured. Thrombus formation was assessed as follows. Thrombi were prepared in the presence and absence of exogenous EMVs and absorbance at 405nm was assessed as described in Section 4.2.3 on thrombi at 90 minutes and blood at 0 minute.

4.2.2. Are EMVs Incorporated Into Thrombi?

In order to determine whether EMVs are incorporated into thrombi, a two method approach was used: Whole mount confocal microscopy was used to identify EMVs within thrombi formed in the presence or absence of exogenous EMVs using AAL and CD41 staining (Section 2.6). Dual staining flow cytometry was carried out to identify EMVs in the blood sample before formation of the thrombus, during and afterwards. Thrombi were prepared in the presence and absence of EMVs as shown in Figure 4.3 and blood/thrombi were collected over a time-course (0 minute, 15 minutes, 30 minutes, 45 minutes, 60 minutes, 75 minutes and 90 minutes). Blood, blood fragments and thrombi

were collected. Blood samples were used to dual stain for EMVs and PMVs using flow cytometry according to the methods described in Section 2.7.
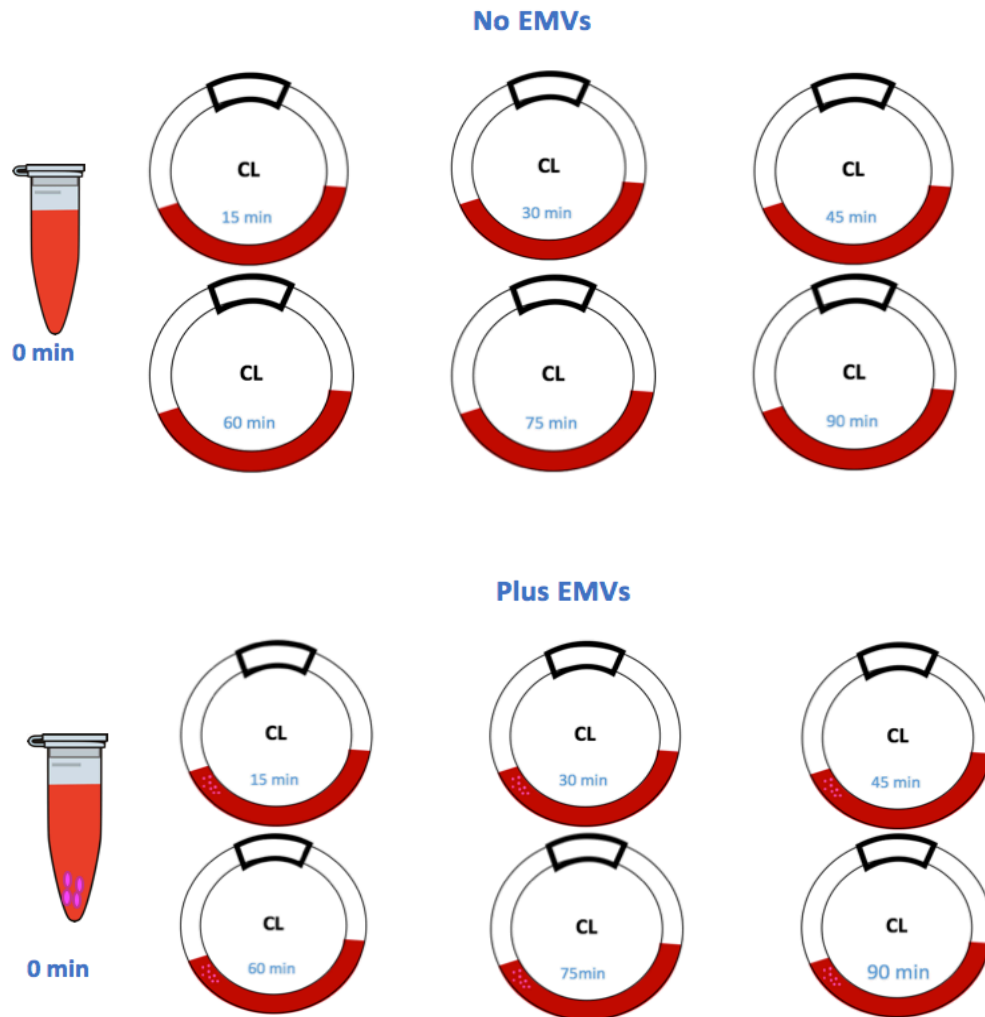
Figure 4.3: Loops of non-added exogenous endothelial microvesicles (EMVs) and added exogenous EMVs. *Loops used to investigate the effect of adding EMVs and allowing thrombi to develop over 0-90 minutes. For each time point, either EMVs (10^3 EMVs/ml) or tissue culture medium (non-EMV control) were added to whole blood before circulating loops on the Chandler Loop apparatus. At the appropriate time point, loops were opened and EMVs in the blood were counted by flow cytometry.*

4.2.3. Measurement of APC Associated with Thrombi Formed in The Presence/Absence of EMVs

4.2.3.1. Preparation of Thrombi for Measurement of APC

Four thrombi with or without exogenous EMVs were prepared as described above. After the thrombi had formed, the following steps were completed in order to investigate whether APC was upregulated in, on or near the thrombus Figure 4.4.

Loop 1 and 3: Plasma was collected from the remaining circulating blood in the loop in Eppendorf tubes. It was centrifuged for 10 minutes at 2,000xg at RT. The plasma directly surrounding the thrombus was also collected separately and centrifuged for 10 minutes at 2,000xg at RT. The thrombus was collected and chopped into small segments, (approximately $1mm^3$) using a scalpel. It was collected in chromogenic assay buffer (20mM HEPES, 150mM NaCl, 5mM $CaCl_2$ at pH 7.5) (ThermoFisher, UK, product number: 124600) and centrifuged for 10 minutes at 2,000xg at RT. Centrifugation at 2000xg removes any large particles but will not remove the MVs.

Loops 2 and 4: The thrombus was collected whole in ECA buffer (ThermoFisher, UK, product number: 33256) in Eppendorf tubes and centrifuged at 2,000xg at RT.
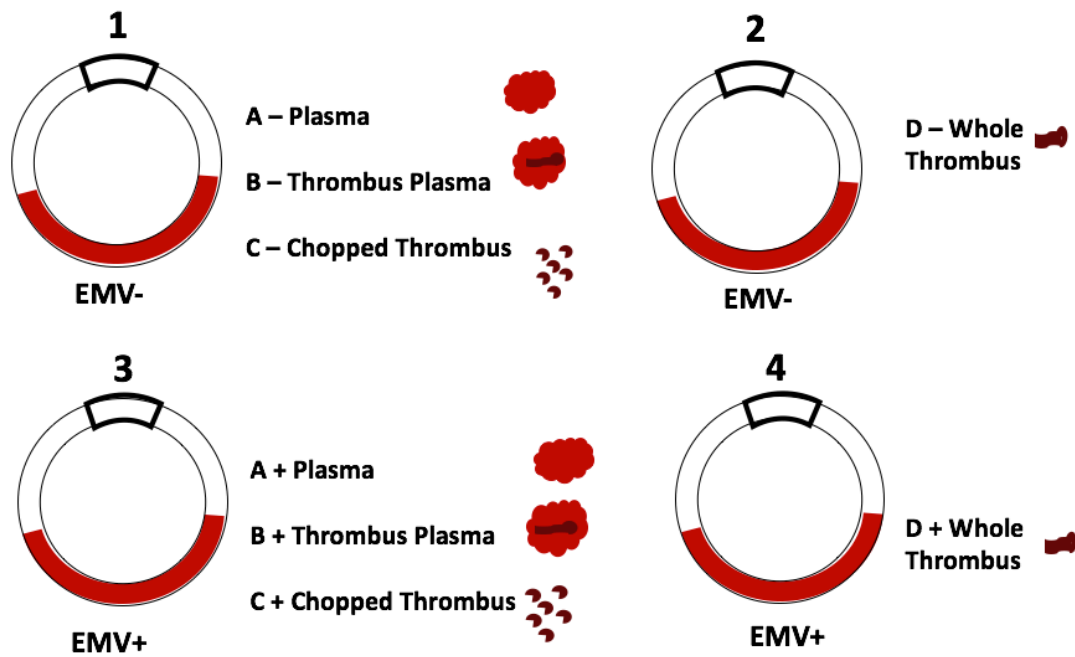
Figure 4.4: Arrangement of loops used to generate thrombi in the presence or absence of endothelial microvesicles (EMVs). *In loop 1, the sample was used to collect plasma from uncoagulated blood, plasma from the surface of the thrombus and for collecting the thrombus to chop it into smaller fractions. In loop 2, the sample was used to collect the thrombus, keeping it whole for further experiments. Loops 3 and 4 consist of the same method but with the addition of EMVs (EMV+). n=8 donors.*

4.2.3.2. APC Generation Assay

Following samples of plasma and thrombus described in Figure 4.4 were kept in Eppendorf tubes. 80μl of supernatant from each Eppendorf was added to wells in a 96 well microtiter plate according to Table 4.1, with negative and positive controls as described below, at a 1:1 ratio with the APC-specific chromogenic substrate (S2336) (ThermoFisher, UK, product number: S2336/36033) in buffer. Negative controls were (1) blood plasma with the absence of exogenous EMVs and absence of S2336 and (2) blood plasma with the presence of EMVs and the absence of S2336. Positive controls were (1) blood plasma without the presence of exogenous EMVs but with the presence of S2336 and (2) blood plasma with the presence of exogenous EMVs and the presence of S2336 as described in Table 4.1. After 30 minutes of incubation, a plate reader was used to measure colour

intensity at wavelength 405nm as summarised in Figure 4.5. Absorbance is directly proportional to APC activity. Each sample had additional controls and these included (1) no addition of exogenous EMVs and no addition of S2336 (2) no addition of S2336 and addition of exogenous EMVs and (3) no addition of exogenous EMVs and addition of S2336. These controls were then added to thrombi samples (blood plasma, blood plasma, thrombus plasma, chopped thrombus and whole thrombus) as shown in Table 4.1.

Table 4.1: Experimental control. *96 wells microtiter plate format using plasma and thrombi as described in Figure 4.5. Blood plasma was prepared by centrifuging blood that had not been in the Chandler Loop to provide a control. Chandler Loop plasma denotes plasma prepared from uncoagulated blood from the Chandler Loop. Thrombus denotes a whole thrombus. Chopped thrombus denotes thrombi that had been cut to expose its interior as described in in Figure 4.4.*

		1	2	3	4
Experimental 96 wells microtiter plate	A	BP -EMVs - S2336 (neg control 1)	BP -EMVs +S2336 (pos control 1)	BP +EMVs –S2336 (neg control 2)	BP +EMVs +S2336 (pos control 2)
	B	CLP -EMVs -S2336 (A-, neg control)	TP -EMVs -S2336 (B-, neg control)	CT -EMVs -S2336 (C-, neg control)	WT -EMVs -S2336 (D-, neg control)
	C	CLP -EMVs +S2336 (A-)	TP -EMVs +S2336 (B-)	CT -EMVs +S2336 (C-)	WT -EMVs +S2336 (D-)
	D	CLP +EMVs -S2336 (A+, neg control)	TP +EMVs -S2336 (B+, neg control)	CT +EMVs -S2336 (C+, neg control)	WT +EMVs -S2336 (D+, neg control)
	E	CLP +EMVs +S2336 (A+)	TP +EMVs +S2336 (B+)	CT +EMVs +S2336 (C+)	WT +EMVs +S2336 (D+)

Key:
BP = Blood Plasma
CLP = Chandler Loop Plasma
TP = Thrombus Plasma
CT = Chopped Thrombus
WT = Whole Thrombus
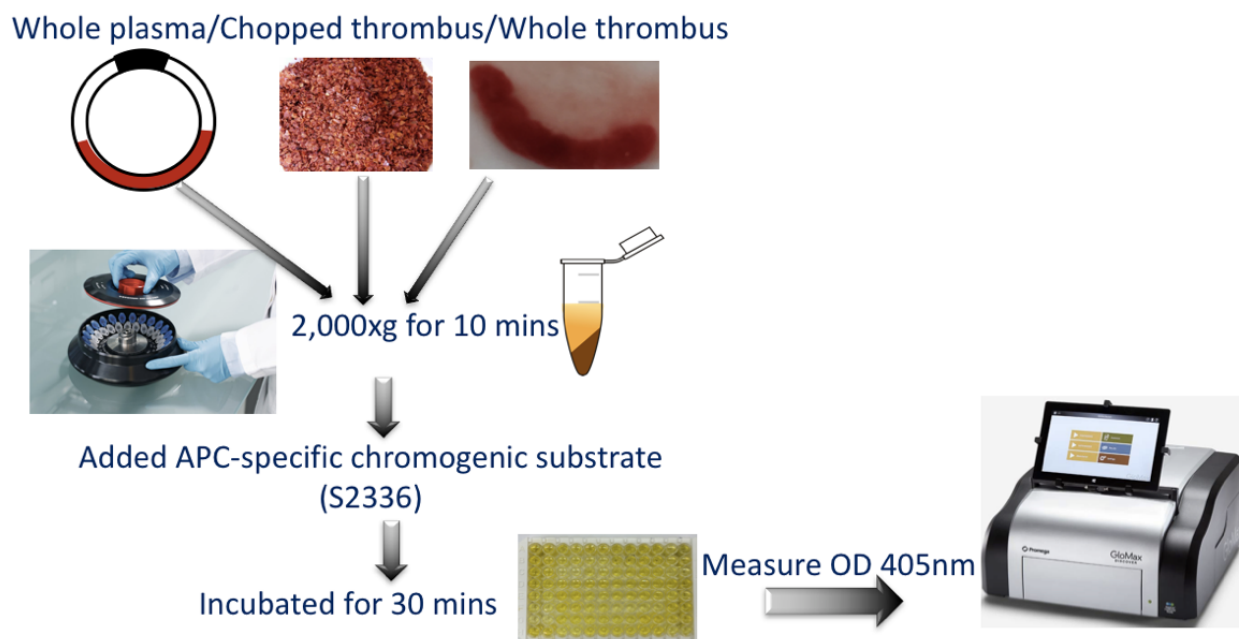
Figure 4.5. A summary of the process of assessing activated protein C (APC) activity. *Whole plasma/ chopped and whole thrombus are centrifuged before addition of APC-specific chromogenic substrate, incubation and measurement.*

4.2.3.3. Thrombomodulin-ELISA

Blood was collected according to method in Section 2.1.2. Four thrombi were formed as described in Section 4.2.3.1, to measure the amount of TM present. The quantity of TM released into the supernatant was identified using the human TM-BDCA-3 Quantikine Enzyme-Linked Immunosorbent Assay (ELISA) Kit (R&D Systems, UK, product number: DTHBD0). All reagents, working standards and samples were prepared as per manufacturer's instructions. Blood samples were diluted using a 2-fold dilution in calibrator diluent RD5P (diluted 1:5), as per manufacturer's suggested preparation. Following preparations and setup of ELISA plate, 100μl of standard assay diluent was added to each well. 50μl of standard solution was added to each well containing blood/ thrombus. Two sets of wells were used for standard serial concentrations. Wells were incubated for 2 hours at RT. Each well was then washed 4 times, with 400μl wash buffer. 200 μl of human TM conjugate was added to each well and incubated for a further 2 hours at RT. Each well was washed four times with 400μl wash buffer to remove any unbound antibody-enzyme reagent. Then 200 μl of substrate solution was added to each well and incubated for 30 minutes at RT. Then 50 μl of stop

solution was added to each well causing reaction/ colour change in the wells from blue to yellow. Then the OD of each well was determined within 30 minutes, using a microplate reader set to 405 nm.

4.2.4. Statistics

The statistical analysis was performed with GraphPad Prism version 7.0. Normality of the data was evaluated by the Kolmogorov-Smirnov and Shapiro-Wilk tests. Data are expressed as mean $\pm$ SD or mean $\pm$ SEM. Predetermined pair-wise differences were analysed by paired t-test and in case of a non-Gaussian distribution, the Wilcoxon matched paired test was used. For non-pairwise comparison, unpaired t-test (Gaussian distribution) and Mann-Whitney test (non-Gaussian) were used. ANOVA with Bonferroni post-test correction (Gaussian distribution) or Kruskal-Wallis test with Dunn's post-test correction (non-Gaussian distribution) were used for multiple group comparison. P values less than 0.05 were considered as statistically significant.

4.3. Results

4.3.1. Do EMVs Modulate Thrombus Formation and Structure?

To investigate the effect of EMVs on thrombus macrostructure, thrombi were produced in the presence and absence of exogenous EMVs and outcomes of thrombus length, weight and macrostructure were assessed.

Adding exogenous EMVs significantly reduced the length of the thrombi (Figure 4.6) p vale = 0.05 for no EMVs vs $x10^4$ EMVs $x10^5$ EMVs and 10^6 EMVs). Furthermore, an effect on length was observed with $x10^6$ EMVs (p value = 0.003). Low numbers of exogenous EMVs had no effect on the weight of the thrombi; however, at higher numbers the thrombi weighed less. When adding low numbers of EMVs, it remains possible to differentiate between the head and tail, although the tail is narrower and sharper in thrombi formed in the presence of EMVs. At higher numbers, the thrombus does not have a distinctive morphology. Adding increasing numbers of EMVs results in increasingly unstable thrombi. The thrombi produced without exogenous EMVs have a solid stable consistency. Adding $x10^5$ EMVs produces thrombi that are wider and less stable (more jelly-like in consistency). When EMVs are added at higher numbers, the thrombi disintegrate when they are removed from the loops suggesting they are highly unstable.
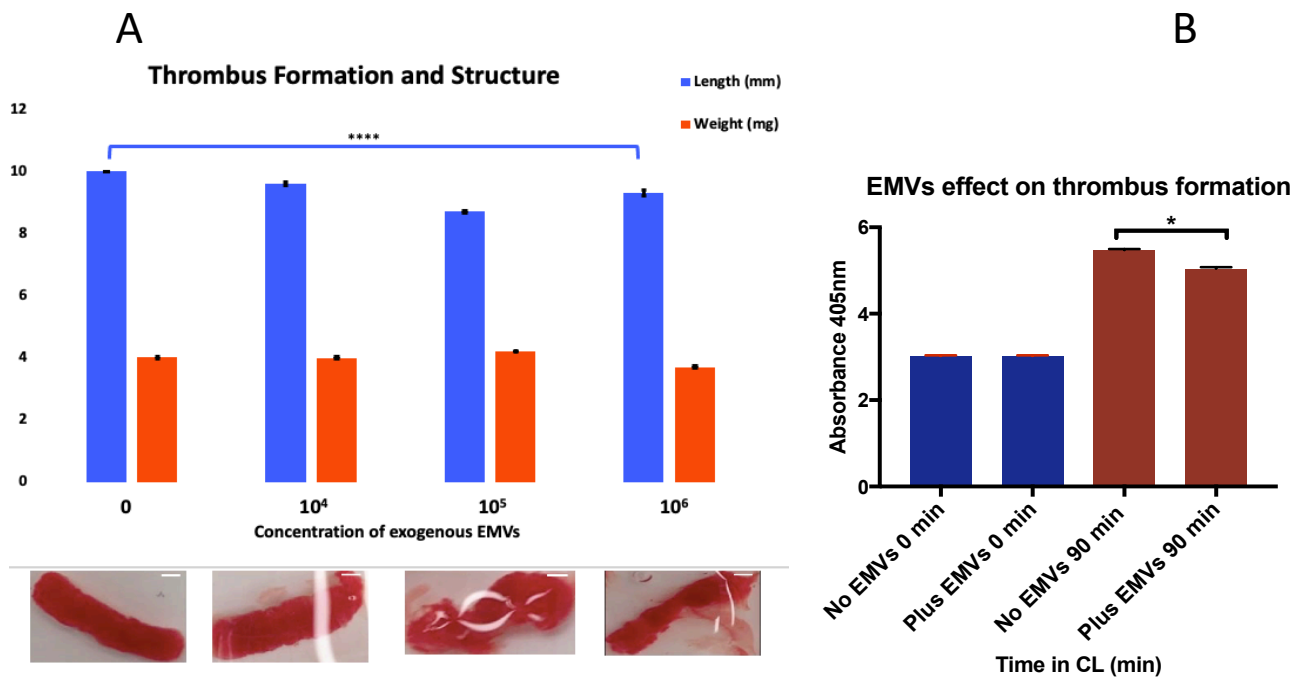
Figure 4.6: The effect of endothelial microvesicles (EMVs) on thrombus formation. A) Thrombi were produced in the presence or absence of exogenous EMVs, and length and weight changes of thrombus were highlighted. The images are representative of thrombus macrostructure at each concentration, showing thrombi morphology changes following addition of exogenous EMVs. B) Effect of exogenous EMVs on thrombus formation. *Effect was measured by absorbance of samples with no time spent in the Chandler Loop v. thrombi produced after 90 minutes. Thrombi were produced in the presence and absence of EMVs at 0 minute and 90 minutes and measured using plate reader. Thrombus formation at 90 minutes is significant compared to 0 minute, showing an effect of EMVs having on thrombus formation.* Asterisks indicate a statistically significant (p value < 0.05) difference between groups. Scale bar = 800μm. n=8.

Adding exogenous EMVs did not change the length of thrombi compared with the length with endogenous EMVs were present in the blood sample (Figure 4.6a). Further investigation was carried out on the effect of EMVs on thrombus formation measured by absorbance (Figure 4.6b). EMVs added to blood samples used for the Chandler Loop resulted in thrombi that were of lower absorbance than the samples that did not contain exogenous EMVs (p value = 0.03; Figure 4.6b), suggesting the EMV-containing thrombi were smaller and therefore take up less space in the well. This contrasts to the samples without added exogenous EMVs, suggesting that EMVs themselves did not physically alter the absorbance.

To summarise, in contrast to the original hypothesis, the presence of EMVs actually makes thrombi that are probably shorter, lighter and less stable.

4.3.2. Are EMVs Incorporated Into The Thrombus?

In order to determine whether exogenous EMVs were incorporated into developing thrombi, whole-mount thrombi were co-stained with AAL (for EMVs) and anti-CD41 (for PMV identification), and nuclei were stained with DAPI for analysis by confocal microscope. MV staining is essential in order to localise them within the thrombus and to recognise the cellular source of each MV. AAL and CD41 were used to differentiate cell types in thrombus.

Staining for AAL and CD41 were absent in the negative control (Figure 4.7 A). Figure 4.7 B shows PMVs stained with anti-CD41 and in terms of size it is plausible that they are PMVs. Figure 4.7 C for AAL shows EMVs labelled with lectin, which shows staining of possible clusters of EMVs within the thrombus or maybe EMVs attached to other cell types.

| **A** | **B** | **C** |
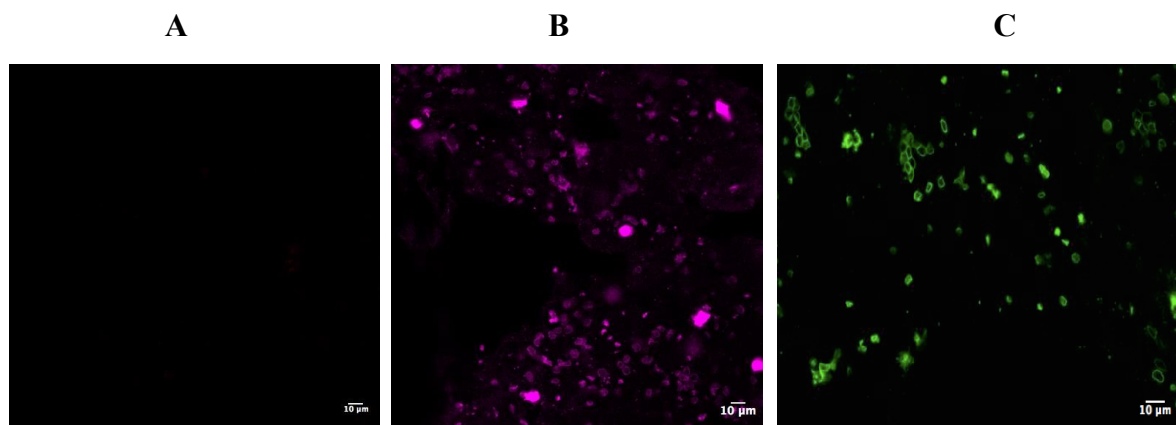
Figure 4.7: Whole-mount confocal thrombi. Image (A) negative control where unstained endothelial microvesicles (EMVs) added to thrombus with IgG1-isotype control antibody. Image (B) staining with antibody against CD41-PE (578nm), a platelet marker and image (C) AAL-FITC (518nm) a reported endothelial marker. Nuclei stained with DAPI (blue). 63 x magnifications. n=1, representative staining.

To further investigate whether exogenous EMVs are incorporated into developing thrombi, samples were prepared in the presence and absence of exogenous EMVs (Figure 4.4). Following collection, supernatants were stained using the F2N12S dye to identify membranes. Samples were then analysed on a two-laser dedicated Attune NxT flow cytometer. PMVs were identified by CD41/42 expression. EMVs were identified as negative for CD41/42 and positive for either or both of CD31/105 or CD106. All staining was compared to isotype controls (Figure 2.4). Histograms are used to show the percentage of EMVs in the population, along with the density of receptor expression (MFI), (Figure 4.8 A). EMVs were identified as negative for CD41/42 and positive for either or both of CD31/105 or CD106 (Figure 4.8 C).
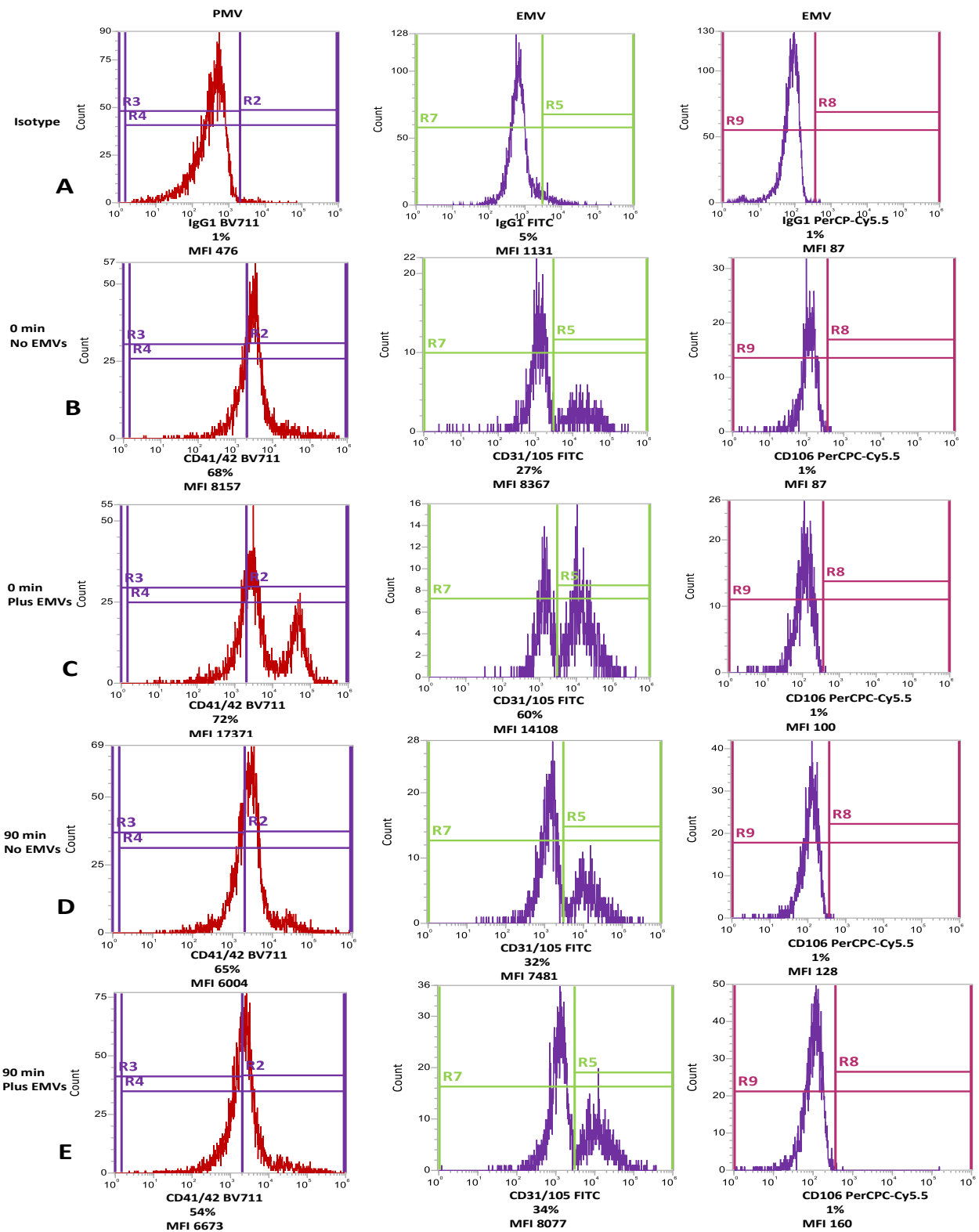
Figure 4.8: Representative flow cytometry histograms. *Thrombi were prepared in the presence and absence of exogenous endothelial microvesicles (EMVs) and blood/plasma were collected at different time intervals. Representative histograms are shown above at each timepoint, and for each phenotype: platelet microvesicles (PMVs) were identified by CD41/42 expression. EMVs were identified as negative for CD41/42 and positive for either or both of CD31/105 or CD106. n=1.*

Samples were stained using F2N12S allowing analysis of membranes. The shorter regions (R2, R5, R8) were used to get the percentage positive, where the histogram region is set using the isotype control. The MFI is only calculated on the whole population and are regions R4, R7, R9. MFI is the median fluorescence intensity of the whole population therefore, R4 shows the MFI of the PMVs. Flow cytometry histograms showing plasma prepared from Chandler Loop. PMVs were identified by CD41/42 expression. EMVs were identified as negative for CD41/42 and positive for either CD31/105 or CD106. Antibodies used were relevant isotype controls (Row A). Plasma prepared from Chandler Loop at 0 minute in the absence of exogenous EMVs, the histograms show surface expression of antibodies (Row B). Plasma prepared from Chandler Loop at 0 minute in the presence of exogenous EMVs, the histograms show surface expression of antibodies (Row C). Plasma prepared from Chandler Loop at 90 minute in the absence of exogenous EMVs, the histograms show surface expression of antibodies (Row D). Plasma prepared from Chandler Loop at 90 minute in the presence of exogenous EMVs, the histograms show surface expression of antibodies (Row E).

The data were collated in Figure 4.9, demonstrating that EMV concentration in the circulating plasma left in the Chandler Loop has reduced numbers of EMVs after 60 and 90 minutes compared to the 0 and 45 minutes time points. This suggests that EMVs are disappearing from the circulation, and with the immunocytochemistry results, suggest that EMVs may be incorporated into the thrombus.

CD31 positive exogenous EMVs concentration
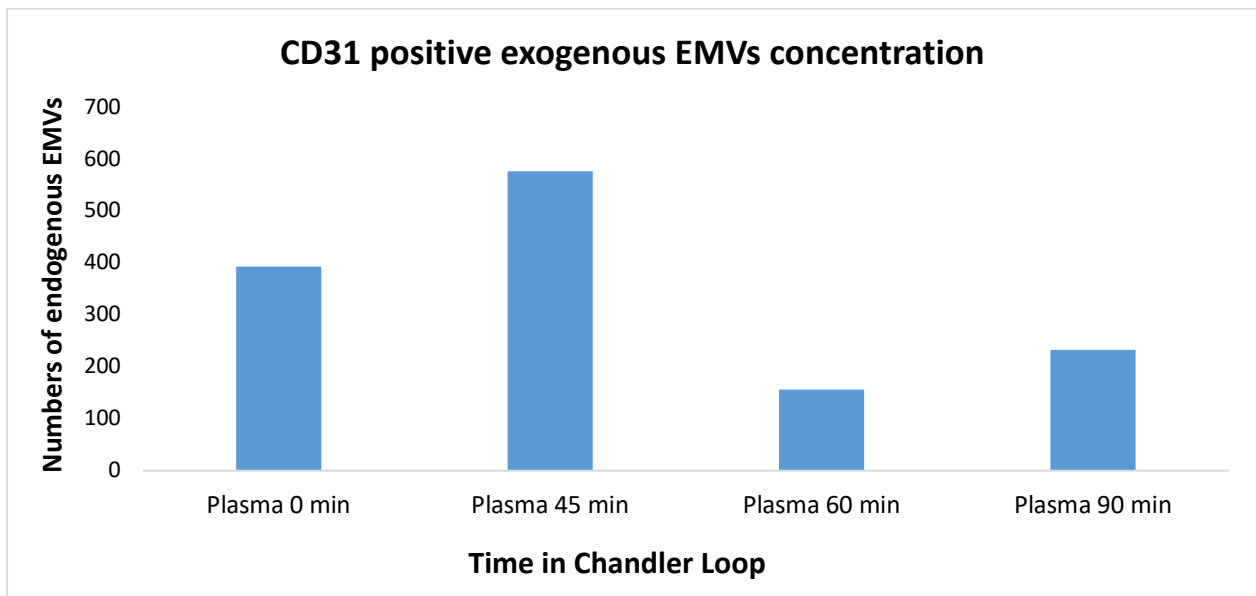
Figure 4.9: Endothelial microvesicles (EMVs) in circulating plasma in the Chandler Loop. *Thrombi were prepared in the presence and absence of exogenous EMVs and blood/plasma. Samples were collected at different time intervals. Supernatants were stained using F2N12S allowing analysis of membranes. Supernatant samples were then analysed on a two-laser dedicated Attune NxT flow cytometry. Added exogenous EMVs at 0 minute show a concentration of approximately 400 EMVs/μL and after 45 minutes the concentration increased to approximately 550 EMVs/μL before decreasing again to 150 EMVs/μL by 60 minutes at a time where a partial thrombus started to form. Concentration has slightly increased again to 200 EMVs/μL at 90 minutes, however, the peak remains approximately half the initial concentration when exogenous EMVs were added (first two bars) which indicates the number of EMVs in plasma decreases and possibly due to incorporation into the thrombus. Blood endogenous EMVs were subtracted and only exogenous EMVs remained. n=1.*

Similarly, when the percentages of CD31/CD105 EMVs and CD41a/42b are investigated, there are more CD31/CD105 EMVs at 0 minutes when exogenous EMVs are added than in the control with no exogenous EMVs added (Figure 4.10). These EMVs are reduced over time, again suggesting that they may enter the growing thrombus. There were not sufficient positive events for CD106 staining to allow data analysis.

125
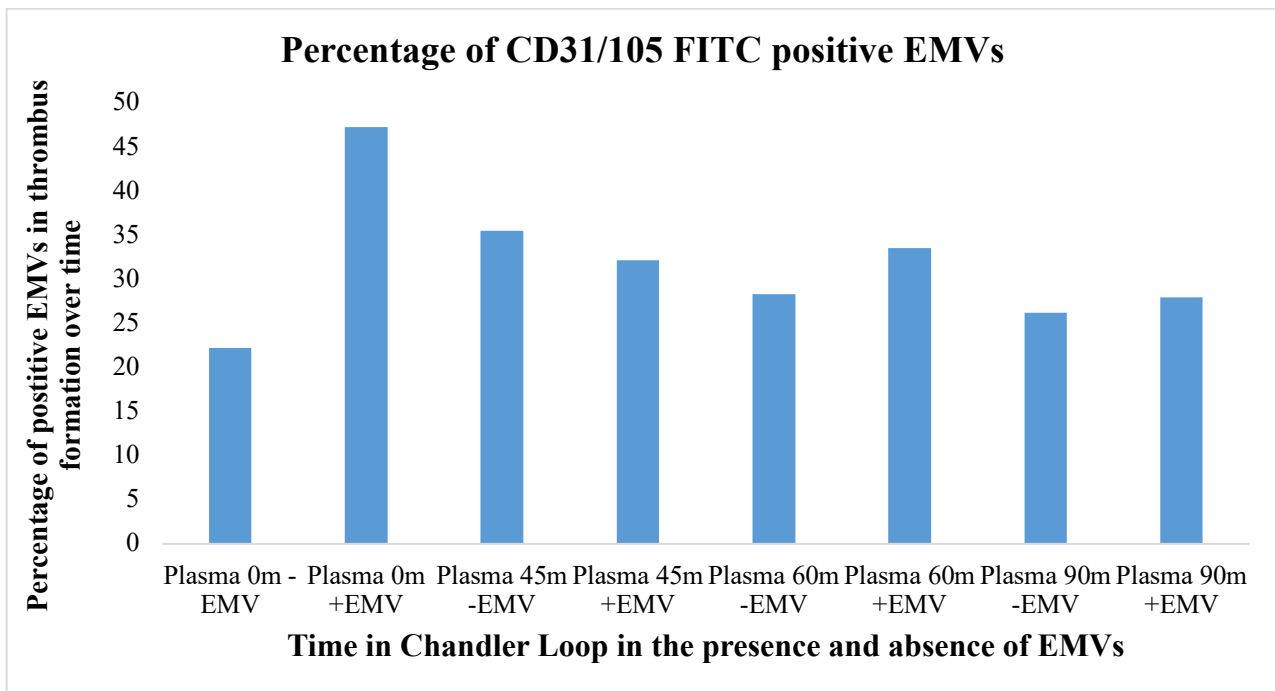
Figure 4.10: Thrombi time-course in the presence and absence of endothelial microvesicles (EMVs). *Thrombi prepared in the presence and absence of EMVs and blood/plasma were collected over a time-course. Supernatants were stained using F2N12S allowing analysis of membranes. Samples were then analysed on a two-laser dedicated Attune NxT flow cytometry. EMVs were identified as negative for CD41a/41b and positive for CD31/105 and background staining was removed using relevant isotype controls. There is a noticeable increase at 0 minute when exogenous EMVs added (46%) in comparison to the absence of EMVs (23%). However, there is a reduction eventually at 90 minutes in the presence of EMVs (28%) in comparison to the initial percentage which suggests the possibility that EMVs leave plasma and are incorporated into the thrombus. n=1.*

In addition to considering numbers of EMVs, the MFI can also be used. This represents the amount of CD31/105 expressed on each EMV. After an initial increase, the MFI stabilises over time (Figure 4.11).

CD31/105 positive EMVs (Corrected MFI)
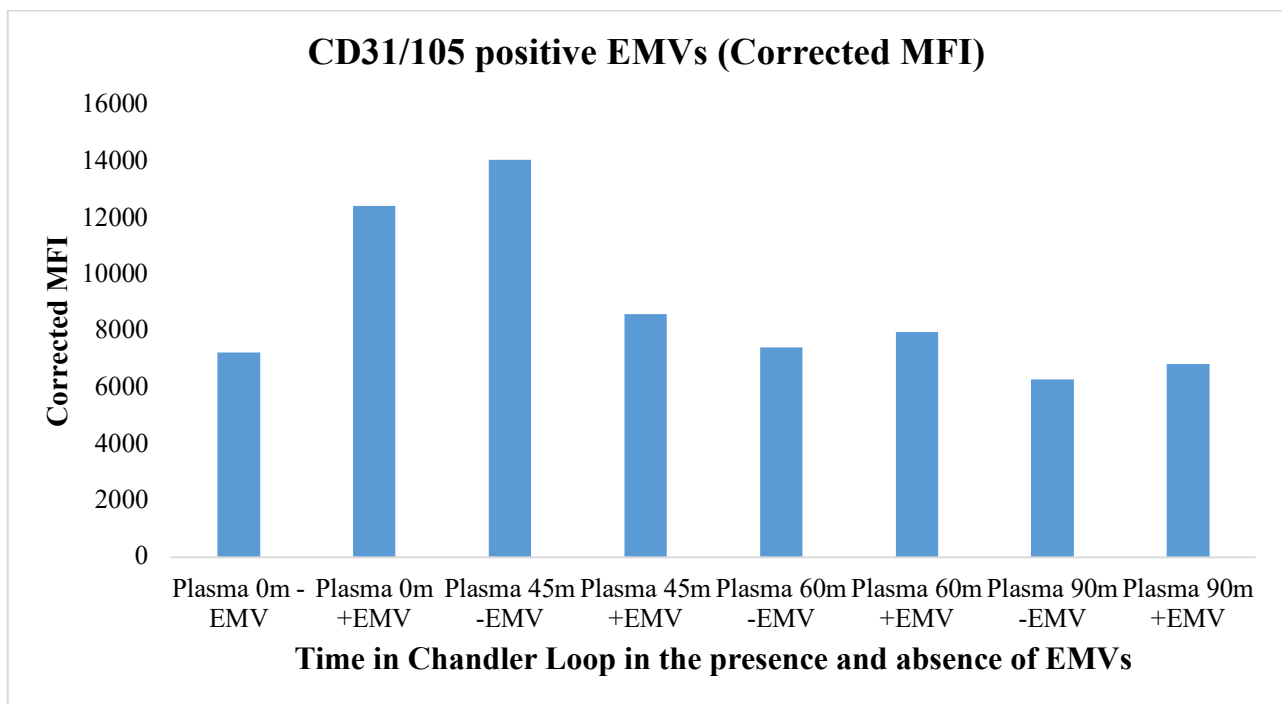
Figure 4.11: Thrombi production in the presence and absence of endothelial microvesicles (EMVs) over 90 minute.
Thrombi were prepared in the presence and absence of exogenous EMVs and blood/plasma were collected over a time-
course. Supernatants were stained using F2N12S allowing analysis of membranes. Samples were then analysed on a two-
laser dedicated Attune NxT flow cytometry. EMVs were identified as positive for CD31/105 given the MFI of added
exogenous EMVs (+EMVs) has exceeded over time. Plasma at 0 minute in the presence of exogenous EMVs (~ 12500)
shows an increase in MFI compared to absence of EMVs at 0 minute (~ 7500). However, at 90 minutes plasma with
added exogenous EMVs shows a noticeable decrease in MFI (~ 7000) whereas without added exogenous EMVs shows a
small reduction (~ 6500) indicating that the numbers of EMVs reduced as thrombus is forming, as EMVs might be left the
plasma and incorporated into the thrombus. n =1.

When the percentage of CD31 EMVs and CD41 are investigated, there is more CD31 EMVs at 0 minutes when exogenous EMVs are added than in the control with no exogenous EMVs added (Figure 4.12). These EMVs are reduced overtime, similarly suggesting that they may enter the developing thrombus.
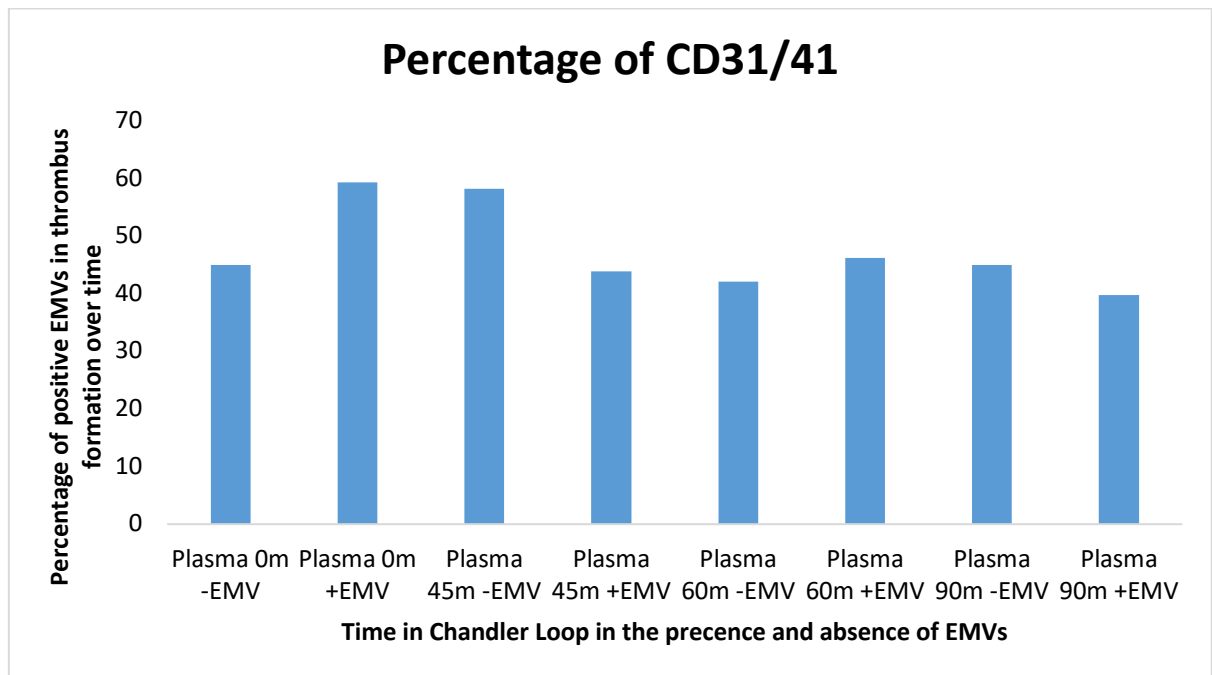
Figure 4.12: Thrombi time-course in the presence and absence of endothelial microvesicles (EMVs). *Thrombi prepared in the presence and absence of EMVs and blood/plasma were collected over a time-course. Supernatants were stained using F2N12S allowing analysis of membranes. Samples were then analysed on a two-laser dedicated Attune NxT flow cytometry. EMVs were identified as negative for CD41a/41b and positive for CD31/105 and background staining was removed using relevant isotype controls. There is a noticeable increase at 0 minute when exogenous EMVs added (59%) in comparison to the absence of EMVs (45%). However, there is a reduction eventually at 90 minutes in the presence of EMVs (39%) in comparison to the initial percentage which may suggests the possibility that EMVs leave plasma and are incorporated into the thrombus. n=1.*

The MFI (Figure 4.13) can also be used complementing the numbers of EMVs (Figure 4.12). The MFI represents the amount of CD31/41 expressed on each MV (Figure 4.13).

CD31/41 (Corrected MFI)
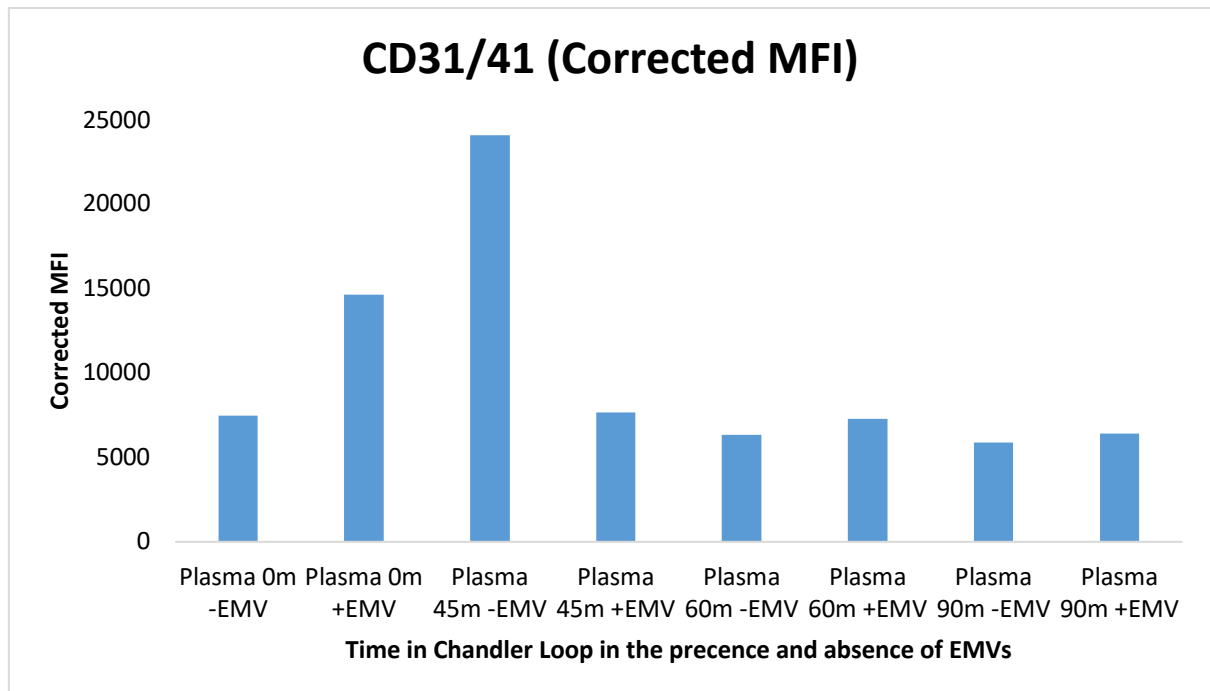
Figure 4.13: Thrombi production in the presence and absence of endothelial microvesicles (EMVs) over 90 minute. *Thrombi were prepared in the presence and absence of exogenous EMVs and blood/plasma were collected over a time-course. Supernatants were stained using F2N12S allowing analysis of membranes. Samples were then analysed on a two-laser dedicated Attune NxT flow cytometry. EMVs were identified as positive for CD31/105 given the MFI of added exogenous EMVs (+EMVs) has exceeded over time. Plasma at 0 minute in the presence of exogenous EMVs (~ 14600) shows an increase in MFI compared to absence of EMVs at 0 minute (~ 7460). However, at 90 minutes plasma with added exogenous EMVs shows a noticeable decrease in MFI (~ 6400) whereas without added exogenous EMVs shows a small reduction (~ 5900) indicating that the numbers of EMVs reduced as thrombus is forming, as EMVs may left the plasma and incorporated into the thrombus. n =1.*

To summarise, these data from the flow cytometer and immunohistochemistry suggest that adding exogenous EMVs to blood under prothrombotic conditions, leads to the incorporation of EMVs into the thrombus.

4.3.3. Do EMVs Increase Anticoagulant APC Activity?

Following the unexpected results of the effect of EMVs on thrombus stability, the effect of EMVs on modulating the generation of APC was examined. Given that APC is a naturally occurring anticoagulant protein that inhibits coagulation, APC may interfere with the balance of haemostasis that is crucial for forming stable thrombi. These experiments were designed to determine whether EMVs contribute directly by carrying/generating APC on their surfaces, whether EMVs contribute indirectly by altering APC generation in the plasma around the thrombus, or whether EMVs contribute indirectly by altering APC generation on the surface of or inside the thrombus.

The findings (Figure 4.14) indicate that there is a significant increase in the quantity of APC associated with surface of the whole thrombus in the presence of EMVs compared to when there are no exogenous EMVs (p value <0.0001, blue bars). There is also an increase in the amount of APC associated with the chopped thrombus in the presence of EMVs in comparison to the absence of EMVs (p value <0.0001, purple bars). However, the plasma directly surrounding the thrombus (p value $=0.18$, pink bars) and plasma collected from the remaining circulating blood (p value $=0.9$, black bars) shows no difference in the amount of APC with or without EMVs. In addition, it is clear from these data that EMVs do not carry appreciable APC activity (p value $=0.96$, green bars). These results support the hypothesis that EMVs alter anticoagulant APC activity during formation of thrombi and therefore EMVs may reduce thrombus formation via the APC pathway.

The effect of EMVs on APC activity associated with thrombi
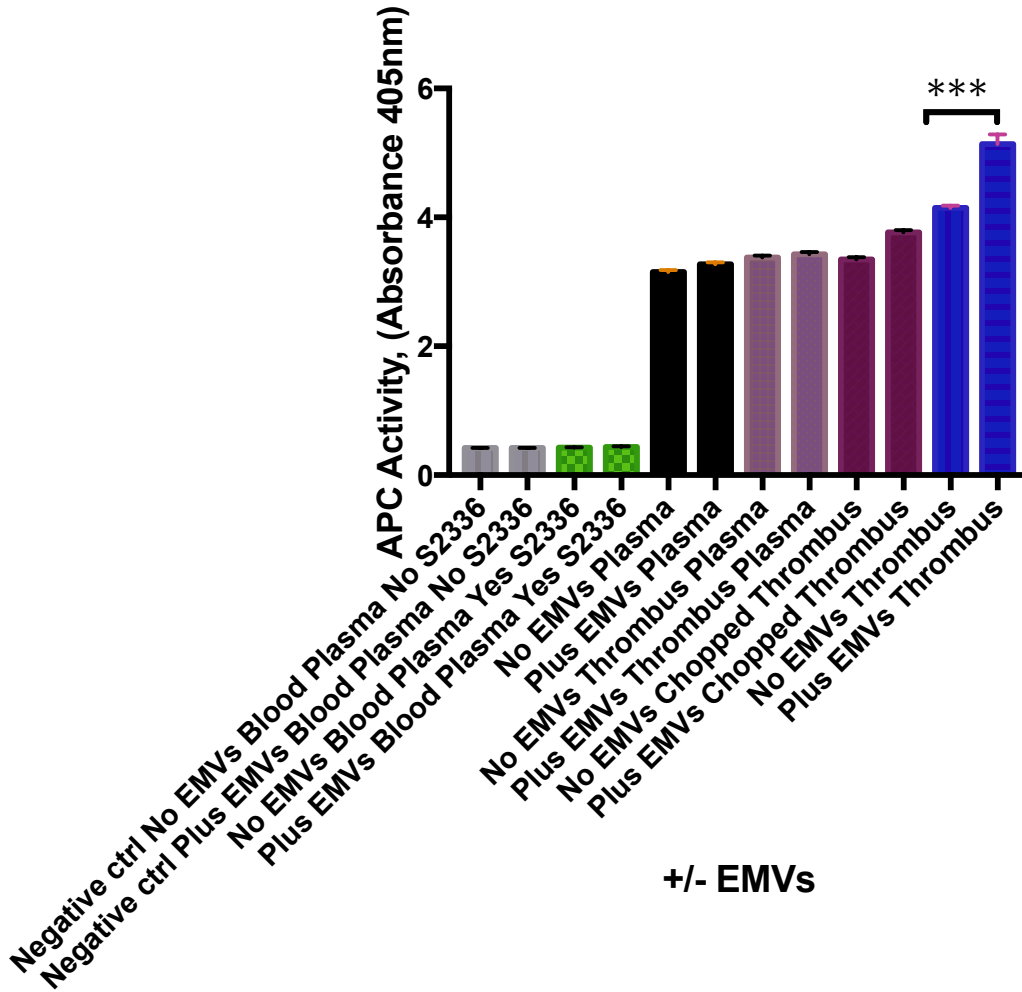
Figure 4.14: Detection of activated protein C (APC) activity on, in and around a thrombus during thrombus formation. Thrombi were made in the presence or absence of exogenous EMVs. Samples collected and used for APC measurements were plasma from the loop (black bars), plasma from around the thrombus (pink bars), thrombus chopped into small sections (purple bars) and whole thrombus (blue bars). In addition, the APC activity of EMVs themselves were assessed (green bars) along with negative control (grey bars). APC activity was assessed using a chromogenic substrate. Asterisks indicate a statistically significant (p value < 0.05) difference between groups. n=8.

TM is one of the key receptors in the generation of APC and is carried on ECs that form the thrombus (Mosnier and Bouma, 2006). The effect of EMVs on the quantity of TM associated with thrombi is shown in Figure 4.15. Due to the low sample number, no statistics could be performed. EMVs did not appear to carry TM in detectable levels (pink bars). In plasma (blue bars) EMVs also were not associated with higher TM. However, in plasma recovered from around the thrombus (brown bars) TM levels were higher when EMVs were present during thrombus formation, but remained under the limit of detection (246.6pg/ml) described in manufacturer's kit. In addition, in samples of the thrombus when the interior was exposed by chopping (purple bar) the amount of TM was considerably higher (1540pg/ml), above the detectable levels. This suggests that it is possible for EMVs to cause increased TM in/on the cells that are incorporated in the thrombus, perhaps leading to an increase in APC generation and instability of the thrombus.
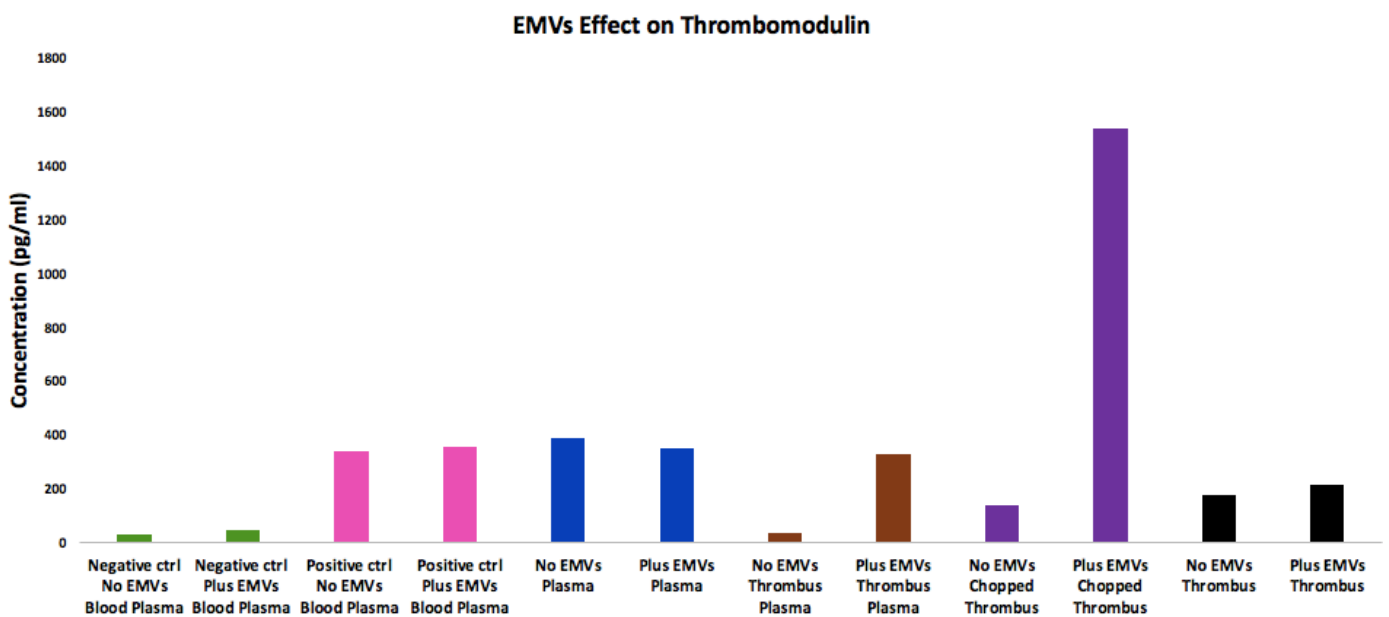
Figure 4.15: Thrombomodulin (TM) production on, in and around a thrombus during thrombus formation. Thrombi were formed in the presence/absence of exogenous endothelial microvesicles (EMVs) in the Chandler Loop. Samples collected and used for TM measurements were plasma from the loop (blue bars), plasma from around the thrombus (brown bars), thrombus chopped into small segments (purple bars), and whole thrombus (black thrombus). In addition, the production of TM of EMVs themselves was assessed (pink bars) along with negative control (green bars). TM production was assessed using TM- ELISA. Experiment conducted once, with two replicate wells of each loop. n =1.

4.4. Discussion

Although present at relatively small concentration in the circulatory system, EMVs have been reported to be associated in several pathologies, particularly in those initiated by endothelial dysfunction such as CVD. However, currently, it is unclear whether elevated EMVs levels are simply a consequence of pathology or are involved in the pathophysiology of disease. Therefore, this chapter aims to determine the role of EMVs in thrombus formation. Following thrombi production (Section 3.3.2), it was hypothesised that adding exogenous EMVs enhance thrombus formation, therefore, the aim was to investigate whether exogenous EMVs contribute to bigger and solider thrombus production. This was determined by preparing thrombi using the Chandler Loop and adding different concentrations of exogenous EMVs. This study demonstrated that EMVs produce smaller thrombi which have a less stable structure (Figure 4.6.). This was not expected, because it has been previously suggested that EMVs have procoagulant activity due to membrane proteins and lipids (Dahlbäck and Villoutreix, 2005) and high EMV levels have been associated with MI. In contrast, in this chapter EMVs appear to support the anticoagulant activity. This may potentially be beneficial in terms of reducing thrombus formation.

EMVs are shed from plasma membranes in response to vascular injury display negatively charged phospholipids on their surfaces as well as the possible presence of TF that can initiate and accelerate coagulation (Burmmez *et al.*, 2011) However, in this chapter, it is hypothesised that they may have some coagulant property at one or more stages during thrombus formation before they indirectly signal to pathways and therefore starting an anticoagulant effect and thrombi initiate retraction, becoming smaller. Therefore, EMVs may have anticoagulant process at later stages limiting thrombus size and promoting dissolution, because, anticoagulant properties may also be found in MVs through binding and promotion of protein C, a vitamin K-dependent anticoagulant protein. This protein activated by thrombin bound to TM, along with protein S cofactor inactivates factors Va and VIIIa. Furthermore, previously, it was identified that approximately 25% of anticoagulant activity was related to the release of MVs from platelet activation by thrombin. Protein S binding with these

133

MVs via the N-terminal domains stimulates the binding and activation of protein C (Kebarle and Verkerk, 2009). Moreover, cultured ECs taken from human blood display presence of EPCR that binds protein C and further develop its activation in the thrombin/TM complex (Dörffler *et al.*, 2003; Nouman, 2019). Another possible hypothesis is that when there is vascular damage, the blood vessels attempt rapid repair by releasing procoagulant EMVs which move rapidly to the plug site and adhere to activating cells to form fibrin. After the vascular breach has been plugged, then the EMVs released are anti-coagulant to prevent the thrombus from growing larger and becoming very stable that it is difficult to remove later by fibrinolysis. This means that EMVs may actually be protective and may simply be found at increased concentrations in conditions such as MI due to their protective role. One consideration is that pharmacological thrombolysis has to occur in a strict timeframe (6 hours for stroke; 1 hour for MI) (Romero *et al.*, 2013; nice.org.uk) and that EMVs may act to allow later natural thrombolysis. However, all these assumptions require validation because currently the research on the role of EMVs as anticoagulant factors is scarce. Nevertheless, if high levels of EMVs present in the body may suggest that the thrombus may not persist for as long which is advantageous for MI infarction and stroke patients. This means potentially they may not require manufactured thrombolytic therapy. Furthermore, the main purpose of haemostasis is mechanical in nature. Independent of the biochemical aspects of thrombus formation, the thrombus must eventually be mechanically stable enough to reduce blood loss. Several mechanical forces that act on bulk blood achieve this by regulating the haemostasis process at the macroscale. Blood cells found in an extremely dynamic environment as they constantly circulate through the vasculature for the entirety of their lifespans (Liu et al., 2006; Romero *et al.*, 2013). The main mechanical stimuli acting on these blood cells include shear stress caused by fluid friction and hydrodynamic forces exerted on the cells by the moving fluid (Vande et al., 2006). However, to exist in such environment, the thrombus formed by these cells must themselves be mechanically stable to form a functional plug while avoiding increased stiffness such that thrombus dissolution cannot occur once the wound is healed. Therefore, adding exogenous EMVs may have some affect and the major affect is caused at

mechanical and macroscales. Although EMVs are generally categorised as procoagulant inducers, they may also possess anticoagulation properties (Vallet and Wiel, 2001). Therefore, possibly, the relative contribution of the procoagulant and anticoagulant properties of MVs to their overall haemostatic function depends on the specific conditions that are being investigated (De Caterina *et al.*, 2013; Pérez-Casal *et al.*, 2009). Therefore, the procoagulant and anticoagulant properties of EMVs in haemostasis require further investigations both *in vitro* and *in vivo* (Mohan Rao, Esmon and Pendurthi, 2014). Furthermore, exogenous EMVs were added to investigate whether they affect thrombus formation and thrombus stability. This was shown in Figure 4.6 which shows that adding exogenous EMVs significantly reduced thrombus formation at 90 minutes in comparison to control (0 minute) which may indicate that the shear stress of the EMVs causing this effect, permitting cells being more susceptible to the effects of EMVs. Furthermore, data from EC research suggest that low shear stress increases the release of EMVs (Loyer *et al.*, 2014), possibly reflecting pathological vascular remodelling. This is logical, since an imbalance between physiologic and pathologic shear stress has traditionally been considered one of the major elements implicated in atherosclerotic plaque formation. These findings (Figure 4.6 A) concurrent with findings from Figure 4.6 B where adding exogenous EMVs reduced thrombi formation which can be observed macroscopically, which indicates the possibility EMVs being involved in anticoagulant function. Therefore, the hypothesis that EMVs make bigger thrombi is rejected. However, further investigation is required analysing various coagulation factors as well as possible pathways which EMVs may influence, because accumulating evidence strongly suggests that EMVs have pro-coagulant and pro-inflammatory effects, indicating that they are not only an indicator of endothelial damage or CVD risk but also possible pathogenic factors. Such pro-thrombotic and pro-coagulation activity of EMVs was studied in an investigation carried out by Abid Hussein et al., which demonstrated that thrombin formation *in vitro* and thrombus formation *in vivo* is triggered by HUVEC-derived EMVs in a TF-dependent manner (Abid Hussein *et al.*, 2007). However, it has also been demonstrated that under healthy conditions, vessel homeostasis is driven by the anti-inflammatory, anti-thrombotic and anti-

atherogenic properties of the endothelial monolayer and it is suggested that endothelial integrity is maintained by cell regeneration and the mobilisation of endothelial progenitor cells from the bone marrow (Curtis *et al.*, 2010). Some studies have found a protective function of EMVs as well, such as that EMVs prevent lipid-induced endothelial damage via Akt/eNOS signalling *in vitro* (Curtis *et al.*, 2009)

This chapter was designed to investigate whether EMVs are incorporated within the thrombus using two complimentary methods (flow cytometry and immunohistochemistry). Data from Figure 4.7 for example show that EMVs are incorporated into the thrombus, as it shows possible clusters of EMVs within the thrombus as well as the possibility of EMVs attached to other cell types. In the future, this could be further analysed and confirmed by using additional techniques such as electron microscopy. The significance of the physical forces involved in the transport and localisation of EMVs in flowing blood cannot be emphasised enough. In order for EMVs to contribute to the growth of thrombus, they must leave the bulk blood flow and localise to the site of thrombus formation. Some studies in animal models of thrombosis illustrated the incorporation of MVs into developing thrombi (Gallart-Palau, Serra and Sze, 2016). Therefore, hypothesising that EMVs are incorporated into thrombus can be accepted. However, the flow and transport factors contribute to this process have not been studied in detail. Therefore, examining the physical influence of EMVs delivery to the injured vessel wall or the site of mural thrombus is important in order to determine the conditions that facilitate or promote the localisation of EMVs into thrombi.

Data presented in this chapter demonstrated an increase in APC activity is associated with thrombi formed in the presence of exogenous EMVs. These findings are consistent with other data demonstrating that EMVs regulate coagulation through anticoagulant or fibrinolytic mechanisms (Pérez-Casal *et al.*, 2009). EMVs have been shown to harbour functionally active TFPI on their membrane (Brummel et al., 2011) and facilitate APC and protein S mediated regulation of coagulation (Koshiar et al., 2014). These preliminary findings suggest that EMVs alter thrombus

formation and caused them to be less stable. A suggested mechanism for APC increases by EMVs is that EMVs are directly or indirectly increasing the presence of APC on ECs or they enhance anticoagulant activity through cell signalling (i.e., platelets or monocytes) which lead to less stable thrombus.

TM overexpression has been reported to reduce thrombus formation in rabbits' femoral arteries (Curtis et al., 2009). In support of this hypothesis, patients with TM-deficiencies have been shown to have a higher risk of early MI (Curtis et al., 2009). Findings from this chapter could be further extended by exploring the distribution of EPCR as some studies have established that EPCR plays a significant role in protein C activation by thrombin-TM complex (Dahlbäck and Villoutreix 2005; Navarro et al., 2011; Mohan et al., 2014). Another suggested mechanism is that the whole thrombus contains more anticoagulant activity on the surface causing an increase in APC production. However, when the thrombus is chopped into small segments there may be protein C inhibitor i.e., serpina5 inhibits APC. Particularly as protein C inhibitor has been reported to act as a procoagulant inhibitor by inhibiting the TM-induced activation of protein C in human plasma (Dörffler *et al.*, 2003). As it was shown that both TM and EPCR are important to protein C activation, TM on EMVs, plasma and thrombus was measured by ELISA. It was hypothesised that adding exogenous EMVs decreases TM production in thrombus formation. The TM-ELISA results provided an idea for EMVs effect on TM production (Figure 4.15). TM levels were particularly increased in chopped thrombus where EMVs were added, however, no difference in TM levels in whole thrombus. This was not expected, as the decreased TM levels did not correspond with the consistent rise in APC production by adding EMVs. Possible explanations for inconsistencies, would be that surface EPCR regulation may have also been altered, as well as the amount of TM released may not accurately reflect membrane TM expression. Furthermore, TM only increased on the chopped thrombi and not the whole thrombi, this could be that EMVs are interacting with the cells to change TM concentration i.e. inhibition of TM on the outside of the thrombus but it is protected from it on the inside of the thrombus. However, future investigation is required repeating the same experiment as well as exploring regulation of surface

EPCR, released EPCR and surface TM to understand the precise mechanism of APC production. Moreover, the effect of TNF-α and EMVs on APC production is explored in Appendix 8.6. Data from the involvement between EMVs and anticoagulant APC showing a possible anticoagulant activity which led to further investigate the coagulant side of the haemostatic balance. This required using coagulation assays such as clot-based tests to provide a global assessment of coagulation function and/or and chromogenic assays to measure the level or function of specific coagulation factors. Unfortunately, due to limited timing this was not possible. Therefore, in the future coagulation testing such as F1+2 and/or thrombin-antithrombin ELISAs or thrombin chromogenic substrates should be used to further investigate the coagulant side of the haemostatic balance (Section 7.4.1).

Despite numerous studies on the role of EMVs in diseases, the functional significance of spontaneously present EMVs is unclear. Circulating EMVs in healthy controls were shown to support low-grade thrombin production by the contact pathway (Raposo and Stoorvogel, 2013). Whether EMVs originating under physiological circumstances can provide sufficient activity to promote blood coagulation is unclear. Furthermore, particularly little is known about potential effects of EMVs on fibrin thrombus formation and lysis, the determinant stages of blood coagulation. The literature suggests that EMVs could act as a potential biomarker of disease stage and CVD risk, as well as a potential therapeutic tool or a signalling mechanism (Hansson et al., 2006). Although, strong correlations between EMVs levels, fibrin thrombus permeability and resistance to lysis in patients with CAD have been discovered (Berckmans et al., 2001), the question remains unanswered as to whether EMVs naturally circulating in blood have a potential to affect haemostasis and can be an additional physiological determinant of the structure and properties of a thrombus determined largely by the fibrin network scaffold. Therefore, it is necessary to gain further understanding of the whole process, including their role in health and disease and their mechanism of action. New knowledge would provide the necessary insight to allow research into developing novel therapies.

4.5. Conclusion

In CVD, inflammation provides a pro-thrombotic state and drives the formation of atherosclerotic plaques. These findings suggest that EMVs may promote APC production during inflammation may provide a use for EMVs in the therapeutic setting, increasing anticoagulant APC activity and therefore reducing inflammation and coagulability, potentially reducing the risk for CVD. Furthermore, the findings in this chapter showed that EMVs increase the production of APC inducing anticoagulant activity possibly via EMVs signalling to cells to carry out anticoagulant properties. These are suggested mechanisms, therefore, although the results are promising, must be taken with caution and expansion of this work could strengthen the role of EMVs in thrombus formation to show their clinical relevance. Therefore, more research is required which would help to understand the mechanisms in which this possible anticoagulant functioning occurs. Links between EMVs and APC pathway is a novel area and could play a vital role in the future.

Chapter 5: The Role of Lipid Composition and Bilayer Structure in EMV Formation

5.1. Introduction

Lipids are a fundamental component of MVs and provide a scaffold into which other cargos, proteins, signalling molecules (both soluble and membrane bound) and nucleic acids (e.g., miRNAs can be packaged) prior to secretion as part of the MV (McMahon and Gallop, 2005; Skotland et al., 2020). Various types of lipids are present on MVs; however, interestingly their lipid composition differs from the membrane of secreting cell (Chen et al., 2020). The formation of MVs demands the creation of a bilayer with a high degree of curvature (Vanni et al., 2014; Record et al., 2018). Particular lipids are known to favour the formation of these curved surfaces, whilst others provide resistance to bending, properties that are encoded both by the structure/shape of the individual lipids and the interactions between them (Doyle and Wang, 2019).

5.1.1. Membrane Curvature and Lipid Packing

Membrane curvature is often observed in membranes and arises as a result of the structure of the lipids present, the types of interactions they exhibit between each other and the asymmetric distribution of lipids in the inner and outer leaflets (Record et al., 2018) (Section 1.2.6). Lipids have intrinsic shapes depending on the size of their headgroups and the size and degree of unsaturation of the acyl chains, therefore, the shape of the constituent lipids affect the curvature. For example, lipids with short tails and large heads induce a positive curvature whereas lipids with long tails induce negative curvature (Figure 5.1) (Harvey and Boucrot, 2018). Collectively the packing of these lipids side-by-side impose a shape on the monolayer. If several lipids with similar shape cluster together, then a monolayer will adopt the spontaneous curvature associated with a particular classes of lipids present (Record et al., 2018). As the two leaflets of the bilayer are coupled the spontaneous curvature of the bilayer mirrors the spontaneous curvature of the inner and outer monolayers (Ratajczak and Ratajczak, 2017). The shape adopted by the bilayer is also influenced by the nature of the interactions occurring between the lipid present, with electrostatic repulsion between the headgroups of charged

lipids contributing to a positive curvature, whilst the presence of cholesterol interrelated between the acyl chain serves to rigidify the lipid bilayer limited elastic deformation. These interactions not only influence the lipid bilayer physical properties but also the formation and secretion of MVs (Ratajczak and Ratajczak, 2017; Record et al., 2018).
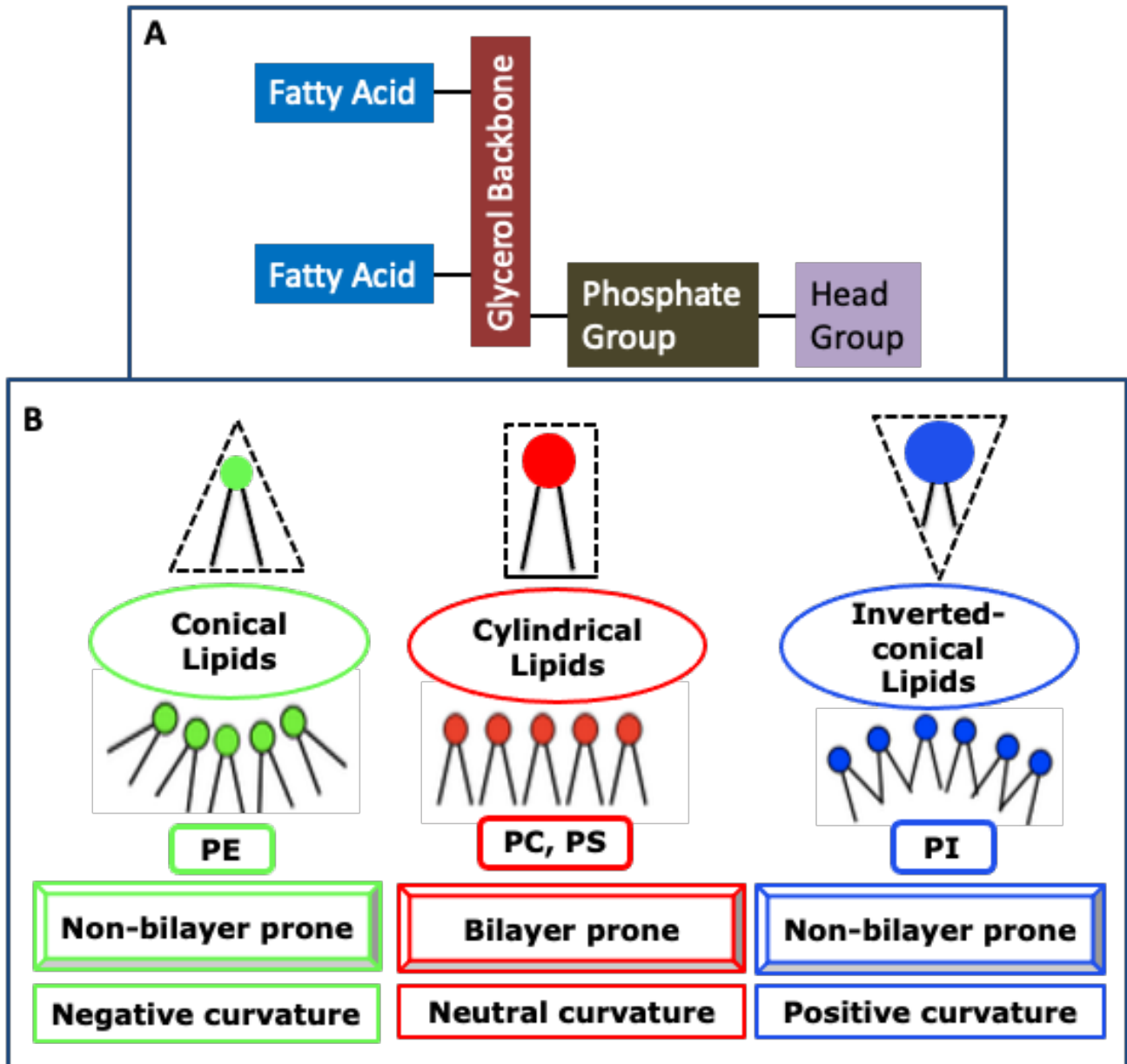
Figure 5.1: Schematic representation of the lipids shape with their representative lipids for each shape. *A) a phospholipid. B) The effect of lipid shape. The size of both the polar head and the tails affect the shape of the lipid bilayer. Lipids with an equal head to chain ratio (cylindrical lipids) are neural such as PC and PS. Lipids with a small area ratio of polar head to acyl chain (conical lipids) induce negative curvature such as PE. Lipids with a larger head compared with the acyl chain area (inverted-conical lipids) induce a positive curvature such as PI. PC=Phosphatidylcholine, PE=Phosphatidylethanolamine, PI=Phosphatidylinositol, PS=Phosphatidylserine.*

5.1.2. MVs-Membrane and Lipids in Coagulation

The highly curved outer membrane of MVs is rich in anionic, unsaturated phospholipids (i.e., PS, PI), whose negatively charged headgroups repel each other driving positive curvature (Chen et al., 2020). This differs from the outer leaflet of the plasma membrane which is typically neutral (Section 1.4.2). Accordingly, MVs present a very different membrane surface than the surrounding cells and the presence of anionic lipids on the outer leaflet, and despite this property being shared with several cancer cells, can be considered as a "universal" marker for MVs alternative or complementary to traditional, characteristic surface-associated proteins (Ridger et al., 2017).

Lipids are involved in coagulation (Section 1.2.6), as well as inflammation (Section 1.4.7 and 1.4.9). Lipids enter the coagulation cascade after it has been initiated by surface contact and other protein interactions (Panfoli et al., 2018). They are also suggested to play a role in anticoagulation activity through membrane lipids (Angelillo-Scherrer, 2012; Ridger et al., 2017). The anticoagulant APC (Section 4.3.3) is centred on inactivation of FVa and VIIIa, and involves lipid cofactors (Levi and Poll, 2017). For instance, PS forms a complex with APC on the phospholipid surface and further elevating the affinity of APC for negatively charged phospholipids (Dasgupta *et al.*, 2009; Dini et al., 2020). Furthermore, PS repositions the APC active site closer to the membrane surface, which includes the activated coagulation factors. In the inactivation of FVIIIa, FV and PS act as synergistic cofactors to APC (Shkair et al., 2021). PS similarly has direct anticoagulant properties independent for APC (Abid Hussein *et al.*, 2008; Ratajczak and Ratajczak, 2017). It was demonstrated to directly inhibit the activity of the prothrombinase complex, presumably by binding to cofactors VIIIa, Va and Xa (Mallia et al., 2020). Moreover, phosphorylated PI species have also been suggested to enhance the membrane binding of APC (Tavoosi et al., 2013; Mallia et al., 2020). Nevertheless, the physiological role of these findings is the subject of active research.

5.1.3. Techniques Employed To Study The Phase Behaviour and Composition of The Bilayer

With the lipid composition of the parent membrane and the MVs playing an important role in influencing the budding of MVs and their subsequent mode of action, this chapter aims to characterise the lipid composition and understand how this may influence the budding of the MVs and subsequent signalling events underpinning haemostasis. To address this, used a combination of ^{31}P magic angle spinning NMR (^{31}P-MAS-NMR) and electrospray ionisation mass-spectrometry (ESI-MS). The relative abundance of the phospholipids present in the membrane can be determined by ^{31}P-MAS-NMR where the different phospholipid species can be identified through their unique chemical shifts and their relative abundance ascertained from the relative signal intensities. Furthermore, analysis of the line-shapes obtained can also provide insights into the types of lipidic phases formed (Luga et al., 2007). This has been complemented with ESI-MS, which is an excellent reporter of the chain composition of the lipids present in the bilayer, allowing the identification of both chain lengths and the degree of unsaturation (Banerjee and Mazumdar, 2012). Collectively, these methods provide an ideal tool with which to characterise both the chemical composition of the bilayers under study and the types of structures that they form. Both techniques are described in Appendix 8.7, which are important for the interpretation of the data presented in this chapter. The overall contribution of this chapter to the global thesis is shown in red in Figure 5.2.
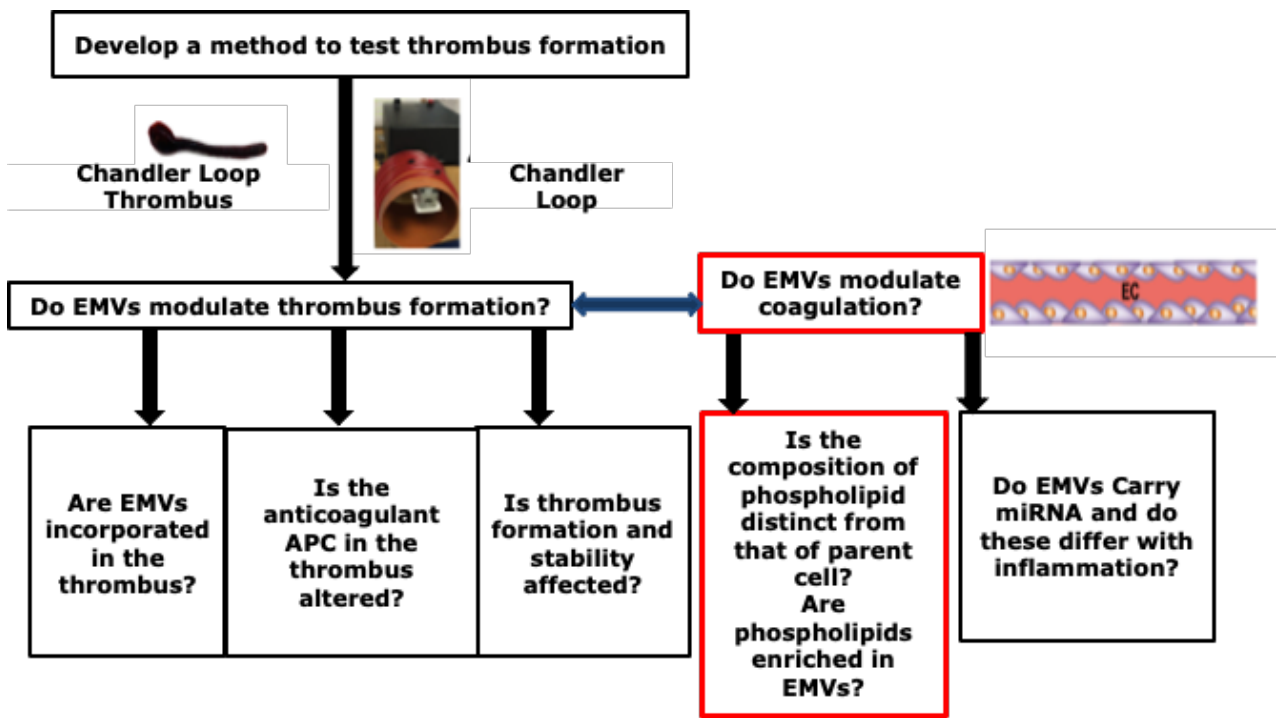
Figure 5.2: Process workflow diagram. *In Chapter 3 the Chandler Loop was developed to test thrombus formation. In Chapter 4 exogenous EMVs were added to blood to investigate whether these EMVs modulate thrombus formation. This chapter will explore the composition of membrane-lipids of parent cells (HUVECs and EA.hy926) and their derived EMVs. Furthermore, will explore whether TNF-α stimulation will influence phospholipid composition. These investigations will be conducted by ^{31}P-MAS-NMR to assess the headgroups and ESI-MS to obtain an understanding of the chain composition of the lipid species present.*

5.1.4. Hypothesis and Aim

Lipid composition and bilayer structure is important in the formation and secretion of EMVs. Therefore, it is important to understand the influence this may have on the formation and secretion of the EMVs and subsequent signalling events underpinning haemostasis.

5.1.4.1. Hypothesis

Lipid composition and bilayer structure of EMVs is distinct from that of their parent cell and this bilayer composition favours vesicle formation.

5.1.4.2. Aims

- To investigate the relative abundance and phase behaviour of the phospholipid species present in both parent cell and derived EMVs.
- To analyse the lipid chains to ascertain the nature of the species present and the influence these may have on bilayer structure.
- To ascertain whether TNF- α stimulation of the cells influences the composition and structure of the parent membrane.

5.2. Methods

5.2.1. ^{31}P-MAS-NMR Analysis of Membrane Lipids

HUVECs and EA.hy926 were collected as described in Section 2.3, and EMVs were collected from the supernatant of growth medium of parent cells as described in Section 2.4. Pelleted membrane samples were collected and packed into a 3.2mm Agilent rotor for ^{31}P-MAS-NMR analysis. Experiments were performed on a Varian DD2 Agilent 600 MHz spectrometer (Yarnton, UK). ^{31}P-MAS-NMR spectra were acquired at 242.02 MHz using a triple-resonance 3.2mm MAS probe. Unless otherwise stated the samples were measured at 25°C with 6 kHz spinning. MAS spectra were acquired using a 3.5 ms 90° pulse for excitation and 75 kHz SPINAL decoupling during acquisition. Chemical shifts were externally referenced using H_3PO_4 (85%) (Sigma-Aldrich, UK, product number: 7664-38-2) as a standard. Prior to Fourier Transform, data were zero filled to 4096 points and 75 Hz line broadening applied. The data were analysed using Mat-NMR (J.D, Van Beek., 2007).

5.2.2. ESI-MS Analysis of Membrane Lipids

HUVECs were collected as described in Section 2.3.1, and EMVs were collected from the supernatant of growth medium of parent cells as described in Section 2.4. Then total lipid was extracted from EMVs using dichloromethane (DCM) (Merck, UK, product number: 270997). Internal quantification standards were added to samples prior to extraction, including 2 nmol dimyristoylphosphatidylcholine (DM-PC14:0/14:0) (Merck, UK, product number: 890809), 0.2nmol lyso-phosphatidylcholine (L-PC 17:0) (Merck, UK, product number: 890808), 0.8 nmol dimyristoylphosphatidylethanolamine (DM-PE14:0/14:0) (Merck, UK, product number: 890810), 0.4 nmol dimyristoylphosphatidylserine (DM-PS14:0/14:0) (Merck, UK, product number: 899800), 0.4 nmol dimyristoylphosphatidylglycerol (DM-PG 14:0/14:0) (Merck, UK, product number: 899500) and 0.2 nmol dimyristoylphosphatidic acid (DM-PA14:0/14:0) (Merck, UK, product number: 899854) per sample. Lipids were extracted by sequential additions of 0.9% NaCl (0.8 ml) (Merck,

UK, product number: 105020), DCM (1 ml) and methanol (1 ml) (Merck, UK, product number: 106018), with vigorous mixing to form one phase. Following the addition of a further DCM (1 ml) and high performance liquid chromatography (HPLC) grade water (1 ml) (Merck, UK, product number: 116754), the sample was vortexed and then centrifuged (1,000xg, 10 min, 20°C) resulting the formation of two distinct phases. The lower lipid-rich organic layer was aspirated, transferred to an MS vial and dried at 37°C under as stream of nitrogen gas. Samples were reconstituted in 200µl of a solution containing 20% butanol (Merck, UK, product number: 71363), 60% methanol (Merck, UK, product number: 67561), 16% water and 4% concentrated aqueous NH_3 (Merck, UK, product number: 105432) and introduced by direct infusion using a syringe pump at 10µl/min into a triple quadrupole MS (Xevo TQ, Micromass, UK) equipped with an electrospray ionisation interface. Phospholipid and neutral lipid species were selectively detected and quantified from a variety of precursor (P) and neutral loss (NL) scans with the diagnostic fragment indicated in parenthesis. Scans in positive ionisation included PC, P184, PE, NL141, Chol ester (CE, P369), ceramide (Cer, P264) and DAG NL35. Scans in negative ionisation included phosphatidylinositol (PI, P241), PA, P153 and PS, NL87. Data were processed using MassLynx-MS Software (Water, v4.2) and analysed using a macro developed at the University of Southampton (Postle et al., 2018) The macro enabled spectra to be smoothed, background subtracted, converted into centroid format and exported into individual Excel sample files, which were imported into the analyser programme. Correction for the ^{13}C isotope abundance was performed prior to calculation of percentage composition of individual lipid classes and as percentage of total lipid analysed. Lipid molecular species were reported if they were greater than 1% of the total abundance detected for each individual lipid class (Bligh and Dyer, 1959).

5.3. Results

5.3.1. ^{31}P-MAS-NMR Analysis of Membrane Lipids

To assess the composition of the parent membranes and derived-EMVs, ^{31}P-MAS-NMR was applied to determine both the types and relative quantity of the phospholipid species present. MAS-NMR permitted to resolve the different phospholipid species in the sample based on their distinctive chemical shifts.
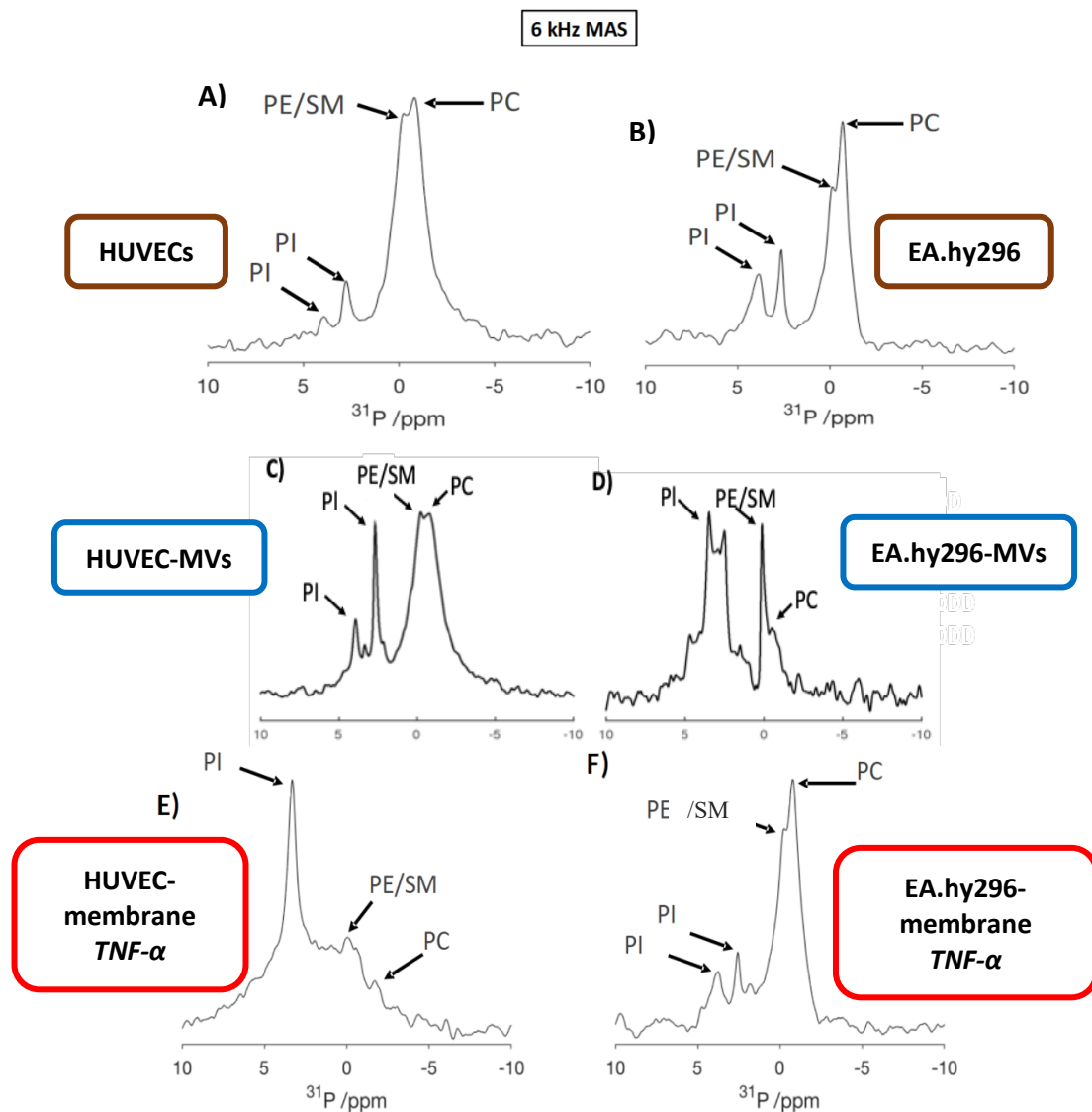
Figure 5.3: ***^{31}P-MAS-NMR spectra of parent cells and derived-MVs.*** *(A) HUVEC membrane; (B) EA.hy926 membrane; (C) HUVEC-MVs and (D) EA.hy926-MVs. Samples (A-D) were cultured in the absence of TNF-α. Whereas samples E and F (HUVEC and EA.hy926 membranes, respectively) were cultured in the presence of TNF-α. The horizontal bar represents the chemical shift anisotropy (CSA) or the isotropic chemical shift (ppm) of each phosphorus in the sample can be observed.*

The ^{31}P-MAS spectrum of HUVEC membranes (Figure 5.3 A) contains two major resonances/peaks at -0.80 ppm and -0.25 ppm. The resonance at -0.80 ppm is consistent with the values reported for isotropic ^{31}P chemical shift for PC (Seelig, 1978; Harris et al., 2001). Based on literature values, this suggests that the chemical shift at -0.25 ppm may arise from the presence of either PE or SM in the samples (Moreau et al., 1999; Harris et al., 2001; Warschawski et al., 2018). In addition to the two major peaks that tentatively assigned to PC and PE/SM there are a further two peaks are observed at 2.73 ppm and 3.96 ppm. Typically signals from the phosphate group that links to headgroup to the glycerol backbone occur in the range of -1.0 ppm to 1.0 ppm (Harris et al., 2001; Grelard et al., 2008; Braunger et al., 2013). Thus, the chemical shifts at 2.73 ppm and 3.96 ppm fall in the same region as resonances observed to phosphates attached to the inositol headgroup in model lipid bilayers (Harris et al., 2001; Michel, 2008).

The ^{31}P-MAS spectrum of EA.hy926 membranes (Figure 5.3 B) reveals a similar distribution of resonances, with peaks at -0.70 ppm and 0.72 ppm, and as for the HUVEC membranes, tentatively assigned to the phosphate linking the headgroup to the backbone in the PC and PE/SM respectively. In addition, as for the HUVEC membranes the spectrum exhibits intensity between 2.0 and 4.0 ppm consistent with the chemical shifts previously reported for phosphates attached to the PI headgroup (Edgar et al., 2009). A more detailed inspection of the data, however, show significant variations in the relative intensities, line-shape and position of some of these resonances, which can provide insight into the relative abundance, bilayer structure and phosphorylation state of PI. The membranes of both parent cells (HUVEC and EA.hy926) show similar lipid composition with resonances tentatively assigned to PC, PE/SM and PI, all showing similar intensities. Furthermore, weak sidebands are observed at +/-6 kHz, which indicate that the lipids are in a liquid crystalline bilayer. Although the peak position should permit the exact characterisation of the inositol species, the sensitivity of the peak positions to variations in pH and membrane surface charge make a definitive assignment challenging (Koijman et al., 2009; Puppato et al., 2007). For example, a study by

Konijman et al., investigated the ionisation properties of the inositol species using ^{31}P-MAS-NMR and demonstrated that an underlying complex ionisation behaviour was linked to the relative positions of each phosphate groups at the inositol rings, and the phosphorylated derivatives hydrogen bond networks which are sensitive to the surrounding pH (Koijman et al., 2009).

The ^{31}P-MAS-NMR spectrum of the HUVEC purified MVs (Figure 5.3 C), reveals dominating resonances at 2.3 and 3.86 ppm. These sharp intense resonances again fall in a region of the spectrum associated with phosphorylated derivatives of PI and the narrow width of the peaks suggest that they are mobile species that are more remote from the surface of the membrane such as an inositol group. Similar resonances are observed in EA.hy926-derived-MVs at 2.93 ppm and 3.66 ppm which tentatively assigned to the phosphorylated derivatives of PI species (Figure 5.3 D). The broader feature underneath, may be additional phospholipid species present in the membrane that are poorly resolved. The width of this peak suggests that the vesicle is tumbling at a similar rate to the MAS, limiting the averaging of the CSA resulting in broad line. This is perhaps expected for EMVs which are between 100 nm and 1 μm in diameter. These data suggest that when EMVs form they undergo tumbling on an intermediate timescale that interferes with the MAS, and in comparison to the parent membranes appear to be tentatively enriched in phosphorylated PIs.

The ^{31}P-MAS-NMR spectrum of TNF-α-treated-HUVECs membrane shows two relatively small resonances at -0.30 ppm and -0.70 ppm (Figure 5.3 E). The resonance at -0.30 ppm which tentatively assigned to PE/SM, whereas the resonance at -0.70 ppm tentatively assigned to PC. In addition, a further dominating peak is observed at 3.3 ppm. This individual peak can be speculated to be a different phosphorylation state of PI, but as highlighted previously given the sensitivity of the groups to surface charge/pH it is difficult to make an unambiguous assignment. In comparison TNF-α treated-EA.hy926 membrane (Figure 5.3 F) is dominated by two resonances at -0.80 ppm and -0.25 ppm. The resonance at -0.80 ppm is consistent with the values reported for isotropic ^{31}P chemical

shift for PC (Moreau et al., 1999; Harris et al., 2001). The resonance at -0.25 ppm could arise from the presence of PC (Harris et al., 2001; Vogt *et al.*, 2014) and thus has been assigned accordingly. In addition, a further two peaks are observed at 2.56 ppm and 3.76 ppm. As eluded previously, these resonances tentatively attribute to negatively charged phosphorylated derivatives of PI. Furthermore, samples prepared in the presence of TNF-α are dominated by phosphorylated PI resonance compared to those prepared in the absence of TNF-α.

In summary, ^{31}P-MAS-NMR was employed to analyse phospholipid composition in parent cells and their derived-EMVs. MAS helps resolve the different phosphate species that present in the lipid bilayer, with the individual species characterised by their chemical shift. The peak intensity is quantitative providing a measure of the relative abundance of a particular lipid species, whilst the width of the peak provides an indication regarding the dynamics experienced by the lipid.

The parent cells and EMVs contain PE/SM and PC. Furthermore, repeatedly throughout ^{31}P-MAS-NMR experiments, there has been resonances appearing between 3 ppm and 4 ppm which consistent with different phosphorylated derivatives of PI.

5.3.2. ESI-MS Analysis of Membrane Lipids

The ESI-MS conducted was able to separate the different classes of lipid (PC, PE etc), measuring the mass-to-charge ratio (m/z) of a charged ion. The resulting spectrum contains a family of charged species that can be used to identify the acyl chains attached to a particular class of lipid. Although not quantitative, for a given lipid species we would expect the efficiency of ionisation to be similar for each number of the family and thus the relative intensity of the peaks for each species provides insight into the chain composition of each lipid. The lipid chain composition of each of the lipid species is reported with distinct peaks in the spectrum corresponding to particular classes of fatty acyl chain, dependent on the mass of the fatty acyl chain.

The ESI-MS data presented below of the chain composition of the species identified by ^{31}P-MAS-NMR. Additional lipids where significancy has been observed are included in Appendix 8.7.4.

3.5.2.1. Phosphatidylcholine (PC)
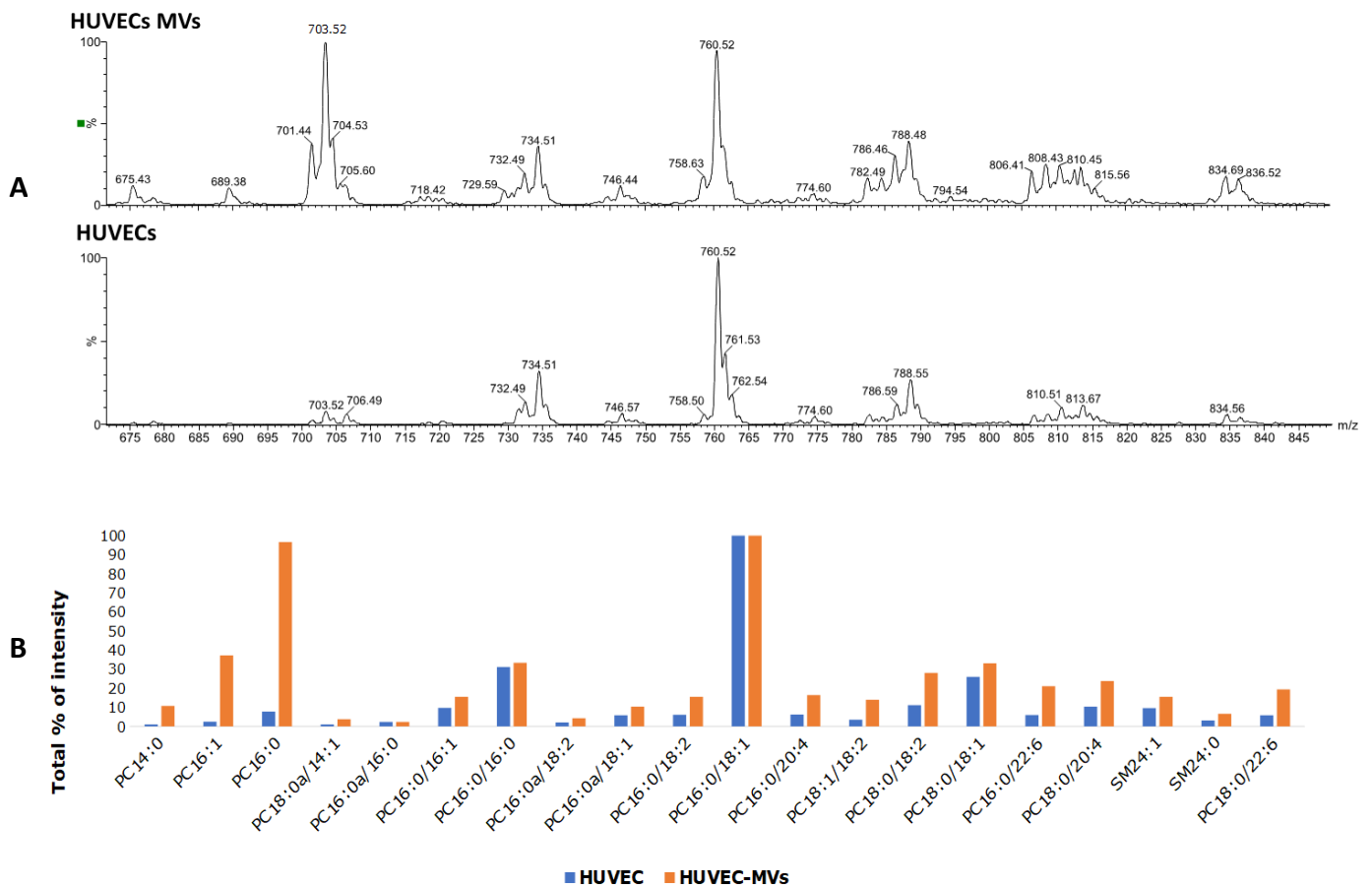
Figure 5.4: ESI-MS quantification of PC species present and normalised intensity of total selected percentage of PC species in HUVEC-membranes and their derived-MVs. *A) The spectra contain a series of different lipid species, where the molecular weight is indictive of the types of chains present. B) Bar chart shows the distribution of PC species between parent cells and EMVs. n=1.*

In the HUVEC membranes, the major species has a m/z ratio of 760.52. This indicates that the PC species is predominantly PC 16:0/18:1. In contrast the EMVs also contain a species with a m/z ratio of 703.52, corresponding to PC 16:0/16:0 indicating the EMVs are enriched in PC16:0/16:0 compared to their parent membrane. Although the change in acyl chain composition is minor, the slight reduction in chain length and the saturated nature of the chain would result in a reduction of the volume occupied by the lipid acyl chains in the PC lipids present.

5.3.2.2. Phosphatidylethanolamine (PE)
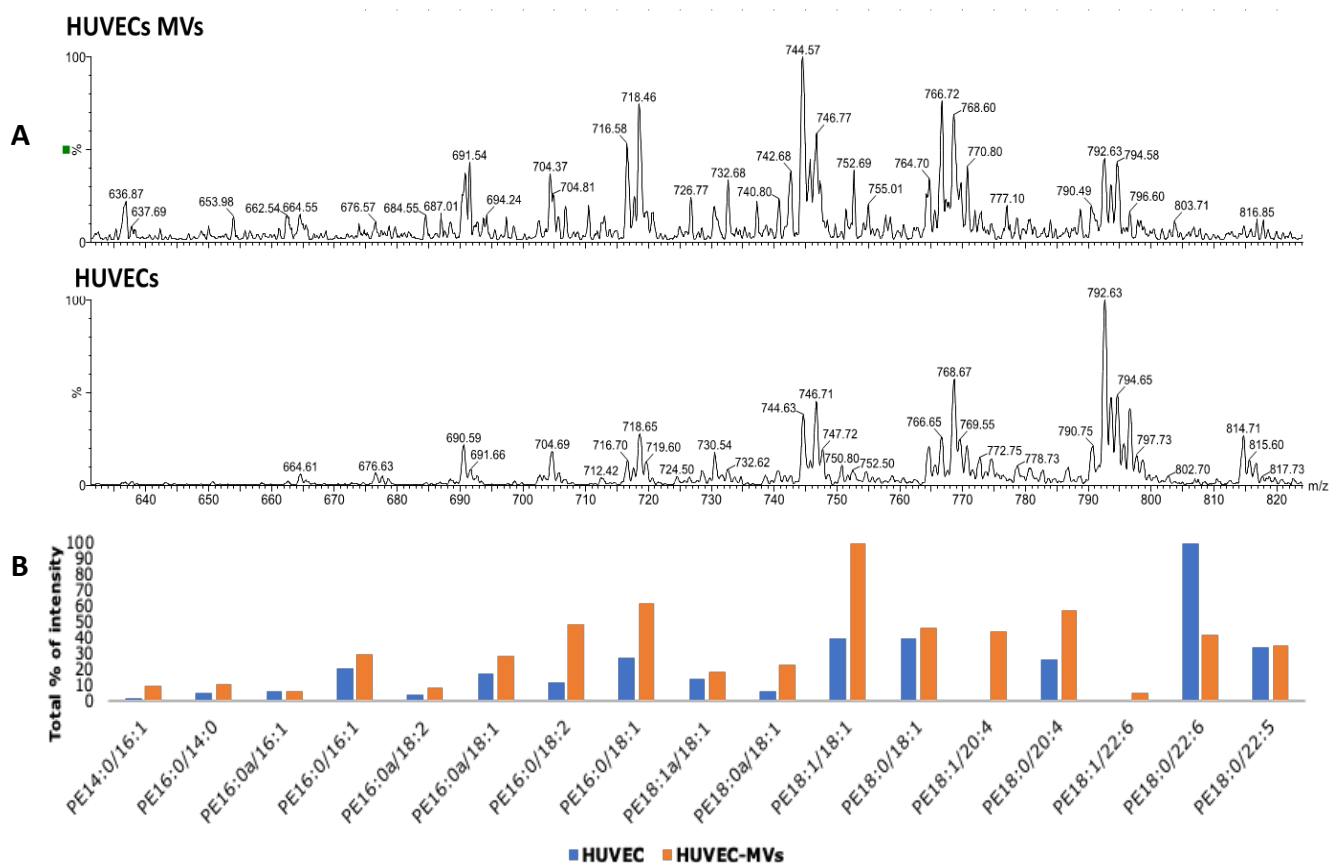
Figure 5.5: ESI-MS quantification of PE species present and normalised intensity of total selected percentage of PE species in HUVEC-membranes and their derived-MVs. *A) The spectra contain a series of different lipid species, where the molecular weight is indictive of the types of chains present. B) Bar chart shows the distribution of PE species between parent cells and EMVs. n=1.*

In the HUVEC membranes, the major species has a m/z ratios of 792.63. This indicates that the PE species is predominately PE18:0/22:6, a species with relatively long acyl chains and a high degree of unsaturation, occupying a relatively large volume. In contrast the EMVs contain species with m/z ratios of 744.57, 718.46, 766.72 and 716.58 corresponding to PE18:1/18:1, PE16:0/18:1, PE18:0/20:0 and 16:0/18:2 respectively, all of which exhibit shorter chains and lower degrees of unsaturation. This indicates the formation of the EMVs, results in the enrichment of the membranes with PE whose acyl chains occupy a lower volume than those found in the parent membrane.

5.3.2.3. Phosphatidyl inositol (PI)
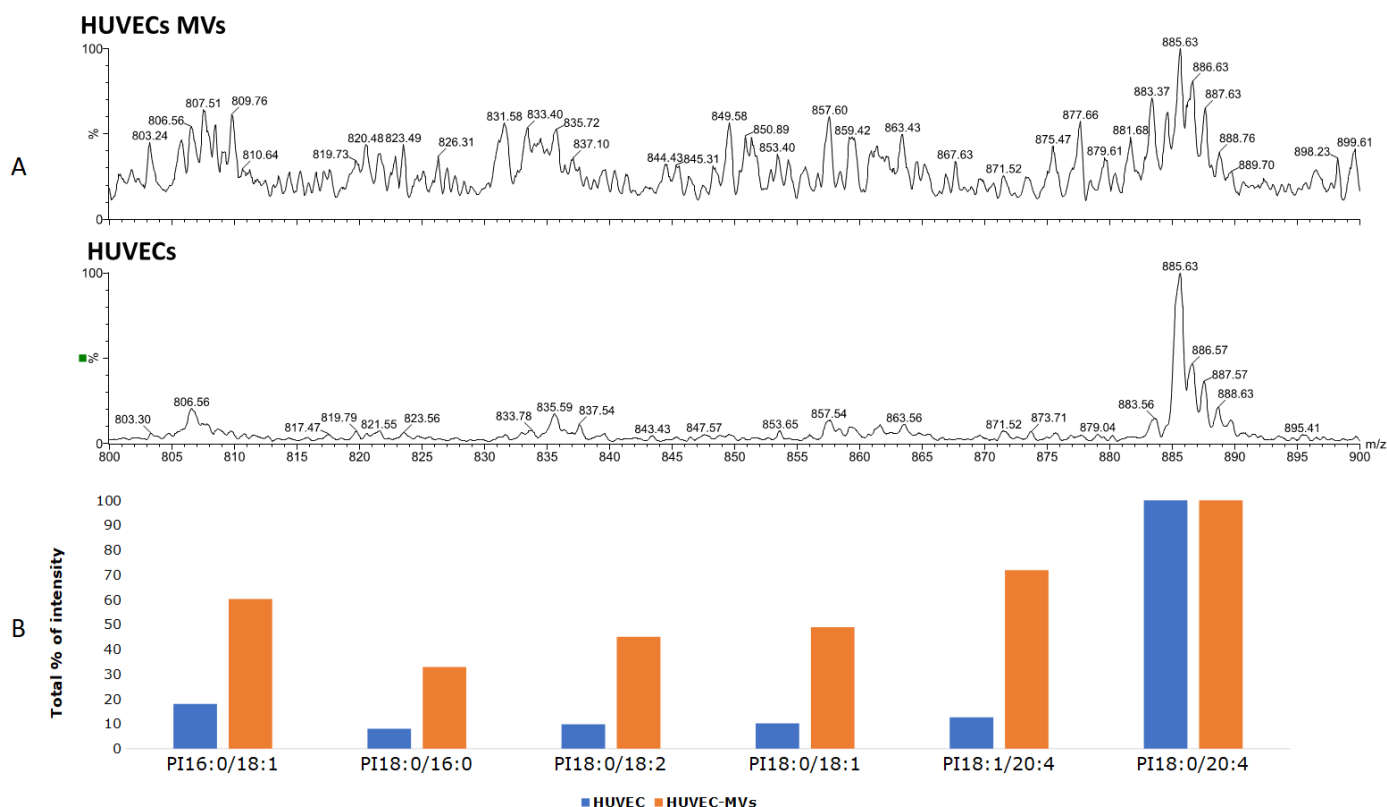
Figure 5.6: ESI-MS quantification of PI species present and normalised intensity of total selected percentage of PI species in HUVEC-membranes and their derived-MVs. *A) The spectra contain a series of different lipid species, where the molecular weight is indictive of the types of chains present. B) Bar chart shows the distribution of PI species between parent cells and EMVs. n=1.*

In the parent membranes, the major species has a m/z ratio of 885.63. This indicates that the PI species is mostly PI 18:0/20:4. In contrast the EMVs also contain species with m/z ratios of 803.24 and 833.40, corresponding to PI 16:0/18:1 and PI 18:1/20:4 respectively. Again this indicates that the budding of the EMVs is accompanied by incorporation of PI whose acyl chains exhibit a lower overall volume than those of the parent membrane. However, the EMV-spectrum does not show an adequate signal. This may be due to difficulties with measuring the different phosphorylated species of PI by MS, as our NMR studies suggest, at least in EMVs, the abundance is relatively high compared to other lipids. The detection of phosphorylated derivatives of PI represents a challenge to MS, as different isomers e.g. PI-3,4-biphosphate, PI-3,5-biphosphate and PI-4,5-biphosphate contain

an identical mass, as well as different charge states reflecting the degrees of phosphorylation (Skotland et al., 2020). These factors can influence the efficiency with which the ions are selected and measured. Moreover, may be the PI concentration in the initial spray solution affected the signal intensity herein.

In summary, ESI-MS was employed to investigate the relative abundance of the main chain composition of the lipid species present in HUVEC membranes and their derived-MVs. The quantifying technique was employed to explore specific lipid species with respect to fatty acyl side chain, backbone and headgroup, by measuring the m/z. Overall the parent membranes and their derived-MVs contain species of PC, PE and PI. The parent cells and EMVs contain relatively similar distribution of PC and PE fatty acyl species. Species with a distribution difference in fatty acyl chains appear to move towards shorter chain lipids. Furthermore, PI species are relatively enriched in shorter chain species compared to parent cells.

5.4. Discussion

Blood coagulation reactions predominantly occur on the surface on injured EC. EMVs are derived from ECs, consisting mainly of phospholipids and proteins, and play a role in coagulation by transporting cargos such as phospholipids. These phospholipids play an important role in blood coagulation as they can alter the rate of clotting reactions depending upon their phospholipid composition and phosphorylation (Record et al., 2018; Ratajczak and Ratajczak, 2020). In addition, blood coagulation has been shown to be localised to the injury site due to most of the coagulation steps occurring on the phospholipid surfaces (Ratajczak and Ratajczak, 2020).

The first aim of this chapter was to assess the type of phospholipid composition in lipid bilayer of the parent cells and their derived-EMVs. This was investigated using ^{31}P-MAS-NMR. The MAS-NMR spectrum resolved the different phosphate species present in lipid bilayer, with the individual species characterised by their chemical shift. The area under the resonance provides insight into the relative abundance, whilst the linewidth provides into the dynamics. Furthermore, the presence of small sidebands at either side of the central isotropic line was consistent with the EMVs retaining a bilayer structure. As expected, all membranes possessed significant PC and PE/SM; however, additional resonances consistent with the negatively charged phosphorylated PI lipids were also present. The assignment of these resonances to phosphorylated PI is consistent with reported chemical shifts (Edgar et al., 2009) and is supported by the longer T_1 relaxation times (Appendix 8.7.3) they exhibit indicative of a more mobile group within the lipid bilayer, remote from the bilayer surface.

The second aim of this chapter was to use ESI-MS to understand the main chain composition of the lipid species present in lipid bilayer of HUVEC-membranes and their derived EMVs (Section 5.3.2). The quantifying technique was employed to explore specific lipid species with respect to fatty acyl side chain, backbone and headgroup, by measuring the m/z. Overall, the parent membranes and their derived-EMVs contained species of PC, PE/SM and PI. In contrast to the parent membrane the

158

EMVs appeared to be enriched in shorter chain lipids. Therefore, overall there was a change in distribution of fatty acyl chains resulting in an overall chain length (and saturation) in derived EMVs which could result in a reduction in the overall volume occupied by the acyl chains.

Relative abundance of PC and PE/SM

Based on the relative intensities of the resonance heights of the relative abundance of the phospholipid present in the parent membranes (Figure 5.3 A-D), overall, it appears that approximately 80% of the intensity of present lipids were PC and PE/SM. This can be used as a quantitative measurement of the different lipid species present which indicates a relative enrichment of PC and PE/SM phospholipids. This agrees with published data, where membranes have been shown to be composed primarily of PC (40 – 50%) and PE/SM (~35%) (Record et al., 2018; Skotland et al., 2020). These phospholipids play essential roles in blood coagulation, therefore, large PC quantities would be projected to act as a substrate to promote coagulation and reduced quantities could be associated with bleeding disorders (Tsuda et al., 2006). For instance, PC has been demonstrated to inhibit APC and protein S activities in a dose-independent manner, as in the FXa-prothrombin reaction system (Tsuda et al., 2006). It appears that coagulation and anticoagulation reactions are modulated by changes in the phospholipid composition of the cellular membrane where the coagulation reaction occurs.

Relative abundance of PI

All the membranes (Figure 5.3 A-D) had chemical shifts present between 2.0 ppm and 4.00 ppm which were tentatively assigned to PI groups. However, relative abundance of the phosphorylated derivatives of PI was higher in the purified EMVs (Figure 5.3 C-D). The observed high level of phosphorylation indicates that there was a high density of negative charge on the surface of the EMVs compared to the parent membrane. Repulsion between these negatively charged headgroups may contribute to the curvature required for the formation of the EMVs. Unfortunately, the analysis

conducted is unable to discriminate between the different phosphorylation states, as the chemical shifts of the individual species are highly dependent on the ions present and the pH of the surrounding buffer. However, the extensive phosphorylation may potentially contribute to differential regulation of processes leading to coagulation. Despite contributing a small proportion to cellular membranes (5 – 8% of total phospholipids), phosphorylated derivates of PI are highly involved in specific lipid-protein interactions and binding that experience a regulatory role (Skotland et al., 2020). The PI headgroup can be phosphorylated at multiple positions and with such reversible phosphorylation resulting in seven phosphorylated derivatives of PI which can be converted into each other by phosphorylation by phosphoinositide kinases that add phosphates to the hydroxyl groups on inositol positions 3, 4 or 5, or by dephosphorylation by phosphatases (Skotland et al., 2020). Phosphorylated derivatives of PI are key components in cellular decision-making processes, i.e., by acting as one of the key targets for lipid-protein binding domains, such as Pleckstrin homology (PH), FYVE and GLA (DiNitto et al., 2003; Poccia 2009). Thus, the presence and recruitment of PI phospholipids have been linked to numerous essential cellular processes including signal transduction, membrane trafficking, cytoskeleton, remodelling and permeability functions of membranes, where specific protein-binding and function known to depend on the presence of PI (DiPaolo and Di Camilli, 2006; Ile et al., 2006; Van Meer et al, 2008). Several studies have suggested supplementary non-specific property of phosphorylated derivatives of PI that involves membrane mechanical forces (Mulet et al., 2008; Koijman et al., 2009). The importance of PI species in protein binding has been associated with coagulation, for instance, a study by Tavoosi et al. has demonstrated that two of the GLA domains containing blood clotting factors (protein C and FVII) bound preferentially to membranes containing monoester phosphates i.e., PI4-phospate or PA, compared to membranes containing PS. Furthermore, they demonstrated that PI4-phosphate also supported membrane binding by enhanced enzymatic activities of both APC and FVIIa (Tavoosi et al., 2013). This suggests that FVII and protein C binding to monoester phosphates may have implications for the function of these proteases *in vivo* (Tavoosi et al., 2013). Nevertheless, the

possible explanation is that PI4-phosphate recruits APC or FVIIa to the surface of the cellular membrane, whilst PS combination recruits the substrate (FX or FVa, respectively) to the surface of the cellular membrane. Additionally, mutations or defects in the regulatory pathways of phosphorylated derivatives of PI are associated with several disease states including CVDs (Majerus, 2009). Although PI has been demonstrated to present in small amounts in EVs, currently, no published data on phosphorylated derivatives of PI (Skotland et al., 2020). Thus, it is a logical question from the preliminary data presented herein if also phosphorylated derivatives of PI present in EVs and therefore in EMVs, as they have been suggested to become phosphorylated upon activation, and speculated to face outward upon MV budding (Ratajczak and Ratajczak, 2017). In Addition, since phosphorylated derivatives of PI confer a unique molecular identity to cellular membranes (Skotland et al., 2020), it is feasible that EMVs may be identified by specific phosphorylated derivatives of PI. Together with the APC data presented in Section 4.3.3, these lipids can be further studied (Section 7.4.2) to determine their functional role in EMVs formation and secretion, as the negative charge of phosphorylated PI headgroup causes bilayer bending leading to EMV repel, suggesting phosphorylated derivatives of PI may have a role in EMV formation and therefore in coagulation signalling.

Effect of TNF-α on lipids relative abundance of cell membranes

Treatment of the cells with TNF-α resulted in parent membranes exhibiting a different distribution of resonances and thus phospholipids (Figure 5.3 E and F). Again, it appears that the addition of TNF-α has increased phosphorylation of PI, similarly increasing the negative charge on the surface of the bilayer and aiding membrane curvature. Interestingly, only one peak was observed in the region corresponding to the phosphorylated derivatives of PI, compared to the two previously observed (Figure 5.3 E). The possible explanations of this finding: I) inflammatory factors induce the signalling of certain derivatives of PI while inhibit the signalling of others; II) a different derivative of PI present. Intriguingly, the peak arising from the phosphodiesters in the lipids was relatively

161

broader maybe reflecting the formation of smaller vesicles whose motion interferes with the averaging by MAS. Furthermore, this spectrum had relatively smaller resonances for PC and PE/SM compared to untreated HUVECs. This challenges the fact that inflammation increases the presence of some of these lipids (Simak and Gelderman, 2006; Ratajczak and Ratajczak, 2020). A possible explanation is that TNF-α may increase the secretion of either EMV, phospholipids or both. We note that the appearance of this spectrum was rather different from the other reported, or to which would be expected, and thus further investigations are required to ascertain the reproducibility of these findings.

Chain composition of PC species

ESI-ES data of HUVEC-derived EMVs showed a relatively similar distribution of lipid chain species of PC to that of parent membranes (Figure 5.4). Studies have demonstrated that PC species play an essential role in signal transduction as a source of lipid signalling molecules, as well as playing a role in the pathological process of atherosclerosis by lipids accumulation at arterial wall which is caused by transporting lipids through blood (Dignat-George and Boulanger, 2011; Paapstel et al., 2017). For instance, lipid species containing PC 16:0/16:0 showed positive correlation with the plasma levels of PC species (Choi and Snider, 2015). This demonstrates that PC lipid species may be induced by atherosclerotic lesions, suggesting that regulating PC-lipid chain biosynthesis can regulate PC levels in the plasma membrane, thus, influencing the process of atherosclerosis (Koskinas, 2020), and with such possible functions, it would not be surprising if PC chain species were implicated in the process of EMV formation also. However, research in this area is scarce (Skotland et al., 2020; Kummerow, 2021).

Chain composition of PE species

The spectra of PE species present in HUVEC membranes and derived EMVs (Figure 5.5), demonstrated that the overall lipids distribution was similar in parent membranes and derived EMVs.

However, longer chain species appeared to be depleted in EMVs. Moreover, EMVs appeared to contain relatively higher content of PE shorter-chain fatty acyls such as PE16:0/18:1 and PE16:0/18:1, demonstrating the importance of these species, for instance, PE16:0/18:1 lipids have been shown to be associated with tumour stage, as well as significantly correlated with patient overall survival (Chakrabarti, 2021). This demonstrates implication of these lipids in different disease states such as CVDs. This is not surprising for a lipid that comprises a large concentration of lipids in inner membrane-leaflets, with its remarkable activities such as by acting as a chaperone that assists in the folding of specific proteins to their folded state and regulating membrane fusion events (Schuiki et al., 2009). Moreover, PE acyl chains impart lateral pressure that can be released by the membrane adopting negative curvature (Ratajczak and Ratajczak, 2017). Excess of PE species with polysaturated acyl chains in the ER membrane can trigger the formation of toxic PE hydroperoxides that can cause cell death (Patel and Witt, 2017), demonstrating the importance of PE species in physiology and excess in certain PE species may result in pathophysiological events.

Chain composition of PI species

The chain composition of PI lipids present (Figure 5.6) was tentatively higher in shorter chain regions in EMVs. This is in alignment with the observations in ^{31}P-MAS-NMR, which showed relative enrichment in phosphorylated derivatives of PI in EMVs, suggesting possible enrichment processes in these phospholipids in the purified EMVs. This change in chain composition would serve to increase the length of the acyl chain which would increase the volume of the lipid chains leading to a more mobile species that is more remote from surface of the membrane. As discussed earlier, the interaction of phosphorylated PI binding with proteins is essential, because they can serve as crucial reference points for a wide range of proteins in terms of docking destination and/or changing their confrontation. This has previously been reported for peripheral membrane proteins with membrane adjacent regions or cytoplasmic "tails" showing interaction with phosphorylated PI (Balla, 2013). The combination of fatty acyls in phosphorylated PI is unique compared to most

phospholipids as they are a rich phosphorylation target at the cytoplasmic surface of all cellular membranes, therefore, research initiated to demonstrate that the acyl chain composition also has an essential function (Barneda et al., 2019). Although numerous acyl species exist, PI species appear to be enriched with one specific acyl chain composition in the sn-1 and sn-1 positions (50-80%) (D'Souza and Epand, 2013). The approximate fatty acid uniformity of phosphorylated derivatives of PI suggests that these phospholipids act as a single rapidly interconverting metabolic pool (Barneda et al., 2019). PI species in various organisms and tissues demonstrated the predominance of a single hydrophobic backbone, which in mammalian-cells is composed of mostly arachidonic chains. Despite evolution having favoured this specific PI species configuration, little is known regarding the mechanisms and functions behind it (Barneda et al., 2019). However, PI acyl chains may be suggested to play a functional role as they are unevenly distributed amongst the different classes of PI containing different headgroups. Moreover, changes in the composition of a lipid acyl chain can affect its function and may lead to disease states (D'Souza and Epand, 2013). Since PI is highly enriched at both sn-1 and sn-2 positions with specific acyl chains; the major species are PI18:0/PI20:4 (D'Souza and Epand, 2013). The HUVEC membranes and derived EMVs demonstrated this reported enrichment (Figure 5.6). In contrast, EMVs also contained PI species enriched in PI 16:0/18:1 and PI 18:1/20:4. Two possible explanations: I) EMV-PI species moves towards shorter chain regions which is consistent with the ability to form high curvature structure, because of the PI negatively charged headgroups repelling providing an increased surface per lipid species; II) the enrichment of PI species with a different acyl chain composition comes from the potential processes resulting in this selective acyl chain incorporation, where the substrate specificity of the enzymes involved leading to acyl chain enrichment, since a number of defects have been linked to enzymes contributing to acyl chain enrichment in PI. However, a unique feature of PI fatty acyl chains remains largely unexplored and currently there is no evidence of these lipids present in MVs (Skotland et al., 2020).

The ^{31}P-MAS-NMR data demonstrate that EMV composition was different from that of the parental cells, with large changes in the amount and composition of the phosphorylated PI lipids present, this suggests that possibly phospholipids enrichment process occurring in the EMVs. However, it is unclear if the differences in lipid composition reflect: a) the preferential budding of particular lipid classes; b) the recruitment of particular lipid classes through their interaction with proteins recruited into the MVs; c) which way the cells enrich EMVs with these different species of phospholipids; or d) the role of phosphorylated PIs in membrane dynamics and vesicular transport, that these lipids may influence EMVs composition and secretion. Additionally, data suggest that the lipid composition of EMVs may be important as EMVs appeared to be either tentatively enriched in lipids or differed in composition. Also, the findings herein suggest that EMV shifts were consistent with the fact that smaller vesicles requiring higher curvature and indicating variations in phospholipid composition of EMVs can affect the function of the membrane.

The ESI-MS data demonstrate that overall, species with a distribution difference in fatty acyl chains, appeared to move towards shorter chain lipids, which is consistent with the ability to favour high curvature structure. Correspondingly, PI species were relatively enriched in shorter chain species compared to parent cells suggesting short chain lipids are required for high membrane curvature. This may be involved in cell signalling between parent cells and recipient cells, as well as in inflammation influencing several cellular processes. Whilst, membrane phospholipids of EMVs are suggested to play a role in cell signalling, the process in which phospholipids carry out that role remains unclear. Also, the composition of MV-phospholipids varies depending on the cell type of origin and the mechanism of MV release (Ratajczak and Ratajczak, 2020). Therefore, these striking observations presented herein can be validated and further studied (Section 7.4.2), as these lipids have been showed to play important roles in regulating cell signalling and membrane dynamics and may potentially play a structural or functional role in cell signalling underlining haemostasis.

5.5. Conclusion

Membrane lipids in the bilayer determine the stresses and the topologies of the membrane they form. An understanding of the link between lipid composition and biochemical parameters such as spontaneous membrane curvature and bending rigidity is fundamental to clarify the mechanisms involved in the formation and secretion of EMVs, as well as lipid-protein interactions. Despite their relatively small fraction of total cellular phospholipids *in vivo*, a class of versatile cell signalling lipids are PI phospholipids. Research of the effect of PI phospholipids cellular membrane systems remains in early stages and have not matched the pace of experimental discoveries with respect to their role in regulation of fundamental cellular processes.

^{31}P-MAS-NMR investigated the different lipid composition and their phase behaviour. The data demonstrated that resonances consistent with phosphorylated derivatives of PI and these resonances were tentatively enriched in EMVs compared to parent cells suggesting possible enrichment of negatively charged phospholipids which is consistent with high membrane curved surfaces. Furthermore, ESI-MS investigated the relative abundance of fatty acyl chains in different lipid species. The distribution of lipids chains associated with each headgroup was measured. For lipid species, whether there was a change in distribution of fatty acyl chains, there was a relative reduction in the overall chain length in EMVs. Additionally, for the PI species where there was a difference in distribution in fatty acyl chains, it moved towards a shorter chain lipid which is consistent with the ability to form high curvature structure. Thus, EMV-lipid composition and bilayer structure are distinct from that of their parent cell and this bilayer composition favours vesicle formation.

Chapter 6: The Role of EMVs Carried miRNAs in Haemostasis

6.1. Introduction

Endothelial-derived MVs reported to carry functional miRNAs mediate cell-to-cell communication (Zeng et al., 2021). The role of miRNAs in EMVs in intercellular communication processes can be considered as consisting of three key concepts: I) miRNAs are released from parent cell and selectively packaged into appropriate carriers such as MVs; II) miRNAs are protected from breakdown (i.e., from circulating RNases) and transported to recipient cell; III) miRNA maintain the ability to recognise and repress mRNA targets inside recipient cell (Raimondo et al., 2020). It has been estimated that 30–60% of all protein-coding genes are regulated by miRNAs and modulate 10–30% of human genome expression (De Rosa et al., 2014; Raimondo et al., 2020). miRNAs play a key role in regulating gene expression by degradation, translational inhibition or translational activation of their target mRNAs (Jansen et al., 2014). Owing to their short base-pairs within miRNA 3'UTR duplex, a single miRNA can bind to a number of mRNA targets (up to hundreds) and multiple miRNAs can target the same mRNA, as well as interaction with each other to form miRNA-miRNA co-targeting networks (Ni and Leng, 2015); (Figure 6.1), demonstrating their regulatory potential even greater.
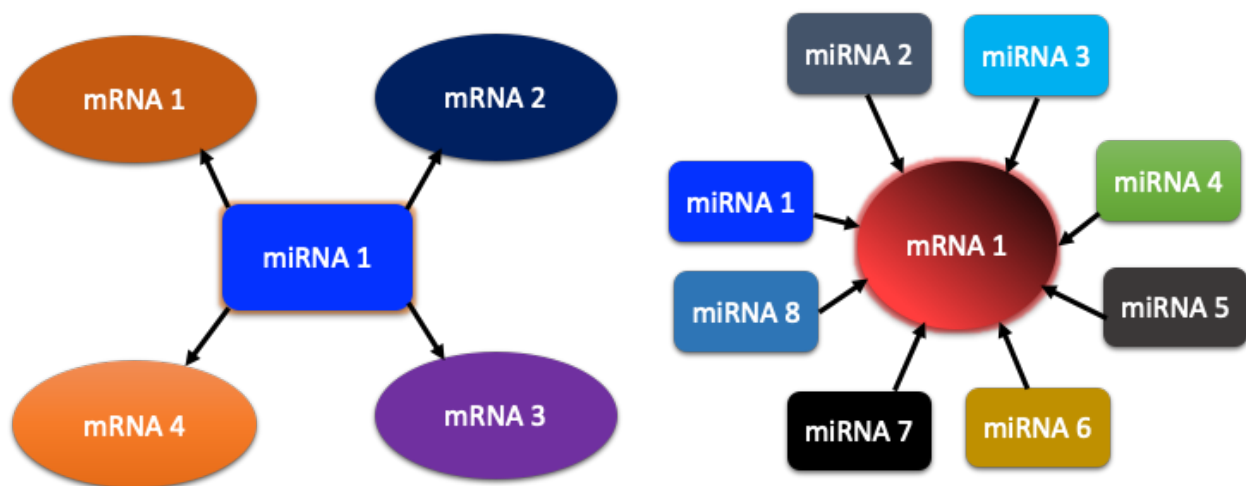
Figure 6.1: Illustrative diagram of common regulation between miRNAs and their mRNA targets. *A single miRNA can target a number of mRNAs and a number of miRNAs can target one mRNA, thus, interactions between miRNAs and their targets may not be one–to–one.*

Studies demonstrated that miRNAs from EMVs regulate the physiological and pathophysiological processes in vascular endothelium, including cell differentiation, proliferation, migration, apoptosis and inflammation (Polyakova et al., 2020). Dysregulation of miRNAs have been linked with a number of CVDs (Jansen *et al.*, 2014; Edwards et al., 2018). It has been reported that removal of Dicer, the key regulatory enzyme in miRNA biogenies, results in decreased EC growth (Pérez-Casal *et al.*, 2009; Raimondo et al., 2020). Mice that have ECs with Dicer knocked out generally have abnormal growth pattern of blood vessels (Raposo and Stoorvogel, 2013). This indicates the role played by miRNA in maintaining the haemostasis in the vascular system (Arroyo et al., 2018). Different mechanisms have been suggested in removal of miRNA from cells (Jansen et al., 2014). For instance, in the case of dead cells, either necrotic or apoptotic, miRNAs are removed via the mechanism of simple leakage (Jansen et al., 2014; Raimondo et al., 2020). The exact role of these miRNA complexes play outside cells remains unclear (Edwards et al., 2018; Zeng et al., 2021). Moreover, it remains unclear whether endothelial-derived MVs carry miRNAs that may play a role in cell signalling and thus in thrombus formation. Additionally, it is not known whether these EMVs have different content in inflammation. In order to address these questions, this study aimed to determine the miRNA content in MVs from cultured ECs and explore potential candidate miRNAs to contribute to a better understanding of their role in EMVs.

In previous chapters the Chandler Loop was developed to test to thrombus formation (Chapter 3), exogenous EMVs were added to blood to investigate whether these EMVs modulate thrombus formation (Chapter 4) and the composition of phospholipid membrane of cultured ECs was compared in stimulated (TNF-α) and unstimulated conditions and quantitatively analysed the different amount of lipids of the lipid bilayer (Chapter 5). This chapter explores whether EMVs that incorporated into the thrombus carry miRNAs involved in cell signalling, underpinning haemostasis. Furthermore, the chapter aims to establish whether TNF-α has any effects on EMV-miRNA content or profile. The overall contribution of this chapter to this thesis is highlighted in red in Figure 6.2.
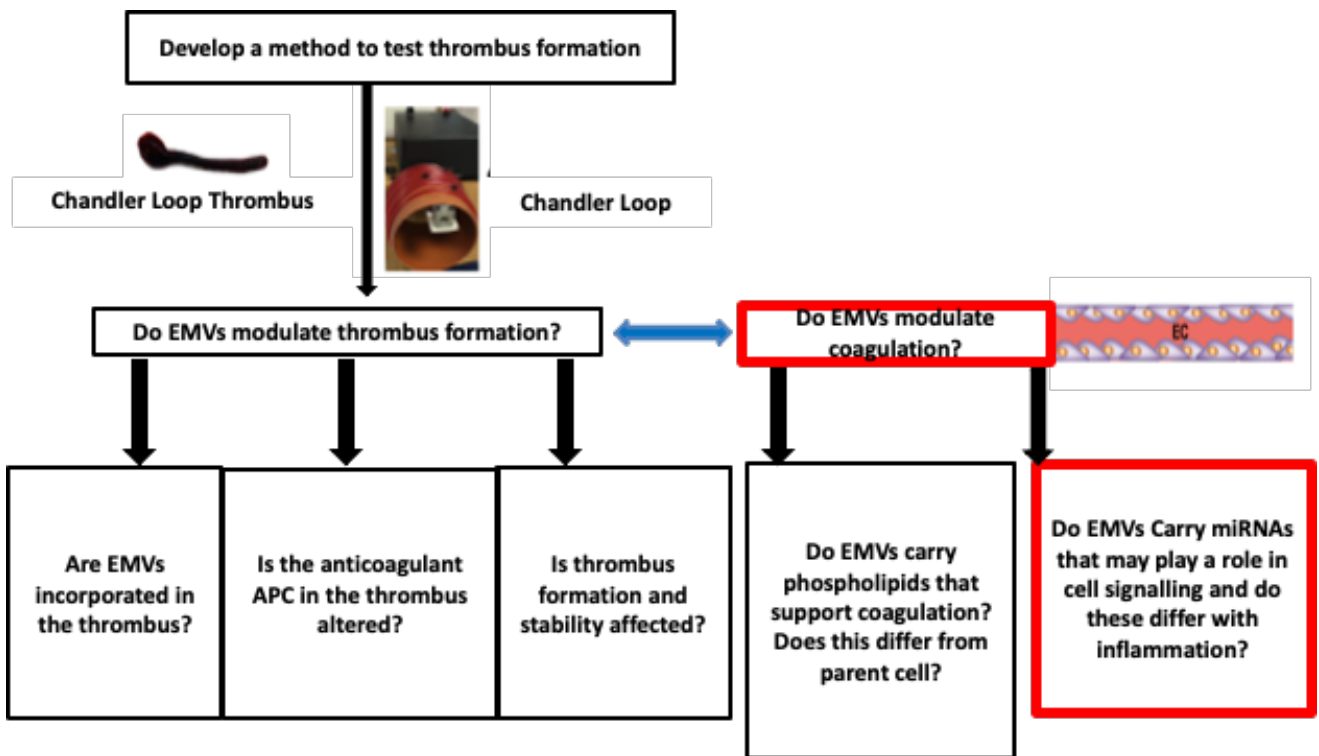
Figure 6.2: The overall contribution of Chapter 6. *This chapter focuses on the role of miRNAs from EMVs generated in normal and stimulated conditions, to explore the differences in miRNAs quantity as well as differentially expressed pathways.*

6.1.2. Hypotheses and Aims

Given that MVs from other cellular sources have been shown to carry miRNAs and regulate biological processes, and further a role for endothelial-derived MVs in regulating haemostasis, the overall aim of this chapter is to establish whether EMVs carry miRNAs that potentially have a role in cell signalling and thrombus formation, and also to explore whether the miRNA content of EC-derived MVs changes (quality and species) in the presence of TNF-α. Below are the hypotheses and aims for each subchapter.

6.1.2.1. Do EMVs carry miRNAs that may play a role in cell signalling and thrombus formation?

Hypothesis: EMVs incorporated into thrombi carry miRNAs whose target genes are associated with cell signalling and thrombus formation.

Aim: To investigate whether EMVs carry miRNAs that may play a role in cell signalling and thrombus formation.

6.1.2.2. Does inflammation (TNF-α treatment) alter the miRNA content of endothelial-derived MVs?

Hypothesis: The miRNA content of EMVs generated in the presence of TNF-α is different to the miRNA content of EMVs generated in the absence of TNF-α.

Aim: To explore the different expression of miRNAs of EMVs derived from TNF-α-treated and untreated cells, and to assess potential pathways targeted by miRNAs carried by EMVs.

6.2. Methods

HUVECs were cultured as described in Section 2.3.1, and EMVs were collected as described in Section 2.4. Total RNA isolation was conducted as described in Section 2.9.1, and the isolated RNA samples were quantified as described in Section 2.9.2. Quantified samples were then shipped to Novogene for NGS. Once samples were received by Novogene, RNA integrity was assessed as described in Section 2.9.3. Samples were subsequently underwent library preparation and construction as described in Section 2.9.4.

6.2.1. Fastq Alignment

Short raw-read sequences were provided by Novogene and were output in fastq files which are text files that contain the sequence data, with quality information, from the clusters that pass filter on a flow cell. Fastq files were processed with the FASTX-Toolkit (v0.014) (Hannon, 2015). Quality control of the sequences from each sequenced library was investigated using FastQC (v0.11.9) to check for homopolymers, adapters and base-quality distribution (Babraham Bioinformatics, 2019). The "fastx_clipper" program was used to trim adaptor sequences and discard reads less than 12 base pairs after clipping. Reads were then mapped to all human miRNAs (mature form) present in the miRbase (v22) (Kozomara, Birgaoany and Griffiths-Jones, 2019). Mapping was performed with the NovoAlign mapper specifically designed for small read sequencing (Thankaswamy-Kosalai, Sen and Nookaew, 2017). Reads were first filtered to require at least 14 bases of good quality present in the read to be kept. Further homopolymer and dinucleotide repeats were filtered out. The default threshold for alignment score (default 4.5) was used, and the miRNA alignment mode was used, where each read is given an additional score based on the Needleman-Wunsch alignment of the read to the opposite strand. Aligned reads were converted to Sequence Alignment Map format (SAM) that stores biological sequences aligned to a reference sequence. These aligned reads were then converted to Binary Alignment Map (BAM) file format, and two sorted files were generated (read name and

read position) with SAMtools, the coordinate sorted file was then indexed by SAMtools (v1.12) (Li, 2011).

6.2.2. Aligned Read Counting

For read counting, a gene transfer format (gtf) file was created for the miRNA database treating each miRNA as a singular "gene" element with no introns. Reads were then counted against this gtf file using High Throughput Sequencing (HTSeq v0.13.5) which calculates the number of mapped reads to each gene (Anders, Pyl and Huber, 2015).

6.2.3. Quality Control of Aligned Reads and Differential Expression

Prior to differential expression analysis of samples, miRNAs were filtered to remove extreme lowly expressed miRNAs and those with no reads present. miRNAs required to reach at least 5 counted reads in at least 8 samples to pass filtering. Thus if an miRNA for instance has 5+ reads in only 7 samples, it is discarded. 8 was chosen because it is the size of the smallest sample group (EMVs from TNF-α-treated HUVECs). This helps to account for reads which are present in one group and absent in the other. Following filtering, a boxplot of primary reads was generated and indicated that library size read normalisation was warranted using trimmed mean of M-values (TMM) normalisation implemented in edgeR (v3.13) (Chen and Smyth, 2012), a Bioconductor package available in the R statistical computing environment (R Core Team, 2018). Differential expression analysis of samples was also performed using edgeR (Robinson, McCarthy and Smyth, 2010; McCarthy, Chen and Smyth, 2012) to compare miRNA expression on EMVs derived from control and TNF-α-treated-cells. EdgeR utilises an over-dispersed Poisson model which accounts for both biological and technical variability coupled with an empirical Bayes method to estimate the degree of dispersion for each miRNA. Data are fitted to a generalised linear model (GLM) that accounts for this over-dispersion, and a GLM likelihood ratio test is performed to determine if the coefficient representing

the contrast between the conditions (control vs treatment) of interest is equal to 0 indicating no differential expression. An miRNA was considered differentially expressed if the GLM likelihood test produced a false discovery rate (FDR) corrected p-value ≤ 0.05. The FDR correction used was the Benjamini-Hochberg's method for controlling the FDR, available in the topTags function in the edgeR.

6.2.4. Pathway Analysis

The differentially expressed miRNA subsequently underwent Gene Ontology (GO) analysis for functional annotation analysis and Kyoto Encyclopaedia of Genes and Genomes (KEGG) analysis to identify the involved enriched pathways. Pathway analysis was performed using GeneCodis (v4.0) (Garcia-Moreno et al., 2021) to run gene set enrichment analysis (GSEA) for functional and enrichment pathway analysis. GeneCodis utilises the miRTarBase database (v8.0) (Huang et al., 2020) that catalogues experimentally validated miRNA-target interactions to identify target mRNAs for each miRNA. This was completed by mapping all target mRNA candidates to GO terms in the database, calculating mRNA numbers for each term using Wallenius non-central hyper-geometric distribution to find significantly altered GO terms in target mRNA candidates compared to the reference background. The p values were corrected for multiple tests using FDR correction (Benjamini-Hochberg's method for controlling the FDR, available in GeneCodis). FDR corrected p-value ≤ 0.05 considered significant. Only the GO terms and pathways with adjusted p values ≤ 0.05 and FDR ≤ 0.05 were selected which were used to generate a heatmap (gplot: R package v2.17.0) (Gregory et al., 2015) of the top differentially expressed miRNAs in relevant pathways across the two conditions. miRNAs with adjusted p value ≤ 0.05 and fold change (FC) ≥ 2 were selected for differential expression analysis (Appendix 8.8.2). An overview of the study design and analysis used in this chapter are presented in Figure 6.3.
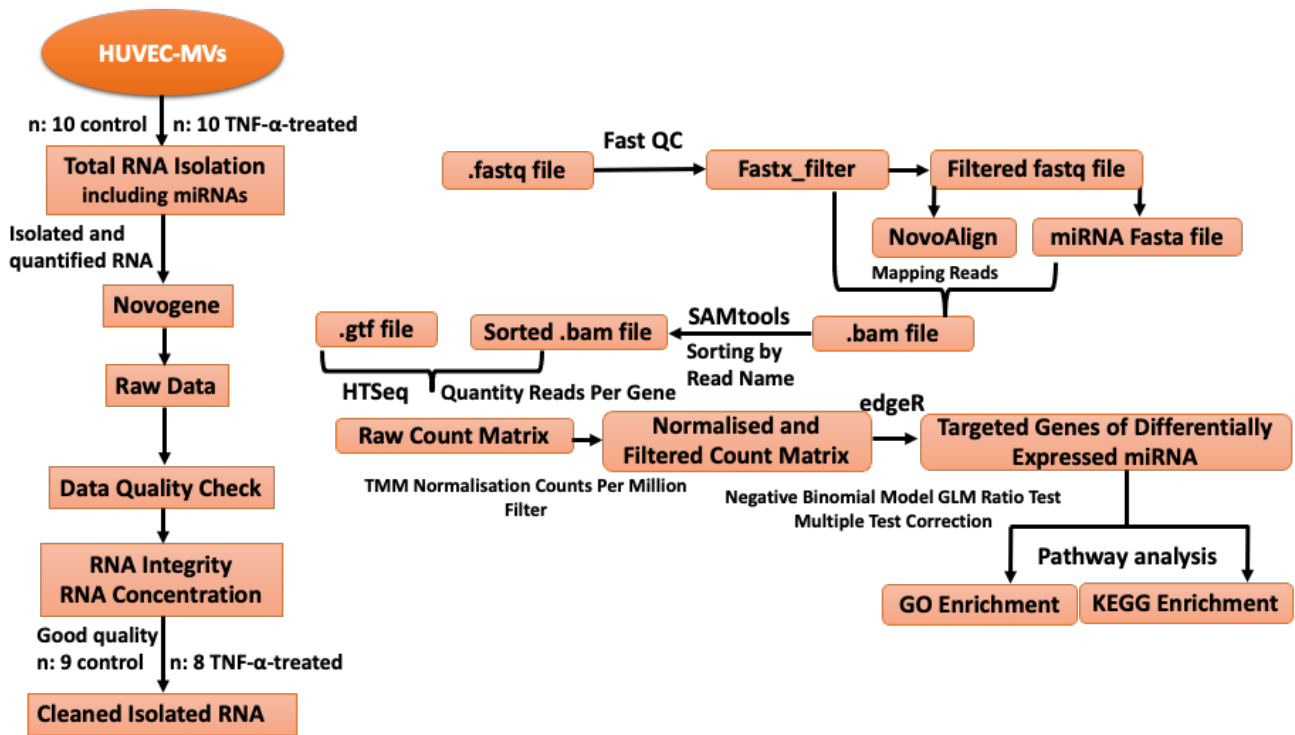
Figure 6.3: Overview of the study design and analysis of EMV-miRNAs. *Endothelial microvesicles (MVs) were collected from primary human umbilical vein endothelial cells (HUVECs) and ribonucleic acids (RNAs) (including mircoRNAs, miRNAs) were isolated and quantified. Next generation sequencing (NGS) conducted by Novogene. Initial quality control of RNA integrity and concentration was performed, as well as quality control of input data (raw reads) were performed. Then the RNA sequence provides a file that generates fastq files (raw sequence data/reads) wherefrom data is filtered to adjust to small RNAs. Data are mapped to the reference genome (human miRNA sequences) which determines which reads align to which miRNA, providing a raw count matrix. This data then require normalisation which is performed by adjusting to different mathematical properties of the data (length of read) which provides a list of different expressed genes. Once specific miRNAs of interest are identified, these can be matched to potential target mRNAs and enrichment of relevant biological pathways assessed.*

6.3. Results

To investigate whether EMVs carry miRNAs that may play a role in cell signalling and thrombus formation, and to explore whether miRNA content of EMVs from quiescent cells differ to EMVs from TNF-α-treated cells, samples were sequenced using NGS. RNA-sequence data were then analysed by obtaining primary reads and aligning to all human miRNAs. The alignment positions were matched with known gene positions and the read counts calculated in order to estimate the level of expression of each gene/mRNA of interest. The read counts of samples between the two groups were compared using differential expression analysis and pathway enrichment analysis.

6.3.1. Fastq Alignment and Read Counting

Following data filtration (Section 6.2.3) a boxplot of log-ratios of gene level read count for each sample was generated and indicated that un-normalised data had a large difference between medians when looking across the treated and untreated EMV groups. These large differences would artificially increase the number of differentially expressed miRNAs due to one group having more overall reads. This indicated that normalisation was warranted to bring the medians for samples closer to together. TMM normalisation accomplished this task thus that overall medians were more easily comparable and differential expression testing would generate fewer false positives (Figure 6.4).
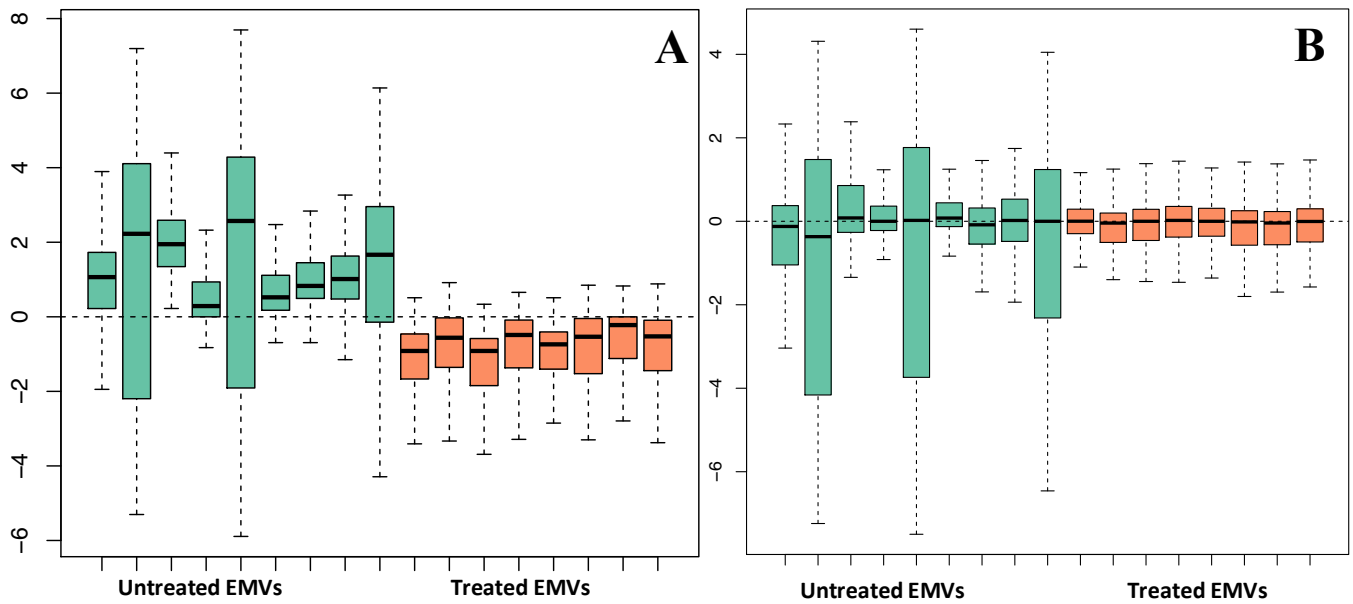
Figure 6.4: Boxplot of primary and normalised relative log expression. *Y-axes of boxplots show log-ratios of the gene level read counts of each sample to a reference defined as the median across samples for EMVs from quiescent vs EMVs from TNF-α treated cells. Panel A shows boxplots without library size normalisation while panel B shows boxplots using TMM (trimmed mean of M values) normalisation. miRNA data suggest that EMVs generated in the presence of TNF-α have different miRNA content. (A) all of the EMVs from quiescent cells showing a higher library size compared with TNF-α-treated cells, (B) indicates miRNA quantity decreased in TNF-α treated samples. n=1.*

6.3.2. Pathway Enrichment

Pathway analysis of significantly and potentially enriched relevant biological pathways targeted by miRNAs carried in EMVs based on the set criteria (FDR adjusted p value ≤ 0.05). Following bar chart demonstrates that miRNAs appear to target mRNAs enriched in cell signalling pathways. For instance, miRNAs with predicted targets in platelet activation pathway (76 miRNAs and 107 predicted mRNA targets) are significantly enriched (p value = 0.003). The top 14 potentially enriched pathways represented in Figure 6.5.
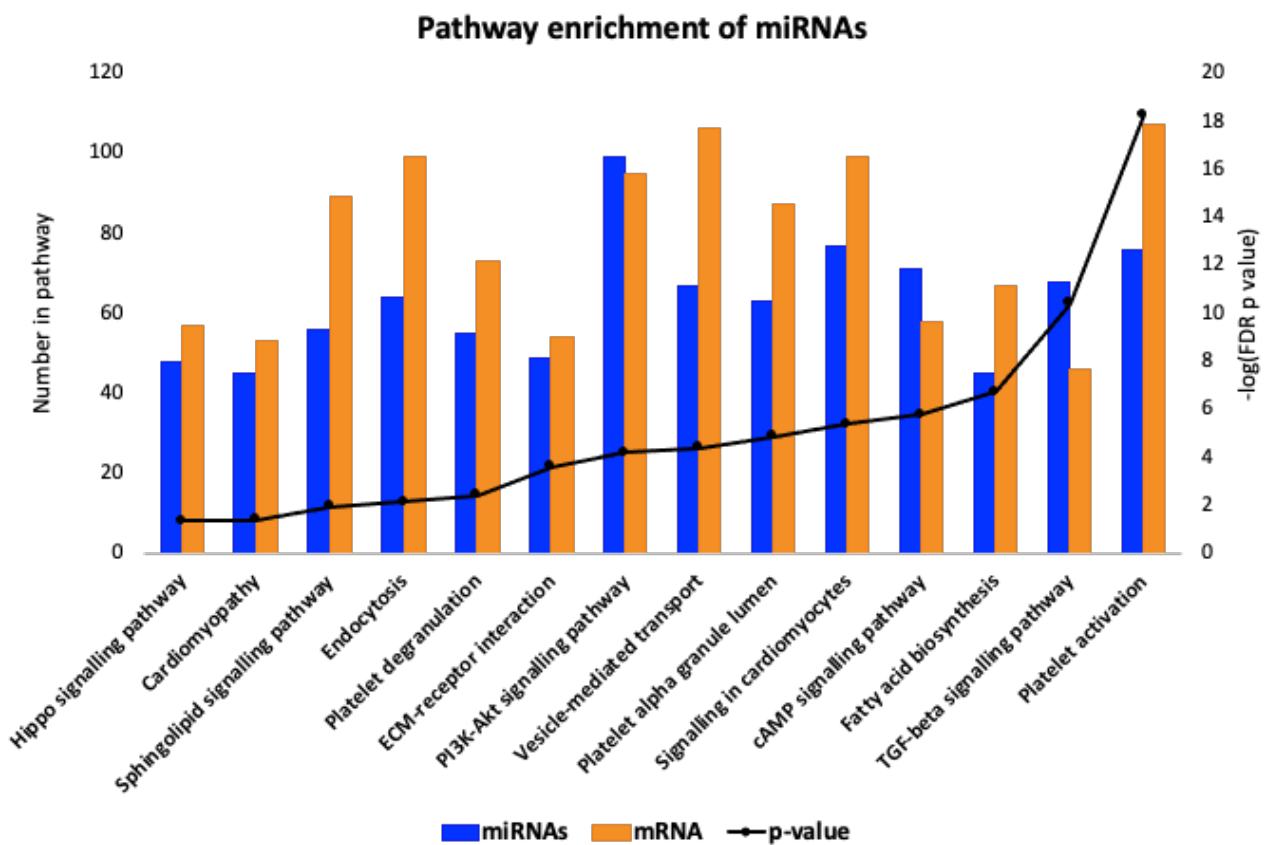
Figure 6.5: Potentially enriched pathways of miRNAs and their targets. *Pathway analysis of potentially enriched pathways in miRNAs in EMVs from quiescent cells. Black line indicates increased enrichment from left to right (-log(FDR p value) and bars indicate the number of miRNAs and their predicted target mRNAs in the pathway. n=1.*

6.3.3. Differential Expression

To assess the effect of TNF-α treatment on the content of miRNAs in EMVs, significantly differentially expressed miRNAs (Appendix 8.8.2) based on the set criteria (FDR adjusted p value ≤ 0.05 with FC ≥ 2) were identified. The heatmap in Figure 6.6 compares the expression of miRNAs in EMVs from quiescent vs EMVs from TNF-α-treated cells. Overexpressed miRNAs represented in yellow to white colours, lighter colours representing higher expression. Down expressed miRNAs represented in light to dark red colours, darker colours representing higher expression (Figure 6.6).
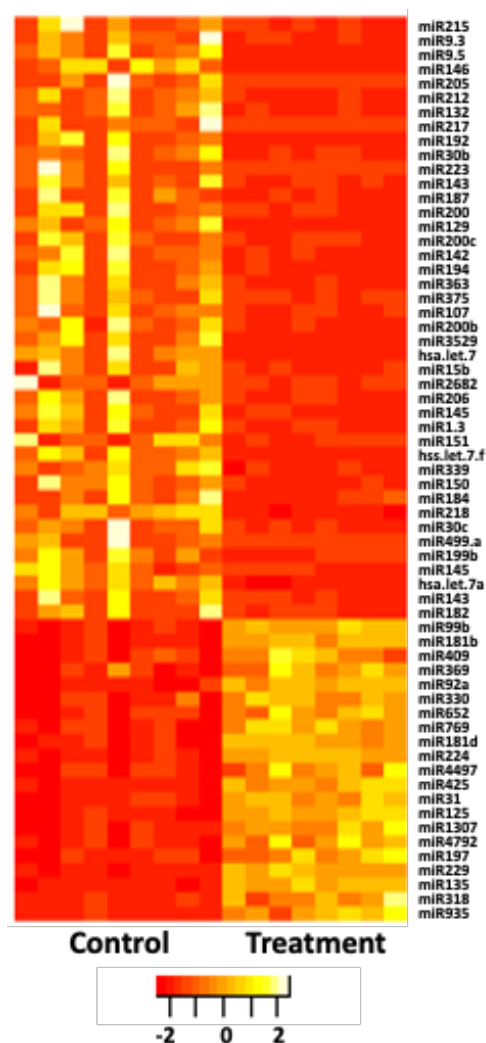
Figure 6.6: Differentially expressed miRNAs. *Differential expression of miRNAs in EMVs from quiescent vs TNF-α-treated cells. Overexpressed miRNAs represented in light yellow to white colour (FC ≥ 2), down expressed miRNAs represented in in light to dark red colour (FC ≥ -2) and miRNAs with normal expression represented in light to dark orange colour (FC 0 to 1.99 or 0 to -1.99) compared to control samples. EMVs generated in the presence of TNF-α contain more overexpressed miRNAs. Nevertheless, the total miRNA quantity is lower in TNF-α-treated samples. n=1.*

6.3.4. Pathway Regulation

Pathway analysis of miRNAs and their predicted target mRNAs was conducted to gain a list of pathways significantly enriched with the number of miRNAs in each pathway plus target mRNA based on the set criteria (FDR adjusted p value ≤ 0.05). Following bar charts represent differentially enriched pathways of differentially expressed miRNAs and predicted targets for upregulated and downregulated miRNAs. For example, upregulated miRNAs with predicted targets in the cAMP signalling pathway (27 miRNAs and 76 predicted mRNA targets) are significantly enriched (p value = 0.006) in the TNF-α-treated cells, and downregulated miRNAs with predicted targets in the platelet activation pathway (54 miRNAs and 122 predicted mRNA targets) are significantly enriched (p value = 0.004). The top 14 (7 upregulated and 7 downregulated) enriched pathways represented in Figure 6.7.
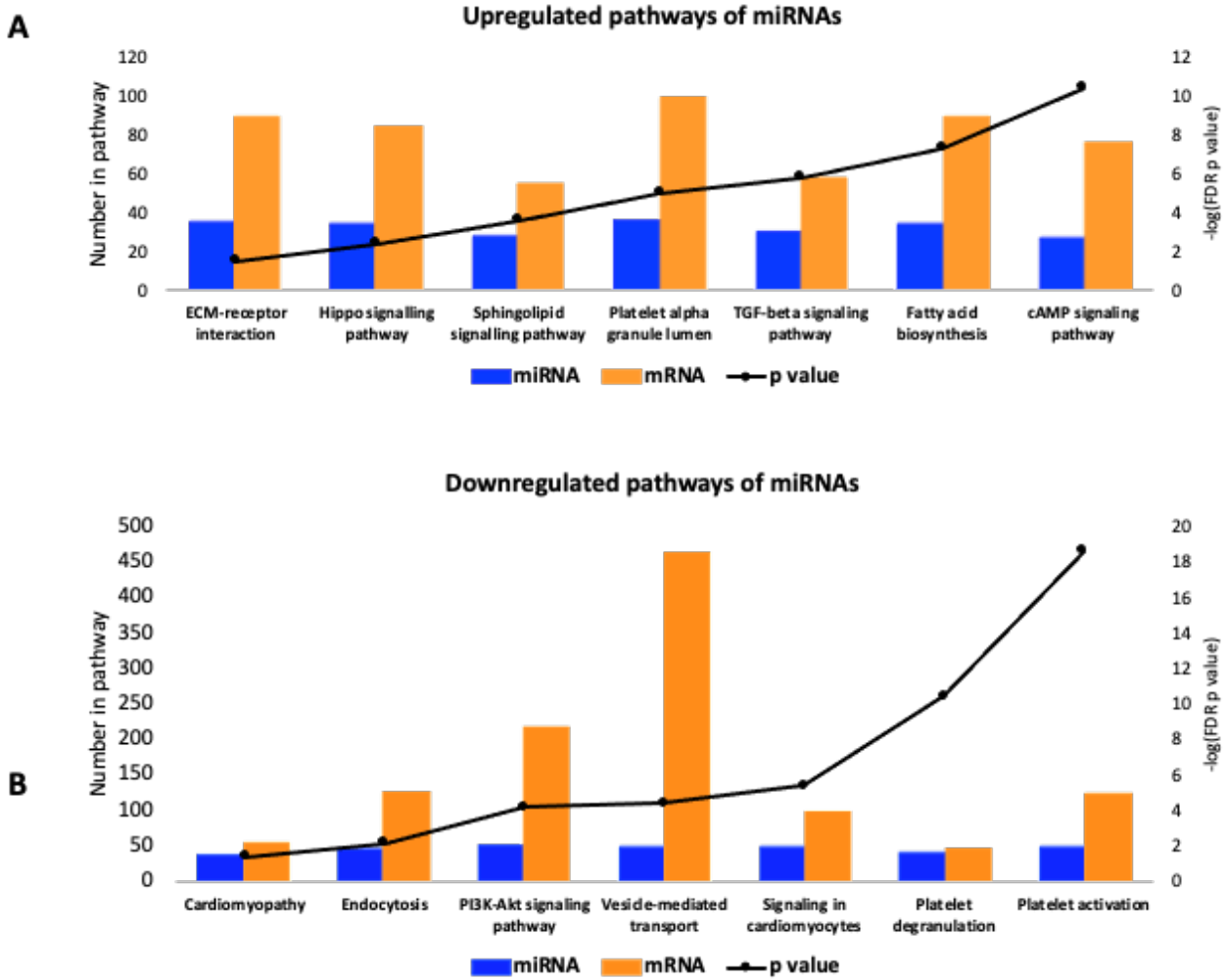
Figure 6.7: Pathways altered by differentially expressed miRNAs. *Pathway analysis of identified enriched pathways of differentially expressed miRNAs in EMVs from quiescent vs TNF-α-treated cells. Black line indicates increased significance from left to right (-log (FDR p value) and bars indicate the number of miRNAs and their predicted target mRNAs in the pathway. A) Represents enriched pathways of upregulated miRNAs and predicted targets. B) Represents enriched pathways of downregulated miRNAs and predicted targets. n=1.*

6.4. Discussion

Endothelial-derived MVs can serve as a delivery system to carry miRNAs from secreting to recipient cells. miRNAs carried by EMVs may induce effects that may be either stimulatory or inhibitory for target cells which can alter gene expression (Raimondo et al., 2020).

 The aim of this chapter was to investigate whether EMVs incorporated in thrombus carry miRNAs whose predicted target genes/mRNAs are associated with cell signalling associated with haemostasis, and whether proinflammatory TNF-α alters the miRNA content of EMVs. EMVs appeared to carry miRNAs whose predicted target genes/mRNAs are associated with cell signalling, particularly those pathways associated with cell signalling in haemostasis. Furthermore, differentially expressed miRNAs in EMVs isolated from quiescent vs treated cells demonstrated that treated samples contained more downregulated miRNAs and lower quantity compared to those of untreated samples. Also, significantly altered pathways by miRNAs and their target genes/mRNAs suggest that EMVs appeared to carry miRNAs involved in the regulating cell signalling pathways. This was indicative that miRNAs were significantly expressed and targeted the most mRNAs encoding genes in pathways associated with cell-to-cell interaction.

In this chapter it was speculated that miRNAs in EMVs incorporated into thrombi carry miRNAs that play a role in cell signalling and thrombus formation. miRNAs in EMVs isolated from quiescent cultured cells were assessed to investigate whether these miRNAs target mRNAs in signalling pathways. Data (Figure 6.5) suggest that the miRNAs appeared to target mRNAs associated with cell signalling in haemostasis (i.e., platelet activation pathway). Besides cell autonomous effects of miRNAs, they are also involved in cellular communication, by two suggested mechanisms: I) effecting cytokines secretion and growth factors; or II) by exerting a direct signalling function (Shu et al., 2019), hence the suggested enrichment of miRNAs and their targets in cell signalling pathways (Figure 6.5). Moreover, following vascular injury, platelets are one of the most essential players in thrombus formation, due to their ability to initiate the initial step of the haemostatic process and close

interaction with endothelium, as well as interaction with sub-endothelial components (Liang et al., 2018) (Section 1.2 and 1.3). In addition, the endothelium is one of the key targets of circulating MVs and miRNAs have been discovered as pivotal regulators of EC function (De Rosa, et al., 2014). MVs play an active and crucial role in regulating vascular endothelium function via delivery of miRNAs (Liang et al., 2018). Therefore, it is not surprising that the preliminary data (Figure 6.5) suggest miRNAs in endothelial-derived MVs appear to target mRNAs enriched in cell signalling pathways (i.e., platelet activation pathway). Moreover, as described previously in Section 1.6 and 4.2, EMVs act as an essential marker of vascular function and key adverse cardiovascular events in patients with endothelial dysfunction. EMVs have a further biological carrier function, which proposes different explanation for their role in pathophysiology (Fan et al., 2017). For instance, it has been reported that EC-derived miRNA-143 and miRNA-145 may be transported to SMCs by EMVs and subsequently prevented SMC differentiation, thus prevented atherogenesis (Shu et al., 2029). Furthermore, Several studies demonstrated that EMVs with a high level of particular miRNAs (i.e., miRNA-19b) may inhibit EC migration as well as angiogenesis via their targets Rho GTPase–activating protein 5 (ARHGAP5) and transforming growth factor-β2 (TGF-β2) which regulate the function of HUVECs (Fan et al., 2017). Beside platelet activation pathway, TGF-β signalling pathway was also significantly enriched of miRNAs and their targets (Figure 6.5), this may further demonstrate that EMVs may modulate signalling in thrombus formation via a number of miRNAs present in a high level. Nevertheless, to confirm these striking preliminary data herein, validating experiments are required.

In this chapter, it was also speculated that inflammatory conditions may affect the quantity and/or diversity of miRNAs in EMVs. miRNA generated in treated and untreated conditions were assessed to explore whether EMVs from quiescent cells have a different miRNA content compared inflammatory conditions. The total miRNA quantity was lower in TNF-α-treated samples (Figure 6.4 and Figure 6.6). However, it is unclear if the differences in total miRNA quantity reflect: I) proinflammatory cytokines such as TNF-α induce the release of certain miRNAs, while inhibit the

183

release of others (Foudi and Legeay, 2021); or II) due to a batch effect, because untreated samples were generated separately to treated samples. Although most of the batch effect was successfully removed using library size correction, as the batch effect directly aligned with the experimental conditions, it is possible removing some biological signals when adjusted for library size which may resulted in a reduction in miRNA quantity. This indicates the possibility of data containing some false negatives. Thus, these potential findings require confirmation in a validation experiment. Nevertheless, there was a number of miRNAs that were differentially expressed between control and TNF-α EMVs (Figure 6.6), suggesting the inflammation results in EMVs with altered miRNA content. Interestingly, when analysing the GO pathways enriched in the differentially expressed miRNAs, the most significantly enriched pathway in the downregulated miRNAs in response to TNF-α was platelet activation pathway (Figure 6.7) containing 27 miRNAs and predicted 76 mRNA targets. This may suggest that EMVs generated in the presence of inflammation may have altered ability to regulate haemostasis. These observations are in line with the study of Alexy et al. that reported proinflammatory cytokine TNF-α in ECs altered release and transfer of miRNAs in EMVs and as a result cells shed EMVs with different levels of miRNA presence (Alexy et al., 2014). Further studies reported the level and transfer of miRNAs from MVs may be regulated by inflammatory factors. For instance, the level of miRNAs such as miRNA-223 in PMVs was upregulated by thrombopoietin (TPO), as well as thrombin (Shu et al., 2019). In addition, the same specific miRNA may have different effects in the presence of inflammation, as the function of miRNAs depends on both its endogenous expression and that of its mRNA target whose expression may also be altered by inflammation. Furthermore, exogenous application of a miRNA may have different effects of endogenous expression (Shu et al., 2019). For instance, it has been reported that miRNA-126-5p preserved EC proliferation following hyperlipidaemic stress and protected from atherosclerosis by surprising Notch-1 inhibitor delta-like 1 homolog (Dlk1); however, endogenous miRNA-126-3p showed no effect (De Rosa 2014). Nevertheless, subsequent studies showed that application of miRNA-126-3p carried by EMVs induced endothelial repair and inhibited

atherosclerosis (Shu et al., 2019). Beside the experimental validation described in Section 7.4.3, the determinants and regulatory factors of miRNAs, as well as their sorting and packaging into EMVs require further studies. Nevertheless, pathway analysis of miRNAs and their mRNA targets in pathways suggests that signalling pathways such as cAMP and platelet alpha granule lumen were significantly upregulated, and signalling pathways such as vesicle-mediated transport and PI3K-Akt were significantly downregulated (Figure 6.7). The regulation of these pathways (i.e., vesicle-mediated and PI3K-Akt) has been reported to affect important biological aspects such as cellular differentiation and apoptosis, and detected in various human conditions including inflammation and CVDs, thereby exerting a broad influence on signalling and developmental pathways (Jansen et al., 2014; Bugueno el al., 2020; Veziroglu, and Mias, 2020). Furthermore, it has been proposed that some miRNA-mediated regulation pathways have several interactions with vesicle-mediated transport pathway, as they share mutual binding sites in mRNA 3'UTRs and share mutual genes and enzymes (Veziroglu and Mias, 2020). For instance, targeting the activation of these pathways (i.e., PI3K-Akt-signalling pathway) may limit inflammation induced conditions. For instance, Schabbauer et al showed that drugs targeting PI3K-Akt activation may limit lipopolysaccharide (LPS)-induced inflammation and coagulation and therefore reducing sepsis mortality (Schabbauer et al., 2004). In addition, the miRNAs uptake by vesicle-mediated transport pathway has been found to target and regulate a number of mRNAs (Sonoda et al., 2021). For instance, several miRNAs have been suggested to regulate vesicle-mediated pathway through Ago2-miRNA complexes in human plasma, which may suggest that Ago2 might have a role in the stability of released miRNAs. However, the precise mechanisms at a molecular level in which this regulation occurs remain under investigation in haemostasis (Shu et al., 2019). Nevertheless, genetic analysis using plasma from 835 participants showed that vesicle-mediated-miRNAs were potentially targeting mRNAs (Rodriguez-Rius et al., 2020). Some studies reported these miRNAs were potentially associated with a number of vascular associated diseases (Shu et al., 2019), i.e., these miRNAs target mRNAs associated with genes encoding proteins in coagulation cascade (Sonoda et al., 2021). Furthermore, research suggests that

miRNAs act as modulators of the haemostatic system by direct or indirect interaction with their targets encoding protein associated with coagulation and dysregulation of miRNA targets have been reported to disturb gene expression (Katarzyna et al., 2020), highlighting the important role miRNAs play modulating cellular processes in coagulation as alterations in levels of proteins mediated by miRNA-mRNA targets may result in bleeding disorders or thrombosis (Shu et al., 2019). For instance, in haemophilia A, miRNAs have suggested to directly target and downregulate the F8 gene encoding FVIII (Katarzyna et al., 2020). Furthermore, it has been reported that miRNA-27 and miRNA-494 directly target 3'UTR of TFPI and downregulate TFPI mRNA, and overexpression of these miRNAs promoted procoagulant activity resulted by elevated FXa generation which promote thrombotic disease (Katarzyna et al., 2020). Additionally, it has been shown that several miRNAs were differentially expressed in EMVs in thrombosis and haemostasis patients, for instance, transfer of miRNA-126 or miRNA-223 is involved with arterial thrombosis that target ICAM-1, VCAM-1 and resulted in endothelial dysfunction (Shu et al., 2019; Katarzyna et al., 2020). Furthermore, miRNA-1 and miRNA-499 which have been suggested to regulate the metabolism of the myocardium, which is associated with cardiac development and disease (Jansen et al., 2014). For instance, it has been shown that miRNA-1 is upregulated in plasma and can be used as biomarker for MI (Sun et al., 2018). It was also reported that deletion of the mature miRNA-1-2 sequence in mouse embryonic stem cells resulted in ventricular septum abnormalities, rapid heart dilatation, rhythm disturbances and ventricular dysfunction (Jansen *et al.*, 2014; Foudi and Legeay, 2021). Moreover, in patients with an acute coronary syndrome, De Rosa et al. showed increased trans-coronary concentration gradients of miRNA-499, which suggests that this miRNA is likely released by the heart. In addition, levels of these miRNAs correlated with MI biomarker high-sensitivity troponin T (De Rosa et al., 2014). These finding may suggest transfer of functional miRNAs into vascular ECs through EMVs which demonstrate an important role in modulating EC-inflammatory response. Moreover, the reference repositories miRbase and miRDB, currently hold over 2,000 human mature miRNAs listed and believed they collectively target over 1.6 million genes and over 29,000 unique

186

gene targets (Kozomara et al., 2019; Chen and Wang, 2020), showing that each miRNA has a mean of approximately 600 potential gene targets. However, the miRNA target database utilised in the GeneCodis software used in this chapter, miRTarBase, only incorporated experimentally verified miRNA-mRNA interactions and not potential interactions based on computational prediction of complementarity between the 3' UTR of mRNAs and the stem-loop of miRNAs. Nonetheless, the number of miRNAs in vesicle-mediated transport (n: 46) target 460 mRNAs, showing that each miRNA has a mean of 10 mRNA targets even using miRTarBase (Figure 6.7). Hence, it can be challenging to ascribe specific roles to a particular miRNA. Nevertheless, due to numerous miRNAs exhibit tissue-specific and developmental-stage specific patterns of expression as well as encapsulation within MVs, the interest in using miRNAs as biomarkers has increased significantly over the past 10 years.

The data presented in this chapter require validation and further investigation as described in Section 7.4.3. MVs and the miRNAs they carry have inspired numerous studies on physiology and pathophysiological states. Therefore, further studies of the precise underlining molecular mechanisms which mediate the effect of miRNAs and the underlining regulation effects of their targets will expand our knowledge, particularly on miRNAs carried by EMVs underpinning haemostasis and CVDs, as further investigations can help understand the biological relevance of these associations, which will greatly facilitate the potential use of miRNAs as potential biomarkers of endothelial dysfunction and recurrence of cardiovascular events.

6.5. Conclusion

Endothelial-derived MVs are suggested to transfer miRNAs from one cell to another, regulating gene expression by the target/activation of their mRNAs. miRNAs carried by EMVs have been proposed to regulate the physiological and pathophysiological processes in endothelium. Data presented herein suggested that EMVs carry miRNAs that are enriched in cell signalling pathways and targeted mRNAs associated with thrombus formation. Furthermore, miRNA quantity was lower in EMVs generated in TNF-α stimulated cells and carry different miRNA cargo. Also, the biological pathways enriched amongst the target mRNAs of the differentially expressed miRNAs, highlighted biological processes relevant to endothelial function and haemostasis, i.e., those mainly associated with cellular communication.

Chapter 7: General Discussion

7.1. Introduction

EMVs are submicron membrane-derived vesicles produced by ECs upon activation, apoptosis or stimulation. Formation of these small membrane vesicles involves membrane blebbing of the parent cell, with specific phospholipid transporters activated through a rise in intracellular calcium. EMVs play an important role as a means of communication between secreting and recipient cells. EMVs, as "multipurpose carriers", carry cargo between these cells, facilitating the intracellular exchange of cellular materials, such as lipids, miRNAs and proteins through which they can change the behaviour of recipient cell (Heemskerk, Bevers and Lindhout, 2002; Vajen, Mause and Koenen, 2015). Evidence suggests that EMVs play a paradoxical role in haemostasis with both procoagulant and anticoagulant activities (Mohan Rao, Esmon and Pendurthi, 2014). Therefore, studies of EMVs to date have produced contrasting data regarding the role of EMVs in haemostasis.

7.2. Thesis Overview and Main Findings

It is clear from the data presented herein, that EMVs do have a potentially important role in haemostasis, targeting a number of different mechanisms: I) In flow conditions, EMVs alter the coagulation/anticoagulation balance to modulate thrombus size and strength, potentially reducing thrombus extent; II) EMVs are produced with an enrichment of particular species of phospholipids, with the potential to support enhanced anticoagulant activity, and III) EMVs carry miRNAs that target cell signalling pathways underpinning haemostasis, that potentially may facilitate anticoagulant EC behaviour in inflammatory conditions. The main findings are highlighted in Figure 7.1.
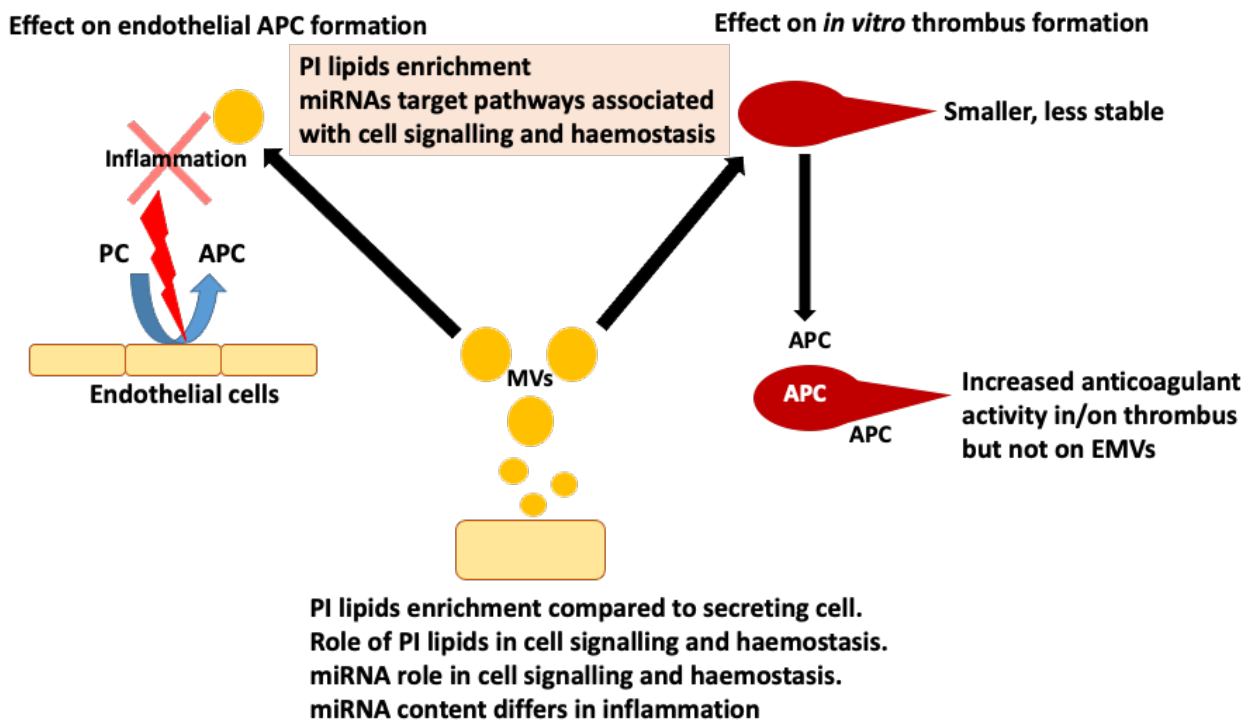
Figure 7.1: A summary of thesis findings. *An overview of thesis highlighting findings of each chapter. Chapter 3 described the development of in vitro methods for assessment of thrombus formation. Chapter 4 investigated the effect of EMVs on thrombus formation. Chapter 5 investigated lipid composition of parent cells and their derived-EMVs, and Chapter 6 investigated the miRNA content of EC-derived MVs (quantity and species). EMVs = microvesicles, EMVs= endothelial microvesicles, APC= activated protein C.*

7.2.1. The Effect of EMVs on Thrombus Formation

Accumulating evidence suggests that EMVs have procoagulant effects due to their PS rich outer membrane and the expression of TF inducing thrombotic activity. Conversely, EMVs have been reported to support anticoagulant APC mediated regulation of coagulation (Iba and Ogura, 2018; Zara et al., 2019). These more recent discoveries point to a more complex role of EMVs in coagulation, where it is possibly the balance between procoagulant and anticoagulant properties ultimately determines their net effects on haemostasis and thrombosis (De Caterina *et al.*, 2013; Zara et al., 2019).

The data presented herein (Chapter 4) demonstrate that adding exogenous EMVs significantly reduced the size and strength of thrombi (Figure 7.2). This outcome was not expected as the majority of studies reported that EMVs induce procoagulant activity in thrombus formation induce procoagulant activity in thrombus formation (Heemskerk, Bevers and Lindhout, 2002; Wohner, 2008; Barteneva *et al.*, 2013) and therefore it may be expected that EMVs would produce larger thrombi. Conversely, studies have demonstrated that EMVs exhibit anticoagulant effects (Oggero, Williams and Norling, 2019), demonstrating the contrasting role of EMVs in haemostasis. Our data also demonstrate that EMVs are incorporated into the thrombus. Currently there is no evidence in the literature regarding incorporation of EMVs in thrombi *in vitro*. These novel findings about the thrombus led us to investigate the anticoagulant properties of EMVs in thrombus formation, indicating a significant increase in APC generation associated with the thrombus in the presence of exogenous EMVs. These novel findings support the hypothesis that EMVs alter anticoagulant APC activity during thrombus formation and therefore EMVs may reduce thrombus formation via the APC pathway. We hypothesise that this might be mediated by modulation of behaviour of cells in the thrombus, such as platelets or monocytes. However, research in this area is scarce (Mathiesen et al., 2021).
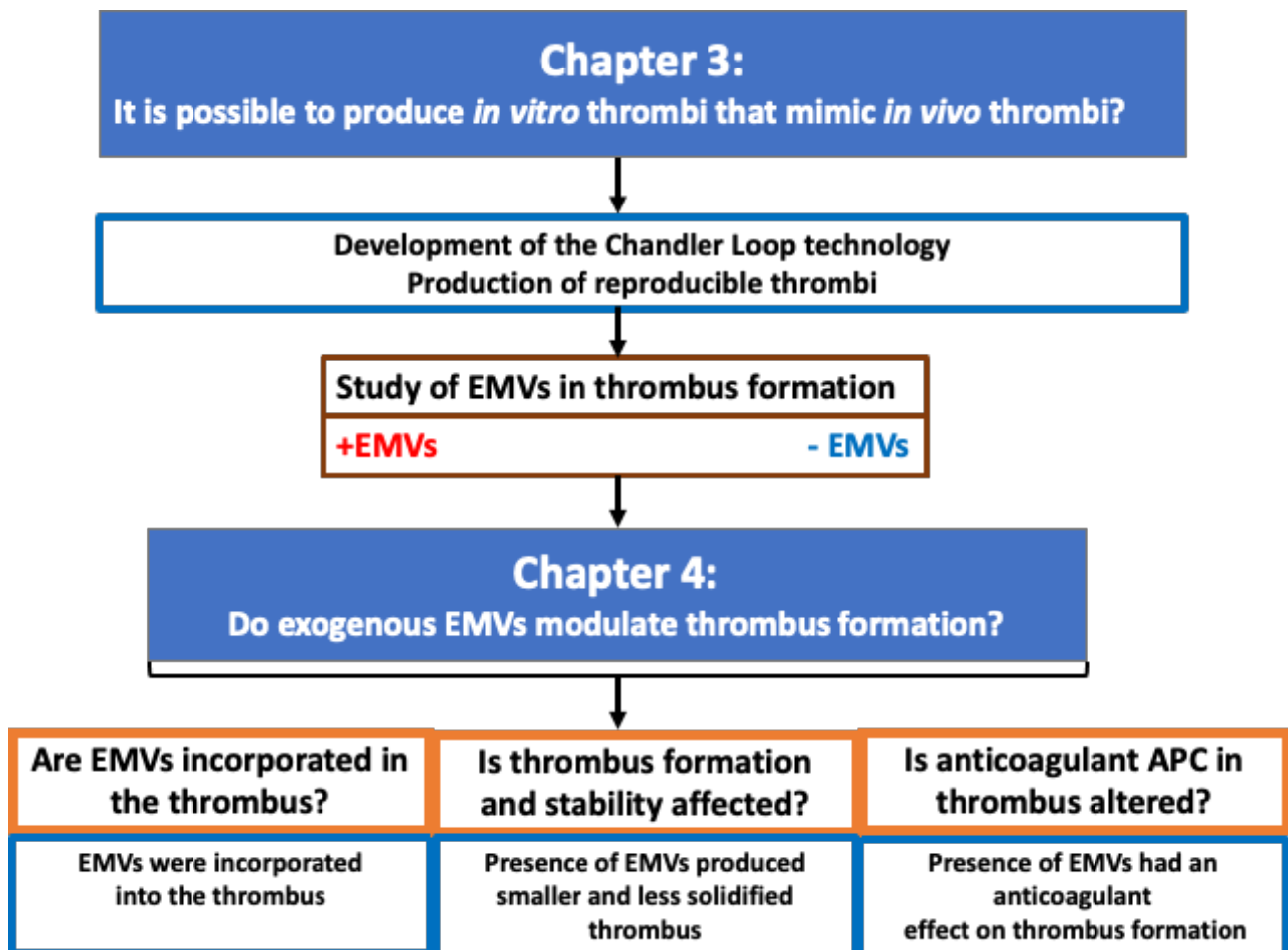
Figure 7.2: Schematic diagram summarising the outcome of Chapter 3 and 4. *In Chapter 3, the Chandler Loop method was developed and produced reproducible thrombi. Chapter 4 investigated the location of exogenous EMVs in thrombus as well as the anticoagulant role of these EMVs in thrombus formation.*

7.2.2. The Role of Lipid Composition and Bilayer Structure in EMV Formation

Lipid composition of EMVs differs from parent membranes, and the production of MV requires the creation of a bilayer with a higher degree of curvature. Particular lipids favour the formation of these curved surfaces. Therefore, lipid composition, bilayer and curvature are important components of MV secretion and formation, and their structure is a key factor in the structure and function of cell membranes and may affect the haemostatic potential of EMVs.

Data presented herein (Chapter 5) suggest that EMVs were enriched in lipids that favour the formation of curved surfaces e.g. phosphorylated derivatives of PI (Doyle and Wang, 2019), suggesting these lipids may play a role in the formation and secretion of MVs, as well as in cell signalling. The contribution and findings of this chapter to the overall thesis are presented in Figure 7.3.

Chapter 5:

I) Do EMVs have a distinct lipid composition and bilayer structure from that of their parent cell?

II) Do EMVs carry lipids that play a role in cell signalling and haemostasis?

| Lipid composition of EMV differs from parent cell | EMVs enriched in specific PI lipids | Bilayer composition with high curvature favours EMV formation |

Phosphorylated derivatives of PI favour the formation of curved surfaces

EMVs were enriched with phosphorylated derivatives of PI

Figure 7.3: Schematic diagram summarising the outcome of Chapter 5. ^{31}P-MAS-NMR showed EMVs were enriched in certain phospholipids in the lipid bilayer and they contained more phosphorylated PIs. ESI-MS showed a reduction in the overall chain length in EMVs, indicating that the budding of EMVs is accompanied by incorporation of PI whose acyl chains exhibit a lower overall volume than those of parent membranes.

7.2.3. The Role of EMV miRNAs in Haemostasis and Inflammation

Endothelial-derived MVs have been suggested to transfer miRNAs from one cell to another, regulating gene expression by the target/activation of their mRNAs. miRNAs carried by EMVs have been proposed to regulate the physiological and pathophysiological processes in haemostasis (Mir and Goettsch, 2020).

Data presented herein (Chapter 6) suggest that EMVs which may be incorporated in thrombus carry miRNAs that target pathways associated with cell signalling pathways underpinning haemostasis. Moreover, the miRNA species differ in inflammatory conditions. The findings are summarised in Figure 7.4.

Chapter 6:
I) Do EMVs contain miRNAs that may play a role in in cell signalling and thrombus formation?
II) Does inflammation alter the miRNA content of EMVs?

Explored miRNAs and assessed biological pathways that may potentially play a role in cell signalling and haemostasis

Preliminary data suggest miRNA in EMVs and their targets are enriched in biological pathways associated with cell signalling and thrombus formation

Preliminary data suggest miRNA content differs between miRNA in EMVs from quiescent vs TNF-α-treated cells, and miRNA may regulate biological pathways associated with haemostasis

***Figure 7.4: Schematic diagram summarising the outcome of Chapter 6.** Endothelial-derived MVs were collected from quiescent cells and from TNF-α-treated cells to investigate the miRNA quantity in both conditions as well as alteration in differentially expressed pathways. Furthermore, relevant miRNAs and their targeted pathways were investigated which may be further studied.*

To summarise, data presented in this thesis demonstrate that EMVs may influence haemostasis in flowing blood and at the cellular level, as well as directly through EMV composition and indirectly through the cargo they carry. Contextualising this with the current knowledge base, it is possible that the relative haemostatic properties of EMVs are influenced by diverse factors including cell activation/stimulation, the inflammatory microenvironment, the local and distant cellular influences, and the physiological and pathological state (Okamoto et al., 2011; Buzas et al., 2014; Enjeti et al., 2019; Katarzyna et al., 2020).

7.3. Thesis Limitations

The field of MV research has rapidly evolved during the course of this research, providing both opportunities and challenges. Pre-analytical and analytical issues included standardisation within this project of blood collection, preparation and then finally analysis of EMVs. These were mainly consistent with the ISEV and ISTH guidelines issued in 2015, however more importantly were consistent within this project. The microscopy studies of whether EMVs were incorporated into thrombi were limited: the staining was weak despite using a variety of methods and numbers of experiments were lower than would be expected due to time constraints. However, combining the limited staining data with the flow cytometry data demonstrating that EMV numbers were reduced during thrombus formation provides an indication that EMVs were incorporated into the growing thrombus. Both the lipid and miRNA investigation protocols from cell/EMV production through to analysis methods were extensively optimised, however they were conducted to the satisfaction of lipidomic laboratories in Southampton and provide novel and exciting data, to be explored further in the future. However, investigations were conducted on small sample number and future studies should increase sample numbers. Working with EMVs was challenging, from ensuring reproducible isolation, enumeration and characterisation, and use as a source material for extractions.

7.4. Thesis Future Perspectives

7.4.1. The Effect of EMVs on Thrombus Formation

In this thesis, EMVs appeared to support anticoagulant activity as measured directly. Moreover, the coagulation properties were explored in terms of the haemostatic balance in the Chandler loop, i.e., if EMVs appeared to enhance pro-coagulant properties, they would participate in the production of bigger thrombi or faster forming thrombi. However, further investigations are required to elucidate the role of EMVs in haemostasis, and therefore, future studies should include investigations of the effect of EMVs on thrombin generation; *in vitro* experiments can be performed using Calibrated Automated Thrombogram (CAT), to investigate samples in the presence and absence of exogenous EMVs in whole blood samples. Furthermore, additional tests can be used to explore thrombin generation (TG) in whole blood such as thromoelastography (TEG). TEG is increasingly being recognised as versatile diagnostic tool in the field of haemostasis and thrombosis. Moreover, anticoagulant pathways such as anticoagulant APC can be further validated by exploring the precise EMVs effect on APC/other cell types such as platelets and/or monocytes *in vitro*. This may also be studied *in vivo* (Diaz et al., 2019). Furthermore, investigation of the role of phosphorylated PIs in supporting APC generation may yield interesting results as these lipids have been reported to induce anticoagulant activity on APC.

7.4.2. The Role of Lipid Composition and Bilayer Structure in EMV Formation

The data presented herein (Chapter 5) may be a starting point for further study and refinement on the phospholipids studies, particularly PI species. Initially, it would be desirable to validate the experiments conducted to date, taking into consideration obstacles encountered in this thesis. The condition for the isolation of the cell and EMV membranes in sufficient quantity for conducting ^{31}P-

MAS-NMR is now established which should facilitate the process. Furthermore, careful control of the pH and the ions present in the sample may enable the identification of the different phosphorylated derivatives of PI to be determined (i.e., PI-3-biphosphate vs PI-4-phosphate vs, PI-5-biphosphate). In contrast to numerous previous studies, it is essential to correlate their presence with the type of lipid chain they possess. Due to time constraints, it was not possible to replicate the ESI-MS and these experiments should be repeated. Methods now exist that permit the separation of different phosphorylation states of PI by HPLC, allowing their quantification prior to analysis by ESI-MS to characterise the types of acyl chains present. Moreover, with the protocols established herein for the isolation of EMVs and parent membranes for both ^{31}P-MAS-NMR and ESI-MS analysis, a more thorough analysis of the lipid composition can be conducted, and the influence of TNF-α more accurately determined. Furthermore, different cells such as platelets and/or monocytes can be explored with different PI derivatives to explore their haemostatic effects.

7.4.3. The Role of EMV miRNAs in Haemostasis and Inflammation

miRNA experiments can be further validated by increasing sample number from both parent cells (HUVECs) and their derived MVs, as well as performing experiments in parallel using same experimental conditions to avoid batch effect. Furthermore, qRT-PCR should be performed to check the sequencing data by independent method to show differences in gene expression. Future studies can explore whether the differences observed in miRNA content count for functional properties observed between TNF-α and control EMVs in selected functional assay of cell culture. Following functional assay, miRNA can be compared to potential target genes of ECs. This can be approached by comparing miRNAs to reduced target list of genes in ECs, to propose that a specific miRNA affected a specific mRNA and protein production and function. In order to achieve the above hypotheses and to test miRNA functions, two experimental methods can be approached by: I) treating cells with collected EMVs and observe changes in gene expression; II) treating collected EMVs with particular miRNAs, followed by addition of miRNAs to EC culture. Subsequently, differences in

proteins expressed by gene can be explored, or alternatively, Dicer/ Antagomirs can be placed to block miRNA activity to observe affect. Moreover, exogenous EMVs can be added to cell culture, followed by flow cytometry count, then miRNA expression can be detected using q-PCR to identify relevant miRNAs. Moreover, coagulation activity on EC can be studied by investigating the interaction of EMVs and miRNAs they carry, on EC-mediated haemostasis. These experiments are highlighted in Figure 7.5.
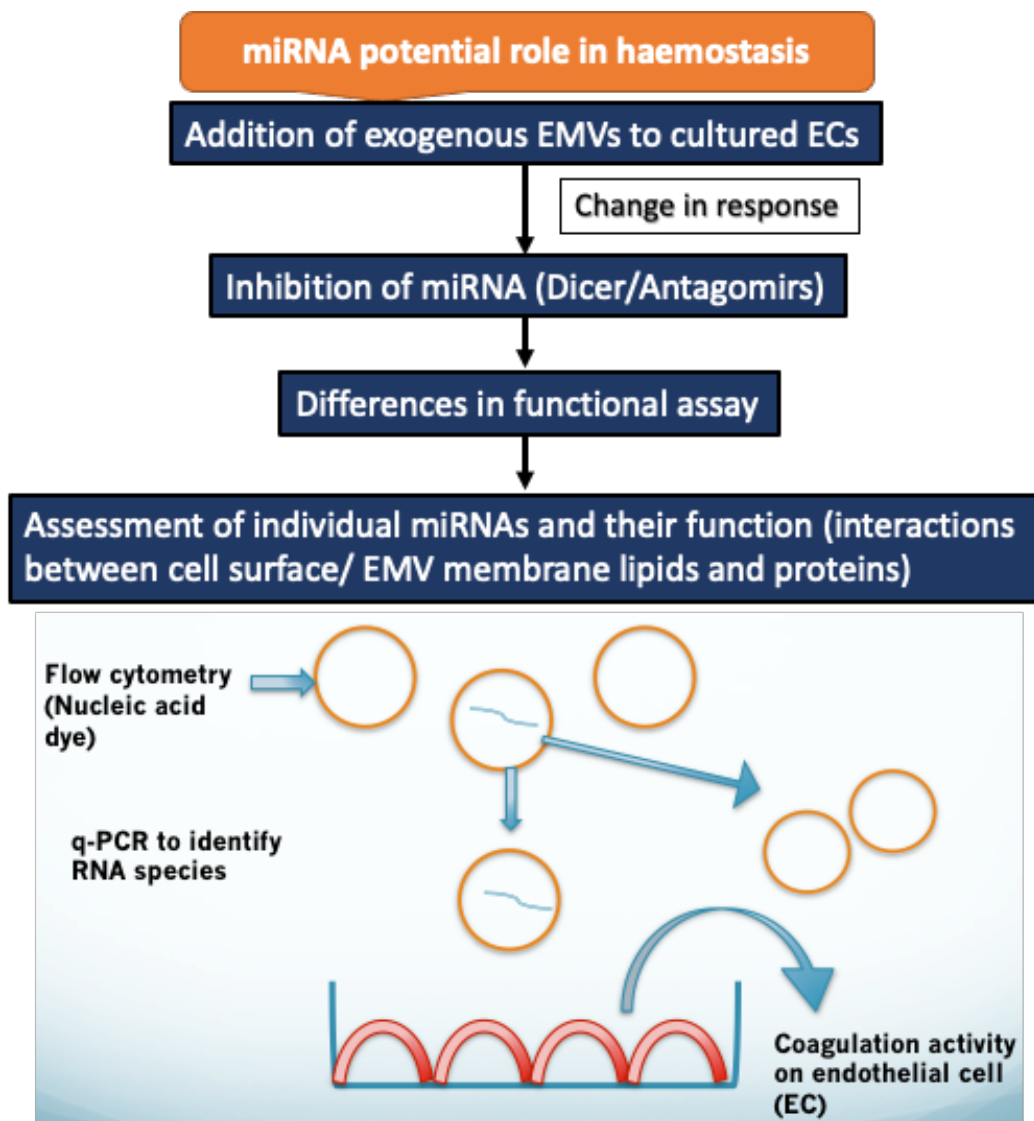
Figure 7.5: Potential roles of miRNAs in haemostasis. EMV carried miRNAs can by identified by flow cytometry, then can apply q-RT-PCR to identify miRNA types, then transfect in cells and add miRNA to show level of reporter is altered (expressed). Then explore whether added exogenous EMVs to cultured ECs change the haemostatic function of the EC.

Individual miRNAs (i.e., miR-1 and miR-499) and their target genes as well as pathways appeared interesting for further study. For instance, the effect of miR-1 and miR-499 can be explored in normal and inflammation groups by the inhibition of PDCD4/SOX6 through PI3K-Akt and vesicle-mediated pathways. Furthermore, can explore the prediction of the relationship between miR-1, miR-499 and PDCD4 or SOX6 3'UTR. Therefore, would be of interest to investigate these selected miRNAs and suggested target genes, to gain a better understanding of the role these miRNAs play in cell-cell communication in haemostasis and in endothelial dysfunction-associated diseases. Further experiments are highlighted in Figure 7.6.
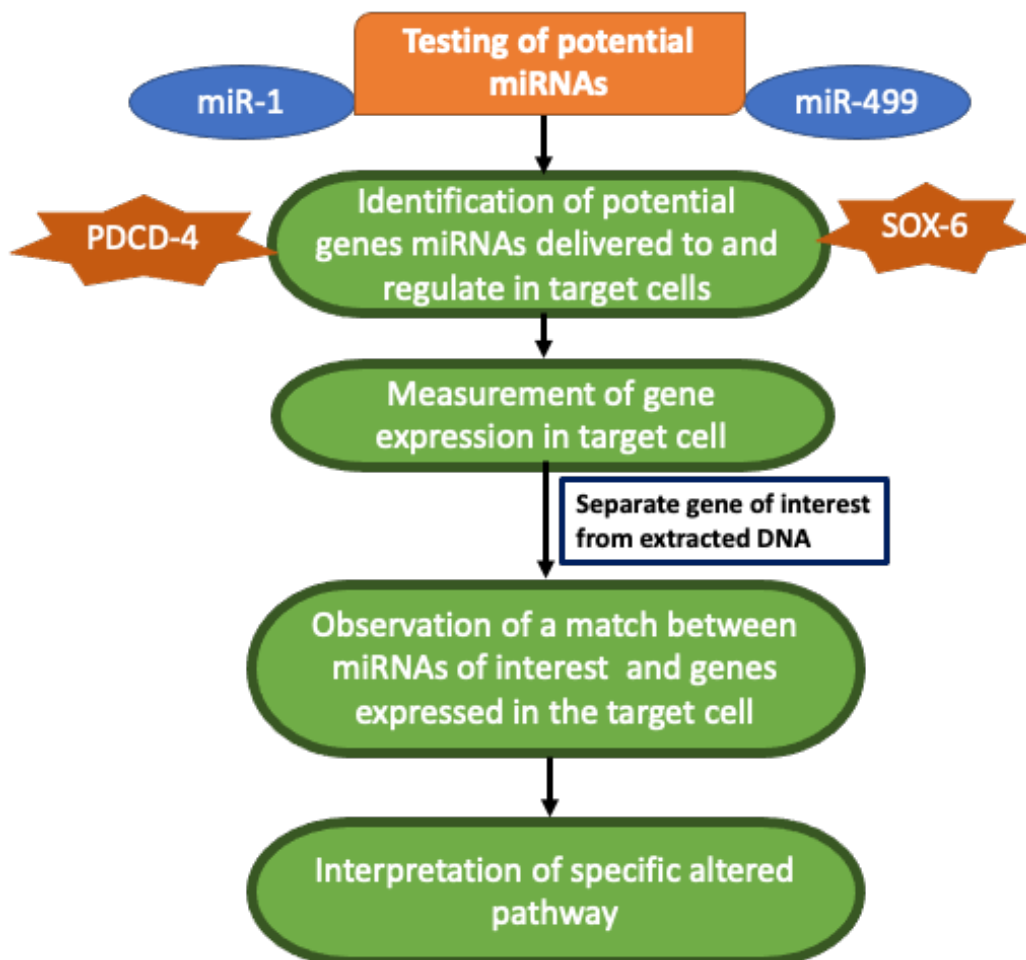
Figure 7.6: Potential miRNAs and predicted target genes. Selected miRNAs (i.e., miR-1 and miR-499) can be identified by creating plasmids that couple the 3'UTR of target genes (PDCD4, SOX6), thus miRNA can bind to reporter gene to report expression in transfected cells.

7.5. Conclusion

This thesis has demonstrated that EMVs reduce the extent of thrombus formation and that this is at least partly related to changes in anticoagulant activity associated with the thrombus; however, not via anticoagulant proteins directly carried on EMVs. These haemostatic changes may be due to the lipids found on EMVs which appear to be enriched compared with their parent cells. This work was extended to consider the effects of EMVs on ECs, building on previous work in our laboratory demonstrating that EMVs protect APC activity on ECs in the presence of inflammation. In this thesis, preliminary experiments with miRNA support the idea that the miRNAs cargo of EMVs could alter EC behaviour, particularly in coagulation. This multi-pronged approach has provided several novel insights into the interaction between EMVs, inflammation and haemostasis.

The *in vitro* preliminary findings presented in this thesis (Figure 7.1) set a foundation for EMVs to be further studied, particularly the potential phosphorylated PI lipids, enriched pathways by EMVs carried miRNAs and anticoagulant role they might play in thrombus formation, because the role of EMVs in coagulation, inflammation and endothelial dysfunction not fully understood. Therefore, exploring the role of EMVs further may promote their use as biomarkers and novel therapeutic treatments.

Appendices

8.1. Ethical Approval

UNIVERSITY OF
Southampton
School of Medicine

NHS
Health Research Authority

South West - Cornwall & Plymouth Research Ethics Committee

Level 3
Block B
Whitefriars
Lewins Mead
Bristol
BS1 2NT

26 October 2016

Dr Nicola Englyst
Level C, IDS Building
Southampton General Hospital
Institute of Developmental Sciences
SO16 6YD

Dear Dr Englyst

Study title:	**Characterising microvesicles and their function in the dynamics of thrombus formation, cell interaction and inflammation.**
REC reference:	**15/SW/0258**
IRAS project ID;	**172734**

This study was given a favourable ethical opinion by the Committee on 25 August 2015.

Research Ethics Committees are required to keep a favourable opinion under review in the light of progress reports and any developments in the study. You should submit a progress report for the study 12 months after the date on which the favourable opinion was given, and then annually thereafter. Our records indicate that a progress report is overdue. It would be appreciated if you could complete and submit the report by no later than one month from the date of this letter.

Guidance on progress reports and a copy of the standard NRES progress report form is available from the Health Research Authority website.

The Health Research Authority website also provides guidance on declaring the end of the study.

15/SW/0258:	**Please quote this number on all correspondence**

Yours sincerely

L Roberts.

Lucy Roberts
REC Manager

8.2. Participant Information Sheet

University of Southampton
School of Medicine

Study Title: Endothelial Microvesicles (EMVs) involvement in the dynamics of thrombus formation

Names of Principal Investigators: Mr Giedo Elamin, Dr Nicola Englyst, Dr Judith Holloway, Prof John Holloway, & Dr Philip Williamson.

Version no: 1.0

Date: October 2014

Study Ethics Number: 12684

Program Funding: Kerkut Charitable Trust and University of Southampton Vice Chancellors Award.

You are being invited to take part in a research study. Before you decide it is important for you to understand why the research is being conducted and what it would involve. Please take time to read the following information carefully and discuss it with friends, relatives and your GP if you wish. Ask us if there is anything that is not clear or if you would like more information. Take time to decide whether or not you wish to participate.

Consumers for Ethics in Research (CERES) publish a leaflet entitled 'Medical Research and You'. This leaflet gives more information about medical research and looks at some questions you may want to ask. A copy may be obtained from CERES, PO Box 1365, London N16 0BW.

Thank you for reading.

Study Background: The physiological response to a wound includes activation of the coagulation cascade, recruitment of specific cells and formation of a fibrin-rich meshwork (thrombus) to prevent excessive bleeding.

EMVs are tiny fragments produced during activation of cells. EMVs are produced by endothelial cells and have been shown to carry pro- and anti-coagulant/fibrinolytic proteins, and therefore may participate in maintaining haemostasis.Increased levels above normal healthy concentrations have been linked to a number of diseases.

What is the purpose of the study
Little is known about the role of EMVs during thrombus formation, and therefore this study aims to further our understanding of the character and actions of EMVs in clot formation.

Methods to be used: Immunohistochemistry, confocal microscopy, coagulation assays, cell culture, flow cytometry, microRNA analysis, solid state-NMR.

Potential clinical impact: Increasing our knowledge of the role of EMVs in the haemostatic response may help our understanding of health, as well as thrombosis and haemorrhagic disease. This research potentially provides a novel route for governing thrombus formation, through use of physiological or manufactured EMVs as vectors for delivering coagulation therapy.

Program Funding:

The Gerald Kerkut Charitable Trust (Known as Kerkut) was established by Professor Kerkut. The objects of the Trust as stated in the Governing Document are :- *"to advance education and research in Physiology at Southampton University by providing bursaries and prizes to students of physiology at Southampton University and publishing the useful results and to or for such other charitable purposes as the trustees shall decide"*.

Currently the trust is supporting more than 20 postgraduate students in the University of Southampton including myself.

Why have I been chosen?

You are healthy and suitable for this study.

Do I have to take part?

It is up to you to decide whether or not to take part. If you decide to take part you will be given this information sheet to keep and be asked to sign a consent form. If you decide to take part you remain free to withdraw at any time and without giving a reason.

What would happen to me if I take part?

If you agree to participate you will be enrolled in this study, which will be conducted at Southampton General Hospital, Tremona Road, Southampton, SO16 6YD. Your participation will be for no more than 30 minutes.

The Visit
• A researcher will ask you some questions about you and medications you are currently taking.

• You will be asked to give up to 60ml of blood (8 teaspoons) from a vein in your arm.

What will happen to the sample I have provided during this study?
Your sample will be coded and those involved in the analysis will not be aware of who these samples came from (unlinked anonymised).

The sample that we take from you will be separated into plasma, refined cells and MVs suspended in plasma and then frozen and later analysed using a variety of scientific techniques in the laboratory in order to gain a better understanding of the role of EMVs populations in blood clotting. The blood containing EMVs will be investigated and phenotyped based upon their size, molecules they express and their DNA/RNA content.

Any DNA/RNA analysis is purely for research purposes and neither you nor your doctor would be informed about any of the results.

The samples may be sent to a third party organisation for analysis if a special technique that we did not have available and was thought to be important to gain further information, was required for the

study. In this case the third party organisation would not know the identity of the sample and will return any sample remaining after the analysis is completed.

What do I have to do?

If you are happy to take part in this project, we will arrange an appointment for you to donate a blood sample.

What are the alternatives for diagnosis or treatment?

This study is of no benefit to you in respect of diagnosis or treatment.

What are the possible risks of taking part?

Occasionally when donating blood some people feel faint and there is a chance of bruising at the site of venepuncture.

What are the possible benefits of taking part?

You would not receive any benefits directly; however, this study will increase our understanding of the role of EMVs in blood clotting, and could possibly lead to changes in treatment in the future.

What if something goes wrong?

This study is covered by indemnity of the University of Southampton. In the unlikely event that you come to any harm as a result of taking part in this study, the usual University complaints mechanisms are open to you.

Would my taking part in this study be kept confidential?

Any information that is collected about you during the course of the research will be kept strictly confidential. Because the samples are given a unique code that is not recorded on your consent form, data generated using your samples cannot be traced back to you. If data is published in scientific/medical journals, data will be anonymous. Your GP will not be notified of your participation in this study.

What will happen to the results of the research?

The results of the research will be evaluated and may be published in scientific papers. You will not be identified from these results. If you wish we can notify you if an article based on the results of this study is published.

Who is organising and funding the research?

This study is sponsored by the University of Southampton, and funded by the Kerkut Charitable Trust and Southampton University Vice Chancellor's Award.

Who has reviewed the study?

The University of Southampton Research Governance Office and South West Research Ethics Committee have reviewed the study.

Contact for further information:

Further information is available from Giedo Elamin on 02380 798226, Dr Nicola Englyst on 023 8079 6925.

If you decide to take part in the study, you will be given a copy of the information sheet and a signed consent form to keep.

8.3. Participant Health Questionnaire

UNIVERSITY OF
Southampton
School of Medicine

Study Title: Endothelial Microvesicles (EMVs) involvement in the dynamics of thrombus formation

Names of Principal Investigators: Mr Giedo Elamin, Dr Nicola Englyst, Dr Judith Holloway, Prof John Holloway, & Dr Philip Williamson.

Version no: 1.0

Date: October 2014

Study Ethics Number: 12684

Subject Identification Number for this trial: ………..

Date: ……………..

Medical History Questionnaire

This is your medical history form, to be completed prior to your blood procedure. All information will be kept **confidential** and will not be given to anyone outside the reseach team without your written permission. This information will be used for the evaluation of study/studies. Please take your time answering all questions carefully and thoroughly, and then review it to be certain you have not left anything out. We understand that some parts of the form may be unclear to you. Therefore, please do not hesitate to ask and we will be happy to go through it with you as many times as you wish.

It might be helpful for you to keep a written list of questions or concerns as you complete the form.

Gender:	Male/ Female
Age (Years)	
Current medication (exclusion criteria: medication that may affect platelet, endothelial cell, or white blood cell function)	Name and details:
Are you taking any anticoagulation medications (i.e. Warfarin, Danaparoid…etc)	Name and details:
Have you taken any anti-inflammatory drugs in the past 48 hours? (i.e. ibuprofen, paracetamol, aspirin)	Name and details:
Are you taking any Non-steroidal anti-inflammatory drugs (NSAIDs), anticoagulants, anti-inflammatory or antiplatelet medication?	Yes/ No
	Comments:
Any self-prescribed medications, dietary supplements, or vitamins you are now taking?	Yes/ No
	Comments:
Do you have any infections, including coughs, colds or flu?	Name and details:
Chronic, recurrent or morning coughs?	Comments:
Episode of coughing up blood?	Comments:
Do you have any known cardiovascular diseases? (i.e. previous cardiac episode, hypertension)?	Name and details:
Do you have diabetes or abnormal blood sugar tests?	Yes/ No
	Comments:
Do you have any hematological disorders? (i.e. anemia, coagulopathy, blood clots)	Name and details:
Do you have pain in your chest or heart?	Yes/ No
	Comments:
Do you Phlebitis (inflammation of a vein)?	Yes/ No
	Comments:
Has a doctor ever mention your cholesterol level was high?	Yes/ No
	Comments:
Have you taken part in any vigorous	Yes/ No

exercise in the past 48 hours?

	Comments:
Are you already participating in an on-going clinical study?	Yes/ No
	Comments:
Have you recently donated blood?	Yes/No
	Comments:
Any allergies?	Yes/ No
	Comments:
Do you smoke cigarettes, cigars or pipe?	Yes/ No
If yes, how many do you smoke per day?	Comments:
Age started?	
If you have stopped smoking, when was it?	
Female participants only:	Yes/ No
Are you pregnant/ possibility that you are pregnant?	
Are you currently breast-feeding?	Yes / No
Would you like to be informed of any publications? If yes please provide an email address.	Yes/ No
	Email:

Additional Comments:

………

………

………

………

………

………

………

Name and Signature: _____

Date:

8.4. Participant Consent Form

UNIVERSITY OF Southampton
School of Medicine

Study Title: Endothelial Microvesicles (EMVs) involvement in the dynamics of thrombus formation

Names of Principal Investigators: Mr Giedo Elamin, Dr Nicola Englyst, Dr Judith Holloway, Prof John Holloway, & Dr Philip Williamson.

Version no: 1.0

Date: October 2014

Study Ethics Number: 12684

Subject Identification Number for this trial: ………..

Date: ……………..

PLEASE **INITIAL** THE BOXES IF YOU AGREE WITH EACH SECTION:

I confirm that I have read the information sheet version 1.0 dated October 2014 for the above study and have been given a copy to keep. I have been able to ask questions about the study and I understand why the research is being conducted and any risks involved. ☐

I understand that my participation is voluntary. I am donating blood for research and that I am free to withdraw at any time. If I withdraw I understand that any remaining donated samples will be disposed of. ☐

I agree to being contacted to be asked to donate a further sample at a later date if necessary (a 30 day interval between blood donation) ☐

I agree that donated blood sample for this study can be used for microparticle analysis as described in the section "What is the purpose of this study" and "What will happen to the samples I have provided" from the information sheet version 1 dated October 2014 for the above study. ☐

I understand that my GP will not be informed of my participation, and that the research will not directly benefit my health. ☐

I understand that by signing this consent form I am releasing the samples, the by-products and derivatives of the sample to the research team and to any third party. ☐

I understand that I will not benefit financially if this research leads to the development of a new treatment or test. ☐

Name of volunteer   Date   Signature

Name of researcher   Date   Signature

1 for volunteer, 1 to be kept by research team

8.5. Participant Details and Baseline Parameters

Study Title: Endothelial Microvesicles (EMVs) involvement in the dynamics of thrombus formation

Names of Principal Investigators: Mr Giedo Elamin, Dr Nicola Englyst, Dr Judith Holloway, Prof John Holloway, & Dr Philip Williamson.

Version no: 1.0

Date: October 2014

Study Ethics Number: 12684

Program Funding: Kerkut Charitable Trust and University of Southampton Vice Chancellors Award.

In order to record participant details and baseline parameters each time conducting venepuncture, participant details were anonymously recorded.

Fifty volunteers in total participated in this study, however, most participants volunteered more than once having a minimum four weeks interval between each participation as highlighted in study ethics.

The study included both male and females (53% and 48% consecutively). 95% of participants were Caucasians and 5% others (consisting of 3% Africans and 2% Asians). Furthermore, study ethics covered participation from anywhere within South East/South West of United Kingdom, however, most participants were from the city of Southampton.

Participants were mainly postgraduates based at the University of Southampton, participants were either BSc, MSc or PhD candidates.

Participants were excluded if they were on NSAIDs, anticoagulants, anti-inflammatory or antiplatelet medication. Moreover, participants were excluded if they had signs of an infection, or diagnosed CVD, diabetes, haematological disorders, hypercholesterolemia, allergies, pregnancy or breast-feeding. Participants were 100% non-smokers.

8.6. Effect of TNF-α and EMV on APC Production

These findings complement the findings from Chapter 4. A MMedSc student in the same research group investigated the effect of EMVs and TNF-α on anticoagulant APC production by ECs (Figure 8.1).
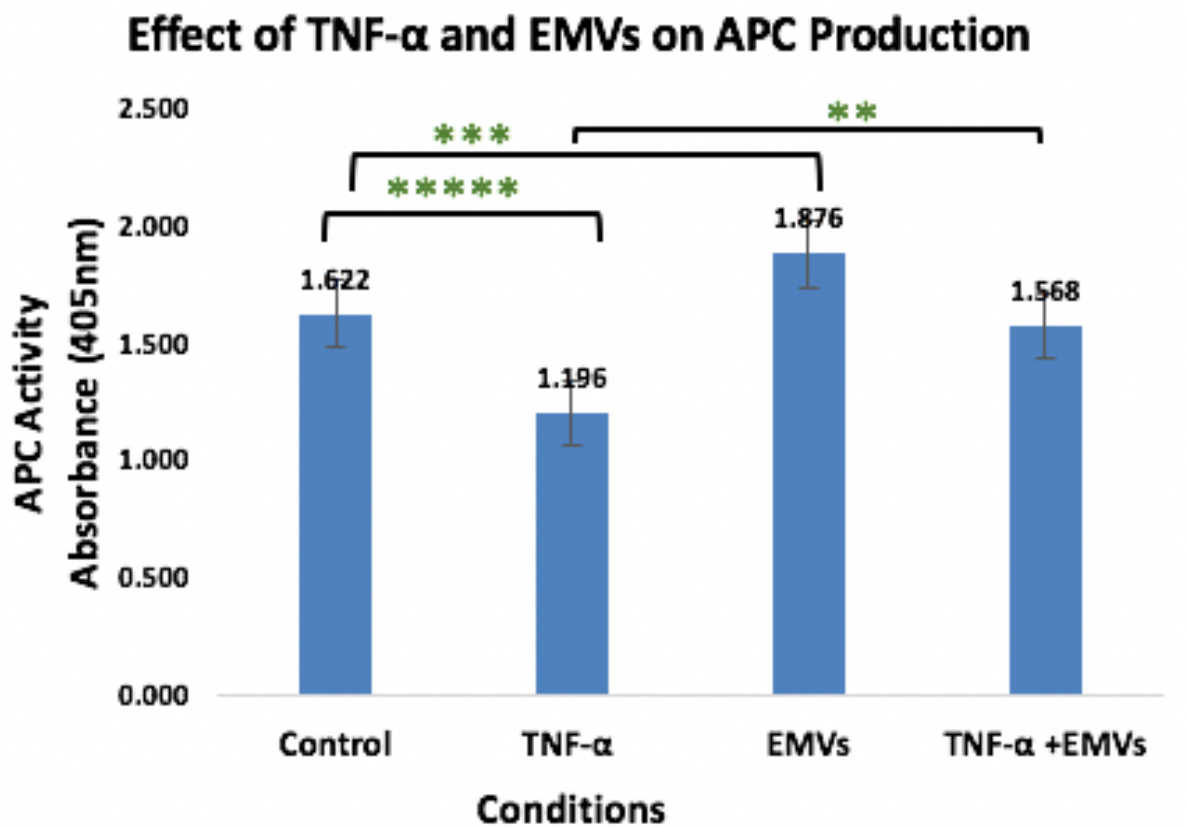
Figure 8.1: Effect of TNF-α and EMVs on activated protein C (APC) production. *Bar chart shows variables (conditions) added to cells measured by absorbance. n=6. This work was conducted by a MMedSc student.*

Under control conditions TNF-α induced a significant decrease in APC generation (P=0.000043). When EMVs are added into the system, there is a significant increase in APC generation (P=0.00244). Furthermore, it shows that after TNF-α stimulation, EMVs reverse the loss of APC generation induced by TNF-α stimulation and caused a significant increase in APC production.

TNF-α partially drives inflammation which is known to promote atherosclerosis and consequently a factor of CVD (Mosnier et al., 2007). These findings exhibit possibly yet another mechanism, through pro-inflammatory mediators lowering APC production from ECs, therefore enhancing coagulability and inflammation, in turn assisting within the development of CVD. As reported in another study, it is understood that ECs stimulated by APC, inhibited TNF-α transcription and for this reason reduced TNF-α production, thus protecting the endothelium from inflammation (Mosnier et al., 2007). Together with these findings, data reported in this thesis demonstrate that APC and TNF-α clearly have opposing roles in the body and possibly a direct physiological outcome on-one-another. In discovering of a direct effect could essentially lead to diagnostic of and therapeutic usage for APC. Furthermore, these findings suggest that EMVs restored APC production of ECs stimulated by TNF-α which means EMVs were able to, in effect, neutralise the negative effects of inflammation and the reduction of APC production (N.A. Englyst unpublished). In addition, EMVs, were able to, in effect, rescue the ECs and restore APC production back to the control (normal) level. There have been no publications on the rescue effect of EMVs. Nevertheless, other publications have observed the outcomes of TNF-α on EMVs production (Zhang et al., 2014). It has been discovered that TNF-α triggered the release of EMVs, proposing the use of EMVs as a potential marker for inflammation (Nan et al., 2005). Findings in this thesis further demonstrate that EMVs enhance APC production, however the study by Zhang J. et al., has demonstrated that TNF-α increases EMV production (Zhang et al., 2014). Therefore, it can be hypothesised that an increase in EMV production may subsequently correlates an increase in APC production. Moreover our findings show the opposing and contradictory situation, thus suggesting that EMVs in both experiments could be phenotypically different and EMVs may have opposing roles. Therefore, extra research is required in this field to phenotypically distinguish EMVs released in different conditions. For instance, EMVs released by activated ECs maybe phenotypically different to those released by stimulated ECs, or EMVs of ECs in health maybe phenotypically different to those secreted in diseased state. One suggested mechanism for the rescue of APC production is that EMVs have EPCR on their cell surface. It has

already been reported that ECs stimulated with APC produce EMVs expressing EPCR on their surface (Dahlback and Villoutreix, 2005). Additionally, the increase in APC production from EMVs could be due to several possibilities, including EMVs directly increasing transcription of EPCR to the cell surface or EMVs protecting EPCR on their surface, significantly increasing the rate and production of APC. Also, APC is known to have anti-coagulant and anti-inflammatory functions, which facilitate its use in treatment of severe sepsis. Furthermore, the novel and significant results in this thesis demonstrate that addition of exogenous EMVs increases APC production in normal conditions which may be a potential use in prophylaxis. Thus, our findings of EMVs rescuing anticoagulant APC production which can lead to further investigation of EMVs for potential therapeutic use in thrombotic and inflammatory conditions. Furthermore, APC has also been reported to increase EC fibrinolytic activity, conversely, it has also been shown to potentially have a pro-inflammatory role through the induction of cytokines IL-6 and IL-8 (Markiewics et al., 2013). Therefore, research investigating the effect of APC production during inflammation may answer some fundamental questions of bidirectional APC functioning.

8.7. Techniques Used To Study The Phase Behaviour and Composition of The Lipid Bilayer

8.7.1. ^{31}P-MAS-NMR

^{31}P-MAS-NMR is a powerful technique to study the composition of phase behaviour of lipids. It provides a common method for characterising the composition and dynamics of lipids in non-crystalline and in an insoluble environment (Berger, 2013). In this thesis, ^{31}P-MAS-NMR was employed as an approach to characterise various phospholipids such as PC, PE and PI, providing dynamic properties of phospholipids.

The principles of NMR: Nuclei possess a spin-angular momentum, as defined by the nuclear spin number, *I*, are observable by NMR and are referred to as "NMR active nuclei" (Yeagle *et al.*, 1975). The nuclear spin is an intrinsic property of the nucleus (Wennerstrom and Lindblom, 2017). The nuclear spin angular momentum, defined by the vector I, gives rise to the nuclear magnetic dipole moment μ, which is aligned in the direction of the spin axis (Oas, Griffin and Levitt, 1988).

Once a single spin in placed in a magnetic field (B_0), it precesses. However overall the ensemble of spins is not aligned coherently with the individual magnetisation vectors distributed evenly about the magnetic field. When a radiofrequency (RF) pulse is applied by the coil, a small magnetic field in the x or y direction is generated, resulting in the bulk magnetisation vector being tilted into the y or x direction respectively (Baum *et al.*, 1985). This results in a bulk magnetisation vector perpendicular to the main field which continues to precess (non-equilibrium magnetisation) resulting in the induction of a current in the detector coil, giving rise to the free induction decay (FID), the Fourier transform of which gives the NMR spectrum (Oas, Griffin and Levitt, 1988). The Larmor frequency, ω_0 about the applied field axis for a given nucleus is simply the negative of the product of the gyromagnetic ratio and applied external magnetic field strength. The ratio of population difference

between energy states is determined by the Boltzmann distribution with the difference determining the amplitude of the signal (Keeler & Maciel, 2003). While the vector can be used to define the behaviour of a single spin under single pulse RF excitation, or during simple pulse sequences, such an approach is insufficient to define the spin evolution during a rather complicated experiment. Generally, a more advanced, quantum-mechanical treatment is required (Jones *et al.*, 2000), however in the context of this work the spectra can be analysed by investigating the chemical shielding anisotropy (CSA) which can be related to the lipid morphology/phase behaviour and in terms of surface charge. The CSA is the shielding of the nucleus by the surrounding electrons, this is anisotropic, i.e., has an orientation dependence, therefore depending on the orientation of lipids, a different position of peak is observed. This anisotropy reflects the anisotropic distribution of electrons surrounding the nucleus (Weingarth *et al.*, 2014). In the case of solid sample, or solid sample that is not moving rapidly, then a CSA can be observed and therefore, produces a particular spectra.

Chemical shielding is caused by interactions among nuclear spins and a local secondary magnetic field. Once an atom/molecule is positioned inside a strong magnetic field (B_0), electrons are induced to circulate within their orbitals and specific orbital pairs are induced to combine with each other (de Kruijff *et al.*, 1978). The induced circulation (magnetically) of electrons and combining of orbitals lead to small local magnetic fields being produced [(very small compared to B_0, typically presented in parts per million) (ppm)] within the molecule (David A Case, 1998) This suggests that the overall effective field encountered at the nucleus is not equal to B_0. Therefore, the event of chemical shielding (nuclear shielding or chemical shifts) emerges from the interaction of the nuclear spin with these small local fields that serves to rise or drop the Larmor precession frequency, determined by the de-shielding or shielding, respectively (Vogt *et al.*, 2014). In the case of ^{1}H, ^{13}C, and [29]Si, trimethylsilane (TMS) is often used as the reference compound (Lindström, Williamson and Gröbner, 2005).

Magic angle spinning: Typically, solution state spectra are highly detailed, with resolution of considerable fine structure. The spectra readily reveal chemical shift and J-coupling (the coupling between adjacent spins) information. However, in the case of solid-state studies, the molecules are generally immobile, and consequently there are no rapid isotropic averaging processes occurring (Castellani *et al.*, 2002).

The aim of MAS-NMR is to apply mechanical averaging techniques so that artificial isotropic averaging can occur, with the ultimate goal of achieving resolution and fine structure comparable to that observed in the solution state. There are mainly two averaging techniques including MAS and high power proton decoupling (HPPD) which removes the interactions with neighbouring protons (Medek, Harwood and Frydman, 1995). Rapid macroscopic rotation was first introduced by Andrew et. Al., in 1958, in an investigation of dipolar coupling interactions (Andrew et. al., 958). It was later recognised independently by Andrew and Jenks that by careful choice of the angle of rotation, line broadening due to dipole-dipole interactions could be reduced to zero (Andrew and Jenks, 1962). The angle of the rotation axis with respect to the static Zeeman field which provided complete removal of the interaction was 54.7°, otherwise referred to as the "magic angle". Subsequently it was demonstrated that magic angle rotation would also remove broadening effects due to the anisotropy in chemical shielding. If the rotation rate is lower than the magnitude of the interaction to be removed, spinning sideband patterns appear, with the centre-band taking the isotropic value. The intensities of the sidebands can be used to recover information regarding the CSA by analysis of the sideband pattern obtained (Tycko and Dabbagh, 1990). In the context of the studies conducted here we employed MAS to average the CSA so that the various lipid species can be resolved by their isotropic chemical shift (Vogt *et al.*, 2014). It is known that, static spectra can provide a quick read out of which type of lipid phase is present. If it is in the alpha phase, the width of that spectrum reflects the surface charge on the bilayer (Lindström, Williamson and Gröbner, 2005). Similar information can be obtained from MAS spectra as the position of these peaks reflect the surface

charge, whilst the resolution obtained allows the number of individual species to be quantitated. Spinning faster than the size of the dipolar and CSA interactions, results in a single isotropic line. At slower spinning speeds sidebands appear that can provide information about the CSA whilst retaining the resolution that MAS provides (Fredrick Lindström, Philip T. F. Williamson and Gerhard Gröbner, 2005).

Studying membrane-EMVs lipids by ^{31}P-MAS-NMR: ^{31}P-MAS-NMR spectroscopy has been particularly valuable in the study of lipid polymorphism, since it provides a quantitative, direct measurement and can be applied non-destructively. An important aspect of the utility of ^{31}P-MAS-NMR spectroscopy in studies of native bio-membranes and model membrane systems is that the head-group ^{31}P nuclei of the different phospholipids have different chemical shifts (Vogt *et al.*, 2014). This method provides unique information about the relative abundance of phospholipid present in the sample (Watts *et al.*, 1999). ^{31}P-MAS-NMR uses a resonance signal of naturally isotopic phosphorus-31 in individual phospholipids which can be directly analysed from a lipid extract in order to identify and reasonably quantify the lipid species in the extract (Aue *et al.*, 1984). The purpose ^{31}P-MAS-NMR in phospholipids can be applied to analyse these characteristics is because ^{31}P has an atomic nucleus which has a nucleus spin that permits it to behave as a magnetic bar (Vogt *et al.*, 2014), which means it is dipolar with only one transition between two energy levels. In fact, the technique is based on the large CSA exhibited by phosphorus in phosphates, the relatively high sensitivity of this nucleus, the fact that it does not require any synthetic labelling as ^{31}P is a 100% abundant nucleus, and that there is generally only one phosphate group present per lipid molecule (Mananga et al., 2015). Furthermore, the unique feature of the method is that it is used to study not only macroscopic properties of lipid systems, such as lipid phases in the system and phase transition between them, but also microscopic properties at the atomic level, such as local environment in a very small sub-molecular region of the membrane (Mananga et al., 2015).

In summary, ^{31}P-MAS-NMR is a great technique investigating the head-groups and applied nearly exclusively for analysis of small biochemicals within the blood, requires comparatively diminutive sample preparation and is non-invasive, permitting further analysis of the same sample. Furthermore, it is a reliable technique to report on the phase, however, it is very challenging to assess the chain composition, it can provide a small information from proton and C_{13} NMR (Juhasz and Biemann, 1994; Wenk, 2005; Wang, Han and Han, 2013). However, the resolution of the different lipid species is challenging, because all CH_2 for example resonate essentially the same place. Therefore, this is a limitation, which requires a more advanced technique more sensitivity to provide a more detail analysis such as mass spectrometer (MS) technique analysing the type of lipid chains present in the lipid bilayer (Vilella, Ramirez and Simón, 2013). Table 8.1 provides an overview of the various approaches employed in lipidomic research.

Table 8.1: Overview of lipidomic. *Technologies used in lipidomic and advantages and disadvantages of each technique.*

Technology	Studied lipids	Advantages	Disadvantages
Mass spectrometry			
ESI	Many lipids	LC combination possible, direct by *m/z*, high sensitivity and selectivity, high turnover	Absolute quantification involves significant effort, ionisation suppression
NMR			
^{31}P	Phospholipids	Non-destructive, direct measurement, quantitative	Low sensitivity, spectra dominated by very abundant lipids, low sensitivity
Chromatography			
Gas chromatography	Non-polar compounds	Detection by mass spectrometry, mainly used for fatty acid	Requires derivatisation of polar lipids or volatile compounds
High-performance liquid chromatography	Many lipids	Quantitative, easy automation	Detection by mass detector or refractive index
Thin-layer chromatography	Many lipids	Technically easy, minor instrumental investment	Low sensitivity and resolution drawbacks

8.7.2. ESI-MS

Several MS-based approaches exist for lipid analysis, such as gas chromatograph mass spectrometry (GC-MS) with electron ionisation (EI), matrix-assisted laser desorption/ionisation (MALDI) and desorption electrospray ionisation (DESI) (Vilella, Ramirez and Simón, 2013). Each of these approaches has been developed and applied depending on different lipid- or sample-type. Due to its intrinsic soft-ionisation feature and capability of analysing intact lipid molecules, the most established and important is electrospray ionisation (ESI)-MS (Vilella, Ramirez and Simón, 2013) which was employed in this thesis. ESI-MS measurements can be performed, fundamentally, by two approaches: I) direct infusion of the sample into the ESI ion source, also called shotgun lipidomics; II) injection of the sample into the ESI ion source via high-performance liquid chromatography (HPLC). The second approach was employed in this thesis, on the whole is much more powerful from the analytical point of view since it permits chromatographic separation of the diverse lipid species avoiding the strong ion suppression effects imposed by the complex chemical matrix and it permits an amplified dynamic range of MS measurements, very important for the detection of minor lipids components (Wenk, 2005; Vilella, Ramirez and Simón, 2013). ESI MS consists of three main elements: an ion source, mass analysers, and an ion detector. The ion source functions to create molecular ions in gas-phase (for instance by ESI), (A Wenk 2005). The ion optics focus and transport molecular ions into the mass analysers which separate the ions according to their m/z before they are finally registered by an ion detector. The ion detector and mass analyser parts are operated at a low pressure to permit unperturbed transmission and detection of the gas-phase ions. All elements are operated by dedicated electronic devices (Bernert *et al.*, 2000). These ions are then separated in the basis of the ions movement in a magnetic field (quadrupole), eventually, depending on how they flow in this field, a master charge ratio is produced which counts the number of ions at a particular master charge ratio which produces a spectra (Gross, 2004; Kreimer *et al.*, 2015).

In conclusion, lipidomic have been extensively employed to study the lipid composition of cell membranes, both plasma membrane and intercellular compartments. However, lipidomic of blood MVs has received little attention (Losito *et al.*, 2013). Furthermore, a comprehensive chemical characterisation of the phospholipids of human blood MVs has not yet been reported (Gallart-Palau, Serra and Sze, 2016). In this theis, lipidomic was employed to understand the main compositions of lipid species present in endothelial cultured cells and their derived EMVs.

8.7.3. T_1 Relaxation

In order to ensure optimum accuracy of data, the delay time between the excitation of nuclei must be considered. Table 8.2 demonstrates that the T_1 relaxation of phosphorylated derivatives of PI values were continuously longer. This suggests that PIs have a different mobility consistent with the different dynamics between the headgroup and the backbone. Moreover, a small difference between the values from the parent cells and their derived EMVs suggesting that the T_1 relaxation is determined by the bilayer properties rather than the reorientation of the EMVs.

Table 8.2: T_1 relaxation of lipids. *T_1 relaxation of PC, PE/SM and PI, the values of the latter show that phosphorylated derivatives of PI are longer compared to that of PC and PE/SM.*

Membrane	T_1 of Membrane Lipids (seconds)		
	PC (ppm)	PE/SM (ppm)	PI (ppm)
HUVEC	-0.80	-0.25	2.73/ 3.96
	1.04	1.82	3.10/ 3.43
EA.hy926	-0.70	0.72	2.81/ 3.86
	1.18	1.76	3.21/ 3.11
HUVEC-EMV	-0.85	-0.25	2.3/ 3.86
	1.98	1.92	3.05/ 3.35
Ea.hy926-EMV	-0.85	0.50	2.93/ 3.66
	1.89	1.92	3.05/ 3.93
TNF-α -HUVEC	-0.70	-0.30	3.3
	1.11	1.81	3.05
TNF-α-EA.hy926	-0.80	-0.25	2.56/ 3.76
	1.42	1.91	2.92/ 3.72

8.7.4. ESI-MS Analysis of Membrane Lipids

The ESI-MS data presented in Chapter 5 of the chain composition of the species identified by ^{31}P-MAS-NMR (PC, PE, PI). Additional lipids where significancy has been observed are presented below. The ESI-MS data presented below demonstrate the total selected percentage of phosphatidylserine (PS), cholesterol (Chol), ceramide (Cer), diacylglycerol (DAG) and lysophosphatidic acid/ lipopolysaccharide (LPA/LPS). Some of these lipids demonstrated a similar chain composition between parent cells and their derived EMVs such as cholesterol which is a major component of the plasma membrane and plays a role in influencing the phase behaviour of the lipid bilayer. In contrast other lipids also suggested a higher content in EMVs such as ceramide, although significancy has been observed in these lipids.
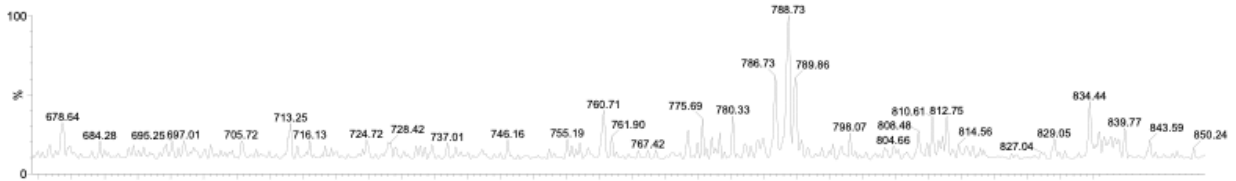
PS
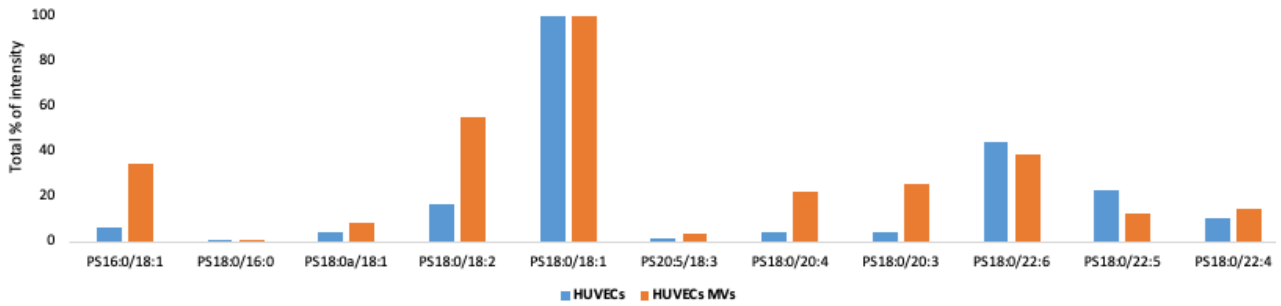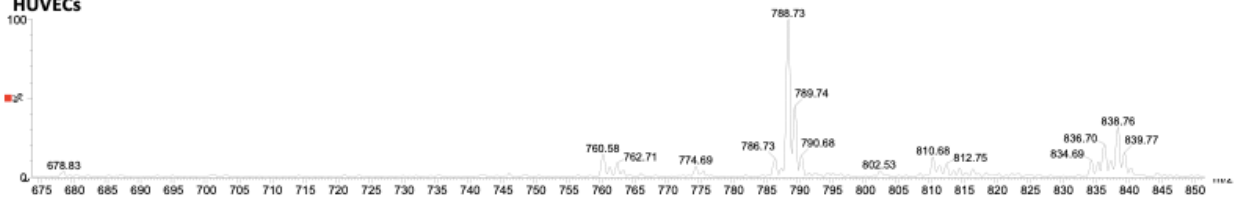
Figure 8.2: ESI-MS quantification of PS species present and normalised intensity of total selected percentage of PS species in HUVEC-membrane and their derived-MVs. *A) The spectra contain a series of different lipid species, where the molecular weight is indicative of the types of chains present. B) Bar chart illustrates the distribution of PI species between parent cells and EMVs. Overall, not an evident change in chain species between parent membranes and EMVs. n=1.*

Chol
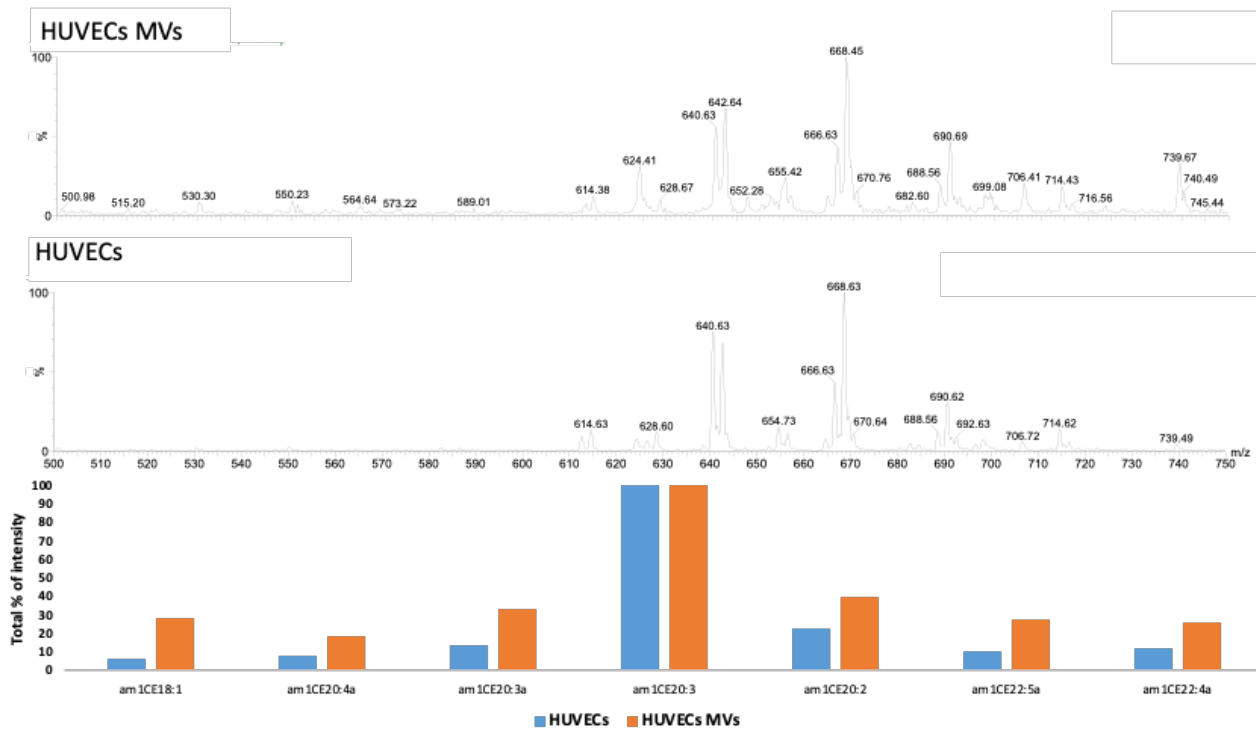
Figure 8.3: ESI-MS quantification of cholesterol (Chol) species present and normalised intensity of total selected percentage of Chol species in HUVEC-membrane and their derived-MVs. A) The spectra contain a series of different lipid species, where the molecular weight is indicative of the types of chains present. B) Bar chart illustrates the distribution of PI species between parent cells and EMVs. Overall, Chol species present in EMVs is similar to that of parent membranes and EMVs. n=1.

Cer
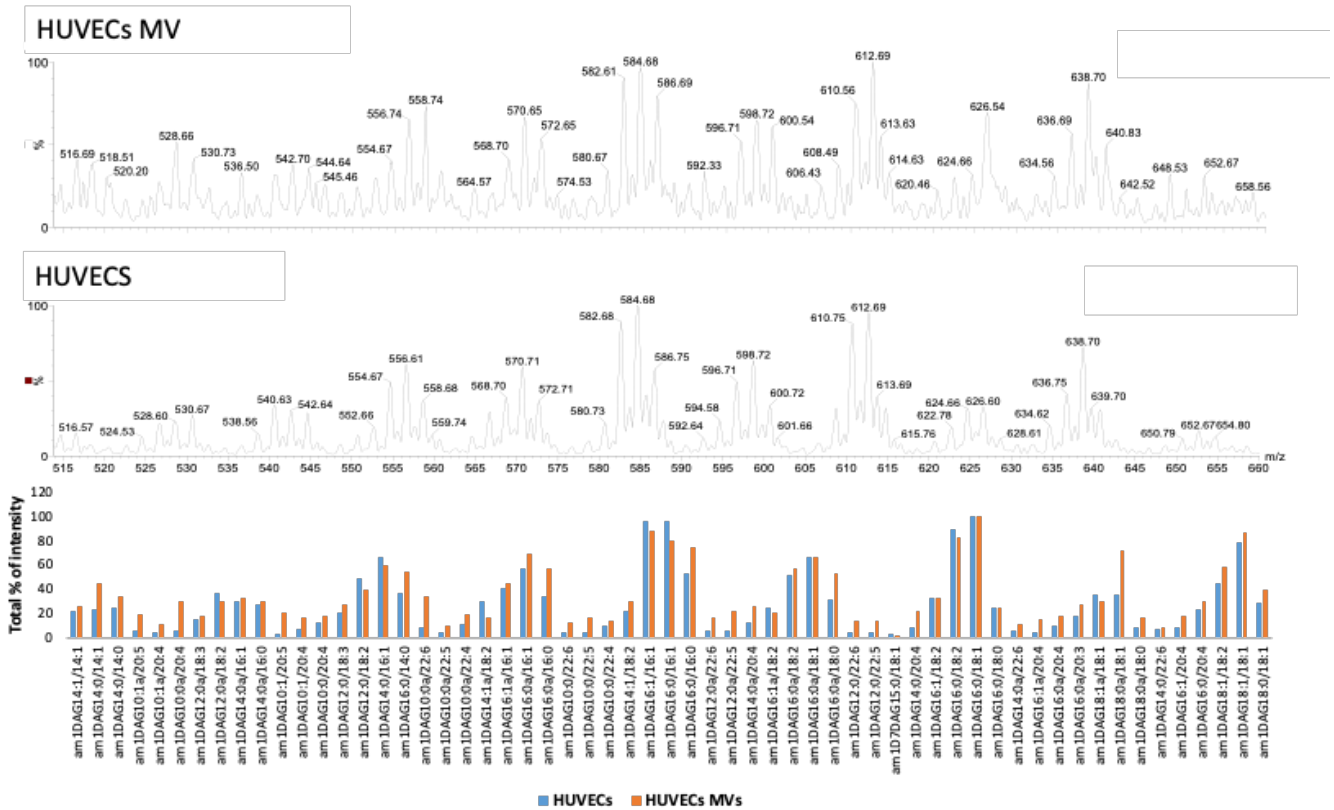
Figure 8.4: ESI-MS quantification of ceramide (Cer) species present and normalised intensity of total selected percentage of Cer species in HUVEC-membrane and their derived-MVs. *A) The spectra contain a series of different lipid species, where the molecular weight is indicative of the types of chains present. B) Bar chart illustrates the distribution of PI species between parent cells and EMVs. Overall, not an evident change in chain species between parent membranes and EMVs. n=1.*

DAG
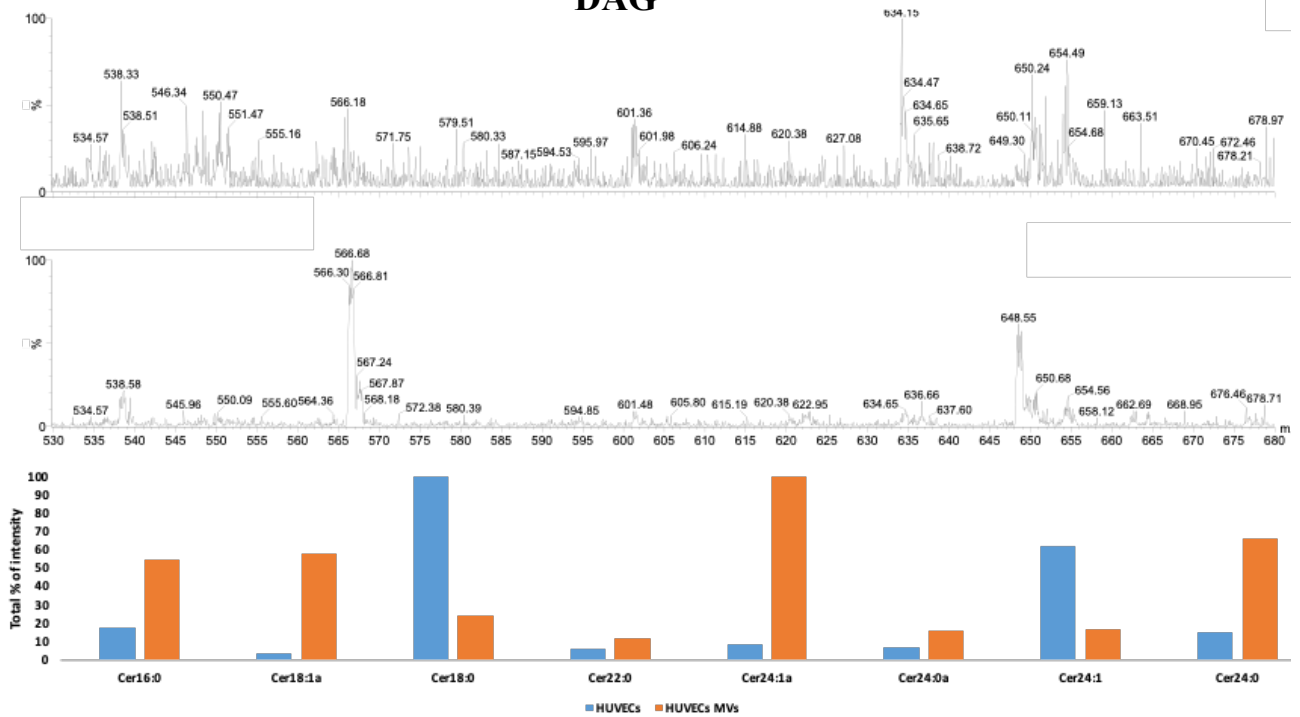
Figure 8.5: ESI-MS quantification of diacylglycerol (DAG) species present and normalised intensity of total selected percentage of DAG species in HUVEC-membrane and their derived-MVs. A) The spectra contain a series of different lipid species, where the molecular weight is indicative of the types of chains present. B) Bar chart illustrates the distribution of PI species between parent cells and EMVs. Overall, there is variation in DAG species present in parent membranes and EMVs, as well as it is evident that the concentration of DAG species may be high. This is may indicate that some DAG species are enriched in EMVs as well as parent cells. n=1.
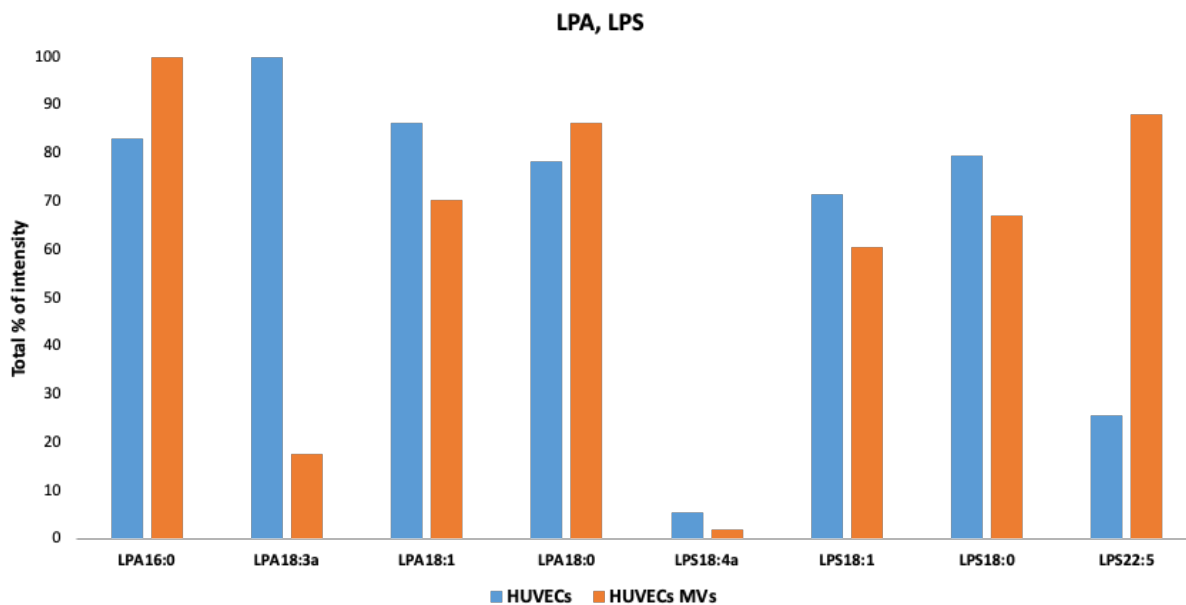
Figure 8.6: Normalised intensity of total selected percentage of lysophosphatidic acid (LPA) and lipopolysaccharide (LPS) species in HUVEC-membrane and their derived-MVs. *Bar chart illustrates the distribution of PI species between parent cells and EMVs. Overall, there is neither evident change nor enrichment in these lipids. n=1.*

8.8. Identification of miRNAs in EMVs

8.8.1. RNA Integrity

Total RNA (including miRNAs) were quantified and table below show the quality of samples. RNA integrity was assessed and samples with RIN values ≥ 7.0 were considered acceptable.

Table 8.3: RNA integrity numbers (RINs). *Samples with RIN values ≥ 7.0 were used for sequencing.*

Sample No	Novogene ID	Sample Name	RIN	Conclusion	Note
1	TR170802457	EMVs – untreated	8.6	Pass	
2	TR170802458	EMVs – untreated	8.6	Pass	
3	TR170802459	EMVs – untreated	8.6	Pass	
4	TR170802460	EMVs – untreated	8.5	Pass	
5	TR170802461	EMVs – untreated	8.7	Pass	
6	TR170802462	EMVs – untreated	8.4	Pass	
7	TR170802463	EMVs – untreated	8.6	Pass	
8	TR170802464	EMVs – untreated	8.4	Pass	
9	TR170802465	EMVs – untreated	8.7	Pass	
10	TR170802466	EMVs – untreated	6.8	Fail	Insufficient
11	TR170802467	TNF-α – treated	8.7	Pass	
12	TR170802468	TNF-α – treated	6.8	Fail	Insufficient
13	TR170802469	TNF-α – treated	8.5	Pass	
14	TR170802470	TNF-α – treated	8.6	Pass	
15	TR170802471	TNF-α – treated	8.6	Pass	
16	TR170802472	TNF-α – treated	8.6	Pass	
17	TR170802473	TNF-α – treated	8.6	Pass	
18	TR170802474	TNF-α – treated	6.5	Fail	Insufficient
19	TR170802475	TNF-α – treated	8.7	Pass	
20	TR170802476	TNF-α – treated	8.2	Pass	

8.8.2. Differential Expression of miRNAs

Table below shows the differentially expressed miRNAs and their direction of expression.

Table 8.4: Differentially expressed miRNAs. *The differentially expressed miRNAs identified in endothelial microvesicles (EMVs) generated in the presence and absence of TNF-α.*

Number	miRNA ID	Main miRNA	P Value	FDR adjusted p value	FC	Expression
1.	hsa-miR-146a-5p	hsa-miR-146a	5.68E-17	1.20E-14	-5.23261	Down
2.	hsa-miR-9-5p	hsa-miR-9	3.51E-15	3.72E-13	-5.33934	Down
3.	hsa-miR-215-5p	hsa-miR-215	1.20E-11	6.38E-10	-5.74225	Down
4.	hsa-miR-192-5p	hsa-miR-192	6.47E-11	2.74E-09	-4.46125	Down
5.	hsa-miR-132-5p	hsa-miR-132	1.05E-10	3.42E-09	-4.5888	Down
6.	hsa-miR-129-5p	hsa-miR-129	1.13E-10	3.42E-09	-3.88809	Down
7.	hsa-miR-30b-5p	hsa-miR-30b	5.70E-10	1.51E-08	-4.36732	Down
8.	hsa-miR-135a-5p	hsa-miR-135a	6.92E-10	1.63E-08	-9.78594	Down
9.	hsa-miR-212-5p	hsa-miR-212	2.23E-09	4.74E-08	-4.61809	Down
10.	hsa-miR-9-3p	hsa-miR-9	3.08E-08	5.45E-07	-5.39998	Down
11.	hsa-miR-3529-3p	hsa-miR-3529	4.94E-08	7.85E-07	-2.85609	Down
12.	hsa-miR-194-5p	hsa-miR-194	5.19E-08	7.85E-07	-3.67339	Down
13.	hsa-miR-219a-2-3p	hsa-miR-219a-2	7.08E-08	1.00E-06	-6.80832	Down
14.	hsa-miR-142-3p	hsa-miR-142	1.20E-07	1.59E-06	-3.68533	Down
15.	hsa-let-7e-5p	hsa-let-7e	1.75E-07	2.18E-06	-2.80734	Down
16.	hsa-let-7f-5p	hsa-let-7f	2.34E-07	2.76E-06	-2.53196	Down
17.	hsa-miR-375	hsa-miR-375	5.42E-07	5.64E-06	-3.4334	Down
18.	hsa-miR-217	hsa-miR-217	5.47E-07	5.64E-06	-4.58797	Down
19.	hsa-miR-200a-3p	hsa-miR-200a	5.59E-07	5.64E-06	-3.96441	Down
20.	hsa-miR-339-5p	hsa-miR-339	2.71E-05	0.000151	-2.48201	Down
21.	hsa-miR-124-3p	hsa-miR-124	7.58E-07	7.11E-06	-5.56006	Down
22.	hsa-miR-223-3p	hsa-miR-223	7.78E-07	7.11E-06	-4.28925	Down
23.	hsa-miR-200c-3p	hsa-miR-200c	1.56E-06	1.28E-05	-3.72362	Down
24.	hsa-miR-143-5p	hsa-miR-143	3.39E-06	2.67E-05	-4.25909	Down
25.	hsa-let-7a-5p	hsa-let-7a	4.42E-06	3.34E-05	-2.05378	Down
26.	hsa-miR-145-5p	hsa-miR-145	5.10E-06	3.73E-05	-2.67266	Down
27.	hsa-miR-363-3p	hsa-miR-363	7.08E-06	5.00E-05	-3.50306	Down
28.	hsa-miR-200b-3p	hsa-miR-200b	7.72E-06	5.28E-05	-3.24085	Down
29.	hsa-miR-218-5p	hsa-miR-218	1.05E-05	6.81E-05	-2.21039	Down
30.	hsa-miR-30c-5p	hsa-miR-30c	3.89E-05	0.000206	-2.19012	Down
31.	hsa-miR-206	hsa-miR-206	1.06E-05	6.81E-05	-2.70463	Down
32.	hsa-miR-499-5p	hsa-miR-499	1.42E-05	8.38E-05	-4.90963	Down
33.	hsa-miR-187-3p	hsa-miR-187	6.53E-05	0.00033	-4.01569	Down
34.	hsa-miR-2682-5p	hsa-miR-2682	0.006984	0.018544	-2.70622	Down
35.	hsa-miR-150-5p	hsa-miR-150	8.02E-05	0.000395	-2.38496	Down

36.	hsa-miR-107	hsa-miR-107	9.84E-05	0.000474	-3.27927	Down
37.	hsa-miR-145-3p	hsa-miR-145	0.00164	0.005432	-2.07191	Down
38.	hsa-miR-15b-5p	hsa-miR-15b	0.000938	0.003313	-2.73589	Down
39.	hsa-miR-1-3p	hsa-miR-1	0.000112	0.000528	-2.65807	Down
40.	hsa-miR-143-3p	hsa-miR-143	0.000339	0.001383	-2.03918	Down
41.	hsa-miR-184	hsa-miR-184	0.001547	0.005291	-2.25807	Down
42.	hsa-miR-151a-3p	hsa-miR-151a	0.000601	0.002315	-2.58981	Down
43.	hsa-miR-499a-5p	hsa-miR-499a	0.001812	0.00582	-2.09423	Down
44.	hsa-miR-199b-5p	hsa-miR-199b	0.000641	0.002428	-2.08586	Down
45.	hsa-miR-182-5p	hsa-miR-182	0.000684	0.002543	-2.01155	Down
46.	hsa-miR-125b-5p	hsa-miR-125b	8.46E-09	1.63E-07	2.769283	Over
47.	hsa-miR-935	hsa-miR-935	2.67E-05	0.000151	4.455116	Over
48.	hsa-miR-3182	hsa-miR-3182	3.04E-05	0.000165	3.819281	Over
49.	hsa-miR-173a-3p	hsa-miR-173a	5.05E-04	0.000253	3.918013	Over
50.	hsa-miR-92a-3p	hsa-miR-92a	8.05E-07	7.11E-06	2.31355	Over
51.	hsa-miR-31-5p	hsa-miR-31	0.000305	0.001294	2.750448	Over
52.	hsa-miR-197-3p	hsa-miR-197	0.000273	0.001206	3.158909	Over
53.	hsa-miR-181b-5p	hsa-miR-181b	1.43E-06	1.22E-05	2.199889	Over
54.	hsa-miR-425-5p	hsa-miR-425	0.000733	0.002633	2.702586	Over
55.	hsa-miR-99b-5p	hsa-miR-99b	0.000198	0.000904	2.098567	Over
56.	hsa-miR-4497	hsa-miR-4497	0.002906	0.008801	2.612186	Over
57.	hsa-miR-181d-5p	hsa-miR-181d	0.000433	0.001733	2.523419	Over
58.	hsa-miR-1307-3p	hsa-miR-1307	0.000519	0.002039	2.92934	Over
59.	hsa-miR-652-3p	hsa-miR-652	0.010878	0.027131	2.40265	Over
60.	hsa-miR-769-5p	hsa-miR-769	0.006998	0.018544	2.425375	Over
61.	hsa-miR-369-3p	hsa-miR-369	0.01475	0.035943	2.288909	Over
62.	hsa-miR-330-3p	hsa-miR-330	0.019056	0.044888	2.31386	Over
63.	hsa-miR-409-5p	hsa-miR-409	0.020629	0.048059	2.236824	Over
64.	hsa-miR-224-5p	hsa-miR-224	0.000709	0.002592	2.557503	Over
65.	hsa-miR-4792	hsa-miR-4792	0.001145	0.003978	3.059836	Over
66.	hsa-miR-361-5p	hsa-miR-361	0.001812	0.00582	1.542057	Over
67.	hsa-miR-148a-3p	hsa-miR-148a	0.002129	0.006737	-1.47833	Normal
68.	hsa-miR-378a-3p	hsa-miR-378a	0.002274	0.00709	-1.62682	Normal
69.	hsa-let-7d-5p	hsa-let-7d	0.002727	0.008378	-1.50607	Normal
70.	hsa-miR-27a-5p	hsa-miR-27a	0.003635	0.010854	-1.81177	Normal
71.	hsa-miR-328-3p	hsa-miR-328	0.003836	0.011294	1.392387	Normal
72.	hsa-miR-92b-3p	hsa-miR-92b	0.00443	0.012864	1.58085	Normal
73.	hsa-miR-320a	hsa-miR-320a	0.006006	0.017207	-1.81293	Normal
74.	hsa-miR-378c	hsa-miR-378c	0.006373	0.01781	-1.88777	Normal
75.	hsa-miR-20a-5p	hsa-miR-20a	0.006393	0.01781	-1.66531	Normal
76.	hsa-miR-423-3p	hsa-miR-423	0.006469	0.01781	1.271038	Normal
77.	hsa-miR-26b-5p	hsa-miR-26b	0.006743	0.018327	-1.63927	Normal
78.	hsa-miR-199a-5p	hsa-miR-199a	0.001614	0.005431	-1.93041	Normal
79.	hsa-miR-126-5p	hsa-miR-126	0.007621	0.019946	1.781247	Normal
80.	hsa-miR-132-3p	hsa-miR-132	0.007867	0.020339	-1.68494	Normal
81.	hsa-miR-128-3p	hsa-miR-128	0.008454	0.021593	-1.25204	Normal

82.	hsa-miR-98-5p	hsa-miR-98	0.008797	0.022203	-1.35026	Normal
83.	hsa-miR-484	hsa-miR-484	0.012103	0.029836	1.952924	Normal
84.	hsa-let-7g-5p	hsa-let-7g	0.01693	0.040786	-1.06318	Normal
85.	hsa-miR-222-3p	hsa-miR-222	0.018019	0.042922	1.475617	Normal
86.	hsa-miR-361-3p	hsa-miR-361	1.42E-05	8.38E-05	1.882955	Normal
87.	hsa-miR-451a	hsa-miR-451a	0.000201	0.000904	-1.76003	Normal
88.	hsa-miR-127-3p	hsa-miR-127	5.41E-05	0.00028	1.665711	Normal
89.	hsa-miR-186-5p	hsa-miR-186	0.000305	0.001294	1.604432	Normal
90.	hsa-miR-21-5p	hsa-miR-21	0.000323	0.001344	1.695064	Normal
91.	hsa-miR-140-3p	hsa-miR-140	0.021656	0.049904	1.535076	Normal

References

Abdelhamed, S., Butler, J.T., Doron, B., Halse, A., Nemecek, E., Wilmarth, P.A., Marks, D.L., Chang, B.H., Horton, T and Kurre, P. (2019). 'Extracellular vesicles impose quiescence on residual hematopoietic stem cells in the leukemic niche' *EMBO Reports,* 20, pp. 1 – 16.

Abid Hussein, Mohammed N., Böing, Anita N., Sturk, Augueste., Hau, Chi M., Nieuwland, Rienk (2007). Inhibition of microparticle release triggers endothelial cell apoptosis and detachment, *Thrombosis and Haemostasis.* 10(4), pp. 121-231.

Abid Hussein, M. N. *et al.* (2008) Phospholipid composition of in vitro endothelial microparticles and their in vivo thrombogenic properties, *Journal of Biological Chemistry,* 143(19), pp. 270 -500.

Adams, R.L.C. and Bird, R.J. (2009) 'Review article: Coagulation cascade and therapeutics update: Relevance to nephrology. Part 1: Overview of coagulation, thrombophilias and history of anticoagulants', *Nephrology.* Blackwell Publishing Asia, 14(5), pp. 462–470.

Ahn, K. *et al.* (1995) 'A permanent human cell line (EA.hy926) preserves the characteristics of endothelin converting enzyme from primary human umbilical vein endothelial cells', *Life Sciences*, 56(26), pp. 2331–2341.

Alexy T, Rooney K, Weber M, Gray WD, Searles CD (2014). TNF-α alters the release and transfer of microparticle-encapsulated miRNAs from endothelial cells. *Physiology Genomics.* 46(22), 833 - 840.

Alia, A., Ganapathy, S. and de Groot, H. J. M. (2009) 'Magic Angle Spinning (MAS) NMR: a new tool to study the spatial and electronic structure of photosynthetic complexes.', *Photosynthesis research.* *Springer*, 102(2–3), pp. 415–25.

An, I. *et al.* (1994) 'A Model for the Tissue Factor Pathway to Thrombin', *Journal of Biological Chemistry*, 269(37), pp. 23357–23366.

Anders, S., Pyl, P. T. and Huber, W. (2015) 'HTSeq-A Python framework to work with high-throughput sequencing data', *Bioinformatics*, 31(2), pp. 166–169.

Andrew E. R. Rradbury A. and Eades, R. G. (1958) 'Nuclear Magnetic Resonance Spectra from a Crystal rotated at High Speed', *Nature.* Nature Publishing Group, 182(4650), pp. 1659–1659.

Andrew, E. R. and Jenks, G. J. (1962) 'The Narrowing of Nuclear Magnetic Resonance Spectra by Molecular Rotation in Solids: II. Further Calculations for a System of Reorienting Nuclear Pairs', *Proceedings of the Physical Society.* IOP Publishing, 80(3), pp. 663–673.

Andrews, A.M., et al., (2018). ' Characterization of human foetal brain endothelial cells reveals

barrier properties suitable for in vitro modelling of the BBB with syngeneic co-cultures'. *Journal of Cerebral Blood Flow & Metabolism*, 38(5), pp. 888 - 903.

Angelillo-Scherrer, A. (2012) 'Leukocyte-derived microparticles in vascular homeostasis', *Circulation Research*, 110(2), pp. 356–369

Animesh Acharjeel *et al.* (2017) 'The translation of lipid profiles to nutritional biomarkers in the study of infant metabolism', *Metabolomics*, 10(1007), pp. 1166–1172.

Antonova, O.A., Yakushkin, V.V and Mazurov, A.V., (2019). 'Coagulation Activity of Membrane Microparticles' *Springer Biochemistry,* 13(3), pp. 169 - 186.

Ardoin, S. P., Shanahan, J. C. and Pisetsky, D. S. (2007) 'The role of microparticles in inflammation and thrombosis', *Scandinavian Journal of Immunology*, 66(2–3), pp. 159–165.

Arroyo, BA., et al., (2018). 'microRNAs in the haemostatic system: More than witnesses of thromboembolic diseases?'. *Thrombosis Research.* 166(3), pp. 1 - 9.

Ashworth Briggs, E. L. *et al.* (2015) 'Interaction between the NS4B amphipathic helix, AH2, and charged lipid headgroups alters membrane morphology and AH2 oligomeric state — Implications for the Hepatitis C virus life cycle', *BBA - Biomembranes*, 1848, pp. 1671–1677.

Aue, W. P. *et al.* (1984) 'Solid-state phosphorus-31 nuclear magnetic resonance studies of synthetic solid phases of calcium phosphate: potential models of bone mineral.', *Biochemistry*, 23(25), pp. 6110–4.

Bak, M., Rasmussen, J. T. and Nielsen, N. C. (2011) 'Simpson: A general simulation program for solid-state NMR spectroscopy', *Journal of Magnetic Resonance*, 213(2), pp. 366–400.

Baker, P. W. *et al.* (2000) 'Phospholipid composition of reconstituted high density lipoproteins influences their ability to inhibit endothelial cell adhesion molecule expression', *Journal of Lipid Research*, 41(8), pp. 1261–1267.

Balla, T., (2013). ' Phosphoinositides: Tiny Lipids With Giant Impact on Cell Regulation'. American Physiological Society, Physiological Reviews. 93(3), pp. 1019 - 1137.

Babraham Bioinformatics (2019). FASTQC: A Quality Control Tool for High Throughput Sequence Data, 2019. http://www.bioinforma- tics.babraham.ac.uk/projects/fastqc/.

Banerjee, S., and Muzumdar, S., (2012). ' Electrospray Ionization Mass Spectrometry: A Technique to Access the Information beyond the Molecular Weight of the Analyte'. *International Journal of Analytical Chemistry*. 8, pp. 282 - 574.

Baranska, P., Jerczynska, H., Pawlowska, Z., Koziolkiewicz, W., and Cierniewski, CS., (2005). 'Expression of integrins and adhesive properties of human endothelial cell line EA.hy926'. Cancer

Genomics and Proteomics. 256(2), pp. 165 - 270.

Barteneva, N. S. *et al.* (2013) 'Circulating microparticles: square the circle.', *BMC cell biology*, 14 (2), pp. 1471-2121.
Batool, S. (2013) 'Microparticles and their Roles in Inflammation: A Review', *Open Immunology*,14(6), pp. 1–14.

Baum, J. *et al.* (1985) 'Multiple-quantum dynamics in solid state NMR', *The Journal of Chemical Physics*. American Institute of Physics, 83(5), pp. 2015–2025.

Behrendts, N. *et al.* (1990) 'The Human Receptor for Urokinase Plasminogen Activator NH2-Terminal amino acid sequence and glycosylation variants, *Open Immunology*, 265(11), pp. 6453–6460.

Berger, S. (2013) 'Book review :" Spin Dynamics ", Wiley Online Library. 42(16), pp. 1787 - 1788.

Bernal-Mizrachi, L. *et al.* (2003) 'High levels of circulating endothelial microparticles in patients with acute coronary syndromes', *American Heart Journal*, 145(6), pp. 962–970.

Bernard, G. R., Vincent, J.-L., *et al.* (2001) 'Efficacy and Safety of Recombinant Human Activated Protein C for Severe Sepsis', *New England Journal of Medicine*, 344(10), pp. 699–709.

Bernard, G. R., Ely, E. W., *et al.* (2001) 'Safety and dose relationship of recombinant human activated protein C for coagulopathy in severe sepsis', *Critical Care Medicine*, 29(11), pp. 2051–2059.

Bernert, J. T. *et al.* (2000) 'Comparison of Serum and Salivary Cotinine Measurements by a Sensitive High-Performance Liquid Chromatography-Tandem Mass Spectrometry Method as an Indicator of Exposure to Tobacco Smoke Among Smokers and Nonsmokers*', *Journal of Analytical Toxicology*, 24 (9), pp.996 - 1009 .

Bertina, R. M. (2009) 'The role of procoagulants and anticoagulants in the development of venous thromboembolism', *Thrombosis Research*, 123 (3), pp. 41–45.

Binder, B. R. *et al.* (2002) 'Plasminogen activator inhibitor 1: Physiological and pathophysiological roles', *News in Physiological Sciences*, 17(2), pp. 56–61.

Biró, É. *et al.* (2003) 'Human cell-derived microparticles promote thrombus formation in vivo in a tissue factor-dependent manner', *Journal of Thrombosis and Haemostasis*, 1(12), pp. 2561–2568.

Blaum, K. (2006) 'High-accuracy mass spectrometry with stored ions', *Physics Reports*, 425(1), pp. 1–78.

Bligh, E.G and W.J. Dyer, W.J (1959) 'Citationclassics.pdf', *Physiology*, (37), pp. 1 -7.

Boerma, Marjan A; et al., (2006). 'Comparative expression profiling in primary and imortalised endothelal cells: changes in gene expression in response to hydroxy methylglutaryl-coenzyme A reductase inhibition'. Blood coagulation and Fibrinolysis. 17(3), 173 - 180.

Bok, J.S., et al, (2018). 'The Role of Human Umbilical Vein Endothelial Cells in Osteogenic Differentiation of Dental Follicle-Derived Stem Cells in *In Vitro* Co-cultures' *International Journal of Medical Sciences,* 15(11), pp. 1160 - 1169.

Bugueno, I.M., et al., (2020). ' *Porphyromonas gingivalis* triggers the shedding of inflammatory endothelial microvesicles that act as autocrine effectors of endothelial dysfunction'. Scientific Reports, *Nature Research*. 1778(10), pp. 98 - 120.

Bouïs, D. *et al.* (2001) 'Endothelium in vitro: a review of human vascular endothelial cell lines for blood vessel-related research.', *Angiogenesis*, 4(2), pp. 91–102.

Breier, G. and Risau, W. (1996) 'The role of vascular endothelial growth factor in blood vessel formation', *Trends in Cell Biology*, 6(12), pp. 454–456.

Brodowski, L., Burlakov, J., Hass, S., von Kaisenberg, C and von Versen-Hoÿnck, F., (2017). 'Impaired functional capacity of fetal endothelial cells in preeclampsia'. *PLOS One,* 1371(10), pp. 1 - 15.

Brummel-Ziedins, K. E. *et al.* (2011) 'Activated protein C inhibitor for correction of thrombin generation in hemophilia A blood and plasma1', *Journal of Thrombosis and Haemostasis*. Blackwell Publishing Ltd, 9(11), pp. 2262–2267.

Burnell, E. E., Cullis, P. R. and de Kruijff, B. (1980) 'Effects of tumbling and lateral diffusion on phosphatidylcholine model membrane 31P-NMR lineshapes.', *Biochimica et biophysica acta*, 603(1), pp. 63–9. Available at: http://www.ncbi.nlm.nih.gov/pubmed/7448188 (Accessed: 13 March 2017).

Capoor, M. N. *et al.* (2015) 'Prothrombin Time and Activated Partial Thromboplastin Time Testing: A Comparative Effectiveness Study in a Million-Patient Sample', *Journal of Thrombosis and Haemostasis,* 5(7), pp.57 - 93

Carrim, N. *et al.* (2015) 'Thrombin-induced reactive oxygen species generation in platelets: A novel role for protease-activated receptor 4 and GPIbα', *Redox Biology*, 6, pp. 640–647.

Castellani, F. *et al.* (2002) 'Structure of a protein determined by solid-state magic-angle-spinning NMR spectroscopy', *Nature*. Nature Publishing Group, 420(6911), pp. 98–102.

Caterina, R. *et al.* (2013) 'General mechanisms of coagulation and targets of anticoagulants (Section I) Position Paper of the ESC Working Group on Thrombosis – Task Force on Anticoagulants in Heart Disease', *Thrombosis and Haemostasis*, 1094(109), pp. 569–579.

Chandler, A. B. (1958) 'In vitro thrombotic coagulation of the blood; a method for producing a

thrombus.', *Laboratory investigation; a journal of technical methods and pathology*, 7(2), pp. 110–4.

Chang, C.-P. *et al.* (1993) 'Contribution of Platelet Microparticle Formation and Granule Secretion to the Transmembrane Migration of Phosphatidylserine', *The Journal of Biology Chemistry,* 268, pp. 7171–7178.

Chavda, V., and Madhwani, K., (2021). ' Coding and non-coding nucleotides': The future of stroke gene therapeutics'. *Genomics*. 113(3), 1291 - 1307.

Collier, ME., Akinmolayan, A., and Goodall, AH., (2017). 'Comparison of tissue factor expression and activity in foetal and adult endothelial cells'. Blood Coagulation and Fibrinolysis. 28(6), pp. 452 - 459.

Contreras, F.X. *et al.* (2010) 'Transbilayer (*flip-flop*) lipid motion and lipid scrambling in membranes', *FEBS Letters*, 584(9), pp. 1779–1786.

Coughlin, S. R. (2000) 'Thrombin signalling and protease-activated receptors', *Nature*. Nature Publishing Group, 407(6801), pp. 258–264.

Cowan, P. J., Robson, S. C. and d'Apice, A. J. F. (2011) 'Controlling coagulation dysregulation in xenotransplantation.', *Current opinion in organ transplantation*. NIH Public Access, 16(2), pp. 214–21.

Crawford, N. (1971) 'The Presence of Contractile Proteins in Platelet Microparticles Isolated from Human and Animal Platelet-free Plasma', *British Journal of Haematology*. Blackwell Publishing Ltd, 21(1), pp. 53–69.

Crawley, J. T. B. *et al.* (2007) 'The central role of thrombin in hemostasis', *Journal of Thrombosis and Haemostasis*. Blackwell Publishing Ltd, 5(1), pp. 95–101.

Crawley, J. T. B. and Lane, D. A. (2008) 'The haemostatic role of tissue factor pathway inhibitor', *Arteriosclerosis, Thrombosis, and Vascular Biology*, 28(2), pp. 233–242.

Creemers, E. E., Tijsen, A. J. and Pinto, Y. M. (2012) 'Circulating MicroRNAs: Novel biomarkers and extracellular communicators in cardiovascular disease?', *Circulation Research*, 110(3), pp. 483–495.

Curtis, A. M. *et al.* (2010) 'Relationship of microparticles to progenitor cells as a measure of vascular health in a diabetic population.', *Cytometry. Part B, Clinical cytometry*. NIH Public Access, 78(5), pp. 329–337.

Curtis, A. M. *et al.* (2009) 'p38 mitogen-activated protein kinase targets the production of proinflammatory endothelial microparticles', *Journal of Thrombosis and Haemostasis*, 11(5), pp. 83 - 97.

Dahlbäck, B. and Villoutreix, B. O. (2005) 'Regulation of blood coagulation by the protein C anticoagulant pathway: Novel insights into structure-function relationships and molecular recognition', *Arteriosclerosis, Thrombosis, and Vascular Biology*, 25(7), pp. 1311–1507.

Dasgupta, S. K. *et al.* (2009) 'Lactadherin and clearance of platelet-derived microvesicles', *Circulation Research,* 113, pp. 1332–1339.

David, A.C. (1998) 'The use of chemical shifts and their anisotropies in biomolecular structure determination' *Current Opinion in Structural Biology*, 8, pp. 624–630.

Dettmer, K., Aronov, P. A. and Hammock, B. D. (2007) 'Mass spectrometry-based metabolomics', *Mass Spectrometry Reviews*. Wiley Subscription Services, Inc., A Wiley Company, 26(1), pp. 51–78.

Dini, L., et al., (2020). 'Microvesicles and exosomes in metabolic diseases and inflammation'. Cytokine and Growth Factor Reviews, *Elsevier,* 51, pp. 27 - 39.

Dignat-George, F. and Boulanger, C. M. (2011) 'The many faces of endothelial microparticles', *Arteriosclerosis, Thrombosis, and Vascular Biology*, 31(1), pp. 27–33.

Doyle, L.M. and Zhuo Wang, M. (2019) ' Overview of Extracellular Vesicles, Their Origin, Composition, Purpose, and Methods for Exosome Isolation and Analysis' Cells Reviews, 8, (727), pp. 2- 24.

Dörffler, J. *et al.* (2003) 'Functional thrombomodulin deficiency causes enhanced thrombus growth in a murine model of carotid artery thrombosis', *Basic Res Cardiol*, 98, pp. 347–352.

Edwards, N., Langford-Smith, AWW., Wilkinson, FL., and Yvonne-Alexander, M., (2018). 'Endothelial Progenitor Cells: New Targets for Therapeutics for Inflammatory Conditions With High Cardiovascular Risk. A Review'. *Frontiers in Medicine, Translational Medicine.* 200 (5), pp. 1 - 10.

Eichacker, P. Q. *et al.* (2002) 'Risk and the Efficacy of Antiinflammatory Agents', *American Journal of Respiratory and Critical Care Medicine*, 166(9), pp. 1197–1205.

Engelmann, B. and Massberg, S. (2013) 'Thrombosis as an intravascular effector of innate immunity', *Nature Reviews Immunology*. Nature Publishing Group, 13(1), pp. 34–45.

English, D., Garcia, J. G. N. and Brindley, D. N. (2001) 'Platelet-released phospholipids link haemostasis and angiogenesis', *Cardiovascular Research*, 49(3), pp. 588–599.

Epstein, F. H., Rosenberg, R. D. and Aird, W. C. (1999) 'Vascular-Bed–Specific Hemostasis and Hypercoagulable States', *New England Journal of Medicine*, 340(20), pp. 1555–1564.

Esmon, Charles T. (2001) 'Protein C anticoagulant pathway and its role in controlling microvascular thrombosis and inflammation', *Critical Care Medicine*, 29, pp. 48–51.

Esmon, C T (2001) 'The normal role of Activated Protein C in maintaining homeostasis and its relevance to critical illness.', *Critical care (London, England). BioMed Central*, 5(2), pp. 7-12.

Esmon, C. T. (2009) 'Basic mechanisms and pathogenesis of venous thrombosis', *Blood Reviews*, 23(5), pp. 225–229.

Esmon, C. T. and Fukudome, K. (1995) 'Cellular regulation of the protein C pathway', *Seminars in Cell Biology*, 6(5), pp. 259–268.

Fan G-C, Ramachandran S, Lowenthal A, Ritner C, Lowenthal S, Bernstein HS., (2017).' Plasma microvesicle analysis identifies microRNA 129–5p as a biomarker of heart failure in univentricular heart disease'. *PLoS ONE*. 12, 183 - 224.

Faure, V. *et al.* (2006) 'Elevation of circulating endothelial microparticles in patients with chronic renal failure', *Journal of Thrombosis and Haemostasis*. Blackwell Publishing Inc, 4(3), pp. 566–573.

Flippov et al., (2015). ' Self-diffusion and interactions in mixtures of imidazolium bis(mandelato)borate ionic liquids with polyethylene glycol: ^{1}H NMR study'. *Magnetic Resonance Chemistry*. 53(1), pp. 493 - 497.

Foudi, N., and Legeay, S., (2021). 'Effects of physical activity on cell-to-cell communication during type 2 diabetes: A focus on miRNA signalling'. *Clinical Pharmacology*. 14(1), pp. 1 - 11.

França, C. N. *et al.* (2015) 'Microparticles as potential biomarkers of cardiovascular disease.', *Arquivos brasileiros de cardiologia*. Arquivos Brasileiros de Cardiologia, 104(2), pp. 169–74.

Fredrick Lindström, Philip T. F. Williamson and Gerhard Gröbner (2005) 'Molecular Insight into the Electrostatic Membrane Surface Potential by 14N/31P MAS NMR Spectroscopy: Nociceptin−Lipid Association'. *American Chemical Society*, 10(2), pp. 42 - 55.

Frey, B. and Gaipl, U. S. (2010) 'The immune functions of phosphatidylserine in membranes of dying cells and microvesicles', *Seminars in Immunopathology*, pp. 1–20.

Fritsch, P. *et al.* (2006) 'Thrombin generation in factor VIII-depleted neonatal plasma: nearly normal because of physiologically low antithrombin and tissue factor pathway inhibitor', *Journal of Thrombosis and Haemostasis*. Blackwell Publishing Inc, 4(5), pp. 1071–1077..

Frydman, L. and Harwood, J. S. (1995) 'Isotropic Spectra of Half-Integer Quadrupolar Spins from Bidimensional Magic-Angle Spinning NMR', *Journal of the American Chemical Society*, 117(19), pp. 5367–5368.

Furie, B. *et al.* (2005) 'Thrombus formation in vivo.', *The Journal of clinical investigation*. American Society for Clinical Investigation, 115(12), pp. 3355–62.

Furie, B. and Furie, B. C. (2008) 'Mechanisms of Thrombus Formation', *New England Journal of*

Medicine. Massachusetts Medical Society , 359(9), pp. 938–949..

Gaamangwe, T., Peterson, S. D. and Gorbet, M. B. (2014) 'Investigating the Effect of Blood Sample Volume in the Chandler Loop Model: Theoretical and Experimental Analysis', *Cardiovascular Engineering and Technology*, 5(2), pp. 133–144.

Gaertner, F. and Massberg, S. (2016) 'Blood coagulation in immunothrombosis—At the frontline of intravascular immunity', *Seminars in Immunology*, 28(6), pp. 561–569.

Gallart-Palau, X., Serra, A. and Sze, S. K. (2016) 'Enrichment of extracellular vesicles from tissues of the central nervous system.', *Molecular neurodegeneration*. BioMed Central, 11(1), p. 41 - 97.

Garcia, J. G. N., Pavalko, F. M. and Patterson, C. E. (1995) 'Vascular endothelial cell activation and permeability responses to thrombin', *Blood Coagulation & Fibrinolysis*, 6(7), pp. 609–626.

García-Moreno, R. López-Domínguez, A. Ramirez-Mena, A. Pascual-Montano, E. Aparicio-Puerta, M. Hackenberg, P. Carmona-Saez (2021). GeneCodis 4: Expanding the modular enrichment analysis to regulatory elements. bio Rxiv.15 (4).439962

Gardner, R. A. (1974) 'An examination of the fluid mechanics and thrombus formation time parameters in a Chandler rotating loop system.', *The Journal of laboratory and clinical medicine*, 84(4), pp. 494–508.

Giancarlo Aquinob, Nicola Pelizzib, Jesus Perez-Gilc, Fabrizio Salomoneb, Howard W. Clarka, d, A. D. P. (2018) 'Metabolism of a synthetic compared with a natural therapeutic pulmonary surfactant in the adult mouse. Jens Madsen', *Journal of lipid research*, 7(6), pp. 44 - 95.

Gleeson, E. M., O'Donnell, J. S. and Preston, R. J. S. (2012) 'The endothelial cell protein C receptor: cell surface conductor of cytoprotective coagulation factor signaling', *Cellular and Molecular Life Sciences*, 69(5), pp. 717–726.

GoretzkP, L. *et al.* (1992) 'Effective activation of the proenzyme form of the urokinase-type plasminogen activator (pro-uPA) by the cysteine protease cathepsin L', *Open Immunology*, 72(1), pp. 112–118.

Graber, ZT., Gericke, A., and Kooijman, EE., (2013). 'Phosphatidylinositol-4,5-bisphosphate ionization in the presence of cholesterol, calcium or magnesium ions'. *Chemistry and Physics of Lipids, Europe PMC*. 182(3), pp.62 - 72.

Gregory R. Warnes, Ben Bolker, Lodewijk Bonebakker, Robert Gentleman, Wolfgang Huber Andy Liaw, Thomas Lumley, Martin Maechler, Arni Magnusson, Steffen Moeller, Marc Schwartz and Bill Venables (2015). gplots: Various R Programming Tools for Plotting Data. R package version 2.17.0.

Griffin, R. G. (1981) 'Solid state nuclear magnetic resonance of lipid bilayers', *Journal of the American Chemical Society*, 43(5), pp. 108–174.

Gumina, D.L and Su, E.J., (2017). 'Endothelial Progenitor Cells of the Human Placenta and Fetoplacental Circulation: A Potential Link to Fetal, Neonatal, and Long-term Health'. Review Article, *Frontiers in Paediatrics,* 41(5), pp. 1 - 7.

Hargett, L. A. and Bauer, N. N. (2013) 'On the origin of microparticles: From platelet dust to mediators of intercellular communication.', *Pulmonary circulation*, 3(2), pp. 329–40.

Harris et al., (2001). 'NMR Nomenclature. Nuclear Spin Properties and Conventions for Chemical Shifts'. Pure Applied Chemistry. 73(11), pp. 1795 - 1818.

Harvey, et al., (2015). ' Modulation of endothelial cell integrity and inflammatory activation by commercial lipid emulsions. Lipids in Health and Disease. 14(9), pp. 2 - 15.

Harvey, T.M and Boucrot, (2018).' Membrane curvature at a glance. Journal of Cell Science. 188, pp. 1065 - 1070.

Heemskerk, J. W. M., Bevers, E. M. and Lindhout, T. (2002) 'Platelet Activation and Blood Coagulation', *Thromb Haemost*, 88, pp. 186–93.

Héliès-Toussaint, C. *et al.* (2006) 'Lipid metabolism in human endothelial cells', *Molecular and Cell Biology of Lipids*, 1761(7), pp. 765–774.

Hellem, A. J., Borchgrevink, Ch. F. and Ames, S. B. (1961) 'The Role of Red Cells in Haemostasis: the Relation between Haematocrit, Bleeding Time and Platelet Adhesiveness', *British Journal of Haematology*, 7(1), pp. 42–50.

Hicks, J. and Bradford, J. (2010) 'A novel violet-laser excitable ratiometric probe for the detection of membrane asymmetry breakdown during apoptosis', *Cancer Research*, 70(8), pp. 3976–3976.

Hoffman, M. and Monroe, D. M. (2007) 'Coagulation 2006: A Modern View of Hemostasis', *Hematology/Oncology Clinics of North America*, 21(1), pp. 1–11.

Hoffman, M. and Pawlinski, R. (2014) 'Hemostasis: Old System, New Players, New Directions', *Thrombosis Research*, 133, pp. 1–27.

Hu, W., Som, A. and Tew, G. N. (2011) 'Interaction between Lipids and Antimicrobial Oligomers Studied by Solid-State NMR', *Journal of Physics Chemistry Biology*, 115, pp. 8474–8480.

Hugel, B. *et al.* (2005) 'Membrane Microparticles: Two Sides of the Coin', *Physiology*, 20(1), pp. 22–27.

Hui, S. W., Stewart, T. P. and Yeagle, P. L. (1980) 'Temperature-dependent morphological and phase behavior of sphingomyelin.', *Biochimica et biophysica acta*, 601(2), pp. 271–81.

Iba, T., and Ogura, H., (2018). 'Role of extracellular vesicles in the development of sepsis-induced coagulopathy'. *Journal of Intensive Care*, 68(6), pp. 2 - 12.

Ishida, M. *et al.* (2004) 'High-resolution analysis by nano-electrospray ionization Fourier transform ion cyclotron resonance mass spectrometry for the identification of molecular species of phospholipids and their oxidized metabolites', *Rapid Communications in Mass Spectrometry*, 18(20), pp. 2486–2494.

Jaffe, E. A. *et al.* (1973) 'Culture of Human Endothelial Cells Derived from Umbilical Veins', *Journal of Clinical Investigation*, 52(11), pp. 2745–2756.

Janmey, P. A. and Kinnunen, P. K. J. (2006) 'Biophysical properties of lipids and dynamic membranes', *Cell Biology*, 16(10), pp. 538–546.

Jankowska, KI., Sauna, ZE., and Atreya, CD., (2020). 'Role of microRNAs in Hemophilia and Thrombosis in Humans'. International Journal for Molecular Sciences. 21(10), pp. 35 - 98.

Jansen, F. *et al.* (2014) 'MicroRNA expression in circulating microvesicles predicts cardiovascular events in patients with coronary artery disease', *Journal of the American Heart Association*, 3(6), pp. 1-16.

Jimenez, J. J. *et al.* (2003) 'Endothelial microparticles released in thrombotic thrombocytopenic purpura express von Willebrand factor and markers of endothelial activation', *British Journal of Haematology*, 123(5), pp. 896–902.

Johansson, P. I. and Stensballe, J. (2009) 'Effect of Haemostatic Control Resuscitation on mortality in massively bleeding patients: a before and after study', *Vox Sanguinis*. Blackwell Publishing Ltd, 96(2), pp. 111– 127.

Jones, J. A. *et al.* (2000) 'Geometric quantum computation using nuclear magnetic resonance', *Nature*. Nature Publishing Group, 403(6772), pp. 869–871.

Juhasz, P. and Biemann, K. (1994) 'Mass spectrometric molecular-weight determination of highly acidic compounds of biological significance via their complexes with basic polypeptides', *Journal of the American Chemical Societ,* 91, pp. 4333–4337.

Kagan, V. E. *et al.* (2004) 'Oxidative lipidomics of apoptosis: redox catalytic interactions of cytochrome c with cardiolipin and phosphatidylserine', *Free Radical Biology and Medicine*, 37(12), pp. 1963–1985.

Kahn, M. L. *et al.* (1999) 'Protease-activated receptors 1 and 4 mediate activation of human platelets by thrombin.', *The Journal of clinical investigation*, 103(6), pp. 879–87.

Kebarle, P. and Verkerk, U. H. (2009) 'Electrospray: From ions in solution to ions in the gas phase, what we know now', *Mass Spectrometry Reviews*, 28(6), pp. 898–917.

Keeler, C. and Maciel, G. E. (2003) 'Quantitation in the solid-state 13C NMR analysis of soil and organic soil fractions', *Analytical Chemistry*, 75(10), pp. 2421–2432.

Khan, A. R. and James, M. N. G. (1998) 'Molecular mechanisms for the conversion of zymogens to active proteolytic enzymes.', *Protein science : a publication of the Protein Society*, 7(4), pp. 815–836.

Koga, H. *et al.* (2005) 'Elevated Levels of VE-Cadherin-Positive Endothelial Microparticles in Patients With Type 2 Diabetes Mellitus and Coronary Artery Disease', *Journal of the American College of Cardiology*, 45(10), pp. 1622–1630.

Kooijman, EE., King, KE., Gangoda, M., and Gericke, A., (2009). *American Chemical Society*. 48(40), pp. 9360 - 9371.

Kozomara, A., Birgaoany, M., and Griffiths-Jones, (2019). 'miRbase: from microRNA sequences to function'. Nucleic Acids Research. 47 (1), pp. D155 – D162.

Kratzer, M. A. A. and Born, G. V. R. (2009) 'Simulation of Primary Haemostasis in vitro', *Pathophysiology of Haemostasis and Thrombosis*. Karger Publishers, 15(6), pp. 357–362.

Kreimer, S. *et al.* (2015) 'Mass-Spectrometry-Based Molecular Characterization of Extracellular Vesicles: Lipidomics and Proteomics', *Journal of Proteome Research*, 14(6), pp. 2367–2384.

Krishnaswamys, S. *et al.* (1992) 'Role of the Membrane Surface in the Activation of Human Coagulation Factors', *The Journal of Biological Chemistry*, 267(36), pp. 26110–26120.

Kruijff, B. *et al.* (1978) 'Evidence for isotropic motion of phospholipids in liver microsomal membranes. A 31P NMR study.', *Biochimica et biophysica acta*, 514(1), pp. 1–8.

Lacroix R., Dubois C., Leroyer A.S., Sabatier F. Dig- George F. (2013). Revisited role of microparticles in arterial and venous thrombosis. *J. Thromb. Haemost*. 11 (Suppl 1), 24–35.

Lee, A. G. (2005) 'How lipids and proteins interact in a membrane: A molecular approach', *Molecular BioSystems*, 1(3), pp. 203–212.

Lee, A. G. (2011) 'Biological membranes: The importance of molecular detail', *Trends in Biochemical Sciences*. Elsevier Ltd, 36(9), pp. 493–500.

Leitinger, N. (2003) 'Oxidized phospholipids as modulators of inflammation in atherosclerosis.', *Current opinion in lipidology*, 14(5), pp. 421–30.

Lemmon, M. A. (2008) 'Membrane recognition by phospholipid-binding domains.', *Nature reviews. Molecular cell biology*, 9(2), pp. 99–110

Leventis, P. A. and Grinstein, S. (2010) 'The Distribution and Function of Phosphatidylserine in

Cellular Membranes', *Annual Review Biophysics*, 39, pp. 407–27.

Levi, M., and Poll, T. von der., (2017). 'Coagulation and Sepsis'. Thrombosis Research. 11(7), pp. 207 - 278.

Lhermusier, T., Chap, H. and Payrastre, B. (2011) 'Platelet membrane phospholipid asymmetry: from the characterization of a scramblase activity to the identification of an essential protein mutated in Scott syndrome', *Journal of Thrombosis and Haemostasis*. Blackwell Publishing Ltd, 9(10), pp. 1883–1891.

Li, H.A., (2011). 'Statistical framework for SNP calling, mutation discovery, association mapping and population genetical parameter estimation from sequencing data'. Bioinformatics. 27(21), pp.2987 - 2993.

Li H, Handsaker B et al., (2009). The sequence alignment/map format and SAMtools. Bioinformatics. 25: 2078—-2079.

Liang H, Li S and Chen, H., (2017).'Endothelial microparticles-mediated trans- fer of microRNA-19b, a novel messenger in cell-cell communication, plays a key role in endothelial migration and angiogenesis. *Journal of The American College of Cardiology*. 70, pp. C34-C49.

Liang H-Z, Li S-F, Zhang F, et al., (2018).' Effect of endothelial microparticles induced by hypoxia on migration and angiogenesis of human umbilical vein endothelial cells by delivering microRNA-19b'. *Chinese Medical Journal.* 13(1), pp. 2726-2733.

Liaw, P. C. *et al.* (2001) 'Identification of the protein C/activated protein C binding sites on the endothelial cell protein C receptor. Implications for a novel mode of ligand recognition by a major histocompatibility complex class 1-type receptor.', *The Journal of biological chemistry*. American Society of Hematology, 276(11), pp. 8364–70.

Lindblom, G. and Rilfors, L. (1992) 'Nonlamellar phases formed by membrane lipids.', *Advances in colloid and interface science*, 41, pp. 101–25.

Lindström, F., Williamson, P. T. F. and Gröbner, G. (2005) 'Molecular Insight into the Electrostatic Membrane Surface Potential by ^{14}N/ ^{31}P MAS NMR Spectroscopy: Nociceptin−Lipid Association', *Journal of the American Chemical Society*, 127(18), pp. 6610–6616.

Losito, I. *et al.* (2013) 'Phospholipidomics of human blood microparticles', *Analytical Chemistry*, 85(13), pp. 6405–6413.

Loyer, X. *et al.* (2014) 'Microvesicles as cell-cell messengers in cardiovascular diseases', *Circulation Research*, 114(2), pp. 345–353.

Luga, A., Ader, C., Groger, and Brunner, E., (2007). 'Applications of Solid-State ^{31}P NMR Spectroscopy'. *Elsevier*, 60, pp. 145 - 189.

Maglott D, Ostell J, Pruitt KD, Tatusova T., (2005). 'Entrez Gene: gene-centered information. National Centre for Biotechnology Information. Nucleic Acids Research. 33, pp. D54-D58.

Mallia, A., Gianazza, E., Zoanni, B., Brioschi, M., Barbieri, SS., and Banfi, C., (2020). 'Proteomics of Extracellular Vesicles: Update on Their Composition, Biological Roles and Potential Use as Diagnostic Tools in Atherosclerotic Cardiovascular Diseases'. *Diagnostics*. 843(10), pp. 1 - 33.

Mananga, E. S. *et al.* (2015) 'Advances in Theory of Solid-State Nuclear Magnetic Resonance.', *Journal of nature and science*, 1(6), pp. 109.

Mann, K. G., Brummel, K. and Butenas, S. (2003) 'What is all that thrombin for?', *Journal of Thrombosis and Haemostasis*. Blackwell Science Inc, 1(7), pp. 1504–1514.

Mareš, T. *et al.* (2012) 'Determination of the Strength of Adhesion between Lipid Vesicles', *The Scientific World Journal*, 1 (3), pp. 1–6.

Martinez-Martin, N. and Nadia (2017) 'Technologies for Proteome-Wide Discovery of Extracellular Host-Pathogen Interactions', *Journal of Immunology Research*. Hindawi Publishing Corporation, 1(5), pp. 1–18.

Massiot, D. *et al.* (2002) 'Modelling one- and two-dimensional solid-state NMR spectra', *Magnetic Resonance in Chemistry*. John Wiley & Sons, Ltd., 40(1), pp. 70–76.

Mathiesen, A., Hamilton, T., Carter, N., Brown, M., McPheat, W., and Dobrian, A., (2021). 'Endothelial Extracellular Vesicles: From Keepers of Health to Messengers of Disease (Review)'. *International Journal of Molecular Sciences*, 4640(22), pp. 2 - 26.

Mavrommatis, A. C. *et al.* (2001) 'Activation of the fibrinolytic system and utilization of the coagulation inhibitors in sepsis: comparison with severe sepsis and septic shock', *Intensive Care Medicine*, 27(12), pp. 1853–1859.

McCarthy DJ, Chen Y and Smyth GK (2012). Differential expression analysis of multifactor RNA-Seq experiments with respect to biological variation. *Nucleic Acids Research* 40, pp. 4288-4297

McMahon, HT., and Gallop, JL., (2005). ' Membrane curvature and mechanisms of dynamic cell membrane remodelling'. Nature. 438, pp. 590 - 596.

Medek, A., Harwood, J. S. and Frydman, L. (1995) 'Multiple-Quantum Magic-Angle Spinning NMR: A New Method for the Study of Quadrupolar Nuclei in Solids', *I . Am. Chem. SOC*, 117, pp. 12779–12787.

Medina-Leyte et al., (2020). 'Use of Human Umbilical Vein Endothelial Cells (HUVEC) as a Model to Study Cardiovascular Disease: A Review'. *Applied Sciences,* 938(10), pp. 1 - 25.

Meer van, G. (2005) 'Cellular lipidomics.', *The EMBO journal*. European Molecular Biology Organization, 24(18), pp. 3159–65.

Meer van, G., Voelker, D. R. and Feigenson, G. W. (2008) 'Membrane lipids: where they are and how they behave.', *Nature reviews. Molecular cell biology*, 9(2), pp. 112–124.

Meng, Z. H. *et al.* (2003) 'The effect of temperature and pH on the activity of factor VIIa: implications for the efficacy of high-dose factor VIIa in hypothermic and acidotic patients.', *The Journal of trauma*, 55(5), pp. 886–891.

Merlo, C. *et al.* (2002) 'Elevated levels of plasma prekallikrein, high molecular weight kininogen and factor XI in coronary heart disease', *Atherosclerosis*, 161(2), pp. 261–267.

Michaelson, L. V. *et al.* (2016) 'Plant sphingolipids: Their importance in cellular organization and adaption', *Biochimica et Biophysica Acta (BBA) - Molecular and Cell Biology of Lipids*, 1861(9), pp. 1329–1335.

Mohan Rao, L. V., Esmon, C. T. and Pendurthi, U. R. (2014) 'Endothelial cell protein C receptor: a multiliganded and multifunctional receptor.', *Blood*. American Society of Hematology, 124(10), pp. 1553–1567.

Monroe, D. M., Hoffman, M. and Roberts, H. R. (2002) 'Platelets and thrombin generation', *Arteriosclerosis, Thrombosis, and Vascular Biology*, 22(9), pp. 1381–1389.

Moran, L., and Janes, N., (1998). ' Tracking Phospholipid Populations in Polymorphism by Sideband Analyses of ^{31}P Magic Angle Spinning NMR'. *Biophysical Journal.* 75(2), pp. 867 - 879.

Moreau, C., Floch, Le M., Segalen, J., Leray, G., Metzinger, L., de Certaines, J.D., and Le Rumeur, E., (1999). ' Static and magic angle spinning ^{31}P NMR spectroscopy of two natural membrane'. Federation of European Biochemical Societies. 461, pp. 258 - 262.

Morel, O. *et al.* (2011) 'Cellular mechanisms underlying the formation of circulating microparticles', *Arteriosclerosis, Thrombosis, and Vascular Biology*, 31(1), pp. 15–26.

Morhayim, J., Baroncelli, M and van Leeuwen, JP., (2014). ' Ectracellular vesicles: Specialized bone messengers'. Archives of Biochemistry and Biophysics. 561(1), pp. 38 - 45.

Mori, N. *et al.* (2003) 'Choline phospholipid metabolites of human vascular endothelial cells altered by cyclooxygenase inhibition, growth factor depletion, and paracrine factors secreted by cancer cells', *Molecular Imaging*, 2(2), pp. 124–130.

Morrissey, J. H. *et al.* (2009) 'Protein-membrane interactions: blood clotting on nanoscale bilayers.', *Journal of thrombosis and haemostasis,* 33(3), pp. 169–72.

Mörtberg,J., Lundwall, K., Mobarrez, F., Wallén, H., Jacobson, S.H. and Spaak, J., (2019). 'Increased

concentrations of platelet- and endothelial-derived microparticles in patients with myocardial infarction and reduced renal function- a descriptive study'. *BMC Nephrology*, 71(20), pp. 2 -9.

Mosnier, L. O. and Bouma, B. N. (2006) 'Regulation of fibrinolysis by Thrombin Activatable Fibrinolysis Inhibitor, an unstable carboxypeptidase B that unites the pathways of coagulation and fibrinolysis', *Arteriosclerosis, Thrombosis, and Vascular Biology*, 26(11), pp. 2445–2453.

Muralidharan-Chari, V. *et al.* (2009) 'ARF6-regulated shedding of tumor cell-derived plasma membrane microvesicles.', *Current biology*, 19(22), pp. 1875–85.

Muralidharan-Chari, V. *et al.* (2010) 'Microvesicles: mediators of extracellular communication during cancer progression.', *Journal of cell science*. Company of Biologists, 123(10), pp. 1603–11.

Mutch, N. J. *et al.* (2003) 'Thrombus lysis by uPA, scuPA and tPA is regulated by plasma TAFI.', *Journal of thrombosis and haemostasis : JTH*, 1(9), pp. 2000–7.

Mutch, N. J. *et al.* (2008) 'The use of the Chandler loop to examine the interaction potential of NXY-059 on the thrombolytic properties of rtPA on human thrombi in vitro.', *British journal of pharmacology*. Wiley-Blackwell, 153(1), pp. 124–31

Mutch, N.J. *et al.* (2007) 'TAFIa, PAI-1 and ? $_2$ -antiplasmin: complementary roles in regulating lysis of thrombi and plasma clots', *Journal of Thrombosis and Haemostasis*. Blackwell Publishing Ltd, 5(4), pp. 812–817.

Narváez-Rivas, M. and Zhang, Q. (2016) 'Comprehensive untargeted lipidomic analysis using core-shell C30 particle column and high field orbitrap mass spectrometer.', *Journal of chromatography. A*. NIH Public Access, 1440, pp. 123–34.

Navarro, S. *et al.* (2011) 'The endothelial cell protein C receptor: Its role in thrombosis', *Thrombosis Research*, 128(5), pp. 410–416.

Oas, T. G., Griffin, R. G. and Levitt, M. H. (1988) 'Rotary resonance recoupling of dipolar interactions in solid-state nuclear magnetic resonance spectroscopy', *The Journal of Chemical Physics*. American Institute of Physics, 89(2), pp. 692–695.

Oeveren, W., Tielliu, I. F. and de Hart, J. (2012) ' Comparison of Modified Chandler, Roller Pump, and Ball Valve Circulation Models for In Vitro Testing in High Blood Flow Conditions: Application in Thrombogenicity Testing of Different Materials for Vascular Applications ', *International Journal of Biomaterials*, 12(3), pp. 1–7.

Okamoto, M., et al., (2012). 'High-curvature domains of the ER are important for the organization of ER exit sites in Saccharomyces cerevisiae'. Journal of Cell Science. 152(14), pp. 3412 - 3420.

Olsen, J. V. *et al.* (2006) 'Global, In Vivo, and Site-Specific Phosphorylation Dynamics in Signaling Networks', *Cell*, 127(3), pp. 635–648.

Onat, D., Brillon, D., Colombo, P.C and Schmidt, A.M., (2012). 'Human Vascular Endothelial Cells: A Model System for Studying Vascular Inflammation in Diabetes and Atherosclerosis'. *Springer*, 11(3), pp.193 - 202.

Palabrica, T. *et al.* (1992) 'Leukocyte accumulation promoting fibrin deposition is mediated in vivo by P-selectin on adherent platelets', *Nature*, 359(6398), pp. 848–851.

Palta, S., Saroa, R. and Palta, A. (2014) 'Overview of the coagulation system.', *Indian journal of anaesthesia*. Medknow Publications, 58(5), pp. 515–23.

Panfoli, et al., (2018). ' Microvesicles as promising biological tools for diagnosis and therapy'. *Expert Review pf Proteomics, Taylor,* 15(10), pp. 801 - 808.

Pérez-Casal, M. *et al.* (2009) 'Microparticle-associated endothelial protein C receptor and the induction of cytoprotective and anti-inflammatory effects.', *Haematologica*. Ferrata Storti Foundation, 94(3), pp. 387–394.

Piccini, J. P. *et al.* (2004) 'New insights into diastolic heart failure: role of diabetes mellitus', *The American Journal of Medicine*, 116(5), pp. 64–75.

Pinton, P. *et al.* (2008) 'Calcium and apoptosis: ER-mitochondria Ca 2 þ transfer in the control of apoptosis', *Oncogene*, 27, pp. 6407–6418.

Raposo, G. and Stoorvogel, W. (2013) 'Extracellular vesicles: Exosomes, microvesicles, and friends', *Journal of Cell Biology*, 200(4), pp. 373–383.

Raimondo, S., et al., (2020). 'Extracellular Vesicle microRNAs Contribute to the Osteogenic Inhibition of Mesenchymal Stem Cells in Multiple Myeloma'. *Cancers*. 12(2), pp. 20 - 49.

Ratajczak, MZ and Ratajczak, J., (2017). 'Extracellular microvesicles as game changers in better understanding the complexity of cellular interactions—from bench to clinical applications'. *The American Journal of The Medical Sciences*. 353(5), 449 - 452.

Ratajczak, MZ and Ratajczak, J., (2020).'Extracellular microvesicles/exosomes: discovery, disbelief, acceptance, and the future?'. *Nature*. 34, pp. 3126 - 3135.

R Core Team (2018). R: A language and environment for statistical computing. R Foundation for Statistical Computing, Vienna, Austria. URL https://www.R-project.org/

Record, M., Silver-Poirot, S., Poirot, M., and Wakelam, M.J., (2018).'Extracellular vesicles: lipids as key components of their biogenesis and functions'. *Thematic Review Series*, 1194(10), pp. 1316 - 1322.

Ridger V.C., et al., (2017). Microvesicles in vascular homeostasis and diseases. Position paper of the

European Society of Cardiology (ESC) Working Group on Atherosclerosis and Vascular Biology. *Thromb. Haemost.* 117, 1296–1316.

Robbie, L. A. *et al.* (1997) 'Thrombi formed in a Chandler loop mimic human arterial thrombi in structure and RAI-1 content and distribution.', *Thrombosis and haemostasis*, 77(3), pp. 510–5.

Robinson MD, McCarthy DJ and Smyth GK (2010). edgeR: a Bioconductor package for differential expression analysis of digital gene expression data. *Bioinformatics* 26, pp. 139-140.

Rodriguez-Rius, A., Lopez, S., Martinez-Perez, A., Souto, JC., and Soria, JM., 2020).'Identification of a Plasma MicroRNA Profile Associated With Venous Thrombosis. *Arteriosclerosis Thrombosis Vascular Biology.* 40(5), pp. 1392 - 1399.

Romero, G. *et al.* (2013) 'Blood clot simulation model by using the Bond-Graph technique.', *The Scientific World Journal.* Hindawi Publishing Corporation, 13(5), pp. 519-47.

Roth, G. J. (1992) 'Platelets and blood vessels: the adhesion event', *Immunology Today*, 13(3), pp. 100–105.

Ruggeri, Z. M. (1997). 'Mechanisms initiating platelet thrombus formation.', *Thrombosis and haemostasis*, 78(1), pp. 611–666.

Sahoo, S. et al. (2021) 'Therapeutic and Diagnostic Translation of Extracellular Vesicles in Cardiovascular Diseases' Circulation, 143(14), pp. 1426 - 1449.

Saitô, H., Ando, I. and Ramamoorthy, A. (2010) 'Chemical shift tensor - the heart of NMR: Insights into biological aspects of proteins.', *Progress in nuclear magnetic resonance spectroscopy.* NIH Public Access, 57(2), pp. 181–228.

Sanders, C. R. and Schwonek, J. P. (1992) 'Characterization of magnetically orientable bilayers in mixtures of dihexanoylphosphatidylcholine and dimyristoylphosphatidylcholine by solid-state NMR.', *Biochemistry*, 31(37), pp. 8898–905.

Santos, A. X. S. and Riezman, H. (2012) 'Yeast as a model system for studying lipid homeostasis and function', *FEBS Letters*, 586(18), pp. 2858–2867.

Satta, N. *et al.* (997) 'Scott syndrome: an inherited defect of the procoagulant activity of platelets', *Platelets*, 8(1), pp. 17–124.

Schabbauer, G., Tencati, M., Pedersen, B., Pawlinski, R., and Mackman, N., (2004). 'PI3K-Akt Pathway Suppresses Coagulation and Inflammation in Endotoxemic Mice'. *Arteriosclerosis, Thrombosis, and Vascular Biology.* 24(10), 1963 - 1969.

Schmieder R and Edwards R (2011): Quality control and preprocessing of metagenomic datasets. Bioinformatics. 27(6): 863–864.

Seelig, J., (1978). ' ^{31}P nuclear magnetic resonance and the head group structure of phospholipids in membranes'. *BBA, Reviews on Biomembranes.* 515(2), pp. 105 - 140.

Shaffer, J., Schlumpberger, M. and Lader, E. (2012) 'miRNA profiling from blood—challenges and recommendations' *The Journal of Immunology*, 511(3), pp. 1111–1130

Shantsila, E., Kamphuisen, P. W. and Lip, G. Y. H. (2010) 'Circulating microparticles in cardiovascular disease: implications for atherogenesis and atherothrombosis', *Journal of Thrombosis and Haemostasis*, 8(11), pp. 2358–2368.

Shkair, et al., (2021). 'Membrane microvesicles as potential vaccine candidates'. International Journal of Molecular Sciences. 22(3), pp. 11 - 42.

Shu, Z., Tan, J., Miao, Y., and Zhang, Q., (2019). 'The role of microvesicles containing microRNAs in vascular endothelial dysfunction'. *Journal of Cellular and Molecular Medicine.* 23(12), pp. 7933 - 7945.

Shet, A. S. (2008) 'Characterizing blood microparticles: Technical aspects and challenges', *Vascular Health and Risk Management*, 4(4), pp. 769–774.

Silini, E. *et al.* (2002) 'Hepatitis C virus infection in a hematology ward: evidence for nosocomial transmission and impact on hematologic disease outcome.', *Haematologica*. Haematologica, 87(11), pp. 1200–8.

Siljander, P., Carpen, O. and Lassila, R. (1996) 'Platelet-derived microparticles associate with fibrin during thrombosis', *Blood*, 87(11), pp.966 - 1077.

Silveira, A. *et al.* (1994) 'Activation of coagulation factor VII during alimentary lipemia.', *Arteriosclerosis and thrombosis : a journal of vascular biology / American Heart Association*, 14(1), pp. 60–69.

Sim, W. J., Ahl, P. J. and Connolly, J. E. (2016) 'Metabolism Is Central to Tolerogenic Dendritic Cell Function', *Mediators of Inflammation*. Hindawi Publishing Corporation, 7(3), pp. 1–10.

Simak, J. and Gelderman, M. P. (2006) 'Cell membrane microparticles in blood and blood products: Potentially pathogenic agents and diagnostic markers', *Transfusion Medicine Reviews*, 20(1), pp. 1–26.

Singh, I. *et al.* (2003) 'Failure of thrombus to resolve in urokinase-type plasminogen activator gene-knockout mice: Rescue by normal bone marrow-derived cells', *Circulation*, 107(6), pp. 869–875.

Skotland, T., Sagini, K., Sandvig, K., and Liorente, A., (2020).' An emerging focus on lipids in extracellular vesicles'. Advanced Drug Delivery Reviews, *Elsevier*. 159, pp. 308 - 321.

Smiley, S. T., King, J. A. and Hancock, W. W. (2001) 'Fibrinogen Stimulates Macrophage

Chemokine Secretion Through Toll-Like Receptor 4', *The Journal of Immunology*, 167(5), pp. 2887–2894.

Soler-Botija, C.; Galvez-Monton, C.; Bayes-Genis, A (2019). Epigenetic Biomarkers in Cardiovascular Diseases. *Front Genetics.* 10, pp.750 - 950.

Sonoda, Y., Kano, F., and Murata, M., (2021). 'Applications of cell resealing to reconstitute microRNA loading to extracellular vesicles'. Scientific Reports, *Nature*, 2900(11), pp. 100 - 226.

Spector, A. A. and Yorek, M. A. (1985) 'Membrane lipid composition and cellular function', *Journal of lipid research*, 26(9), pp. 1015–1035.

Stringer, H. A. *et al.* (1994) 'Plasminogen activator inhibitor-1 released from activated platelets plays a key role in thrombolysis resistance. Studies with thrombi generated in the Chandler loop.', *Arteriosclerosis and thrombosis : a journal of vascular biology*. American Heart Association, Inc., 14(9), pp. 1452–85.

Suárez-García, S. *et al.* (2017) 'Development and validation of a UHPLC-ESI-MS/MS method for the simultaneous quantification of mammal lysophosphatidylcholines and lysophosphatidylethanolamines in serum', *Journal of Chromatography B*, 1055, pp. 86–97.

Sustar V., Bedina-Zavec A., Stukelj R., Frank M., Ogorevc E., Jansa R., Mam K, Veranic P., Kralj-Iglic V., (2011). Post-prandial rise of microvesicles in peripheral blood of healthy human donors. *Lipids Health Disease.* 10, pp. 10 - 47.

Suzuki, K. *et al.* (1987) 'Structure and expression of human thrombomodulin, a thrombin receptor on endothelium acting as a cofactor for protein C activation', *The EMBO Journal*, 6(7), pp. 1891–1897.

Szafraniec, E. *et al.* (2018) 'Diversity among endothelial cell lines revealed by Raman and Fourier-transform infrared spectroscopic imaging', *Analyst. Royal Society of Chemistry*, 143(18), pp. 4323–4334.

Tanaka, K. A., Key, N. S. and Levy, J. H. (2009) 'Blood Coagulation: Hemostasis and Thrombin Regulation', *Anesthesia & Analgesia*, 108(5), pp. 1433–1446.

Tavoosi, B., Smith, S.A., Davis-Harrison, R and Morrissey, JH., (2013). 'Factor VII and Protein C are Phosphatidic Acid-Binding Proteins'. *Biochemistry*. 52(33), pp. 5545 - 5552.

Thankaswamy-Kosalai,S., Sen, P., and Nookaew, I., (2017). ' Evaluation and assessment of read-mapping by multiple next-generation sequencing aligners based on genome-wide characteristics'. Genomics. 109(4), pp. 186 – 191.

Théry C, Witwer KW, Aikawa E, Alcaraz MJ, Anderson JD, Andriantsitohaina R, Antoniou A, Arab T, Archer F, and Atkin-Smith GK. (2018) 'Minimal information for studies of extracellular vesicles a position statement of the International Society for Extracellular Vesicles and update of the

MISEV2014 guidelines', *Journal of Extracellular Vesicles*, 7 (3), pp. 53 - 75.

Thomas, M. C., Mitchell, T. W. and Blanksby, S. J. (2005) 'A Comparison of the Gas Phase Acidities of Phospholipid Headgroups: Experimental and Computational Studies', *ournal of the American Society for Mass Spectrometry*, 6(16), pp. 926–939.

Thornhill, M.H., Li, J and Haskard, O., (1993). 'Leucocyte Endothelial Cell Adhesion: a Study comparing Human Umbilical Vein Endothelial Cells and the Endothelial Cell Line EA-hy-926'. *Scandinavian Journal of Immunology*, 38(3), pp. 279 - 286.

Todoroki, H. *et al.* (2000) 'Neutrophils express tissue factor in a monkey model of sepsis', *Surgery*, 127(2), pp. 209–216.

Topper, J. N. *et al.* (1996) 'Identification of vascular endothelial genes differentially responsive to fluid mechanical stimuli: cyclooxygenase-2, manganese superoxide dismutase, and endothelial cell nitric oxide synthase are selectively up-regulated by steady laminar shear stress.', *Proceedings of the National Academy of Sciences*, 93(19), pp. 10417–10422.

Touma, H. *et al.* (2014) 'Numerical Investigation of Fluid Flow in a Chandler Loop', *Journal of Biomechanical Engineering*, 136(7), pp. 704 - 767.

Travers, R. J., Smith, S. A. and Morrissey, J. H. (2015) 'Polyphosphate, platelets, and coagulation', *International Journal of Laboratory Hematology*, 37(S1), pp. 31–35.

Tripisciano, C., Weiss, R., Eichhon, T., Splittler, A., Heuser, T., Bernhard, M and Weber, V., (2017). Different Potential of Extracellular Vesicles to Support Thrombin Generation: Contributions of Phosphatidylserine, Tissue Factor, and Cellular Origin' Nature, 6522(7), pp. 2 - 11.

Tycko, R. and Dabbagh, G. (1990) 'Measurement of nuclear magnetic dipole—dipole couplings in magic angle spinning NMR', *Chemical Physics Letters*, 173(5–6), pp. 461–465.

Undas, A. and Ariëns, R. A. S. (2011) 'Fibrin clot structure and function: A role in the pathophysiology of arterial and venous thromboembolic diseases', *Arteriosclerosis, Thrombosis, and Vascular Biology*, 31(12), pp 61 - 83.

Vafa Homann, M. *et al.* (2016) 'Improved ex vivo blood compatibility of central venous catheter with noble metal alloy coating.', *Journal of biomedical materials research. Part B, Applied biomaterials*. Wiley-Blackwell, 104(7), pp. 1359–65.

Vajen, T., Mause, S. F. and Koenen, R. R. (2015) 'Microvesicles from platelets: Novel drivers of vascular inflammation', *Thrombosis and Haemostasis*, 114(2), pp. 228–236.

Vallet, B. and Wiel, E. (2001) 'Endothelial cell dysfunction and coagulation', *Critical Care Medicine*, 29, pp. 36–41.

Vanni, S., Hirose, H., Barelli, H., Antonny, B., and Gautier, R., (2014). ' A sub-nanometre view of how membrane curvature and composition modulate lipid packing and protein recruitment'. *Nature Communications*, 4916(5), pp. 1 - 9.

Van Beek, J.D., (2007). 'matNMR: a flexible toolbox for processing, analyzing and visualizing magnetic resonance data in Matlab'. Journal of Magnetic Resonance. 187(1), pp. 19 - 26.

Vervloet, M., Thijs, L. and Hack, C. (1998) 'Derangements of Coagulation and Fibrinolysis in Critically III Patients with Sepsis and Septic Shock', *Seminars in Thrombosis and Hemostasis*, 24(01), pp. 33–44.

Veziroglu, EM., and Mias, GI., (2020).' Characterizing Extracellular Vesicles and Their Diverse RNA Contents. A Review. *Frontiers in Genetics*. 700(11), pp. 1 - 22.

Vilella, F., Ramirez, L. B. and Simón, C. (2013) 'Lipidomics as an emerging tool to predict endometrial receptivity', *Fertility and Sterility*, 99(4), pp. 1100–1106.

Villoutreix, B. O., Teleman, O. and Dahlbäck, B. (1997) 'A theoretical model for the Gla-TSR-EGF-1 region of the anticoagulant cofactor protein S: from biostructural pathology to species-specific cofactor activity.', *Journal of computer-aided molecular design*. American Heart Association, Inc., 11(3), pp. 293–304.

Vogt, F. G. *et al.* (2014) 'Solid-State NMR Analysis of a Complex Crystalline Phase of Ronacaleret Hydrochloride', *The Journal of Physical Chemistry B*, 118(34), pp. 10266–10284.

Volk, T. and Kox, W. J. (2000) 'Endothelium function in sepsis', *Inflammation Research*, 49(5), pp. 185–198.

Wanger, D. D. and Bonfanti, R. (1991) 'Von Willebrand Factor and the Endothelium', *Mayo Clinic Proceedings*, 66(6), pp. 621–627.

Wang, C-C. *et al.* (2014) 'Circulating endothelial-derived activated microparticle: a useful biomarker for predicting one-year mortality in patients with advanced non-small cell lung cancer.', *BioMed research international*. Hindawi Publishing Corporation, 2014, p. 173401.

Wang, J.-M. *et al.* (2009) 'Elevated circulating endothelial microparticles and brachial–ankle pulse wave velocity in well-controlled hypertensive patients', *Journal of Human Hypertension*. Nature Publishing Group, 23(5), pp. 307–315.

Wang, M. *et al.* (2016) 'Novel Advances in Shotgun Lipidomics for Biology and Medicine HHS Public Access', *Prog Lipid Res*, 61, pp. 83–108.

Wang, M., Han, R. H. and Han, X. (2013) 'Fatty acidomics: global analysis of lipid species containing a carboxyl group with a charge-remote fragmentation-assisted approach.', *Analytical chemistry*. NIH Public Access, 85(19), pp. 9312–20.

Warschawski, D.E., Arnold, AA., and Marcotte, I., (2018). 'A New Method of Assessing Lipid Mixtures by ^{31}P Magic-Angle Spinning NMR'. *Biophysical Journal.* 114(22), pp. 1368 - 1376.

Watts, A. *et al.* (1999) 'Membrane protein structure determination by solid state NMR.', *Natural product reports*, 16(4), pp. 419–23.

Weiler, H. *et al.* (2001) 'Characterization of a Mouse Model for Thrombomodulin Deficiency', *Arteriosclerosis, Thrombosis, and Vascular Biology*, 21(9), pp. 1531–1537.

Weingarth, M. *et al.* (2014) 'Quantitative Analysis of the Water Occupancy around the Selectivity Filter of a K $^+$ Channel in Different Gating Modes', *Journal of the American Chemical Society*, 136(5), pp. 2000–2007.

Welsh, J., Holloway, J. and Englyst, N. (2014) 'Microvesicles as Biomarkers in Diabetes, Obesity and Non-Alcoholic Fatty Liver Disease: Current Knowledge and Future Directions', *Internal Medicine: Open Access*, 2014.S6-009.

Wenk, M. R. (2005) 'The emerging field of lipidomics', *Nature Reviews Drug Discovery*. Nature Publishing Group, 4(7), pp. 594–610.

Wenk, M. R. (2010) 'Lipidomics: New Tools and Applications', *Cell*, 143, pp. 888–895.

Wennerstrom, H. and Lindblom, G. (2017) 'Biological and model membranes studied by nuclear magnetic resonance of spin one half nuclei', *Quarterly Reviews of Biophysics*, 10, pp. 67–96.

Wennerström, H. and Lindblom, G. (1977) 'Biological and model membranes studied by nuclear magnetic resonance of spin one half nuclei.', *Quarterly reviews of biophysics*, 10(1), pp. 67–96.

White, B. and Perry, D. (2001) 'Acquired antithrombin deficiency in sepsis', *British Journal of Haematology*, 112(1), pp. 26–31.

Williamson, P. and Schlegel, R. A. (2002) 'Transbilayer phospholipid movement and the clearance of apoptotic cells', *Biochimica et Biophysica Acta (BBA) - Molecular and Cell Biology of Lipids*, 1585(2–3), pp. 53–63.

Wohner, N. (2008a) 'Role of cellular elements in thrombus formation and dissolution.', *Cardiovascular and hematological agents in medicinal chemistry*. Europe PMC Funders, 6(3), pp. 224–228.

Wohner, N. (2008b) 'Role of cellular elements in thrombus formation and dissolution.', *Cardiovascular and hematological agents in medicinal chemistry*, 6(3), pp. 224–8.

Wolberg, A. S. *et al.* (2005) 'High dose factor VIIa improves clot structure and stability in a model of haemophilia B', *British Journal of Haematology*. Blackwell Science Ltd, 131(5), pp. 645–655.

Wolberg, A. S. *et al.* (2012) 'Procoagulant activity in hemostasis and thrombosis: Virchow's triad revisited.', *Anesthesia and analgesia*. NIH Public Access, 114(2), pp. 275–285.

Wolf, P. (1967) 'The Nature and Significance of Platelet Products in Human Plasma', *British Journal of Haematology*. Blackwell Publishing Ltd, 13(3), pp. 269–288.

Wu, K. K. and Thiagarajan, P. (1996) 'Role of endothelium of in thrombosis and haemostasis, *Annu. Rev. Med*, 47, pp. 315–31.

Yamamoto, K. and Loskutoff, D. J. (1996) 'Fibrin deposition in tissues from endotoxin-treated mice correlates with decreases in the expression of urokinase-type but not tissue-type plasminogen activator.', *Journal of Clinical Investigation*, 97(11), pp. 2440–2451.

Yáñez-Mó M., et al., (2015). Biological properties of extracellular vesicles and their physio- logical functions. *Journal of Extracellular Vesicles*. 4, pp. 27 - 66.

Ya-Ting Chen et al., (2020). 'Microparticles (Exosomes) and Atherosclerosis'. Current Atherosclerosis Reports, *Springer*. 23(22), pp. 4 - 8.

Yau, J. W., Teoh, H. and Verma, S. (2015) 'Endothelial cell control of thrombosis.', *BMC cardiovascular disorders*. BioMed Central, 15, pp. 13 - 130.

Yeagle, P. L. *et al.* (1975) 'Headgroup conformation and lipid--cholesterol association in phosphatidylcholine vesicles: a 31P(1H) nuclear Overhauser effect study.', *Proceedings of the National Academy of Sciences*. Cambridge University Press, 72(9), pp. 3477–3481.

Yong, P. J. a, Koh, C. H. and Shim, W. S. N. (2013) 'Endothelial microparticles: missing link in endothelial dysfunction?', *European journal of preventive cardiology*, 20(3), pp. 496–512.

Yoshida, H. *et al.* (2005) 'Phosphatidylserine-dependent engulfment by macrophages of nuclei from erythroid precursor cells' Nature, 77(13), pp.77 - 85.

Zachowski, A. (1993) 'Phospholipids in animal eukaryotic membranes: transverse asymmetry and movement', *Biochem. J*, 294, pp. 1–14.

Zeng, W., Lei, Q., Ma, J., Gao, S., and Ju, R., (2021). 'Endothelial Progenitor Cell-Derived Microvesicles Promote Angiogenesis in Rat Brain Microvascular Endothelial Cells In vitro'. *Frontier Cell of Neuroscience.*638 (15), pp. 1 - 7.

Zimmerman, G. A. *et al.* (1990) 'Endothelial cells for studies of platelet-activating factor and arachidonate metabolites', *Circulation*, 33(5), pp. 520–607.

Zwaal, R. F. A. and Schroit, A. J. (1997) 'Pathophysiologic Implications of Membrane Phospholipid Asymmetry in Blood Cells',*Circulation*, 89(15). pp.701 - 733.